CT Perfusion in Acute Ischaemic Stroke within 24 Hours of Onset

Viveka Biswas MBChB, MRCP (UK)

Submitted in fulfilment of the requirements for the Degree of Doctor of Philosophy

Institute of Neurology and Psychology

College of Medical, Veterinary & Life Sciences

Queen Elizabeth University Hospital

University of Glasgow

August 2024

Abstract

This work, presented for examination, addresses how advanced imaging in acute stroke may be used across time windows, to identify the population who will benefit the most from reperfusion therapy at a time when resources are limited.

The time windows for reperfusion therapy have been extended (from 4.5 and 6 hours) to 9 and 24 hours for thrombolysis and endovascular therapy respectively. This extension depends on advanced imaging of penumbra and collateral circulation. However, uncertainties exist surrounding the proportion of patients with prolonged penumbral survival tissue, failure to recruit leptomeningeal collaterals and validation of current thresholds for prediction of tissue fate in late time windows.

We conducted a prospective, single-centre, observational study. Our primary objective was to identify the proportion of patients with salvageable brain tissue, at different time windows up to 24 hours after onset of acute ischaemic stroke. We also assessed collateral circulation (using both perfusion and angiographic imaging), the biological factors which may predict its demise and the time thresholds for ischaemia. We analysed imaging using three commonly used commercial software which process scans using Artificial Intelligence and found systematic differences which may influence treatment decisions.

Improved understanding of the mechanisms underpinning collateral flow, particularly the relevance of hyperglycaemia, is important in identifying a group of patients in whom very early intervention may sustain viable tissue for longer, opening the door for therapeutic interventions such as delayed revascularisation in a wider clinical group.

Table of Contents

List of Tables

List of Figures

Preface

The work presented in this thesis was performed at the Imaging Centre of Excellence, Queen Elizabeth University Hospital, Glasgow from 2018 to 2022.

A substantial component of this work has been presented at various national and international scientific conferences.

Presentations

Visualisation of Ischaemic Stroke on Computed Tomography Perfusion Maps: A Comparison of Automatic Stroke Volume Calculation versus Manual Stroke Volume Calculation using the MIStar Program.
Biswas V, Muir KW.
Oral presentation at the Visualisation in Science Conference (2018), Glasgow 03/12/2018.

A Comparison of Hypoperfusion Lesion Volumes on CT Perfusion Derived from Different Software Programs.
Biswas V, McVerry F, MacDougall N, Huang X, Parsons M, Bivard A, Campbell BCV, Levi C, Davis S, Muir KW.
Poster presentation at the European Stroke Organisation Conference (2019), Milan 22-24/05/2019.

Interaction of Hypoperfusion Intensity Ratio and Hyperglycaemia Predicts Functional Outcome in Ischaemic Stroke.
Biswas V, McVerry F, MacDougall N, Huang X, Muir KW.
Oral Presentation at the Scottish Imaging Network: A Platform for Scientific Excellence (SINAPSE) Annual Meeting (2019), Dundee 21/06/2019.

Whole brain Human Ischaemic Stroke Perfusion and Extended Re-canalisation study (WHISPER).
Biswas V, El Tawil, Porter D, Jampana R, Muir KW.
Poster presentation at the UK Stroke Forum (2019), Telford 3-5/12/2019.

Two Clinical Cases of Migraine with Aura Demonstrating Increased Delayed Tmax on CT Perfusion Maps.

Biswas V, Muir KW.

Oral presentation at the Scottish Imaging Network: A Platform for Scientific Excellence (SINAPSE) Annual Meeting (2020) 19/06/2019.

A Systematic Review of the Relevance of Hyperglycaemia in Collateral Flow in Acute Ischaemic Stroke.

Biswas V, Mahmood A, Neilson S, Muir KW.

Poster presentation at the European Stroke Organisation Conference/ World Stroke Organisation (2020), Vienna 7-9/11/2020.

Prevalence of "Target Mismatch" within 24 hours after Stroke Onset.

Biswas V, Muir KW.

Poster presentation at the European Stroke Organisation Conference (2022), Lyon 4-6/05/2022.

Comparison of Hypoperfusion Lesion Volumes and Target Mismatch on CT Perfusion from Different Software Programs.

Biswas V, McVerry F, MacDougall N, Huang X, Parsons M, Bivard A, Campbell BCV, Levi C, Davis S, Muir KW.

Poster presentation at the European Stroke Organisation Conference (2022), Lyon 4-6/05/2022.

Hyperglycaemia Predicts Collateral Status in Patients Presenting Within 24 Hours of Acute Ischaemic Stroke

Biswas V, Muir KW.

Poster presentation at the European Stroke Organisation Conference (2022), Lyon 4-6/05/2022.

Regional leptomeningeal collateral score versus hypoperfusion intensity ratio in large vessel occlusion

Biswas V, Sitaram A, Pollard CRJ, Izzath MWKI, Muir KW

Poster presentation at the European Stroke Organisation Conference (2023), Munich 24-26/05/2023.

Thresholds of ischaemia differ depending on recanalisation in patients presenting within 24 hours of acute ischaemic stroke with large vessel occlusion

Biswas V, Sitaram A, Pollard CRJ, Neilson S, Izzath MWKI, Muir KW

Poster presentation at the European Stroke Organisation Conference (2023), Munich 24-26/05/2023.

Variable penumbra but not core volume by occlusion site in large vessel occlusion

Biswas V, Sitaram A, Pollard CRJ, Izzath MWKI, Muir KW

Poster presentation at the European Stroke Organisation Conference (2023), Munich 24-26/05/2023.

Clinical and radiological characteristics of AIS patients with no perfusion lesions on admission CTP

Biswas V, Neilson S, Sitaram A, Pollard CRJ, Izzath MWKI, Muir KW

Poster presentation at the UK Stroke Research Workshop (2023), London 26-27/09/2023

Comparison of eASPECTS with Clinical Raters in AIS within 24 hours

Biswas V, Sitaram A, Pollard CRJ, Neilson S, Izzath MWKI, Muir KW

Poster presentation at the European Stroke Organisation Conference (2024), Basel 15-17/05/2024.

Comparison of Routinely Used Acute Stroke Imaging Software for CTA

Biswas V, Sitaram A, Pollard CRJ, Neilson S, Izzath MWKI, Muir KW

Poster presentation at the European Stroke Organisation Conference (2024), Basel 15-17/05/2024.

Comparison of Three CT Perfusion Processing Software Systems in Acute Stroke

Biswas V, Mahmood A, Sitaram A, Pollard CRJ, Izzath MWKI, Muir KW

Poster presentation at the European Stroke Organisation Conference (2024), Basel 15-17/05/2024.

The Impact of Covid-19-Related Restrictions

The COVID-19 pandemic and subsequent cessation of research (23rd March 2020) with national and international lockdowns both directly and indirectly affected this work.

Owing to the COVID-19 pandemic, all clinical research work was suspended (March to August 2020). As an NHS doctor, I was also redeployed to work full-time for the NHS from (March to August 2020).

Stroke research recommenced in August 2020. However, disruption to patient recruitment and delayed data gathering persisted. My return to research was made more difficult by continuing redeployment of staff and prioritisation of COVID activities. These staff were essential to my data gathering and included radiographers, clinical research fellows and radiologists. Furthermore, a planned component of the study involving blood sampling was not possible due to restrictions on access to laboratories and sample processing.

Consequently, the recruitment period of the study was extended but there remained a protracted impact on clinical services which affected data analysis. We continued recruitment up until the end of the funding period which coupled with a reduction in availability of clinical staff contributed to prolonged data analysis.

My Contribution to this Work

This work was performed as part of a team (an acknowledgement succeeds this section) of which my contribution is as follows.

I designed and performed the searches for the systematic review (Chapter 2) and was the first assessor for abstract and paper inclusion. I extracted the data from the included papers and performed the statistics and meta-analysis.

I performed the software comparison (Chapter 4). I was fortunate to be in Glasgow where Professor Muir and his research colleagues have established an extensive research database of international trials. I uploaded CTP scans to the three software: MIStar version 3.2 (Apollo), Brainomix (versions 9.001 to 11.001) and RAPID version 4.7 (Ischemaview). I performed the first manual analysis of scans on MIStar (my colleague Ammad Mahmood performed the second) and all of the analyses on RAPID and Brainomix. I collated the data and performed the statistical analyses.

The WHISPER study (Chapters 5, 6 and 7) began before I joined the team. I contributed to recruitment of participants and arranged imaging and follow up. I uploaded the clinical data and all imaging into the research database. I co-ordinated the analysis of the non-contrast CT, CTA and MRI imaging by more experienced assessors and uploaded the CTP scans to the RAPID software for analysis. I performed all statistical analyses.

None of the above would have been possible without a great deal of help and guidance from Professor Muir who has considerable interest and expertise in stroke.

Acknowledgement

I would like to offer my deep gratitude to Professor Keith Muir. Against an unprecedented and challenging environment, his time and generosity continue to be unfailing. His patience and good humour persisted during my statistical efforts. His curiosity invariably took my thinking to a new level. I remain deeply indebted to him and I thank him for the lifelong escape route.

My other supervisors (internal and external) also guided progress and provided invaluable advice. They are Professor Matthew Walters, Professor Jesse Dawson and Professor David Porter.

The ATTEST, POSH, MASIS and Australian TNK trial data analysed in chapter four were accumulated at multiple centres over several years. I thank the trial investigators Dr Xuya Huang, Dr Neil McDougal, Dr Ferghal McVerry, Professor Andrew Bivard, Professor Christopher Levi, Professor Stephen Davis, Professor Bruce Campbell and Professor Keith Muir who allowed access to this data.
Dr Ammad Mahmood provided second manual readings for CTP scans. The CTA and MRI scans were analysed by Marta Guarisco, Dr Amith Sitaram, Dr Sin Yee Foo, Dr Christopher Pollard and Professor Keith Muir. I appreciate the alliances (both historic and recent) which led to the software comparison's being possible.

The design of the WHISPER study described in chapters five, six and seven was the brainchild of Professor Keith Muir. The research nurses who recruited to the study were Angela Welch, Wilma Smith and Kim Hatherly. Dr Salwa El Tawil, Dr Jennifer Elliot, Dr Amith Sitaram, Dr Ammad Mahmood, Dr Cameron Brown and Dr Sam Neilson also recruited patients. Other members of Professor Muir's research team included Shirley Mitchell, Emma MacRae, Monica Crone and Dr Alicia Murray -all of whom enabled the study to progress. Zanariah Mohd assisted in data upload. Tracey Hopkins and her team of research radiographers performed the imaging. The NCCT, CTA and MRI imaging were analysed by Dr Christopher Pollard and Dr Amith Sitaram with verification by Dr Wazim Izath and Professor Keith Muir. Dr Ammad Mahmood provided second manual CTP

readings. MRI volumes were measured by Dr Sam Neilson with guidance from Professor Keith Muir. I am grateful to all for their persistence and hard work.

My clinical supervisor Dr Andy Breckenridge's formidable combination of gentle persuasion and steely determination made my transition from research back to clinical medicine (amidst a training restructure) seamless. Dr Tracy Baird and Dr Fozia Nazir also provided much-appreciated encouragement, career advice and interview practice. To each, I owe a debt of gratitude.

My thanks go to the patients and relatives who agreed to participation in the studies with special thanks to the nursing staff in the Hyper-Acute Stroke Unit for their care (from which I too benefited) and assistance.

I received generous funding from the Chief Scientist Office, NHS Research Scotland and the Neurosciences Foundation for which I am grateful.

My current colleagues at Charing Cross Hospital and St Mary's Hospital were understanding about leave; their flexibility and optimism directly contributed to the thesis and corrections being completed.

For my part, I am sure that without the close friendship and support of my research colleagues Ammad Mahmood, Cameron Brown, Sam Neilson and Katerina Pappa, I would have found my time in research a much less enjoyable experience. I must also acknowledge the tolerance of my family and friends. This has been an immersive experience amidst a huge transition; I would have become increasingly dissociated without them.

I dedicate this work to my parents, Kamalaksha Biswas and Anushua Biswas.

Viveka Biswas, August 2024

Declaration

I declare that this thesis has been composed by myself and is a record of work performed by myself. It has not been submitted previously for a higher degree.

The work described in this thesis was carried out under the supervision of Professor Keith Muir in the Department of Stroke Medicine and Imaging Centre of Excellence at the Queen Elizabeth University Hospital, Glasgow.

Viveka Biswas

August 2024

List of Abbreviations

ACA – Anterior Cerebral Artery

ACIS – Acute Cerebrovascular Ischaemic Syndrome

ADC – Apparent Diffusion Coefficient

AGC – The American Society of Interventional and Therapeutic Neuroradiology Collateral Grading System

AHA-ASA – American Heart Association–American Stroke Association

AIF – Arterial Input Function

AIS – Acute Ischaemic Stroke

AMI – Acute Myocardial Infarction

ANGEL-ASPECT – Endovascular Therapy in Acute Anterior Circulation Large Vessel Occlusive Patients with a Large Infarct Core

aPTT – Activated Partial Thromboplastin Time

ASA – Acetylsalicylic Acid

ASL – Arterial Spin Labelling

ASPECTS – Alberta Stroke Program Early Computed Tomography Score

ATP – Adenosine Triphosphate

ATTEST2 – Alteplase-Tenecteplase Trial for Evaluation of Stroke Thrombolysis 2

AUC – Area Under the Curve

BBB – Blood-Brain-Barrier

BMI – Body Mass Index

BP – Blood Pressure

CASP – Critical Appraisal Skills Program

CAST – Chinese Acute Stroke Trial

CBF – Cerebral Blood Flow

CBV – Cerebral Blood Volume

CI – Confidence Intervals

CMRG – Cerebral Metabolic Rate of Glucose

CMRO2 – Cerebral Metabolic Rate of Oxygen

cOR – Common Odds Ratio

COX – Cyclo-Oxygenase

CPP – Cerebral Perfusion Pressure

CT – Computed Tomography

CTA – Computed Tomography Angiography

CTP – Computed Tomography Perfusion

CVR – Cerebrovascular Resistance

DALY- Disability-Adjusted Life Year

DAPT – Dual-Antiplatelet Therapy

DEFUSE – Diffusion and Perfusion Imaging Evaluation for Understanding Stroke Evolution

DM – Diabetes Mellitus

DVT – Deep-Vein Thrombosis

DWI – Diffusion-Weighted Imaging

ECASS – European Cooperative Acute Stroke Study

EEG – Electroencephalogram

EIC – Early Ischaemic Change

ELVO – Emergent Large Vessel Occlusion

ESOC – European Stroke Organisation Conference

ESUS – Embolic Stroke of Undetermined Source

EVT – Endovascular Thrombectomy

EXTEND – Extending the Time for Thrombolysis in Emergency Neurological Deficits

FLAIR – Fluid-Attenuated Inversion Recovery

GI – Gastrointestinal

GISSI – Gruppo Italiano per lo Studio della Sopravvivenza nell'Infarto Miocardico Acuto

GIST-UK – Glucose Insulin in Stroke Trial

GRE – Gradient Recalled Echo

HASU – Hyper-Acute Stroke Unit

HEPA – Human Extrinsic Plasminogen Activator

HERMES – Highly Effective Reperfusion Evaluated in Multiple Endovascular Stroke Trials

HIR – Hypoperfusion Intensity Ratio

HMG-CoA – Hydroxymethylglutaryl-Coenzyme A

IA – Intra-arterial

ICA – Internal Carotid Artery

ICC- Intraclass Correlation Coefficient

ICD – International Classification of Diseases

ICH – Intracranial Haemorrhage

IE – Infective Endocarditis

ILCD – International List of Causes of Death

INTERSTROKE – International Study of Risk Factors for Stroke

INR – International Normalised Ratio

IQR – Inter-quartile Range

ISIS – International Study of Infarct Survival

IST – International Stroke Trial

IV – Intravenous

IVO – Intracranial Vessel Occlusion

LACS – Lacunar Stroke

LDL – Low-Density Lipoprotein

LMWH – Low Molecular Weight Heparin

LVO – Large Vessel Occlusion

MCA – Middle Cerebral Artery

MCA – Middle Cerebral Artery

MERCI – Mechanical Embolus Removal in Cerebral Ischaemia

MHRA – Medicines and Healthcare products Regulatory Agency

MI – Myocardial Infarction

MMD – Moyamoya Disease

MR – Magnetic Resonance

MR CLEAN – Multicentre Randomized Clinical Trial of Endovascular Treatment for Acute Ischemic Stroke

MR CLEAN LATE – Multicentre Randomized Clinical Trial of Endovascular Treatment for Late Arrivals

MRA – Magnetic Resonance Angiography

MRI – Magnetic Resonance Imaging

mRS – modified Rankin Scale

MT – Mechanical Thrombectomy

MTT – Mean Transit Time

NCCT – Non-Contrast Computed Tomography

NHS – National Health Service

NICE – National Institute for Health and Care Excellence

NIH – National Institutes of Health

NIHSS – National Institutes of Health Stroke Scale

NNT – Number Needed to Treat

OR – Odds Ratio

ORIGINAL - Study in Chinese Patients to Compare How Tenecteplase and Alteplase Given After a Stroke Improve Recovering of Physical Activity

OSA – Obstructive Sleep Apnoea

PA – Plasminogen Activator

PACS – Partial Anterior Circulation Stroke

PAI-1 – Plasminogen Activator Inhibitor 1

PCA – Posterior Cerebral Artery

PE – Pulmonary Embolism

PFO – Patent Foramen Ovale

POCS – Posterior Circulation Stroke

PRISMA – Preferred Reporting Items for Systematic Reviews and Meta-Analyses

PSH – Post-Stroke Hyperglycaemia

PT – Prothrombin Time

PWI – Perfusion-Weighted Imaging

QALY- Quality-Adjusted Life Year

QEUH – Queen Elizabeth University Hospital

rCBF – Regional Cerebral Blood Flow

RCT – Randomised-Controlled Trial

RCVS – Reversible Cerebral Vasoconstriction Syndrome

RESCUE-Japan LIMIT – Recovery by Endovascular Salvage for Cerebral Ultra-Acute Embolism Japan-Large Ischemic Core Trial

rFTD – Relative Filling Time Delay

rLMC – Regional Leptomeningeal Score

ROC – Receiver Operating Characteristic

RR – Relative Risk

rTPA – Recombinant Tissue Plasminogen Activator

SAH – Sub-arachnoid Haemorrhage

SD – Standard Deviation

SELECT2 – Randomized Controlled Trial to Optimize Patient's Selection for Endovascular Treatment in Acute Ischemic Stroke

SHINE – Stroke Hyperglycaemia Insulin Network Effect

SICH – Symptomatic Intracranial Haemorrhage

SITS-ISTR – Safe Implementation of Treatments in Stroke International Stroke Thrombolysis Register

SNIS – Society of Neuro-Interventional Surgery

SSNAP – Sentinel Stroke National Audit Programme

SWI – Susceptibility-Weighted Imaging

TACI – Total Anterior Circulation Infarct

TACS – Total Anterior Circulation Stroke

TASTE – Tenecteplase versus Alteplase for Stroke Thrombolysis Evaluation

TEMPO-2 – Tenecteplase versus Standard of Care for Minor Ischaemic Stroke with Proven Occlusion

TENSION – Efficacy and Safety of Thrombectomy in Stroke with Extended Lesion and Extended Time Window: A Randomized-Controlled Trial

TIA – Transient Ischaemic Attack

Tmax – Time to Maximum

TNK – Tenecteplase

TOAST – Trial of Org 10172 in Acute Stroke Treatment

tPA – Tissue Plasminogen Activator

TRACE III – Tenecteplase Reperfusion Therapy in Acute Ischaemic Cerebrovascular Events-III

TTP – Time to Peak

VISTA – The Virtual International Stroke Trials Archive

VOF – Venous Outflow Function

WHO – World Health Organisation

WSC – World Stroke Congress

Chapter 1 Introduction

Definitions of Stroke

The current definition of stroke is based upon clinical findings and was introduced by the World Health Organisation [WHO] in 1970 as an epidemiological tool. Acute ischaemic stroke [AIS] manifests as 'rapidly developed clinical signs of a focal (or global) disturbance of cerebral function, lasting more than 24 hours or leading to death, with no apparent cause other than of vascular origin' (Aho et al., 1980).

Current advice by the WHO for the naming of conditions is to use 'specific descriptive terms'; by comparison the word 'stroke' can seem ambiguous and broad (WHO, 2015).

Historical 'Apoplexy'

The first term used for AIS - 'ἀποπληξία' (Greek -*apoplexia*), channels the same spirit of sudden violence as '*stroke*', the German '*Schlaganfall*' and the French '*coup de sang*'(Clarke, 1963).

'Apoplexy' can be traced from Antiquity to its appearance in Oscar Wilde's 19th century play "The Importance of Being Earnest" to its final appearance in the 4th Revision of the International List of Causes of Death [ILCD/ICD] in 1929 (Engelhardt, 2017, Wilde, 1895). It indicated a sudden collapse - 'as if struck by lightning'. When searching for an excuse to put an end to his alter-ego, Oscar Wilde's protagonist Jack Worthing says: "Apoplexy will do perfectly well, lots of people die of apoplexy, quite suddenly, don't they?" (Wilde, 1895).

Associated terms included 'paraplegia', 'paresis' and 'paralysis' -which continue to be associated with AIS (Cooke, 1820). If the term 'stroke' is broad, 'apoplexy' is broader still. It included collapse of any nature -even myocardial infarction, pulmonary embolism and mental instability (Cooke, 1820, Clarke, 1963).

Autopsy divided the classification of ‘apoplexy’ into anatomical subsidiary branches (Engelhardt, 2017). ‘Haemorrhage’ was distinguished as separate in 1658 and the word ‘stroke’ was first substituted for ‘apoplexy’ in medical writing in 1689 (Cole and Kimberley, 1689).

The Term ‘Stroke’

‘Stroke’ first appeared in the *Oxford English Dictionary* in 1599, in which the first synonym for the ‘stroke of the palsy’ is given as ‘stroke of God’s hands’ (Schiller, 1970). It did not appear in the ILCD until the 9th revision (1975) (WHO, 1975). The first case report to be published on the subject was a case of sudden, transient mutism in *Brain* (1898) by Byron Bramwell -a Scottish Neurologist (Mohr et al., 1978).

Stroke

Cerebral Circulation

The cerebral circulation exists as a series of anastomoses allowing continuous blood flow between two internal carotid and two vertebral arteries which converge to form the circle of Willis at the base of the brain. Arteries arising from the circle of Willis give rise to pial arteries which further branch into penetrating arteries and arterioles. Penetrating arteries are separated from brain tissue by the Virchow-Robin space (an extension of the subarachnoid space) and pass through the brain tissue as intracerebral arterioles which divide into capillaries allowing for the exchange of oxygen, nutrients, carbon dioxide and metabolites to occur (Hall JE, 2011). Anastomoses with the external carotid artery branches also exist but are not functional in most unless there is pathology. The anatomy varies from individual to individual and thus impacts tolerance for ischaemia and subsequent neurological disability caused by a stroke (Riggs HE, 1963, Vander Ecken HM, 1953).

Cerebral Blood Flow

A measure of rate, cerebral blood flow [CBF] is defined as the blood volume that flows per unit mass per unit time in brain tissue and is expressed in units of ml (blood)/ 100g (brain tissue) /minute (Hall JE, 2011). The average value of CBF in adults is 50ml/100g/min

(Lassen, 1985). CBF is lower in white matter (~20ml/100g/min) and greater in grey matter (~80ml/100g/min) (Vavilala MS, 2002).

Ohm's law of current (I) being equal to the voltage difference (δV) divided by resistance (R) can be applied to blood flow (F). The voltage difference being the perfusion pressure difference (δP) between the two ends of the vessel and resistance determined by the diameter of the vessel and blood viscosity. (Hall JE, 2011, Markus, 2004).

CBF is determined by the cerebral perfusion pressure [CPP] (the difference between systemic arterial pressure and venous back pressure) and the cerebrovascular resistance [CVR]. If CPP remains the same, CVR must reduce in order to increase CBF by way of dilation of the smaller intracranial arteries– which provide the most intracranial resistance (Markus, 2004).

Cerebral Autoregulation

Brain tissue receives a consistent supply of blood despite wide variations in systemic blood pressure affecting CPP due to CBF autoregulation -first observed in cats (Fog, 1938). CBF remains constant between the mean arterial pressures of 60 and 150 mmHg; these limits are shifted upwards in hypertensive patients causing arteriolar wall hypertrophy. Reduction below these limits endangers brain tissue through hypoxia, increase risks cerebral oedema (Strandgaard et al., 1973).

Classification of Stroke Syndromes

There are two categories of stroke. Ischaemic, defined as brain, spinal cord or retinal cell infarction, account for 80% of AIS presentations. Haemorrhagic, include either intracerebral haemorrhage [ICH] or subarachnoid haemorrhage [SAH] (Bamford et al., 1991, Sacco et al., 2013).

There is heterogeneity in terminology describing time from onset. The definitions below (Table 1-1) were declared by the international Stroke Recovery and Rehabilitation

Roundtable in recognition of potentially different physiological processes at each stage (Bernhardt et al., 2017).

Table 1-1 Agreed Definitions of Time-Windows for Ischaemic Stroke

Phase	**Time-Window**
Hyper-acute	0-24 hours
Acute	1-7 days
Early Subacute	7 days – 3 months
Late Subacute	3-6 months
Chronic	>6 months

(Bernhardt et al., 2017)

Ischaemic strokes were further classified by Bamford et al. (1991) based on the clinical pattern at presentation, to identify subgroups who may benefit from targeted therapies. The Oxfordshire Community Stoke Project [OCSP] was an epidemiological study, undertaken with limited access to brain imagine (especially in the acute phase) (Bamford et al., 1991). The syndromes were based on a long history of neurological classification and are listed in Table 1-2.

Table 1-2 The Bamford Classification of Acute Ischaemic Stroke Syndromes

Bamford Classification	Presentation
Total anterior circulation syndrome [TACS]	Combination of the following: - New higher cerebral dysfunction (e.g. dysphasia, dyscalculia, visuospatial disorder) - Homonymous visual field defect Ipsilateral motor and/or sensory deficit of at least two of face, arm and leg
Partial anterior circulation syndrome [PACS]	Two of the three components of TACS
Lacunar syndrome [LACS]	Pure motor stroke Pure sensory stroke Sensori-motor stroke Ataxic hemiparesis
Posterior circulation syndrome [POCS]	Any of the following: - Ipsilateral cranial nerve palsy with contralateral motor and/or sensory deficit - Bilateral motor and/or sensory deficit - Disorder of conjugate eye movement - Cerebellar dysfunction without ipsilateral long-tract deficit - Isolated homonymous visual-field defect

LACS=Lacunar Syndrome, TACS=Total Anterior Circulation Syndrome, PACS=Partial Anterior Circulation Syndrome, POCS=Posterior Circulation Syndrome (Bamford et al., 1991)

Epidaemiology

Stroke (both ischaemic and haemorrhagic) affects 12.2 million people globally per year and is the second leading cause of death with 6.5 million deaths per year. An estimated 1 in 4 adults (>age 25) will experience a stroke in their lifetime and there are >101 million survivors of stroke globally (WSO, 2022). These stroke survivors indicate a high-risk population and are the target of secondary prevention stroke therapies.

The Global Burden of Disease Study (2019) showed a substantial increase in absolute number of cases from 1990 to 2019. Whilst population growth and aging are contributing risk factors so too are high body mass index [BMI], high fasting plasma glucose, high systolic blood pressure, alcohol consumption, low physical activity, kidney dysfunction, high temperature and ambient particulate matter pollution (Feigin et al., 2021).

Risk factors and Aetiology

Risk factors which cannot be modified include age, sex and genetic susceptibility.

From 1990 to 2019, there has been an increase in the total number of stroke-related disability-adjusted life years [DALYs] due to high BMI, high fasting plasma glucose, high systolic blood pressure, high low-density lipoprotein [LDL] cholesterol, kidney dysfunction, a diet high in red meat, alcohol consumption and second hand smoking (Feigin et al., 2021).

Other (non-traditional) risk factors include poor quality sleep (including obstructive sleep apnoea [OSA]), chronic inflammation -including periodontal disease, chronic kidney disease and psycho-social stress (Boden-Albala et al., 2012, Dregan et al., 2014, Grau et al., 2004, Go et al., 2004, O'Donnell et al., 2010).

The second-phase analysis of the International Study of Risk Factors for Stroke [INTERSTROKE] found differences in prevalence of risk factors among region, ethnic

groups, between men and women and in younger and older subgroups (O'Donnell et al., 2016).

Mechanisms

The most used classification system was developed for the Trial of Org 10172 in Acute Stroke Treatment [TOAST] (a randomised-control trial of low-molecular weight heparinoid given within 24 hours of AIS) which grouped AIS into five aetiologies (Table 1-3).

Table 1-3 Types of Acute Ischaemic Stroke Based on the TOAST Classification with Distribution of Subtype Based on North American and European Studies

Stroke type	Causes	Percentage
Large-artery atherosclerosis (embolus/thrombosis)	Atherosclerotic plaques or stenosis >50% occlusive leading to ischaemia and infarction	25%
Cardioembolism	Identifiable cardiac source for an embolism	20%
Small-artery occlusion (lacune)	Small vessel disease	25%
Stroke of other determined aetiology	e.g. Dissections, arteritis	5%
Stroke of undetermined aetiology (cryptogenic)	a. Two or more causes identified b. Negative evaluation c. Incomplete evaluation	25%

(Adams et al., 1993, Hart et al., 2014)

Atherosclerosis

When the lipid core of an atherosclerotic plaque in the aortic arch, carotid or intracranial vessels is exposed to the bloodstream following inflammation or ulceration of the fibrous cap, thrombi form. Either the atherosclerotic vessel is occluded or the thrombus embolises more distally.

Intracranial atherosclerosis is responsible for 5-10% of strokes in Caucasian people and up to 30-50% of strokes in Asian populations (Huang et al., 1997).

Small Vessel Disease

Vascular disease can manifest silently, causing asymptomatic injury (Miller-Fisher, 1965).

The early 19th century concept of 'cerebral softening' consisted of Dechambre's lacunae (1838) and Durand-Fardel's description of a sieve -'l'état criblé' (1842) (Poirier and Derouesné, 1985). More sophisticated and detailed brain imaging has resulted in the expansion of the description. On a pathological level there is loss of smooth muscle cells from the tunica media, deposits of fibro-hyaline material causing narrowing of the lumen with thickening of the vessel wall (Furuta et al., 1991). Other pathological definitions refer to cerebral amyloid angiopathy, genetic small vessel diseases (CADASIL, CARASIL, MELAS, Fabry's disease), immunologically mediated small vessel diseases (Wegener's, Churg-Strauss or HSP), venous collagenosis or other small vessel diseases such as post-radiation angiopathy (Pantoni, 2010).

Imaging features include lacunes (Vermeer et al., 2007), white matter lesions (Rost et al., 2010), enlarged perivascular spaces (Doubal et al., 2010) and microbleeds (Cordonnier et al., 2007) and are detected in 20% of healthy elderly people (Vermeer et al., 2007). The Standards for Reporting Vascular Changes on Neuroimaging [STRIVE] (Wardlaw et al., 2013b) and STRIVE-2 (Duering et al., 2023) guidelines have attempted to consolidate terminology of SVD imaging features to promote international consistency.

Arterial Dissection

A dissection or tear (through trauma or exercise) within the intimal layer of an artery causes stroke through thrombus formation or distal embolism with the most common sites being the internal carotid artery and the vertebral arteries.

Pregnancy (specifically the post-partum period) is also associated with increased risk of dissection (Debette et al., 2011, Dziewas et al., 2003, Salehi Omran et al., 2020).

Overall, in the context of other risk factors dissection accounts for a smaller proportion of stroke in older adults leading to the belief that dissection is a relatively common cause of young stroke (Atalay et al., 2021).

Cerebral Vasculitis

Vasculitis is characterised by inflammation of small or medium cerebral arteries with or without systemic involvement. Vessel wall inflammation leads to narrowing and thromboembolism which can cause both ischaemic and haemorrhagic stroke. Diagnostic criteria include symptoms of a multifocal or diffuse CNS-disorder, with remitting or progressive course, exclusion of systemic disease, angiography demonstrating segmental arterial narrowing and CSF or biopsy consistent with vascular inflammation. This is important to distinguish as treatment is with steroid therapy and cyclophosphamide (Moore, 1989) – different to other causes of AIS.

Reversible Cerebral Vasoconstriction Syndrome

Reversible cerebral vasoconstriction syndrome [RCVS] presents as severe headache -often thunderclap (or recurring thunderclap). Around 37% are spontaneous, secondary causes include the post-partum period and exposure to vasoactive substances (such as cannabis, selective-serotonin reuptake inhibitors and nasal decongestants) (Ducros et al., 2007). It is characterised by vasoconstriction and dilation predominantly involving arteries around the circle of Willis (Call et al., 1988). This is typically viewed on angiography as a “string and beads” and resolves 1-3 months following onset. The pathophysiology is unknown – arterial histology is normal without infection or inflammation (Singhal et al., 2011). TIA and AIS are potential complications, if these manifest they present typically in the second week following onset (Ducros et al., 2007).

Atrial Fibrillation

Atrial fibrillation interrupts normal flow through the heart causing stasis in the left atrial appendage leading to the formation of thrombosis with or without embolism. In first presentation of AIS, the prevalence of AF is 25% - particularly affecting older populations (especially women). AF induced AIS is also associated with higher 30-day mortality, 1-year fatality rates and stroke recurrence rate within the first year (Marini et al., 2005).

Patent Foramen Ovale

Overall incidence of a patent foramen ovale [PFO] is around 27.3% with a mean diameter of 4.9mm -neither of which is affected by gender. PFO is significantly associated with cryptogenic AIS in young patients suggesting a mechanism of paradoxical emboli crossing from venous to arterial circulation (Overell et al., 2000). Certainly in adults with cryptogenic AIS, closure is associated with reduction in subsequent AIS compared with medical therapy alone (Saver et al., 2017).

Infective Endocarditis

In a prospective study of cerebral MRI within 7 days of presentation with infective endocarditis [IE], MRI was abnormal in 87% of patients with microhaemorrhages and ischaemic lesions being the most common finding (Duval et al., 2010). The increased risk of haemorrhagic events presents difficulties with management.

Hypokinetic Segment with Mural Thrombosis

Severe apical-wall-motion abnormalities following acute transmural myocardial infarction [MI] can lead to formation of left-ventricular thrombosis (typically diagnosed 5 days following MI) which may cause embolic AIS (Asinger et al., 1981).

Haematological Disorders

Haematological disorders are estimated to account for 1.5% of first presentation AIS (Arboix et al., 2001). Sickle cell anaemia is an important cause of stroke in children (Earley et al., 1998). Cerebral infarction secondary to venous thrombosis, essential thrombocytopaenia and polycythaemia vera are the most common haematological causes in adults. Other causes include anti-phospholipid syndrome, aplastic anaemia, leukaemia and lymphoma (Arboix et al., 2001).

Pathophysiology of Acute Ischaemic Stroke

The current model of AIS was described in an editorial summarising the background to the understanding of the reversible element of brain ischaemia in animal studies (Astrup et al.,

1981). In the same year, Jones et al. (1981) demonstrated the relationship between severity of CBF reduction, duration and probability of infarction. Focal ischaemia of the middle cerebral artery [MCA] in *Macaca irus* monkeys was reversible up to 3 hours later. Post-mortem confirmed the size of the infarct to be proportional to the duration of MCA occlusion. Some of the brains (after just fifteen minutes' occlusion) showed no evidence of infarction (Jones et al., 1981).

Haemodynamic Compromise

Three stages of haemodynamic compromise were described by Powers and Raichle (1985) and are illustrated by Figure 1-1.

1. Compensatory cerebral autoregulation: Cerebral perfusion pressure [CPP] falls, compensatory pre-capillary arterioles dilate to increase cerebral blood volume [CBV], cerebral blood flow [CBF] and the metabolic rate of oxygen [CMRO2].
2. Maximal autoregulatory vasodilation: compensatory vasodilation culminates, decrease of CPP causes CBF to fall, the oxygen extraction fraction [OEF] increases to maintain CMRO2.
3. The limit of OEF is reached: further decrease of CBF causes cerebral ischaemia. CMRO2 decreases and tissue infarcts (Powers and Raichle, 1985).

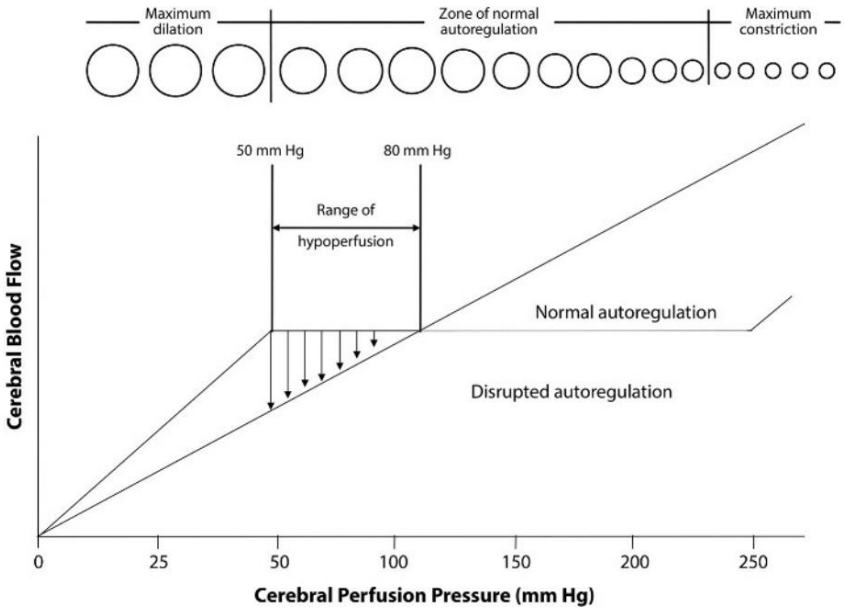

(Lassen, 1959, Lin and Liebeskind, 2016)

Figure 1-1 Schematic of Cerebral Autoregulation

Cerebral Ischaemia

Cerebral ischaemia ensues when disruption in cerebral blood flow [CBF] leads to loss of glucose/nutrient supply, loss of waste product removal and hypoxia (Sharbrough et al., 1973). Hypoxia pauses neuronal electrical activity causing deterioration of the energy state and ion homeostasis. Depletion of high energy phosphates, failure of the membrane ion pumps, efflux of potassium, influx of sodium, chloride and water and membrane depolarisation follow. Irreversible cell damage may occur after 5-10 minutes (Astrup et al., 1981).

Ischaemic Thresholds for Vital Brain Functions

Neurological deficit may resolve if the occlusion is removed however this is time dependent.

Trojaborg and Boysen (1973) provided a flow threshold for failure of neuronal electrical function in humans. Carotid artery clamping was used to show that slowing of the electroencephalogram [EEG] occurs when CBF falls to a mean rate of 18ml/100g/min with flattening at 14 ml/100g/min.

Primates, cats and rodents were used to established CBF thresholds (Molinari and Laurent, 1976). In *Macaca irus* monkeys, occlusion of the MCA (15 minutes up to 3 hours or permanent surgical occlusion) demonstrated that hemiparalysis is reversible when CBF<23ml/g/min but irreversible when CBF< 18ml/g/min (Thomas et al., 1981).The survival of brain tissue is dependent on continued protein synthesis and glucose metabolisation (Mies et al., 1991, Paschen et al., 1992). In rats, protein synthesis is inhibited by 55% at a CBF rate below 55ml/g/min and completely suppressed below 35ml/g/min (Mies et al., 1991). In Mongolian gerbils, glucose utilisation i.e. the cerebral metabolic rate of glucose [CMRG] increases when CBF falls below 35ml/g/min before declining sharply at values below 25ml/g/min (Paschen et al., 1992). Mongolian gerbils, however, have an incomplete circle of Willis; synthesising data from different species and models adds complexity.

Differential Neuronal Vulnerability

Grey matter (having greater metabolic activity) is more vulnerable to ischaemia than white (Marcoux et al., 1982).

Mechanisms of Cell Death: 'Necrosis' or 'Apoptosis'

Originally it was believed that cells within the infarct core perished through 'necrosis' whereas cells within the ischaemic penumbra through 'apoptosis' or cell-mediated death. However the mechanism of cell death in the ischaemic brain probably involves both (MacManus and Buchan, 2000).

Oedema

Cerebral oedema develops when regional cerebral blood flow [rCBF] falls below 10-20ml/100g/min -the threshold required to maintain structural integrity (Schuier and Hossmann, 1980, Symon et al., 1979). Capillary dysfunction causes oedema which leads to swelling and can result in haemorrhagic transformation (Hossmann and Schuier, 1980).

The Infarct core

Jennet et al measured rCBF in a carotid endarterectomy patient sample during carotid ligation. Hemiparesis consistently occurred when CBF dropped below 25% (Jennett et al., 1966).

Following the initial obstruction or alteration of CBF in AIS and the failure of electrical, metabolic and functional processes mentioned above, ischaemia necrosis of neurones, glia and other supportive brain cells. Ischaemic brain damage is a complex process with many potential mechanisms – summarised by Pulsinelli (1992) in Figure 1-2. The ischaemic core refers to brain tissue which is destined for infarction or is already infarcted i.e. unsalvageable by any form of treatment.

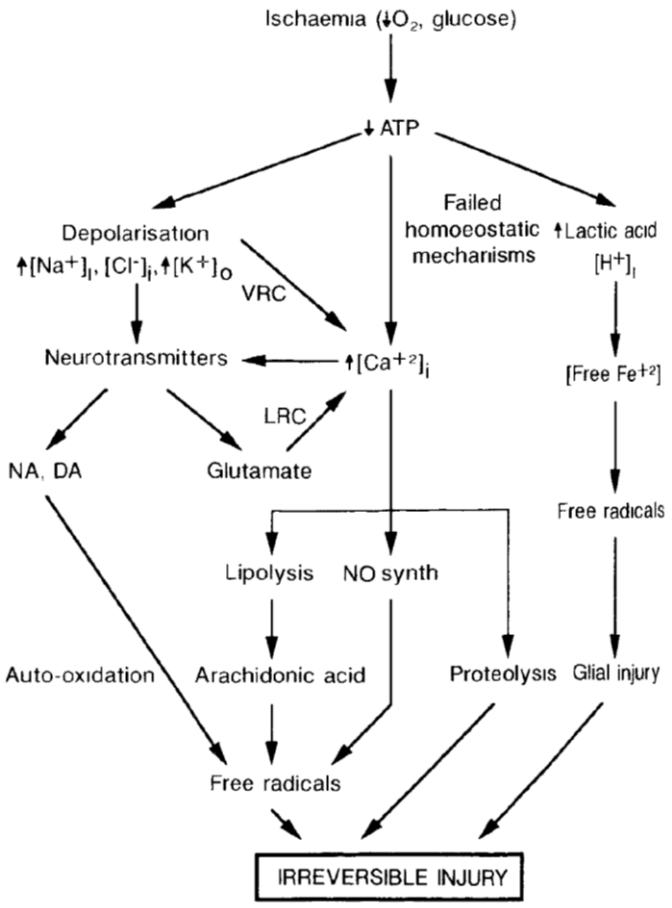

(Pulsinelli, 1992)

Figure 1-2 Potential Mechanisms of Ischaemic Brain Damage

The 'Penumbra'

Referencing the partially shaded region around the centre of a solar eclipse, the area of the ischaemic brain with CBF between the upper limit of electrical failure and the lower limit of energy and ion pump failure was labelled the ischaemic 'penumbra' by Astrup et al. (1981). This review brought together years of research and offered a conceptual framework for stroke treatment. It also notes an anatomical distinction between core and penumbra i.e. central core surrounded by a ring of penumbra, which set the visualisation agenda (Astrup et al., 1981).

Neurological disability may be observed below certain thresholds of cerebral blood flow - demonstrated in Figure 1-3 with a modified version shown beside the original (Jones et al., 1981, Lin and Liebeskind, 2016). Infarction may occur within minutes or hours depending on degree of reduction of CBF and duration of ischaemia (Heiss and Rosner, 1983).

Collateral flow dictates how long a patient may remain asymptomatic following occlusion before ischaemia evolves (Liebeskind et al., 2014b).

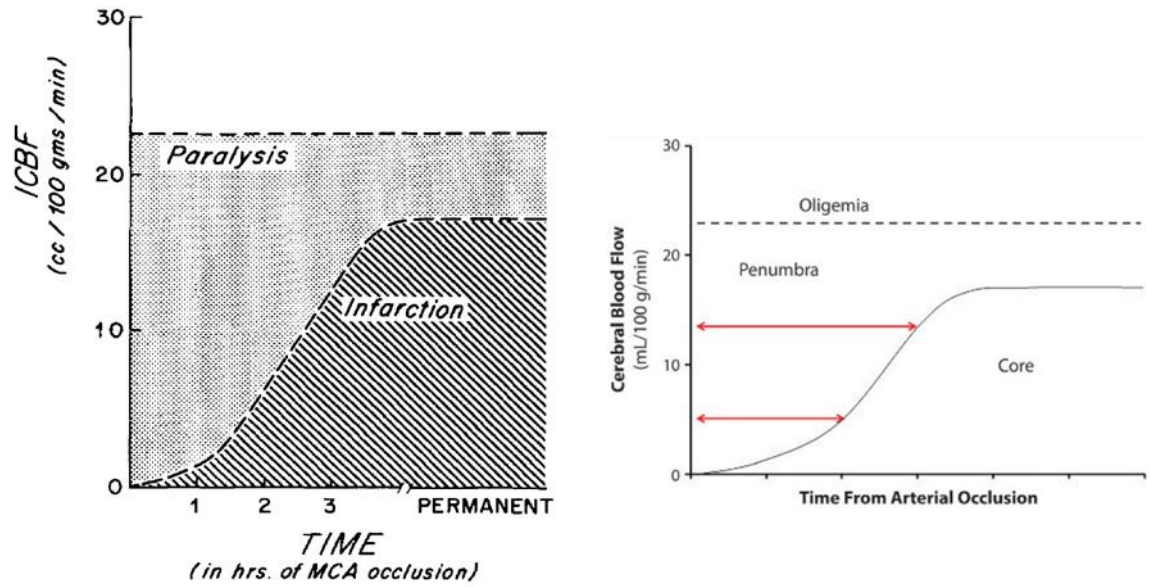

lCBF=local cerebral blood flow. MCA = middle cerebral artery. (Jones et al., 1981, Lin and Liebeskind, 2016)

Figure 1-3 Ischaemia Thresholds for Time versus Cerebral Blood flow

The Leptomeningeal Collateral Circulation

The existence of a primary collateral circulation to protect brain tissue against ischaemia due to obstructed arteries was observed by Astley Cooper, a surgeon who ligated the common carotid artery in a human patient and cerebral vessels in a dog (Cooper, 1836a, Cooper, 1836b). In this instance, the collateral flow refers to the primary communicating arteries of the Circle of Willis.

A secondary collateral circulation of leptomeningeal anastomoses [LMA] also play a role in sustaining perfusion to penumbral tissue. LMA are believed to be preexisting pial arteries with the ability to dilate in response to ischaemic stress (alongside small arteries and arterioles in autoregulation). They form a temporary collateral supply of blood flow (in which blood can flow in both directions) between cerebral arteries supplying different cortical territories (Meyer and Denny-Brown, 1957, Vander Ecken HM, 1953, Kono et al., 1990).

Both penumbra and LMCs represent a target for reperfusion therapy. Whilst we accept that the two terms are not interchangeable, in this thesis we examine both with the aim of assessing potentially salvageable tissue.

Anatomic Evidence of Leptomeningeal Collaterals

LMA were first identified as a form of compensation in 1875 but not accepted until the 1950s. Several pieces of work identified that the occlusion of the MCA near its origin results in the slowing of but not the cessation of blood flow in the MCA branches in monkeys and dogs (Heubner, 1875, Petersen, 1937, Meyer, 1958, Symon, 1960). Vander Eecken and Adams provided the first extensive anatomical account of LMA after injecting Schlesinger lead solution into 20 human cadaver brains, fixating the brains and dissecting them under a magnifying glass. They reported interhemispheric variability in size, number, location as well as variability between individuals (Vander Ecken HM, 1953).

Functional Importance of Leptomeningeal Collaterals

As an artery in which blood can flow in both directions, LMAs connect vascular territories and better LMAs associated with good clinical outcome and educed risk of developing ICH (both spontaneously and after thrombolysis) (von Kummer and Hacke, 1992, von Kummer et al., 1994, Bozzao et al., 1989).

LMA compensation is also evidenced in the absence of neurological disability following therapeutic anterior circulation occlusion for aneurysm treatment (Drake et al., 1994, Drake and Peerless, 1997, Lownie et al., 2000).

Historical Controversy Surrounding Collateral Circulation

Before reperfusion therapy (described later in this chapter) was established into routine practice, the existence of LMA was controversial. Some considered the ACA, MCA and PCA as terminal arteries with no further capacity to exchange blood flow (Sorteberg et al., 1989, Pansera, 1990). Others considered their compensatory blood flow abilities ‘marginal’ with poor response to ischaemic stress (Day, 1984, Müller and Schimrigk,

1996). LMA were deemed neither adaptable nor versatile, unlikely to develop in patients without pre-existing cerebrovascular disease and of little use (Hoksbergen et al., 1999).

Determinants of Collateral Status

Little is known about the biological determinants leading to variability in leptomeningeal collateral filling contributing to good or poor collateral status.

In mice, the extent of the pre-existing cerebral collateral circulation and remodelling following obstruction vary widely with genetic background which is significantly correlated with infarct volume (O'Donnell et al., 2010). Genetic factors are also thought to influence human collateral status (Wiegers et al., 2020).

In Moyamoya Disease [MMD] -a chronic condition leading to intracranial vessel narrowing and increased susceptibility to AIS, increased age but not RNF123 mutation, MMD type, clinical presentation, the outer diameter of the MCA, external carotid collateral status or cortical neovascularization is significantly associated with poor collateral status as measured by CTA (Chung et al., 2016).

As well as increased age, diabetes mellitus, hypertension, hyperlipidaemia, occlusion location, poor hydration status and presence of ICA stenosis were traditionally associated with poor collateral status (Wiegers et al., 2020). A post-hoc analysis of the MR CLEAN data demonstrated worse collateral status in patients with increased age, male status, higher admission glucose and ICA-T occlusion (Wiegers et al., 2020).

Age and occlusion site cannot be modified but risk factors such as hypertension, hyperlipidaemia and hydration status can be managed. Admission hyperglycaemia is also modifiable. The relationship between hyperglycaemia (independent to diabetes mellitus status) and poor collateral is explored in the following sub-section.

The Effect of Blood Glucose on Penumbra

Many AIS patients without DM present with post-stroke hyperglycaemia [PSH] (Gray et al., 1987). It has been suggested that PSH represents undiagnosed DM, impaired glucose tolerance or a stroke-related neurohumoral stress response (Oppenheimer et al., 1985, Gray et al., 1987, Murros et al., 1993).

A meta-analysis by Capes et al. (2001) suggests that hyperglycaemia in non-diabetic stroke patients increases the relative risk of death by 3.3 (95% CI, 2.3 to 4.6). Hyperglycaemia within 48 hours of onset predicts higher mortality and poorer functional outcome independent of age, stroke sub-type or severity and is therefore less likely to represent a stress response (Muir et al., 2011, Weir et al., 1997).

In animal models, high plasma glucose concentration is associated with increased infarct volume (Courten-Myers et al., 1988, Ginsberg et al., 1980, Nedergaard, 1987). The penumbra is particularly susceptible (Prado et al., 1988). The mechanism is unclear. In hyperglycaemic rats, post-reperfusion endothelial cell swelling decreases the capillary luminal diameter and may occlude flow (Paljärvi et al., 1983). Increased lactic acid production, tissue acidosis and cerebral oedema were also observed (Rehncrona et al., 1981, Chopp et al., 1987, Venables et al., 1985).

In spontaneously hypertensive stroke-prone [SHRP] rats, acute hyperglycaemia (at clinically relevant levels) exacerbates early ischaemic damage in both normal and metabolic syndrome rats (Tarr et al., 2013). This contributed to the belief that early glucose-lowering therapy may benefit stroke patients with evolving lesions. The detrimental effect of hyperglycaemia presented at 1 hour post-MCA occlusion and persisted for 3 hours (Tarr et al., 2013). This acceleration of early lesion growth on imaging is akin to the previously mentioned 'fast progressor' phenotype i.e. potentially poor collaterals with rapid core development.

In humans, PSH is associated with reduced salvage of mismatch tissue from infarction, greater final infarct volume and worse functional outcome (Parsons et al., 2002).

The Post Stroke Hyperglycaemia and Brain Arterial Patency Study [POSH] was a prospective study with the aim to investigate the relationship between PSH, infarct growth and brain arterial patency (MacDougall, 2013). In this dataset, 54.6% of patients developed PSH within 6 hours' onset and 29.6% within 48 hours - only 15.7% remained euglycaemic throughout. Patients were separated in to three categories: normoglycaemia, admission hypergylcaemia and late hyperglycaemia. Admission blood glucose (alongside admission NIHSS and systolic blood pressure) was significantly predictive of infarct growth. However, outcome infarct volumes in the normoglycaemia group were smaller (79.4ml versus 135.7ml and 92.4ml, p=0.273) but this difference did not reach statistical significance. There was also reduced penumbral salvage in this group - again not reaching statistical significance (MacDougall, 2013).

Achieving normoglycaemia during the acute phase does not improve outcome in AIS patients (Ntaios et al., 2011, Bruno et al., 2008, Johnston et al., 2009, Gray et al., 2007, Johnston et al., 2019). Insulin therapy is labour-intensive to monitor and hypoglycaemia is common (and clinically unsafe); PSH is currently not corrected (Reshi et al., 2017).

Given that the contribution of admission hyperglycaemia to poor collateral status, reduction in penumbral salvage and accelerated infarct expansion is clear, it is unclear why correction therapy does not improve outcome (Wiegers et al., 2020, MacDougall, 2013). Other approaches to blood glucose therapy may be worth exploring.

Imaging in Stroke

As mentioned, the concept of the penumbra was determined from the tip of a micro-electrode and based on this definition, non-invasive neuroimaging is not able to accurately measure volumes.

Traditionally the role of neuroimaging in stroke was to exclude other non-ischaemic aetiologies such as haemorrhage, space-occupying lesions such as neoplasms or infection. With recent advances, this role has evolved to aid diagnosis and eligibility for treatment and intervention (Kamalian and Lev, 2019).

Shetty and Lev (2005) summarised the aims of imaging in AIS to four questions:

1. Is there haemorrhage?
2. Is there an intravascular thrombus?
3. Is there a core of irreversibly infarcted brain tissue?
4. Is there a penumbra of severely ischemic but potentially salvageable tissue?

Non-Contrast Computed Tomography

CT scanning uses soft-tissue absorption values of X-ray transmissions taken at a multitude of angles to create a snapshot of the brain (Hounsfield, 1973). Non-contrast CT [NCCT] is the first-choice imaging assessment in the Emergency Department to answer question 1. It has a high sensitivity for excluding intracranial haemorrhage; acute blood appears hyperdense due to the protein fraction of haemoglobin which has a high-density mass (Wolverson et al., 1983). Increased density of intracranial vessels on NCCT is a marker of thrombus within the vessel (Gács et al., 1983).

Computed Tomography Angiography

CT angiography [CTA] involves injection of IV contrast followed by thin-section helical CT images ideally taken in the arterial phase to identify stenosis, occlusion and contrast-enhanced arteries beyond the occlusion as an estimate of collateral flow -which has been proven to correlate independently with clinical outcome (Knauth et al., 1997, Verro et al., 2002). It addresses the second question listed above. Contra-indications include allergy to contrast and severe renal failure.

Computed Tomography Perfusion Imaging

CT Perfusion [CTP] imaging offers an insight into CBF at tissue-level and aims to differentiate between and provide estimates of penumbra volume and ischaemic core volume. CTP addresses the final two questions necessary for AIS imaging. The viable penumbra is the target for reperfusion therapy. This imaging modality is used for screening patients eligible for reperfusion therapy, assessing ischaemia in cases of diagnostic uncertainty and clarifying large vessel occlusion [LVO] status if CTA is equivocal (Christensen and Lansberg, 2019).

At the time of acquisition, an IV iodine contrast bolus is administered and tracked through repeated brain scans. As contrast flows through brain tissue, the contrast is tracked over time. An attenuation curve depicting the increase, peak and decrease in contrast-intensity (measured in Hounsfield units) is calculated for each voxel. This is measured against an arterial input function [AIF] and a venous outflow function [VOF] which allows measurement of perfusion for each voxel as illustrated in Figure 1-4 (Wing and Markus, 2019). Post-processing software analysis is necessary to generate the following series of maps of haemodynamic compromise which are illustrated in Figure 1-5(Gobbel et al., 1991, Ostergaard et al., 1996):

- Cerebral blood volume [CBV] – the total volume of blood in a given volume of brain (ml/100g)
- Cerebral blood flow [CBF] – the volume of blood moving through a given volume of brain per unit time (ml/100g/minute)
- Mean transit time [MTT] – the average of the transit time of blood through a given brain region (seconds) (Konstas et al., 2009)
- Time to maximum [Tmax] – is the time for contrast to reach tissue in comparison to normal flow (i.e. Tmax>0s would indicate normal flow) (Calamante et al., 1999, Calamante et al., 2010)
- Time to peak [TTP] – time at which the largest signal drop occurs in gradient echo images signalling the most distinctive boundary between normal and abnormal perfusion (Beaulieu et al., 1999)

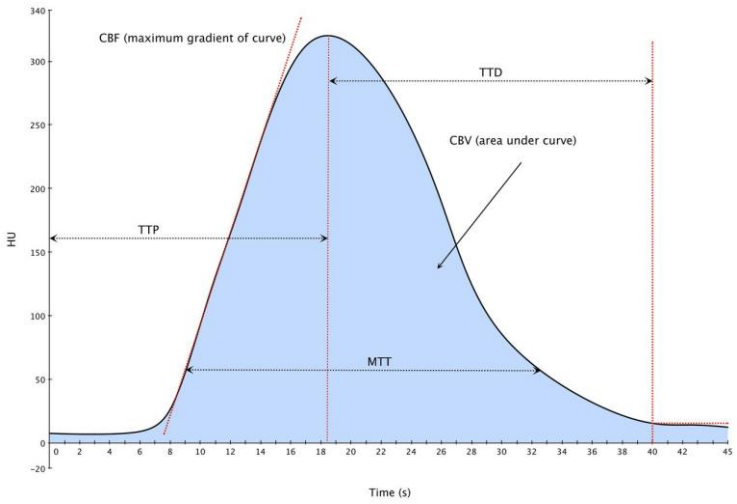

CBF=cerebral blood flow, TTP=time to peak, MTT=mean transit time, TTD=time to drain, CBV=cerebral blood volume. (Wing and Markus, 2019)

Figure 1-4 Attenuation-Time Curve for a Given Voxel

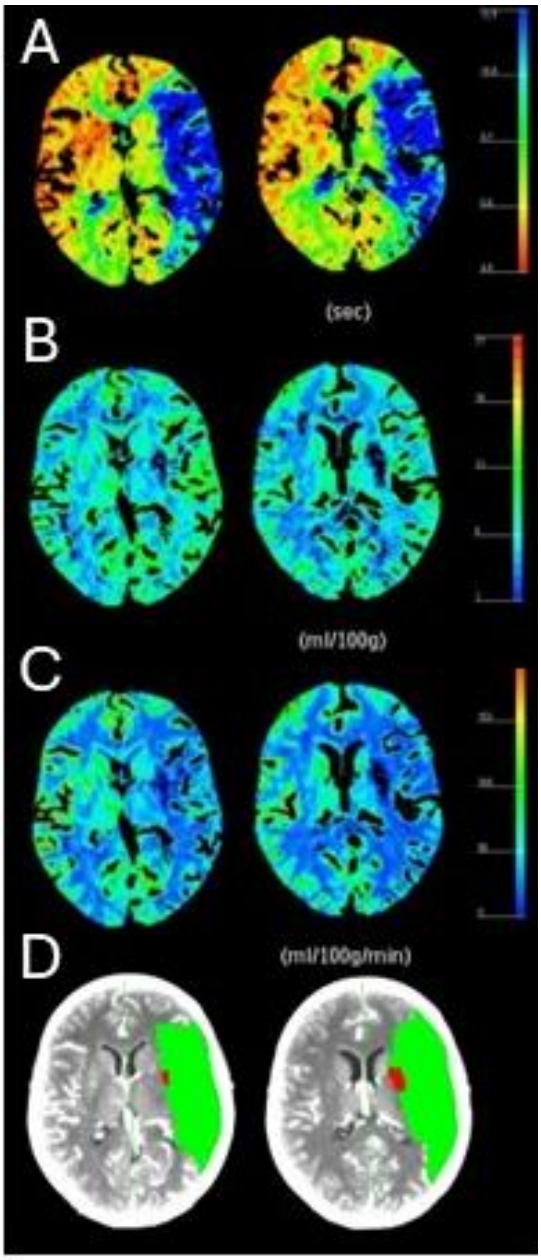

A. Mean transit time. B. Cerebral Blood Volume. C. Cerebral Blood Flow. D. Application of predictive thresholds by post-processing software depicting core and penumbra

Figure 1-5 CTP Output Depicting Left Hemisphere MCA Occlusion with Associated Tissue Delay.

Table 1-4 Haemodynamic Parameters in Cerebral Ischaemic Infarct provides an insight into how the maps are used to distinguish between core and penumbra tissue.

Table 1-4 Haemodynamic Parameters in Cerebral Ischaemic Infarct

	MTT/TTP/Tmax	CBV	CBF
Ischaemic penumbra	Mildly increased	Mildly increased or normal	Mildly decreased
Infarct core	Markedly increased	Mildly decreased	Markedly decreased

MTT = mean transit time; Tmax = time to maximum; TTP = time to peak, CBV=cerebral blood volume, CBF=cerebral blood flow (Lin and Liebeskind, 2016)

Order of Imaging

The order of acquisition in a CT stroke protocol i.e. CTP before CTA and vice versa, has no significant difference in quantitative CTP parameters (Dorn et al., 2012). Practically, scheduling the CTP after the CTA avoids venous contamination of the CTA from CTP contrast (Christensen and Lansberg, 2019).

Magnetic Resonance Imaging

Diffusion weighted imaging [DWI] can be used to identify early ischaemic change, cytotoxic oedema and the infarct core (Le Bihan et al., 1988) by measuring the molecular diffusion of water molecules through cells (Wesbey et al., 1984). Each water molecule is tagged and net movement over the time of observation results in signal loss -darkening of images. Regions of acute ischaemic injury accumulate intracellular water and have slower diffusion which manifests as signal hyperintensity. DWI is sensitive to acute ischaemic injury within minutes after AIS onset (Warach et al., 1992).

The apparent diffusion coefficient [ADC] map identifies acute ischaemia and can differentiate from oedema(Le Bihan et al., 1988). Acutely infarcted tissue has a lower ADC than non-infarcted tissue (Warach et al., 1992). Whilst ADC remains low when tissue is reperfused, improvement is quicker than in those who do not reperfused (An et al., 2011).

Perfusion weighted imaging [PWI] uses injected gadolinium chelates to assess CBV and CBF which indicate cerebral perfusion (Villringer et al., 1988). MMT or TTP maps are generated and like CTP the penumbra can be identified through the difference between the DWI defect and the PWI defect (Birenbaum et al., 2011).

Time of flight Magnetic resonance angiography [MRA] does not require contrast to assess blood flow and is also used to evaluate for LVO or stenosis (Nederkoorn et al., 2003).

Arterial spin labelling [ASL] also measures perfusion but is rarely used in AIS due to low signal-to-noise ratio, long acquisition times and difficulty in distinguishing CBF and transit times (Williams et al., 1992).

Digital Subtraction Angiography

Digital subtraction angiography [DSA] is the gold standard imaging modality for detection of cerebrovascular disease, occlusion and delayed filling of vessels. It is however invasive as it involves passing a catheter through a peripheral artery up into the brain (Birenbaum et al., 2011).

Artificial Intelligence

Artificial intelligence [AI] technology can help with various aspects of the AIS treatment paradigm. Techniques such as convolutional neural networks are evolving and there are several commercially available platforms providing automated information about various components of the AIS triage pathway. Following use in the EXTEND-IA and SWIFT PRIME trials, post-processing software have been integrated into routine clinical practice (Campbell et al., 2015, Saver et al., 2015). These software offer fast analyses which optimise the delivery of AIS care and impact treatment decision making and time to treatment.

The Regulatory Environment around Imaging Assessment Platforms

RAPID-AI (Ischemaview, Inc) is the only clinically validated software with an FDA indication to assist patient selection for reperfusion therapy (FDA, 2024).

In the UK, the framework for medical devices verses medical drugs is separate. The Medicines and Healthcare products Regulatory Agency [MHRA] is responsible for UK

medical devices. When used for a medical purpose, AI falls under the definition of a medical device; at the time of writing the MHRA is in the process of reforming regulation for medical devices with a view to incorporating AI (MHRA, 2024).

NICE provided a recent evidence overview of AI software highlighting key issues and questions which require answering – the main issues being both clinical and cost effectiveness (NICE, 2022). There is an ongoing Health and Innovation Oxford and Thames Valley study of e-Stroke which aims to compare the time periods before and after AI software was introduced. Of 107 stroke units in England, 99 are using AI technology (NICE, 2024).

Treatment of Acute Ischaemic Stroke

Immediate treatment of AIS aims to restore anterograde perfusion to salvage ischaemic brain through recanalisation. Without treatment, spontaneous recanalisation occurs in 24.1% although as previously discussed, timing of recanalisation is also a factor in preventing irreversible tissue damage (Rha and Saver, 2007).

Proven treatments for AIS include antiplatelet therapy, stroke unit care, hemicraniectomy for malignant middle cerebral artery infarction and reperfusion therapy in the form of IV thrombolysis and more recently endovascular thrombectomy [EVT].

The target of reperfusion therapy is the penumbra – salvageable tissue which can be identified using advanced imaging techniques and would likely infarct if the haemodynamic compromise persisted.

Intravenous Thrombolysis

Thrombolysis aims to restore perfusion by the administration of drugs which promote fibrinolysis.

Plasminogen Activator

It was first observed in 1933 that cultures of β-haemolytic Streptococci were capable of producing a substance which rapidly liquefies a human fibrin clot (Tillett and Garner, 1933). The active agent was termed "fibrinolysin" (Garner and Tillett, 1934). The subsequent thrombolytic drug (called Streptococcal fibrinolysin or Streptokinase) was first used to dissolve intrapleural fibrin clots in 1948 (Tillett and Sherry, 1949). In 1953, a purified preparation successfully dissolved artificially-induced intravascular clots in 23 out of 25 rabbits who received an intravenous infusion paving the way for lysis of intravascular thrombi (Johnson and Tillett, 1952).

Streptokinase interacts with plasminogen to form a complex which changes the plasminogen molecule by exposing the active catalytic site; the plasminogen within the complex is converted to plasmin. Both plasmin as well as plasminogen can form activator complexes with streptokinase (Reddy and Markus, 1972). Dissolution of thrombus results from endogenous lysis caused by the formation of plasmin by the activator complex from plasminogen (Alkjaersig et al., 1959).

Human extrinsic plasminogen activator [HEPA] was first used to treat humans in 1981. The successful lysis of a 6-week-old thrombus (as a 24-hour infusion of 7.5mg of HEPA – extracted from a human melanoma cell-line) in the renal and iliofemoral veins of a 30-year-old female renal-allograft recipient provided a new therapy for thromboembolic disease (Weimar et al., 1981).

The first generation of plasminogen activators [PA] comprised Streptokinase and Urokinase which activate both circulating and fibrin-bound plasminogen resulting in a systemic fibrinolytic state which raised concerns about bleeding risk; they were non-fibrin specific (Staniforth et al., 1983).

Streptokinase and Urokinase were initially authorised as treatments for the management of deep vein thrombosis [DVT] and pulmonary embolism [PE]. AIS and acute myocardial infarction [AMI] were not listed as eligible conditions to receive thrombolytic drugs due to fears about bleeding. However, the potential benefits to AIS and AMI were recognised;

further research into the use of thrombolysis for both of these pathologies was strongly encouraged at the National Institutes of Health [NIH] consensus development conference (1980).

The evidence from the 1950s was promising but the number of patients within these trials were too small to give a statistically reliable answer. The aim of the International Study of Infarct Survival [ISIS] trials in the 1980s was to use large data to demonstrate both safety and efficacy of the use of streptokinase and aspirin in AMI (Keating, 2015). The Gruppo Italiano per lo Studio della Sopravvivenza nell'Infarto miocardico acuto [GISSI] trial demonstrated that high-dose streptokinase dissolves thrombi and promotes recanalisation of coronary arteries following MI (GISSI, 1986). The results of ISIS-2 were compelling: streptokinase and aspirin, administered within 1 hour of onset reduced the risk of 5-week mortality by 20% and 23% respectively (ISIS-2, 1988).

The first major randomised controlled trial [RCT] to assess the efficacy of thrombolysis in AIS was the Multicentre Acute Stroke Trial–Italy [MAST-I] trial in 1995. Patients with AIS who were in 6 hours' onset were recruited. Owing to an indication of early harm, the trial was stopped early. There were 662 patients recruited of the planned 1500. There was no difference in mortality or morbidity at 6 months (MAST-I, 1995). This trial formed the basis for the idea of thrombolytics being either live-saving or life-threatening. The subsequent MAST-Europe [MAST-EU] which focused on moderate to severe MCA AIS was also stopped early due to concerns about mortality (Hommel et al., 1996). There was no success in thrombolysis with streptokinase, thrombolysis within 6 hours onset or thrombolysis in moderate to severe stroke.

Recombinant Tissue Plasminogen Activator

The second generation of thrombolytics include extrinsic (tissue-type) plasminogen activators [PA] specifically activate plasminogen associated with fibrin -localising the formation of the fibrinolytic enzyme (plasmin) to the environment of the thrombus; they are fibrin specific.

Alteplase (Activase; Genentech, Inc., South San Francisco, CA), is a recombinant form of the naturally occurring tissue plasminogen activator [tPA] produced by endothelial and other vascular cells. It is the first recombinant tissue plasminogen activator [rtPA] to be licensed for use in thrombolysis of acute ischaemic stroke [AIS] (2002, 1996). It converts fibrin-bound plasminogen to plasmin which in turn converts fibrin to fibrin degradation products (Hoylaerts et al., 1982, Zamarron et al., 1984).

The safety of intravenous [IV] rtPA for the treatment of AIS was examined in two open-label, dose escalation studies (Urgent Therapy for Stroke Parts I and II, n= 94). It was demonstrated that doses higher than 0.95mg/kg were significantly associated with symptomatic ICH but early treatment reduced this risk and with considerably better clinical improvement (Brott et al., 1992, Haley et al., 1992).

rtPA was approved for use in AIS in 1996 (within 3 hours of onset) on the basis of the National Institute of Neurological Disorders and Stroke (NINDS) rt-PA study (1995). In this study of two parts, 624 patients presenting with suspected AIS within 3 hours of onset were randomly assigned to treatment with 0.9mg/kg of intravenous rtPA (Alteplase) or placebo. Neurological improvement did not differ between the two groups at 24 hours but outcomes were significantly better in the treated group at 90 days (1995). The 2008 European Cooperative Acute Stroke Study III [ECASS III] demonstrated a benefit of intravenous alteplase beyond 3 hours, extending the window for treatment to 4.5 hours (Hacke et al., 2008).

The efficacy of alteplase is highly time dependant: early administration of rtPA after ischaemic stroke improves outcome (Lees et al., 2010). Alteplase has a short half-life which is estimated to be between 3.3 to 4.4 minutes (Tanswell et al., 1989, Tanswell et al., 1992). Maintaining plasma concentration when early recanalisation improves outcome involves a continuous infusion following bolus administration. The current recommendation is for the initial 10% of dose to be administered by intravenous injection over 1 minute with the remainder by intravenous infusion over 1 hour. Considering the short half-life of alteplase, bolus-infusion delays may result in a suboptimum concentration within the bloodstream which could adversely influence outcome.

None of the trials of Alteplase in AIS reported bolus-infusion delays. A single-centre retrospective analysis of patients (n=229, treated between 2008 to 2013) treated with Alteplase following AIS observed bolus-infusion delays of >8 minutes (~2 half lives) in 47% of patients which were not associated with significantly worse outcomes although functional independence rate was lower and the death rate was higher in this group (Acheampong et al., 2014). A smaller series (n=120) documented a median bolus-infusion delay of 15 minutes with no significant effect on clinical outcome or recanalisation (Huang, 2012). Both series may be too small to conclusively define the relationship between bolus-infusion delay and clinical outcome however they suggest bolus-infusion delay to be common in clinical practice.

A systematic review and meta-analysis revealed 46.3% of patients allocated rt-PA were alive and independent (mRS 0-2) after 3 months compared with 42.1% allocated control (Wardlaw et al., 2012). It is likely the treatment effect is even greater; this review included the IST-3 trial which was large and neutral because it excluded all of those where treatment was beneficial.

Advanced imaging has been used to extend the treatment window for thrombolysis. The WAKE-UP trial used DWI-FLAIR mismatch to identify patients who had woken up with symptoms for randomisation between IV rtPA and placebo. The trial demonstrated significantly better functional outcome in the rtPA arm (Thomalla et al., 2018). This opened reperfusion therapy to the wake-up population -around 14% of AIS patients (Mackey et al., 2011). These results were supported by the Statistical Analysis Plan for Extending the Time for Thrombolysis in Emergency Neurological Deficits [EXTEND] trial which identified patients to randomise presenting between 4.5 to 9 hours post onset using CT and MR perfusion and randomised between placebo or IV rtPA. The treatment group had better outcomes (Ma et al., 2019). Following the publication of these trials, the European Stroke Organisation [ESO] guidelines were updated and suggested an extended thrombolysis window up to 9 h or if presenting after waking up based on CTP or DWI-FLAIR (Berge et al., 2021, Bhalla A, 2023).

Other intravenously administered thrombolytic agents exist including reteplase, anistreplase, staphylokinase, desmoteplase and tenecteplase.

Tenecteplase

Tenecteplase [TNK] (a manufactured tPA variant) is the most promising alternative thrombolytic agent.

It has been bioengineered with improved properties compared with alteplase (Keyt et al., 1994). These include 14-fold higher fibrin specificity, 80-fold higher resistance to the physiological plasminogen activator inhibitor 1 [PAI-1] and a 4-fold slower plasma clearance allowing single bolus administration (Keyt et al., 1994, Modi et al., 2000).

Multiple trials presented at both the World Stroke Congress [WSC] 2023 and the European Stroke Organisation Conference [ESOC] 2024 demonstrated that TNK is an effective and probably preferred alternative to Alteplase. The Alteplase-Tenecteplase Trial for Evaluation of Stroke Thrombolysis [ATTEST2] was presented at the WSC and demonstrated non-inferiority of TNK in comparison with alteplase in suitable AIS patients within 4.5 hours onset (Muir, 2023). Both the Tenecteplase versus Alteplase for Stroke Thrombolysis Evaluation [TASTE] and the Study in Chinese Patients to Compare How Tenecteplase and Alteplase Given After a Stroke Improve Recovering of Physical Activity [ORIGINAL] trials were presented at ESOC and provided additional evidence for treatment within 4.5 hours onset (Parsons, 2024, Li, 2024). The Tenecteplase Reperfusion Therapy in Acute Ischaemic Cerebrovascular Events-III [TRACE III] trial indicated that TNK may improve outcome beyond 4.5 hours in patients without EVT access (Xiong, 2024). A meta-analysis of 9 randomised-controlled trials [RCTs] assessing TNK within 4.5 hours of onset was also presented at ESOC and demonstrated higher likelihood of excellent functional outcome and reduced disability in the TNK arm with a number needed to treat [NNT] of 34 (Palaiodimou, 2024). This meta-analysis is promising but requires updating with the above trials once published.

Intra-arterial Fibrinolysis

Intra-arterial fibrinolytic therapy was explored with initially promising results. The small, phase 3 intra-arterial prourokinase for acute ischaemic stroke [PROACT] II trial demonstrated significantly improved clinical outcome in patients with endovascular delivery of thrombolysis to MCA occlusion but there was also increased sICH (Furlan et

al., 1999).There was no confirmatory larger trial. Subsequent meta-analysis of three small trials (including PROACT II) demonstrated increased odds of good outcome (OR 0.58, 95% CI 0.36 to 0.93, p=0.91) but this estimate was imprecise and non-significant.

Endovascular Mechanical Thrombectomy for Large Vessel Occlusion

Patients with proximal LVO benefit significantly less from IV rTPA with lower rates of recanalisation and worse outcome (Bhatia et al., 2010). Other limitations of IV rTPA are ineligibility, availability of serum plasminogen, the resistance to fibrinolysis (i.e. longer thrombi) and the risks of both cerebral and systemic haemorrhage (IST, MAST-I, Riedel et al., 2011). Endovascular mechanical thrombectomy [EVT] uses a mechanical embolectomy device to restore patency of occluded intracranial vessels (Smith et al., 2005).

The Mechanical Embolus Removal in Cerebral Ischaemia [MERCI] trial was the first to report data on the safety and efficacy of EVT in AIS. MERCI used the Merci corkscrew device -approved for use despite not having been validated in RCTs and was associated with SAH (Smith et al., 2005). The development of stent retrievers (2013) improved clot removal and led to their being approved by the American Food and Drug Administration [FDA] for use in eight subsequent randomised clinical trials MR CLEAN, EXTEND-IA, ESCAPE, SWIFT PRIME, REVASCAT, THRACE, THERAPY and PISTE (Berkhemer et al., 2014, Campbell et al., 2015, Goyal et al., 2015, Saver et al., 2015, Jovin et al., 2015, Bracard et al., 2016, Mocco et al., 2016, Muir et al., 2017). A meta-analysis of data from the five trials published in 2014-2015 (n=1287) demonstrated significantly reduced disability at 90 days (OR 2.49, 95% CI 1.76 to 3.53, p<0.0001) with a number needed to treat [NNT] of 2.6 (Goyal et al., 2016). Subsequent trials were stopped early but demonstrated that EVT was non-inferior to the control group.

HERMES: A Messenger for Stroke Interventional Treatment

The Highly Effective Reperfusion Evaluated in Multiple Endovascular Stroke Trials [HERMES] collaboration formed a unique dataset to meta-analyse data from 7 major trials: the MR CLEAN, ESCAPE, EXTEND-IA, SWIFT PRIME, REVASCAT, PISTE and THRACE trials (Berkhemer et al., 2014, Campbell et al., 2015, Goyal et al., 2015, Saver et

al., 2015, Jovin et al., 2015, Bracard et al., 2016, Muir et al., 2017). Data from the 7 landmark RCTs allowed better estimation of overall treatment effects and further post-hoc analyses of collateral circulation (Muir and White, 2016).

Late-Window Endovascular Thrombectomy

In 2017-2018, two trials demonstrated EVT in the 6 to 24 hour patient group, expanding the window of treatment. These were the DWI or CTP Assessment with Clinical Mismatch in the Triage of Wake Up and Late Presenting Strokes Undergoing Neurointervention with Trevo [DAWN] and Diffusion and Perfusion Imaging Evaluation for Understanding Stroke Evolution [DEFUSE] 3 trials (Nogueira et al., 2017, Albers et al., 2018). Both trials used perfusion imaging (DAWN – clinical -core mismatch on DWI or CTP at 6-24 hours and DEFUSE-3 – CTP or MR mismatch at 6-16 hours) to select patients. The criteria were narrow and have been critiqued as "over-selecting" patients, excluding a large proportion of AIS patients (Albers et al., 2018). Treatment effects were large and subsequent trials with less rigorous selection criteria, notably MR CLEAN late still showed significant benefit (Olthuis et al., 2023b).

Large-Core Endovascular Thrombectomy

More recently, trials have sought to assess the treatment effect of EVT in large core patients. RESCUE-Japan LIMIT and TENSION demonstrated better functional outcome with EVT in patients with LVO and ASPECTS 3-5 within 24 and 12 hours' onset respectively (Yoshimura et al., 2022, Bendszus et al., 2023). Both SELECT2 and ANGEL-ASPECT also demonstrated better functional outcome within 24 hours' onset and introduced additional optional inclusion criteria of core volumes of >50ml and between 70 to 100ml respectively (Sarraj et al., 2023, Huo et al., 2023). The trials recruiting up to 24 hours' onset demonstrated a significantly higher haemorrhagic transformation rate or vascular complications in the EVT arm (Yoshimura et al., 2022, Sarraj et al., 2023, Huo et al., 2023). The median core volumes for the EVT arms of SELECT2 and ANGEL-ASPECT were 74ml (IQR 50 to 111.5ml) and 60.5ml (IQR 29 to 86ml) respectively, which are relatively conservative for large core trials (Sarraj et al., 2023, Huo et al., 2023).

Large Vessel Occlusion

Definitions of anterior circulation LVO varied across the trials. All included occlusion of the ICA and M1 (SWIFT PRIME, REVASCAT, DAWN, DEFUSE-3) and some included M2 (MR CLEAN, EXTEND-IA, PISTE, ESCAPE). ESCAPE included multiple branch M2 occlusion (Goyal et al., 2015). Our analyses in Chapters 5, 6 and 7 also explored definitions of intracranial vessel occlusion.

Target Mismatch

WAKE UP and EXTEND SWIFT PRIME, EXTEND-IA, DAWN, DEFUSE-3 used perfusion imaging to select patients for EVT (Saver et al., 2015, Campbell et al., 2015, Nogueira et al., 2017, Albers et al., 2018, Thomalla et al., 2018, Ma et al., 2019).

The target mismatch profiles most commonly adopted for clinical use are based on the inclusion criteria used by DEFUSE 3 and EXTEND (Albers et al., 2018, Ma et al., 2019). DEFUSE 3 trial included patients with ICA or MCA-M1 occlusions and a favourable target mismatch profile, defined as ischaemic core lesion<70ml, a ratio of total volume of ischaemic lesion to ischaemic core (Tmax>6s over CBF<30%) of $\geq$1.8 and a penumbra lesion $\geq$15ml (Albers et al., 2018). The EXTEND trial defined target mismatch as ischaemic core lesion<70ml, a ratio of volume of ischaemic lesion to ischaemic core (Tmax>6s over CBF<30%) of >1.2 and an absolute difference in volume >10ml (difference between perfusion lesion and core lesion).(Ma et al., 2019) The mismatch ratio 1.2 was first used in EPITHET (a rtPA trial using mismatch to select patients between 3 to 6 hours) and again in EXTEND (Davis et al., 2008, Ma et al., 2019). Both mismatch approaches are analysed in Chapter 5.

The Hypoperfusion Intensity Ratio

The hypoperfusion intensity ratio [HIR] was devised by the DEFUSE investigators to describe the proportion of hypoperfused tissue with severely delayed contrast arrival, providing an index of collateral flow. HIR is defined as Tmax>6s/Tmax10s (Olivot et al., 2014). The Tmax >6s and Tmax >10s values were taken from the DEFUSE and DEFUSE-2 studies (Olivot et al., 2009, Lansberg et al., 2012). Tmax >6s provides the most accurate assessment of penumbra volume compared with Tmax >2s, Tmax >4s, Tmax 8s and

Tmax >10s. Penumbra salvage volume only defined by a Tmax >6 second delay was significantly increased in patients with favourable outcomes, patients who experienced reperfusion and among mismatch patients (Olivot et al., 2009). Tmax >6s lesions encompass regions of variable delay – including severe hypoperfusion associated with irreversible necrosis regardless of reperfusion and tissue with delays of >8s and >10s (Calamante et al., 2010, Olivot et al., 2014, Guadagno et al., 2008). Tmax >10s was associated with poor outcome following reperfusion in the DEFUSE and the Echoplanar Imaging Thrombolytic Evaluation Trial (EPITHET) meta-analysis (Mlynash et al., 2011).

Higher HIR reflects poorer collateral flow and has been associated with faster infarct growth and poor clinical outcome.(Olivot et al., 2014, Guenego et al., 2018)

Antiplatelet Therapy

Antiplatelet therapy is a key component of AIS and TIA regardless of eligibility for reperfusion therapy.

Aspirin

Originally derived from willow bark which was used as an analgaesic during the time of Hippocrates, acetylsalicylic acid [ASA] or aspirin was introduced in the 1890s (Stone, 1763, Dresser, 1899). Vane (1971) demonstrated that aspirin inhibits the activity of cyclo-oxygenase [COX], an enzyme whose action generates prostaglandin formation causing inflammation, pain and fever.

The International Stroke Trial [IST] and the Chinese Acute Stroke Trial [CAST] tested the effects of Aspirin (at 300mg and 160mg doses respectively) in AIS (IST, 1997, Chen, 1997). A combined analysis of 40,000 patients demonstrated significant reductions in recurrence of stroke and mortality (Chen et al., 2000).

Dual-Antiplatelet Therapy

The trials of dual-antiplatelet therapy [DAPT] have superseded Aspirin in the acute treatment of minor stroke or TIA. The superiority of the combination of clopidogrel and aspirin versus aspirin alone was first demonstrated in a Chinese population and further tested at international level (Wang et al., 2013, Johnston et al., 2018). DAPT during the first twenty-one days post AIS reduces the risk of recurrent major ischaemic events (Prasad et al., 2018).

The Role of Thrombolysis in Minor Stroke

The Tenecteplase Versus Standard of Care for Minor Ischaemic Stroke with Proven Occlusion [TEMPO-2] trial was the first phase 3 study to examine the efficacy of thrombolysis with tenecteplase in minor AIS with proven intracranial occlusion within 12 hours onset. There was no benefit and possibly increased risk of harm from tenecteplase treatment (Coutts et al., 2024).

The Role of Statins in Acute Ischaemic Stroke

Statins lower serum cholesterol by inhibiting hydroxymethylglutaryl-coenzymeA [HMG-CoA] reductase (Endo et al., 1976). In addition, they improve endothelial function, inhibit thrombus formation, attenuate inflammatory and oxidative stress damage and facilitate angiogenesis (Anderson et al., 1995, Obi et al., 2009, Rasmussen et al., 2001, Wagner et al., 2000).

Immediate statin initiation following AIS is associated with both improved functional outcome and reduced incidence of early seizure (Matsubara et al., 2020, Gao et al., 2024).

Hyper-Acute Stroke Unit Care

Randomised controlled trials and subsequent meta-analyses have shown that regardless of risk factor, stroke category or even stroke severity, patients who receive care in a multidisciplinary stroke unit have reduced morbidity and mortality rates and are less likely to be institutionalised (SUTC, 2013).

The hyper-acute stroke unit [HASU] provides immediate care for stroke patients including assessment, treatment and primary intervention before discharge or step-down to downstream wards, typically within 48 hours (Fulop et al., 2013).

This model coincided enabled the centralisation of stroke care (in the UK this initially took place first in both London and Manchester in 2008) which demonstrated increased thrombolysis rates, reduced mortality, reduced length of stay and overall a reduction in cost to the NHS (Morris et al., 2014).

Secondary Prevention

The aim of secondary prevention is to reduce the risk of AIS recurrence which is highest within the first few days following the index event with a second phase of lower recurrence rate over the subsequent months (Bulwa et al., 2021).

Management strategies target aetiology and include the use of antiplatelet or anti-coagulant therapy, risk factor modification (i.e. hypertension management, diabetes mellitus management, hypercholesterolaemia management, smoking cessation, reduction of alcohol consumption), left atrial appendage occlusion, patent foramen ovale closure, carotid surgery and carotid artery stenting (Jensen and Thomalla, 2020).

The Scottish Clinical Context

During the study period there was a lack of access to mechanical thrombectomy in Scotland.

A pilot thrombectomy programme began in the North of Scotland at NHS Tayside on 9th November 2020. In 2023, the Queen Elixabeth University Hospital (NHS Greater Glasgow and Clyde) and NHS Lothian started ‘hub’ thrombectomy services for the West and East of Scotland respectively.

The clinical context is relevant because the thrombectomy should be available as routine treatment. In England, as of 2023, 3.3% of patients receive thrombectomy and treatment rates vary between London and regions such as the East or North East (SSNAP, 2023). Availability remains an issue.

We understand the need for data to contribute to service planning as described below in the thesis aims.

Rational for Focus on CT imaging

We focused entirely on CTP as opposed to MR imaging – which can also provide estimates of penumbral tissue.

In practice CTP is more widely available and easier to implement in routine stroke care. CTP can be performed in a few minutes on modern CT scanners.

CTP provides an assessment of blood flow throughout brain tissue as opposed to CTA which provides an assessment of blood flow throughout intracranial blood vessels. The aim of reperfusion therapy is to save brain tissue therefore we believe that cerebral perfusion provides a more detailed understanding. However, we accept that many acute stroke centres favour CTA over CTP at the front door and have compared the two modalities in Chapter 6. We hope to demonstrate that there need not be a choice and CTP can offer different and equally valuable information.

Out of the HASUs across the UK, only a few have access to MR imaging 24 hours per day but CT remains the first-line brain imaging modality. In France, MR as first-line brain imaging is more common (Leys et al., 2022). Our research is aimed at the population who will be treated on the NHS.

Thesis Aims

This thesis investigated the penumbra and its relevance within a changing clinical environment -specifically reperfusion treatment availability and eligibility.

We addressed this with the following aims:

1. To describe the proportion of patients with prolonged penumbral survival within the first 24 hours after onset of symptoms.
2. To investigate biological mechanisms underlying failure to recruit leptomeningeal collaterals with a focus on hyperglycaemia.
3. To assess observational data regarding the effect of hyperglycaemia on collateral circulation in a systematic review and meta-analysis.
4. To validate current thresholds for prediction of tissue fate in later presentations
5. To compare how current software estimates tissue viability

Chapter 2 Hyperglycaemia and Collateral Status in Acute Stroke: A Systematic Review and Meta-Analysis

One of our aims to determine the effect of hyperglycaemia on collateral circulation. We present a systematic review and meta-analysis (first performed in 2018 and updated in 2023) to analyse the current evidence.

Introduction

We previously described the modifiable determinants of collateral status: hypertension, hyperlipidaemia and hydration status. A link exists between admission hyperglycaemia and collateral status which is independent to diabetes mellitus status which is more evident in animals than humans (Tarr et al., 2013). Whilst many studies have reported data on hyperglycaemia and collateral status in humans, few have found a significant association.

Hyperglycaemia within 48 hours of onset is associated with higher mortality and poorer functional outcome independent of age, stroke sub-type or severity and is therefore less likely to represent a stress response (Muir et al., 2011, Weir et al., 1997). In animal models, high plasma glucose concentration is associated with increased infarct volume (Nedergaard, 1987).

Whilst many studies have reported data on hyperglycaemia and collateral status, few have found a significant association. This was explored in greater detail in Chapter 1. A series of rodent experiments demonstrated more rapid infarct expansion and smaller core in SHRP rats. The behaviour on imaging is akin to the “fast progressor” phenotype, with poor collaterals and rapid core development (Tarr et al., 2013). The POSH study showed reduced penumbral salvage and greater infarct expansion in humans with hyperglycaemia further providing the experimental underpinning for the link (MacDougall, 2013).

As EVT expands – not just by increase of numbers but also by time window expansion, more data is becoming available with specific emphasis on collateral circulation and modifiable determinants. Further understanding of the effect of admission hyperglycaemia

on collateral circulation may guide future clinical trial design for front-door treatment which in turn may lead to improved patient outcome.

We performed a systematic review and meta-analysis to assess the relationship between hyperglycaemia and collateral status.

Methods

This review was conducted in adherence with the Preferred Reporting Items for Systematic Reviews and Meta-Analyses [PRISMA] guidelines (Moher et al., 2009).

Search Strategy

We developed a search strategy and registered it with the PROSPERO database (reference CRD42019116876, see Appendix A). We adapted the search strategy to the focus of our review: limiting to studies of humans only. We included studies published in peer-reviewed journals that included patients who had AIS and reported data on collateral circulation and admission glycaemic status. We accepted any clinical diagnostic assessment of collateral circulation provided it was based on neuroimaging. No restrictions were placed on country or year of publication but for practicality we limited the language to English. Conference abstracts were excluded on the basis of the restricted word count yielding limited data. Case reports were also excluded as they would not give representative population data. Review articles were excluded but their references were assessed.

Three databases -MEDLINE, EMBASE (through the Ovid portal) and Cochrane, were searched using separate strategies from inception until 26/10/2018 using the search strategies detailed in Appendix B. Our search syntax used a combination of exploded medical subject headings “stroke”, “collateral circulation” or “cerebral blood flow” and “blood glucose”, “hypoglycaemia” or “hyperglycaemia”. To identify further studies, we assessed the reference lists of the included papers. If relevant abstracts were identified but the papers were not available, we contacted the author to request access. However, where

relevant data were not available in the published manuscript, we excluded the paper and did not contact the author for practicality reasons.

There were three reviewers: VB (author), AM (Clinical Research Fellow, University of Glasgow) and SN (Clinical Research Fellow, University of Glasgow). VB performed the search of three databases: VB and AM identified additional papers from reference lists of the papers included (including from review articles).

An updated search was conducted for publications between 2018 and 18/09/2023 with the same strategy. Additionally, we searched for papers who had referenced the included papers since the original search date.

VB and AM reviewed titles and abstracts separately, before reviewing full papers (separately) and selected those meeting the inclusion and exclusion criteria stipulated below. SN resolved disagreements.

Manuscript Inclusion Criteria

1) English language (due to the cost and lack of resources to translate foreign language articles)
2) Acute ischaemic stroke in adults
3) Randomised controlled trials, cohort-studies, cross-sectional studies
4) Papers which reported the effect of blood glucose levels on human collateral circulation status (if not directly mentioned then any perfusion imaging, scoring of blood vessel appearance or mention of the hypoperfusion intensity ratio or penumbra)
5) Neuroimaging including CT, multiphasic CT, CT angiography, CT perfusion, MRI, MR perfusion, ASL MRI, DSA, SPECT, PET

Manuscript Exclusion Criteria

1) Case reports or case series

2) Any papers measuring infarct size without measurement of collateral status or penumbra
3) Review articles – references were followed
4) Conference abstracts

Data Extraction

We extracted data from eligible papers using a proforma based on the Cochrane data extraction tool (Higgins JPT, 2023). VB and AM performed the data extraction (VB performed the data extraction for the updated search). We collected data on the effect of hyperglycaemia on collateral status or penumbra and glycaemic status in patients with good/moderate collateral status versus poor collateral status.

Analysis

The primary outcome for the analysis was the effect of glycaemic status on collateral status.

A secondary analysis compared the mean blood glucose in favourable and unfavourable collateral status. Some studies only reported mean glucose without the individual data. We calculated the mean of means for blood glucose in favourable and unfavourable collateral subgroups, and the standard deviation using the following formula: $\sqrt{(\text{mean}(sd^2))}$.

Quality Analysis

We used the Critical Appraisal Skills Programme [CASP] checklist to assess the quality of the studies (CASP, 2018). Reviewers VB and AM performed the checklist separately with issues resolved by the third assessor, SN.

Assessment of Bias

Publication bias was assessed visually using a funnel plot alongside Egger's weighted regression and Begg's rank correlation test. Statistically significant publication bias was defined by $p<0.05$ (Egger et al., 1997).

Meta-analysis

We performed a meta-analysis to examine the relationship between hyperglycaemia and the quality of collateral status.

We extracted data from studies with clearly defined groups of collateral blood flow. We defined favourable collateral flow as ‘good collateral flow’ or ‘medium/partial collateral flow’ and unfavourable flow as ‘poor collateral flow’ or ‘collaterals not present’.

Stats Direct version 4.0.4 was used to generate a Der Simonian-Laird random effects model. This method of meta-analysis summarises an effect across several studies. This model was designed to evaluate the efficacy of a variable on a specified medical condition whilst addressing heterogeneity and expressed the difference between groups through an odds ratio with 95% confidence intervals (DerSimonian and Laird, 1986).

Sensitivity Analysis

We aimed to remove studies considered as outliers to examine the overall effect on the pooled data. We defined outliers as studies whose 95% CI did not overlap with the 95% CI of the pooled effect (Viechtbauer and Cheung, 2010). Sensitivity analyses where dominant datasets were removed were run.

Results

Search Results

Figure 2-1 summarises the combined screening of papers (both 2018 and the 2023 update).

We identified twenty-four papers (ranging from 1994 to 2023) which provided information on the effect of glucose or hyperglycaemia on collateral status as determined by neuroimaging. These have been described in Table 2-2. Of these, seven provided data for meta-analysis.

Table 2-1 demonstrates our data-extraction tool and Table 2-2 summarises the data extraction. Clinical details are recorded in Table 2-3. Many studies did not report clinical details or risk factors. The available data shows that the populations of the studies are widely different. The ages are similar but there are wide variations in sex, vascular risk factors and reperfusion therapy rate. There are wide variations in patients receiving EVT (not least because the earliest study is in 1994 when this was not available). Genceviciute et al. (2022a) (the largest study with n=1020) was a sub-analysis of the MR CLEAN data and 100% of the patients received EVT. Whilst we know what proportion of the available data received EVT, it is difficult to know what proportion were eligible, especially as the admission NIHSS throughout tends to be on the higher side, especially when compared with the SSNAP data.

We excluded one paper following assessment using the CASP Cohort Study Checklist (Table 2-1). We found data extraction from Gong et al. (2021) difficult due to lack of clarity surrounding patient recruitment, collateral scoring and data presentation.

Table 2-2 summarises data extraction with papers separated by imaging modalities. There were eighteen (75%) cohort studies and six (25%) analyses of randomised-controlled trials – two of which reported analyses of the SWIFT-PRIME trial: one CTA analysis and one CTP analysis. Neither was included in the meta-analysis and only one was included in the mean analysis.

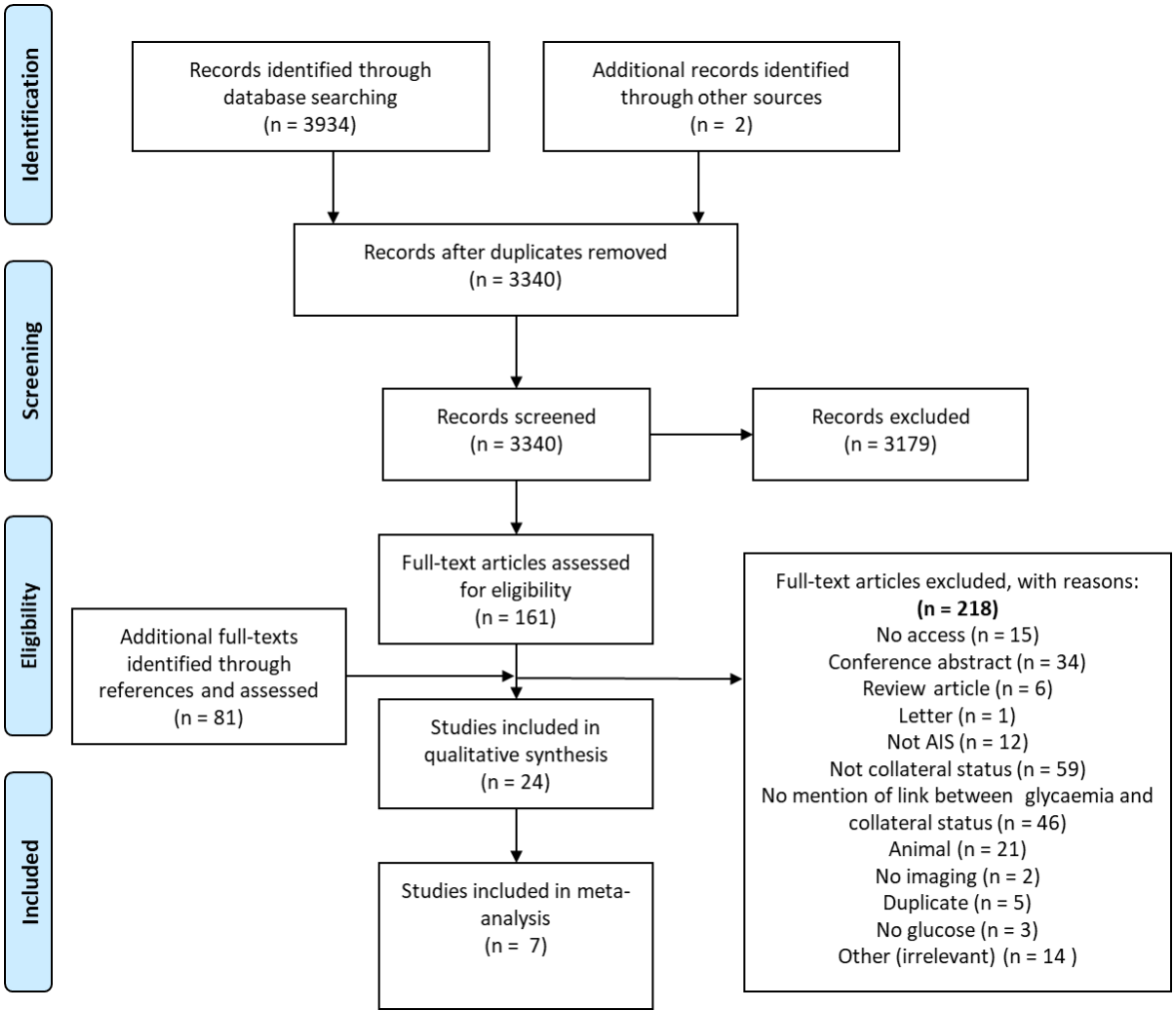

Figure 2-1PRISMA Search Flow.

Quality Analysis

Table 2-1 uses the CASP checklist to demonstrate that addressing bias, identifying confounding factors, follow up and implications for practice were the main issues identified (CASP, 2018). As mentioned, we excluded one study following the validity assessment: Gong et al. (2021).

Table 2-1 Systematic Review Quality Assessment: Critical Appraisal Skills Program (CASP) checklist

Paper	1	2	3	4	5a	5b	6a	6b	7	8	9	10	11	12
Toni et al. (1994)	Y	Y	Y	Y	N	N	C	N	Y	Y	C	N	C	C
Parsons et al. (2002)	Y	Y	Y	Y	Y	C	C	C	Y	Y	Y	Y	Y	Y
Moreton et al. (2007)	Y	Y	Y	Y	Y	Y	C	C	Y	Y	Y	Y	C	C
Ribo et al. (2007)	Y	Y	Y	C	C	C	N	N	Y	Y	Y	Y	Y	C
Rosso et al. (2011)	Y	Y	Y	Y	Y	C	C	C	Y	C	C	C	Y	C
Shimoyama et al. (2013)	Y	Y	Y	Y	Y	N	C	C	Y	Y	Y	C	C	C
Menon et al. (2013)	Y	Y	Y	Y	C	C	Y	Y	Y	Y	Y	Y	Y	C
Luitse et al. (2013)	Y	Y	Y	Y	Y	N	N	N	Y	Y	Y	C	Y	C
Liebeskind et al. (2014a)	Y	Y	Y	Y	Y	N	Y	Y	Y	Y	Y	C	Y	C
van Seeters et al. (2016)	Y	Y	Y	Y	Y	Y	Y	Y	Y	Y	Y	C	Y	C
Mi et al. (2017)	Y	C	C	Y	C	C	N	N	Y	C	C	C	Y	Y
Borggrefe (2018)	Y	Y	Y	Y	Y	Y	Y	Y	Y	Y	Y	Y	Y	Y
Kim et al. (2018)	Y	Y	Y	Y	Y	N	Y	Y	Y	C	C	Y	C	C
Wang et al. (2018)	Y	Y	Y	Y	Y	Y	Y	Y	Y	Y	Y	C	C	C
Broocks et al. (2020)	Y	Y	Y	Y	Y	Y	Y	Y	Y	Y	Y	Y	Y	Y
Gür-Özmen et al. (2019)	Y	Y	Y	Y	C	C	Y	Y	Y	Y	Y	Y	Y	Y
Wiegers et al. (2020)	Y	Y	Y	Y	Y	Y	Y	Y	Y	Y	Y	Y	Y	Y
Gong et al. (2021)*	Y	N												
Scheidecker et al. (2022)	Y	Y	Y	Y	Y	Y	Y	Y	Y	Y	Y	Y	Y	Y
Arteaga et al. (2022)	Y	Y	Y	Y	Y	Y	Y	Y	Y	Y	Y	Y	Y	Y
Genceviciute et al. (2022a)	Y	Y	Y	Y	Y	C	Y	Y	Y	Y	Y	Y	Y	Y
Liebeskind et al. (2022)	Y	Y	Y	Y	Y	Y	Y	Y	Y	Y	Y	Y	Y	Y
Kersten et al. (2022)	Y	Y	Y	Y	Y	Y	Y	Y	Y	Y	Y	Y	Y	Y
Mannismäki et al. (2023)	Y	Y	Y	Y	Y	Y	Y	Y	Y	Y	Y	Y	Y	Y

*Excluded following assessment of validity
1 = Did the study address a clearly formed issue?
2 = Was the cohort recruited in an acceptable way?
3 = Was the exposure accurately measured to minimise bias?
4 = Was the outcome accurately measured to minimise bias?
5a = Have the authors identified all important confounding factors?
5b = Have they taken account of the confounding factors in the design and/or analysis?
6a = Was the follow up of subjects complete enough?
6b = Was the follow up of subjects long enough?
7 = What are the results of this study?
8 = How precise are the results?
9 = Do you believe the results?
10 = Can the results be applied to the local population?
11 = Do the results of this study fit with other available evidence?
12 = What are the implications of this study for practice?

Descriptive analysis

There were sixteen studies which were not used in the meta-analysis that provided descriptions of the link between collateral status and glucose.

There were five studies which reported no significant association. Two were CTP studies: Moreton et al. (2007) focused on insular cortex hypoperfusion whereas Luitse et al. (2013) compared perfusion deficit across hyperglycaemia and normoglycaemia subgroups. Of the CTA studies, van Seeters et al. (2016) suggested higher admission blood glucose [ABG] was related to poor collateral flow, Broocks et al. (2020) suggested patients with normoglycaemia exhibited better collateral flow and Arteaga et al. (2022) focused on intensive blood glucose control and with no finding of a connection to collateral flow.

Of the eight studies which reported a significant association, six used CTA to demonstrate a relationship between either high ABG and poor collateral flow (Menon et al., 2013, Liebeskind et al., 2014a, Mi et al., 2017, Wiegers et al., 2020, Scheidecker et al., 2022) or low ABG and good collateral flow (Liebeskind et al., 2022). There were two studies which used CTP to link hyperglycaemia to baseline perfusion deficit -specifically ischaemic core volume and core-penumbra ratio (Kersten et al., 2022) and total hypoperfusion lesion in a non-diabetic subgroup (Mannismäki et al., 2023).

Outcome was used by three studies to postulate a connection between hyperglycaemia and collateral circulation. Ribo et al. (2007) found significant reduction in salvage of mismatch tissue and Rosso et al. (2011) found that normoglycaemia was significantly associated with reduction of transformation of penumbra to infarct. Wang et al. (2018) found significantly reduced day 90 mRS in patients with good collaterals at baseline but higher fasting plasma glucose [FPG].

Table 2-2 Table of Studies Fulfilling Inclusion Criteria

Lead Author	Study type	Total (N)	Time window	Glucose Assessment	Hyperglycaemia definition	Collateral assessment	Collateral assessment tool	Definition of favourable collaterals
Angiography Studies								
Toni et al. (1994)	Cohort	73	<4 hours	Admission	≥6.6mmol/L	DSA	Present: yes/no	Present
Shimoyama et al. (2013)	Cohort	93	<24 hours	Admission	>140mg/dL	CTA	AGC (0 to 4)	Partial (2) + good (3 to 4)
Menon et al. (2013)	Cohort	206	Unavailable	Admission	Unavailable	CTA	rLMC (0 to 20)	rLMC=11 to 20
Liebeskind et al. (2014a)	RCT	119	<8 hours	Admission	Unavailable	CTA	AGC (0 to 4)	Partial (2) + good (3 to 4)
van Seeters et al. (2016)	Cohort	484	<9 hours	Unavailable	Unavailable	CTA	Good/bad	>50% filling
Mi et al. (2017)	Cohort	45	<24 hours	Fasting glucose	Unavailable	CTA	Higashida (0 to 4)	3 to 4
Borggrefe (2018)	Cohort	313	<8 hours	Admission	>7mmol/L	CTA	Tan (0 to 3)	TAN 0-2
Kim et al. (2018)	RCT	309	<8 hours	Admission	>140mg/dL	CTA	AGC (0 to 4)	Partial (2) + good (3 to 4)
Wang et al. (2018)	Cohort	270	<4.5 hours	Fasting glucose	≥7.8mmol/L	CTA	rFTD	rFTD≤4s
Broocks et al. (2020)	Cohort	178	<6 hours	Admission	>140	CTA	Scale 0-4	3 to 4
Wiegers et al. (2020)	RCT	1988	<6 hours	Admission	>7.8	CTA	Tan (0 to 3)	Tan: 2-3
Gong et al. (2021)	Cohort	30	Unavailable	Admission	Unavailable	CTA	rLMC (0 to 5)	rLMC>4
Scheidecker et al. (2022)	Cohort	230	Unavailable	Admission	Unavailable	CTA	mCTA (0 to 5)	intermediate + good (2 to 5)
Arteaga et al. (2022)	RCT	57	<12 hours	Unavailable	Unavailable	CTA	Unavailable	Unavailable
Genceviciute et al. (2022a)	Cohort	1020	Unavailable	Admission	≥7.8	CTA	AGC (0 to 4)	Moderate + good
Liebeskind et al. (2022)	RCT	161	6 to 24 hours	Admission	>150	CTA/DSA	Tan (0 to 3) ASITN (0 to 4)	Tan: 2-3, ASITN: 2-4
CTP Studies								
Moreton et al. (2007)	Cohort	35	<6 hours	Admission	≥7.0mmol/L	CTP	rCBF	rCBF>0.5
Luitse et al. (2013)	Cohort	80	<24 hours	Admission	≥7.0mmol/L	CTP	N/A	N/A
Kersten et al. (2022)	RCT	173	<6 hours	Admission	>7.8	CTP	N/A	N/A
Mannismäki et al. (2023)	Cohort	832	Unavailable	Admission	>6, >7.8, >8.2	CTP	N/A	N/A
MRI Studies								
Parsons et al. (2002)	Cohort	63	<24 hours	Admission	≥8.0mmol/L	MRI	PWI-DWI mismatch	mismatch ratio >1.2
Ribo et al. (2007)	Cohort	47	<6 hours	Admission	>140mg/dL	MRI	PWI-DWI mismatch	Unavailable
Rosso et al. (2011)	Cohort	94	<6 hours	Admission	≥7.0mmol/L	MRI	ADC-DWI	Unavailable
Gür-Özmen et al. (2019)	Cohort	193	<12 hours	Admission	>140	MRI	PWI-DWI mismatch	mismatch>20%

CTA= Computed Tomography Angiography. CTP= Computed Tomography Perfusion. MRI= Magnetic Resonance Imaging. AGC= The American Society of Interventional and Therapeutic Neuroradiology Collateral Grading System. rLMC= Regional Leptomeningeal Score. rFTD= Relative Filling Time Delay. PWI= Perfusion Weighted Imaging. DWI= Diffusion Weighted Imaging.

Table 2-3 Clinical Characteristics

Lead Author	Age (mean±SD or median with IQR)	Female, %	Admission NIHSS (mean±SD or median with IQR)	HTN, %	DM, %	IHD, %	Dyslipidaemia, %	Smoker, %	Previous AIS/TIA, %	Previous AIS, %	Previous TIA, %	AF, %	rTPA, %	EVT, %
Toni et al. (1994)*	70±7 65±8				12									
Parsons et al. (2002)**	73 (64-78) 70 (66-75)		12 (8-17) 10 (4-15)											
Moreton et al. (2007)	68±13	51	15 (11-19)	71	6	29	32	43		27	27		57	
Ribo et al. (2007)	73	60	18≠	55	19		32	17				38		
Rosso et al. (2011)*	60 (51-61) 62 (55-67)		17 (15-20) 14 (11-16)											
Shimoyama et al. (2013)*	68.5±13.9 66.2±13.3	30	10.7±7.9 8.2±6.8	75	31		29					30		
Menon et al. (2013)***	65.6±12.2 69.1±10.1	48		53	31	31			20					
Luitse et al. (2013)*	59±15.3 69±10.9	0	9.9±5.6 13.2±6.2	41	16								46	
Liebeskind et al. (2014a)														
van Seeters et al. (2016)	66.6±14.6	45	13 (8-17)	51	13		28		18					
Mi et al. (2017)	61.9± 11.4	36	13	51	20	24		42	27			20		
Borggrefe (2018)	70±14.5	51		65	15	28	19	14				53		
Kim et al. (2018)***	68±12 67±12 67±13	55	18 (13-21) 17 (13-19) 16 (13-19)	63	19		37	17		10	6	41	63	
Wang et al. (2018)	71.3±13.4	46	14.2±6.9	66	27	18	41	24		14	7	39		
Broocks et al. (2020)****	73 (57-80) 78 (69-92)	48	14 (11-18) 18 (15-20)		19									
Gür-Özmen et al. (2019)	73 (62-80)	41	10±7	70								40		
Wiegers et al. (2020)	69 (58-79)	45	16 (12-20)	49	16		29			15		24		
Gong et al. (2021)														
Scheidecker et al. (2022)***	74.4±13.2 73.5±13.9 74.1±11.7	55		68	21	25	25					48		
Arteaga et al. (2022)		53		86	70		63			14		62	53	63
Genceviciute et al. (2022a) α	75 (18-101) 78 (45-94)	51	13 (0-36) 16 (0-36)	75	22	25	70			13		39 46		100
Liebeskind et al. (2022)***	70.7±14.2 69.7±14.4 68.1±11.3	55	16.3±4.5 18.1±5.7 19.7±5.5	78	23	30	57	21		11	8	34		
Kersten et al. (2022)*	60±14 64±12	47	18 (13-19) 17 (14-21)	39	8		23	30					98	100
Mannismäki et al. (2023)	69±13	43	5 (3-11)	66	23		51			13	8	18		
SSNAP, 2023	76 (65-85)	47	4 (2-10)	56	24						24	19	10	3

Pink cells represent data not provided within individual papers. *Data separated into two groups: "hyperglycaemic" and "normoglycaemic", **Data separated into "mismatch" and "no mismatch", ***Data separated into groups (two or three) based on collateral status, ****Data separated into mRS 0-2 and 3-6, α Data separated into DM and non-DM, ≠presumably mean or median but no SD or IQR given. SD=standard deviation, IQR=interquartile range, NIHSS=National Institute of Health Stroke Scale, HTN=hypertension, DM=diabetes mellitus, IHD=ischaemic heart disease, AIS=acute ischaemic stroke, TIA=transient ischaemic attack, AF=atrial fibrillation, rTPA=recombinant tissue plasminogen activator, EVT=endovascular thrombectomy.

Mean Admission Glucose

There were nine studies which provided data on blood glucose in patients with favourable and poor collaterals. We excluded three from this analysis on the basis of two studies providing median with IQR (Parsons et al., 2002, Wiegers et al., 2020) and another which provided information on fasting plasma glucose [FPG] (Mi et al., 2017). All studies except one (Moreton et al., 2007) provided data in mg/dL form, therefore we converted the mean and SD of the exception using the basis 1mmol/L of blood glucose is equivalent to 18mg/dL.

Table 2-4 demonstrates that the overall mean admission glucose in patients with unfavourable collaterals was higher with a wider SD.

Table 2-4 Mean Admission Glucose in Favourable and Unfavourable Collaterals

	Favourable collateral circulation			**Unfavourable collateral circulation**		
Study	**N**	**Mean**	**sd**	**N**	**Mean**	**sd**
Moreton et al. (2007)	16	112.4	25.8	19	120.9	21.8
Shimoyama et al. (2013)	59	157.9	71.5	34	147.4	43.4
Menon et al. (2013)	133	133.1	48.1	73	164.5	95.5
Kim et al. (2018)	109	124	38	105	136	61
(partial/fair)	95	134	63			
Scheidecker et al. (2022)	117	121.8	35	25	141.6	52.1
(partial/fair)	88	129.5	45			
Liebeskind et al. (2022)	54	128.8	32.3	35	158	64.8
(partial/fair)	72	132.4	49.9			
Overall	**743**	**130.8**	**47.5**	**291**	**146.6**	**60.7**

N=number, sd=standard deviation

Meta-Analysis

There were seven papers in which data was available for the number of patients with glycaemic status and related collateral status included in the meta-analysis in the forest plot depicted in Figure 2-2.

Meta-analysis (n=2064) found no significant increased odds of poor collaterals with hyperglycaemia (pooled random OR 0.85, 95% CI 0.63 to 1.13, p=0.26).

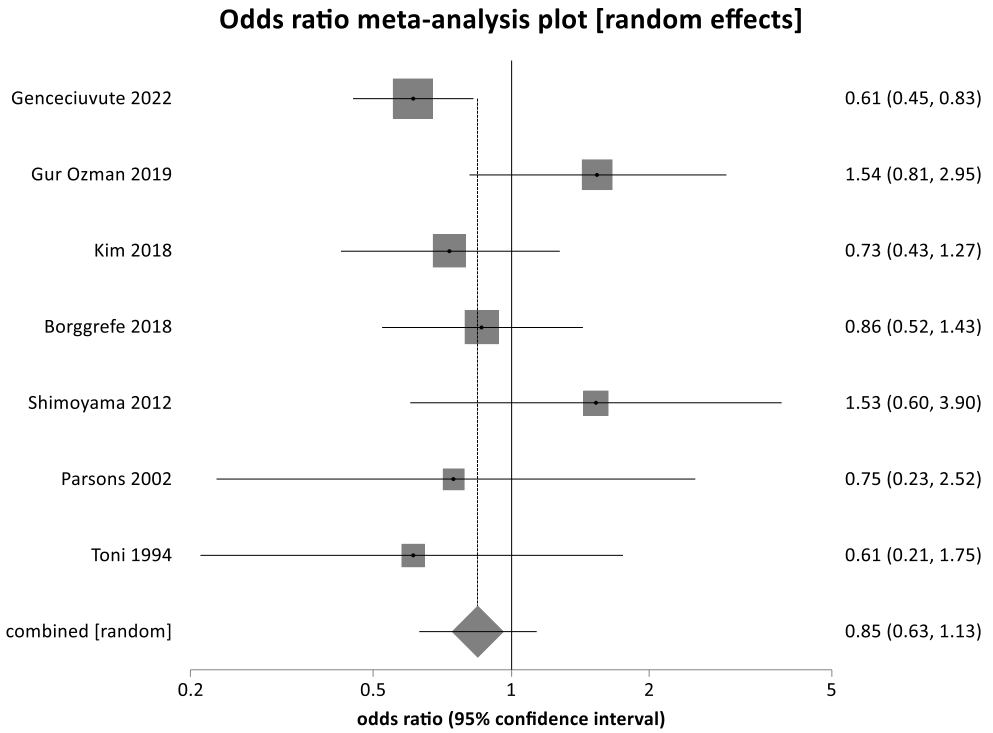

An odds ratio statistically lower than 1 reflects a preference for poor collateral status, whereas an odds ratio statistically higher than 1 reflects a preference for good collateral status

Figure 2-2 Odds Ratio Meta-Analysis Plot of Hypergylcaemia and Collateral Status

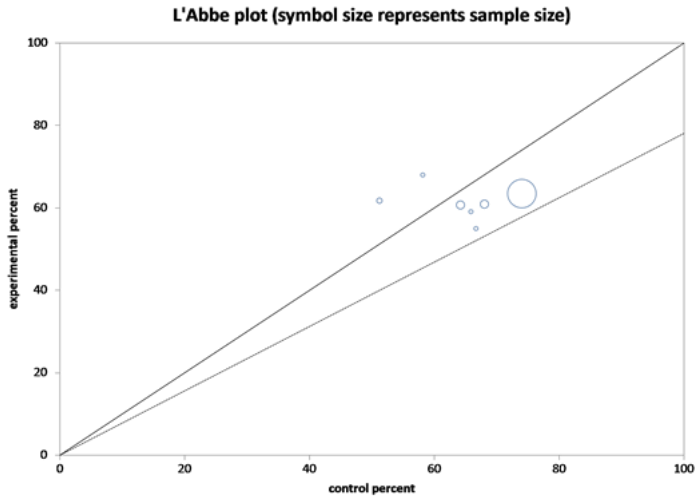

Figure 2-3 L'Abbé Plot demonstrating Heterogeneity

Figure 2-3 illustrates the heterogeneity across the populations explored revealing one dominant dataset. There were no studies in keeping with our definition of outliers as defined by Viechtbauer and Cheung (2010).

A sensitivity analysis excluding for the largest study (Genceviciute et al., 2022a) gave a similarly non-significant result with a random effects pooled odds ratio of 0.95, 95% CI 0.71 to 1.27, p=0.72.

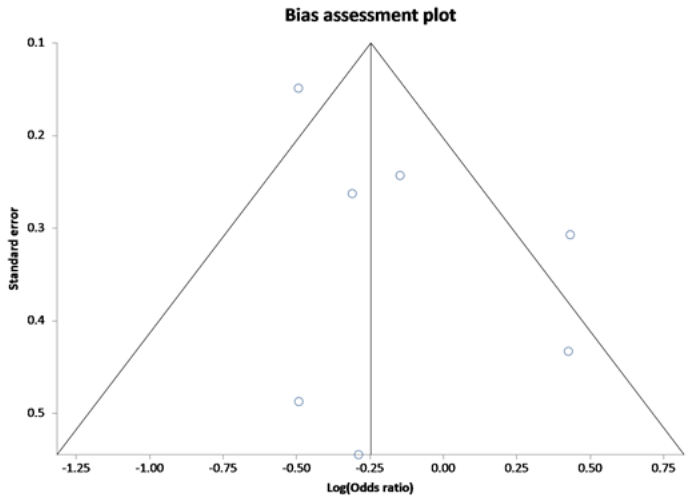

Figure 2-4 Bias Assessment Funnel Plot

The funnel plot does not suggest publication bias. Kendall's tau is 0.14 with p=0.77. For Egger's test, the intercept is 1.56, with a 95% CI from -1.33 to 4.46, and one-tailed p=0.22.

Discussion

Our systematic review and meta-analysis did not find a significant association between admission hypergylcaemia and poor collateral status.

Of the seven papers included in the meta-analysis, only two had reported individually a significant link: Parsons et al. (2002) reported significantly reduced salvage of penumbral tissue and Borggrefe (2018) reported an association between glucose and poor collaterals in a diabetic subgroup only. Additionally, we identified 8 papers reporting a significant link between hyperglycaemia and poor collaterals but where data were not presented in a form suitable for meta-analysis (Menon et al., 2013, Liebeskind et al., 2014a, Mi et al., 2017, Wiegers et al., 2020, Scheidecker et al., 2022, Liebeskind et al., 2022, Kersten et al., 2022, Mannismäki et al., 2023).

Of the papers which did not find an association, two did not measure collateral score over all - Moreton et al. (2007) focused on insular hypoperfusion as a potential mechanism for hyperglycaemia and Arteaga et al. (2022) focused specifically on glucose control. van Seeters et al. (2016) reported a link between higher ABD and poorer collateral flow but did not back this up with data. No study suggested that hyperglycaemia was related to improved collateral flow.

The thresholds of hyperglycaemia ranges widely from >118.9mg/dL to >150mg/dL which is a broad range. Similarly, there were three imaging modalities assessing collateral status. This risks the effect of hypergylcaemia on collaterals being diluted. Nevertheless, the mean ABG was higher in patients with poorer collaterals.

Many studies did not report clinical details or risk factors which would have been useful in terms of fully assessing the heterogeneity of the results. What is clear is that the populations are widely different especially in terms of sex, vascular risk factors and reperfusion therapy rate. The wide variation in patients receiving EVT can be explained both by the earliest study being in 1994 (before both thrombolysis and EVT were established) but also by some studies being sub-analyses of patients recruited to reperfusion therapy trials. Genceviciute et al. (2022a), the largest study with 1020 patients, was a sub-analysis of the MR CLEAN data and 100% of the patients received EVT. Whilst we know what proportion of the available data received EVT, it is difficult to know what proportion were eligible, especially as the admission NIHSS throughout tends to be on the higher side, especially when compared with the SSNAP data.

The assumption of most meta-analyses is that the studies are sufficiently comparable that they can be combined to answer a question. We chose a random effects model for our meta-analysis as opposed to a fixed effects given the substantial differences between the individual studies – as a more conservative approach. However as mentioned above, the studies were widely different. This may be the reason we were not able to prove a link between hyperglycaemia and poor collaterals (as well as there not being a link to find).

There was no suggestion of publication bias, but the total number of studies remains quite small and the settings diverse. Definitions may not be the same.

Additional and more recent data with robust assessment of collateral vessels would be of value.

Conclusion

Admission hyperglycaemia is not significantly associated with poorer collateral circulation as determined by CTA, CTP and PWI-DWI imaging. Thresholds for hyperglycaemia varied widely within our dataset and when further studies are published, a repeat meta-analysis would be useful.

Chapter 3 General Methods

Introduction

This chapter describes the patients and general methods used in the series of studies analysed in this thesis. Methodology, protocols and endpoints are described in detail in the relevant chapter.

Imaging Data Analysed

Several sources of imaging data were used for this research. The key features of the MASIS, Australian TNK, POSH and ATTEST studies which form the basis of Chapter 4 are described here.

MASIS

The Multi-Centre Acute Stroke Imaging Study [MASIS] was a multi-centre prospective observational study performed between August 2008 to March 2010 designed to investigate different imaging modalities, blood biomarkers and clinical aspects of AIS. Patients (total=81) were recruited from the Aberdeen Royal Infirmary the Western General Hospital, Edinburgh and the Southern General Hospital, Glasgow, United Kingdom (Wardlaw et al., 2013a).

The inclusion/exclusion criteria are listed in Table 3-1 MASIS Inclusion and Exclusion Criteria. Imaging comprised of baseline NCCT, CT perfusion and CT angiography or baseline MRI including DWI, PWI, T2, FLAIR post-contrast, gradient echo and circle of Willis time-of-flight MRA. Follow up imaging included MRI with DWI, PWI, T2, FLAIR post-contrast, gradient echo and circle of Willis MRA at 72 hours and the same (minus the circle of Willis MRA) at day 30. If MR was contraindicated, follow up imaging comprised of NCCT and CTA. NIHSS was assessed at baseline, 24 hours, 72 hours, day 7 and day 30 (Wardlaw et al., 2013a).

Arterial occlusion/early recanalisation on angiography were more consistently associated with clinical outcome than perfusion lesion/reperfusion regardless of the perfusion parameter used (Wardlaw et al., 2013a).

Table 3-1 MASIS Inclusion and Exclusion Criteria

Inclusion:
1. Clinical diagnosis of acute ischaemic stroke 2. ≤6 hours after onset 3. ≥18 years
Exclusion:
1. Known non stroke diagnosis (e.g. Primary intracerebral haemorrhage, tumour, subarachnoid haemorrhage, epilepsy) 2. Inability to lie in a recumbent position for the duration of additional imaging (e.g. severe cardiac failure, desaturation on lying flat, high risk of aspiration) 3. Intercurrent illness likely to limit survival to less than 30 days 4. Coma 5. Chronic or acute renal failure 6. Known sensitivity to iodinated contrast media (including previous contrast reactions or severe asthma) for CT based imaging studies 7. Known sensitivity to gadolinium contrast, recently implanted ferromagnetic foreign bodies, intracranial aneurysm clip, or dependence on a cardiac pacemaker or implantable defibrillator for MRI studies

CT=computed tomography, MRI=magnetic resonance imaging

Australian TNK

The Australian Tenecteplase [TNK] trial was a multi-centre phase 2 PROBE trial to compare the efficacy of standard dose Alteplase therapy (0.9mk/kg) to 0.1 and 0.25mg/kg TNK in AIS patients who had a CTP-defined ischaemic penumbra and associate vessel occlusion within 6 hours of stroke onset which took place between 2008 and 2011. Patients (total=75) were recruited from the John Hunter Hospital, Newcastle, Australia and two other centres (Parsons et al., 2012).

The inclusion/exclusion criteria are listed in Table 3-2. Patients were randomly assigned (1:1:1) to receive thrombolytic treatment with Tenecteplase (0.1mg/kg or 0.25mg/kg) or Alteplase (0.9mg/kg). Imaging comprised of baseline NCCT, CT perfusion and CT angiography, 24 hour NCCT and MRI and day 90 MRI. NIHSS was assessed at baseline and 24 hours. The primary imaging outcome was extent of reperfusion at 24 hours; the primary clinical outcome being clinical improvement at 24 hours.

TNK significantly improved reperfusion and clinical outcomes in patients selected on the basis of CT perfusion imaging.

Table 3-2 Australian TNK Inclusion and Exclusion Criteria

Inclusion:
Clinical inclusion criteria: 1. Symptoms and signs of clinically definite stroke with measurable deficit on NIHSS 2. Age 18 years or older 3. Treatment can be initiated within 6 hours of stroke onset *Imaging inclusion criteria:* 1. CT scanning has excluded intracranial haemorrhage 2. CTA shows a visible vessel occlusion (complete or partial) – this may be in the middle, anterior or posterior cerebral artery, and should be anatomically correlated with the CTP 3. CTP shows at least 20% 'mismatch' between mean transit time (MTT) lesion and cerebral blood volume (CBV) lesion (i.e. significant penumbral tissue) – this is visually assessed, as previously validated.
Exclusion:
Clinical exclusion criteria: 1. Minor stroke symptoms, or major stroke symptoms rapidly improving 2. Clinically suspected brainstem stroke 3. Clinical presentation suggesting subarachnoid haemorrhage 4. Pregnancy 5. Known bleeding diathesis and/or platelet count 1.5 6. Patients who have received heparin within 48 hours must have a normal aPTT 7. Major surgery or serious trauma within 14 days, serious head trauma within 3 months 8. GI or urinary tract haemorrhage within last 21 days 9. Arterial puncture at a noncompressible site or lumbar puncture within 7 days 10. Systolic BP > 185, diastolic BP > 110mmHg 11. Clinical stroke within 3 months or history of ICH 12. Unable to gain consent from patient or person responsible *Imaging exclusion criteria:* 1. Known severe renal impairment (GFR < 15mls/min) 2. Contraindication to MRI (pacemaker, aneurysm clips) 3. No perfusion lesion visible and/or no visible vessel occlusion (in middle, anterior, or posterior cerebral arteries) 4. 'Match' between CBV lesion and MTT lesion (i.e. no penumbra) 5. Large area of irreversible ischaemia (>1/3 MCA territory on CBV) 6. ICA occlusion on side of acutely affected hemisphere or carotid 'T' thrombus (as this may be more effectively treated with intra-arterial therapy) 7. Evidence of acute brainstem ischaemia

TNK= Tenecteplase, NIHSS=National Institute of Health Stroke Scale, CT=computed tomography, CTA=computed tomography angiography, CTP=computed tomography perfusion, MTT=mean transit time, CBV=cerebral blood volume, APTT=activated partial thromboplastin time, GI=gastro-intestinal, BP=blood pressure, ICH=intracerebral haemorrhage, GFR=glomerular filtration rate, MCA=middle cerebral artery, ICA=internal carotid artery

POSH

The Post-Stroke Hyperglycaemia and Brain Arterial Patency study [POSH] was a single-centre prospective observational study with the aim to define the interaction of early and

delayed hyperglycaemia with arterial patency and brain perfusion. Patients (total=113) who presented within 6 hours of AIS were recruited from the Acute Stroke Unit, Southern General Hospital, Glasgow, United Kingdom between January 2009 and December 2011 (MacDougall, 2013).

The inclusion/exclusion criteria are listed in Table 3-3. Imaging comprised of baseline NCCT and CTA with some patients also undergoing CTP. NIHSS was assessed at baseline, 24-48 hours in some patients, 72 hours, day 7 and day 30.

Higher admission and mean glucose levels correlated with larger infarct volumes. Admission hyperglycaemia was more harmful than hyperglycaemia after 6 hours.

Table 3-3 POSH Inclusion and Exclusion Criteria

Inclusion:
1. Clinical diagnosis of acute ischaemic stroke 2. ≤6 hours after onset 3. ≥18 years
Exclusion:
1. Known non-stroke diagnosis (eg. ICH, tumour, SAH, epilepsy) 2. Known sensitivity to iodinated contrast media (including previous contrast reactions or severe asthma) 3. Inability to lie in a recumbent position for the duration of additional imaging (e.g. severe cardiac failure, desaturation on lying flat, high risk of aspiration) 4. Intercurrent illness likely to limit survival to less than 30 days

POSH=Post-Stroke Hyperglycaemia and Brain Arterial Patency study, ICH=intracerebral haemorrhage, SAH=subarachnoid haemorrhage

ATTEST

The Alteplase-Tenecteplase Trial Evaluation for Stroke Thrombolysis [ATTEST] was a single-centre phase 2 prospective randomised open-label blinded end-point [PROBE] study that compared markers of biological activity to assess the efficacy and safety of Tenecteplase versus Alteplase within 4.5 hours of AIS onset, in a population not selected on the basis of advanced neuroimaging, to inform the design of a definitive phase 3 clinical trial. Patients (total=105) were recruited from the Acute Stroke Unit, Southern General

Hospital, Glasgow, United Kingdom from January 2012 to September 2013 (Huang et al., 2015).

The inclusion/exclusion criteria are listed in Table 3-4. Patients were randomly assigned (1:1) to receive thrombolytic treatment with Tenecteplase (0.25mg/kg, maximum 25mg) or Alteplase (0.9mg/kg, maximum 90mg). Imaging comprised of baseline NCCT, CT perfusion and CT angiography with follow-up NCCT and CTA at 24-48 hours. The primary endpoint was percentage of penumbra salvaged (defined by baseline CT perfusion minus follow-up CT infarct volume at 24-48 hours). NIHSS was assessed at baseline, 24 hours, 72 hours, day 30 and day 90 (Huang et al., 2015).

Neurological and radiological outcomes did not differ between Tenecteplase and Alteplase arms suggesting further evaluation of Tenecteplase in larger trials would be of use – we summarised the most recently published (at the time of writing) data in Chapter 1 (Huang et al., 2015).

Table 3-4 ATTEST Inclusion and Exclusion Criteria

Inclusion:
1. Clinical diagnosis of supratentorial acute ischaemic stroke with score of ≥1 on the NIH Stroke Scale
2. Male or non-pregnant female ≥18 years of age
3. Within 4.5 hours of onset as defined by time since last known well
4. CTP and CTA examinations acquired prior or immediate after the initiation of treatment
5. mRS ≤2 pre-admission
Exclusion:
1. Contraindications to thrombolytic drug treatment for stroke
2. Evidence of intracranial haemorrhage or significant non-stroke intracranial pathology (including CNS neoplasm, aneurysm or arteriovenous malformation) on pre-treatment CT
3. Established hypodensity on pre-treatment brain CT of more than one third of the MCA territory or ASPECT score <4 (sulcal effacement or loss of grey-white differentiation in cortical territories alone are not counted towards ASPECT score)
4. Hypodensity consistent with recent cerebral ischaemia other than the presenting event
5. Very severe stroke (e.g. NIHSS>25)
6. Systolic BP> 185 or diastolic BP> 110 mm Hg, or aggressive management (intravenous pharmacotherapy) necessary to reduce BP to these limits
7. If on warfarin, INR >1.4
8. Current prescription of direct oral anticoagulant drugs
9. Significant abnormality of coagulation parameters pre-treatment (prolonged INR or APTT, or platelet count <100,000/mm3)
10. Administration of heparin within the previous 48 hours and a thromboplastin time exceeding the upper limit of normal for laboratory, or use of therapeutic dose low molecular weight heparin within 48h
11. Clinical history suggestive of subarachnoid haemorrhage even if no blood is evident on CT
12. Risk of bleeding (Major surgery within previous 1 month; intracranial or spinal surgery; recent trauma to the head or cranium; prolonged cardiopulmonary resuscitation (> 2minutes) within the past 2 weeks; acute pericarditis and/or subacute bacterial endocarditis; acute pancreatitis; severe hepatic dysfunction, including hepatic failure, cirrhosis, portal hypertension (oesophageal varices) and active hepatitis; active peptic ulceration; any known history of haemorrhagic stroke or stroke of unknown origin; arterial aneurysm and known arteriovenous malformation)
13. Dependent (mRS 3-5) pre-stroke
14. Blood glucose <2 mmol/l or >18 mmol/l
15. Seizure at onset of symptoms unless brain imaging identifies positive; evidence of significant brain ischaemia (e.g. CTA confirmed arterial occlusion, early ischaemic change on plain CT, hypoperfusion on CTP)
16. Pregnancy
17. Known history of impaired renal function with an eGFR <30 mL/min pre-treatment precluding contrast CT
18. Known allergy to radiological contrast
19. History of allergies to active substances in either trial medication, or to excipients including Gentamicin
20. Severe concurrent medical condition that would prevent participation in study procedures (e.g. cardiac failure with severe pulmonary oedema) or with life expectancy ≤ 3 months

ATTEST=Alteplase-Tenecteplase Trial Evaluation for Stroke Thrombolysis, NIH Stroke Scale=National Institute of Health Stroke Scale, CTP=computed tomography perfusion, CTA=computed tomography angiography, mRS=modified Rankin Scale, CNS=central nervous system, CT=computed tomography, MCA=middle cerebral artery, ASPECT=Alberta Stroke Programme Early CT score, BP=blood pressure, INR=international normalised ratio, APTT=activated partial thromboplastin time.

WHISPER

The Whole Brain Ischaemic Stroke Perfusion and Extended Recanalisation [WHISPER] will be described in detail in Chapter 5.

The Research Database

The MASIS, Australian TNK, POSH and ATTEST studies formed a local stroke research imaging database in which data were pooled. Informed consent was obtained in all studies; consent forms included explicit permission for secondary analyses as part of collaboration. Data were used according to ethical approval and consent for secondary analysis. Data governance was ensured: data were shared using an encrypted external hard drive and saved to an internal shared research folder within the University of Glasgow. Users must apply for access.

CT and MR Imaging Protocols

For all studies, acute CT imaging included whole brain NCCT, CTP and single-phase CTA using 64 or 320 slice scanners. Study specific imaging is detailed in the relevant chapter.

For the MASIS, POSH and ATTEST cohorts, this was performed using a multi-detector Scanner (Philips Brilliance 64 Slice). Whole brain NCCT was acquired first, followed by CTP with 40 mm slab coverage (8 x 5 mm2 slices), using a 50 ml contrast bolus administered at 5 ml/second via a large-gauge peripheral venous cannula. Finally, a CT angiogram was performed from aortic arch to the top of the lateral ventricles using bolus tracking to enable correct timing of image acquisition.

The WHISPER study used whole brain (16cm detector) on Toshiba Aquilion One Vision research scanner or Emergency Department scanner - GE 660: 8cm detector in jog mode which moves the examination table in and out of the gantry to provide 2x8cm brain volumes throughout the acquisition (approximately 60s in total). Jog mode is necessary as CT scanners do not typically have sufficient axial coverage (van Ommen et al., 2019).

The TNK cohort had whole brain NCCT followed by CTP and CTA. CTP was acquired (16 slice Phillips Mx8000 scanner) as two separate (consecutive) 24mm slabs positioned to maximize supratentorial coverage. Iodinated contrast (40ml) was injected at 5ml/s and 35 images acquired every 1.3s (total acquisition time 45s). CTA was performed from the carotid bifurcation to the top of the lateral ventricles.

The MASIS, Australian TNK and WHISPER cohorts had MRI follow up imaging. Only the WHISPER MRI data is used in this work. The stroke MRI protocol included diffusion and perfusion imaging with the majority of patients also having MR angiography, T2* gradient echo and T2/FLAIR imaging.

Imaging Processing and Analysis

Imaging analysis is described in depth in subsequent chapters; a brief overview is described here.

ATTEST, POSH, MASIS and Australian TNK

For the ATTEST, POSH, MASIS and Australian TNK cohorts, CT perfusion and CTA imaging were of interest.

Study imaging records were transferred from clinical scanners or radiology archives after removal of individual identifiers from the Digital Imaging and Communications in Medicine [DICOM] file and were identifiable by study number.

CT perfusion analysis was repeated using MIStar version 3.2 (Apollo Medical Imaging Technology, Melbourne, Australia), RAPID version 4.7 (Ischemaview) and Brainomix versions 9.001 to 11.001 -the software automatically updated on a regular basis. An account of analysis on each software is described below.

CTA data was used from the study data bases.

WHISPER

For the WHISPER cohort, NCCT, CTP, CTA and MRI imaging were analysed.

The WHISPER imaging records were transferred as previously described. Many patients had study specific imaging processed by relevant software (for clinical reasons) prior to recruitment. In these cases, data was recorded from the local imaging database -PACS Radiology Software (InsigniaMedical) and the processing software version noted.

Baseline NCCT was assessed for early ischaemic change using the ASPECT score with 5mm thickness slices imaging (Barber et al., 2000).

CT perfusion analysis was performed using MIStar version 3.2 (Apollo Medical Imaging Technology, Melbourne, Australia), RAPID version 4.7 (Ischemaview) and Brainomix versions 9.001 to 11.001 (updates were automatic).

CTA analysis was performed using RAPID version 4.7 (Ischemaview) and RAPID (clinical version), and Brainomix versions 9.001 to 11.001. Scans were also scored separately for presence of LVO with subsequent leptomeningeal collateral assessment by consensus of one experienced stroke neurologist with one neuroradiologist (AS and CP) using the regional Leptomeningeal Collateral [rLMC] score (Menon et al., 2011).

MRI infarct volume analysis was performed by a Clinical Research Fellow (SN) using Multi-image Analysis GUI [Mango] version 4.1 (RII-UTHSCSA, University of Texas. AM and CP assessed the ASPECTS on MRI and used the Arterial Occlusive Lesion [AOL] recanalisation score to assess MRA.(Barber et al., 2000, Khatri et al., 2005) Scans were also reported clinically by local radiologists (either by a Consultant Radiologist or by a trainee with subsequent assessment by a Consultant).

MIStar (Apollo Medical Imaging Technology, Melbourne, Australia)

The MIStar version 3.2.63 (Apollo Medical Imaging Technology, Melbourne, Australia) software was used to analyse CT perfusion imaging.

Imaging was analysed by two Clinical Research Fellows (VB and AM) on a workstation separately following the completion of the studies analysed. Inter-observer agreement was assessed. Disagreements in readings were resolved by each reader analysing the scan separately for a second time (four readings in total) and by discussion if this did not resolve the issue.

The MIStar software package uses a modified singular value decomposition [SVD] deconvolution algorithm to provide the following four parameters: cerebral blood flow [CBF], cerebral blood volume [CBV], mean transit time [MTT] and delay time [DT](Yang, 2005). Motion correction and 3D registration are applied automatically by the software. Arterial input function [AIF] and Venous Output Function [VOF] are automatically selected by the software but this is user-supervised and can be altered. The contra-lesional anterior cerebral artery [ACA] or middle cerebral artery [MCA] and superior sagittal sinus were favoured when possible. The attenuation curves are measured for all pixels as the contrast bolus travels from the arteries, through the parenchyma to the veins to produce a lesion map. The region of interest [ROI] is manually drawn and volumes of core and penumbra calculated.

RAPID (Ischemaview)

The RAPID version 4.7 (Ischemaview) is a fully automated software used to analyse both CTP and CTA scans.

Imaging data is sent directly from the scanner to RAPID which measures attenuation curve height, width and arrival time for each pixel. AIF is automatically generated; pixels with early arrival time, above average height, and narrow width compared to the average are selected. The VOF time attenuation curve is identified similarly; a 3 to 12 second delay from the AIF is assumed. The VOF is usually located in a posterior location, on a major

deep cerebral vein or venous sinus. The algorithm corrects for motion and timing. A circular deconvolution model is used to estimate contrast concentration within the vessels based on CT attenuation. This information is used calculate the following parameters: relative CBV, MTT, time-to-peak concentration (Tmax) and CBF for each pixel. The VOF is corrects for volume averaging. The artery, being relatively smaller in calibre, is subject to volume averaging effects and more sensitive to motion. The VOF, located on a much larger vessel, is not as affected by volume averaging and is therefore used to correct the AIF curve. Additional corrections are made for noise, signal regularization, oscillatory artifact, and haematocrit differences between large vessels and capillaries (Laughlin, 2019).

Brainomix

There is little to no published information available with regards to Brainomix perfusion methods. Similarly, to RAPID, it is a fully automated software and imaging data is sent directly from the scanner. Thresholds for core and total perfusion deficit are CBF<30% and Tmax>6s. The software automatically selects AIF and VOF.

Assessment and Scales

The National Institutes of Health Stroke Scale (NIHSS)

The NIHSS is the most widely used measure of neurological deficit in modern practice. It became the gold standard for AIS severity assessment following its use in the first successful clinical trial in reperfusion therapy, the National Institute of Neurological Disorders and Stroke recombinant tissue-type plasminogen activator [NINDS r-tPA] Acute Stroke Trial.(1995) The version used today (Table 3-5) was developed by the NINDs r-tPA trial designers to standardise the use of examination scales with emphasis on speed and reproducibility in large clinical trials (Lyden et al., 1994).

The NIHSS is a 0-42 point, non-linear scale; a normal examination scores 0 and death scores 42. An NIHSS<5 is deemed ‘mild’ and is a relative contraindication to IV rtPA; the AHA guidelines do not recommend the use (Powers et al., 2019). The NIHSS should not replace comprehensive neurological examination. The simplicity of the scale being weighted towards gross motor and language tasks makes it quick, reliable and reproducible

(Lyden et al., 1994). This weighting means that right hemisphere lesions are, however, consistently larger than left for a given NIHSS score which must be taken into account when deciding stroke severity (Woo et al., 1999). Posterior circulation strokes are also under-weighted by the scale (Linfante et al., 2001).

The NIHSS is reproducible by users with good interrater agreement following training on most scale points except for facial paresis and ataxia assessment (Lyden et al., 1994).

Table 3-5 National Institutes of Health Stroke Scale

Activity	Score	
Level of consciousness	Alert	0
	Not alert, arousable	1
	Not alert, obtunded	2
	Unresponsive	3
LOC questions	Answers both correctly	0
	Answers one correctly	1
	Incorrect	2
LOC commands	Obeys both correctly	0
	Obeys both incorrectly	1
	Incorrect	2
Gaze	Normal	0
	Partial gaze palsy	1
	Forced deviation	2
Visual fields	No visual loss	0
	Partial hemianopia	1
	Complete hemianopia	2
	Bilateral hemianopia	3
Facial palsy	Normal	0
	Minor paralysis	1
	Partial paralysis	2
	Complete paralysis	3
Motor arm	Normal	0
a. Left	Drift	1
b. Right	Some effort against gravity	2
	No effort against gravity	3
	No movement	4
Motor leg	Normal	0
a. Left	Drift	1
b. Right	Some effort against gravity	2
	No effort against gravity	3
	No movement	4
Ataxia	Normal	0
	Present in one limb	1
	Present in two limbs	2
Sensory	Normal	0
	Mild loss	1
	Severe loss	2
Language	Normal	0
	Mild aphasia	1
	Severe aphasia	2
	Mute	3
Dysarthria	Normal	0
	Mild	1
	Severe	2
Extinction/Inattention	Normal	0
	Mild – to one modality	1
	Severe – to more than one modality	2

LOC=level of consciousness

The modified Rankin Scale (mRS)

The Rankin Scale for severity of stroke outcome was developed by Rankin (1957). It was revised –'modified' to its current form in the 1980s as part of the United Kingdom Transient Ischaemic Attack [UK-TIA] trial (Farrell et al., 1991).

The mRS is a 7 point ordinal scale (Table 3-6) ranging from 0 (no symptoms at all) to 6 (death) (Farrell et al., 1991). Excellent outcome is usually defined as functional independence i.e. 0-2 (Furlan et al., 1999).

A clear limitation is the potential for interobserver variability (Quinn et al., 2009). This is important considering a single-point difference on the scale will always be clinically relevant.

Table 3-6 Modified Rankin Scale

Score	Description
0	No symptoms at all
1	No significant disability and able to carry out all duties
2	Slight disability. Unable to carry out some previous activities but able to look after own affairs without assistance
3	Moderate disability. Requiring some help but able to walk without assistance
4	Moderately severe disability. Unable to walk without assistance and unable to attend to own bodily needs without assistance
5	Severe disability. Bedridden, incontinent and requiring constant nursing care and attention
6	Death

The Alberta Stroke Programme Early CT Score (ASPECTS)

The Alberta Stroke Programme Early CT Score [ASPECTS] was proposed to measure the extent of early ischaemic change in MCA AIS on NCCT (Barber et al., 2000).

It is a topographic 10-point scoring system in which each point represents a defined territory of the middle cerebral artery as demonstrated in Figure 3-1. For each area of early

ischaemic change -for example focal swelling or parenchymal hypoattenuation, 1 point is subtracted. A normal NCCT will have an ASPECTS value of 10 points whereas a score of 0 indicates diffuse ischaemia throughout the entire MCA territory in one hemisphere (Barber et al., 2000).

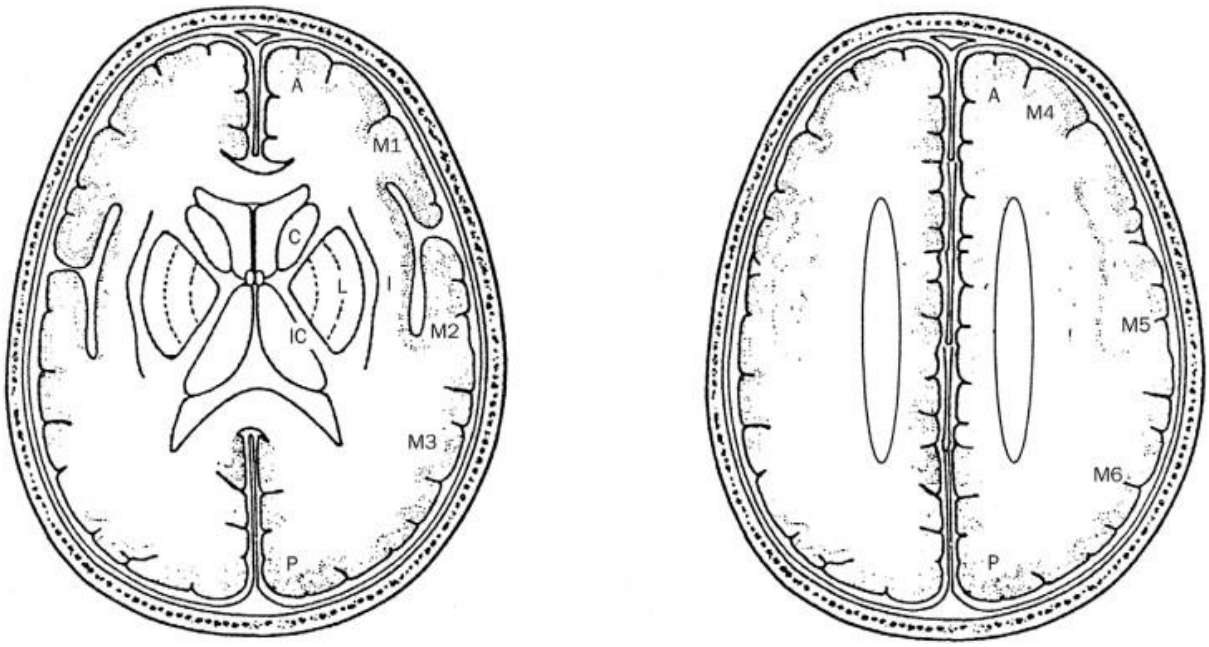

A=anterior circulation; P=posterior circulation; C=caudate; L=lentiform; IC=internal capsule; l=insular ribbon; MCA=middle cerebral artery; M1=anterior MCA cortex; M2=MCA cortex lateral to insular ribbon; M3=posterior MCA cortex; M4, M5, and M6 are anterior, lateral, and posterior MCA territories immediately superior to M1, M2, and M3, rostral to basal ganglia. Subcortical structures (C, L and IC) are allotted 3 points, MCA cortex (insular ribbon, M1, M2, M3, M4, M5 and M6) is allotted 7 points.(Barber et al., 2000)

Figure 3-1 Alberta Stroke Programming Early CT Score

ASPECTS forms key selection criteria in the updated American Heart Association guidelines on the management of AIS: endovascular therapy in patients with baseline ASPECTS≥6 is recommended (Powers et al., 2019). As ASPECTS assessment became increasingly incorporated into treatment decision making in EVT randomised clinical trials, this cut-off is also applied to rtPA therapy treatment decisions (Goyal et al., 2015). The AHA IV rTPA contraindications which advises against rtPA when NCCT demonstrates ‘extensive regions of clear hypoattenuation >1/3 MCA territory’ (Powers et al., 2019). The original publication suggested a cut-off of ≤7 (Barber et al., 2000).

NCCT-ASPECTS has been proven to predict functional outcome and symptomatic ICH following tPA treatment (Barber et al., 2000).

A major limitation is that intra-observer agreement is variable (Nicholson et al., 2020, Coutts et al., 2004).

The Hypoperfusion Intensity Ratio HIR

The HIR was described in detail in Chapter 1. It is defined as the proportion of Tmax >6 second delay lesion with Tmax >10 second delay and is a method of assessing collateral circulation using CTP (Olivot et al., 2014).

CTA Collateral Flow Assessment Scores

A systematic review of collateral flow assessment scores revealed that there were forty-one methods for grading collateral flow on the basis of conventional angiography (McVerry et al., 2012). Now the number is probably higher. We describe below two common methods in current use.

The Modified Tan Score

The modified Tan score is a simple system of grading collateral vessels in patients with LVO that appears to be attributed to both Tan et al. (2007) and Tan et al. (2009a) -two separate people. What is clear is that the score appears to be based on the original scoring system derived from Kim et al. (2004) using the PROACT II data but this scoring system is less prescriptive with regards to filling definition. There are various versions proposed with subtle differences, the now named ‘modified Tan score’ has become the universally acknowledged score and is displayed below in Table 3-7. Both proposed score by Tan et al. (2009a) and Kim et al. (2004) focus on MCA occlusions which is why the Tan score has a reputation for being validated for MCA occlusions only. It is, however, universally used for all occlusions.

Table 3-7 The Modified Tan Score

Score	Definition
0	absent collaterals
1	collaterals filling ≤50% of the occluded territory
2	collaterals filling >50%, but <100% of the occluded territory
3	collaterals filling 100% of the occluded territory

The regional Leptomeningeal Collateral (rLMC) score

The regional Leptomeningeal Collateral [rLMC] score (Table 3-8) is a semi-quantitative system of scoring the leptomeningeal pathways as divided into anatomic regions in accordance with the ASPECTS method, based on the extent of contrast opacification in multi-phase CTA. Arteries in the Sylvian sulcus are given a higher weighting because of their being more distant from the ACA to MCA and MCA to PCA anastomoses; flow here indicates strong retrograde flow and good collateral networks. Better collateral status is indicated by higher total scores. Interrater reliability is good. This score too was developed on a patient population with ICA and/or MCA occlusions (Menon et al., 2011). The rLMC score correlates with ASPECTS and clinical outcome at 90 days (Chatterjee et al., 2020).

Table 3-8 Regional Leptomeningeal Collateral Score

Regions	**Score** 0 – artery not seen 1 – less prominent 2 – equal or more prominent when compared to a matching region in the opposite hemisphere **Sylvian sulcus only** 0 – artery not seen 2 – less prominent 4 – equal or more prominent when compared to a matching region in the opposite hemisphere
M1	
Sylvian Sulcus	
M2	
M3	
M4	
M5	
M6	
ACA	
Basal Ganglia	

The Arterial Occlusive Lesion (AOL) recanalisation score

The primary Arterial Occlusive Lesion [AOL] recanalisation score was defined to specifically focus on recanalisation at the primary occlusive site. It grades the severity of vessel occlusion from 0 (no flow) to 3 (normal flow) (Khatri et al., 2005).

Before the introduction of the AOL score, two other scales were widely used to describe vessel patency. The Thrombolysis in Myocardial Infarction [TIMI] scale was originally developed to grade coronary blood flow based on assessment of contrast opacification of the infarct artery in myocardial infarction [MI](1985). A variation of this scale (Thrombolysis in cerebral infarction [TICI]) was developed to grade perfusion in the intracranial cerebral circulation (Higashida and Furlan, 2003). Both of these scales represent global reperfusion distal to the lesion but not necessarily recanalisation of the occlusion.

Table 3-9 Arterial Occlusive Lesion Recanalisation Score

Score	AOL Recanalisation
0	No recanalisation of the primary occlusive lesion
1	Incomplete or partial recanalisation of the primary occlusive lesion with no distal flow
2	Incomplete or partial recanalisation of the primary occlusive lesion with any distal flow
3	Complete recanalisation of the primary occlusive lesion with any distal flow

AOL=arterial occlusive lesion

Statistics

The statistical analyses presented were chiefly performed using IBM SPSS Statistics for Windows (version 24.0, Armonk, New York: IBM Corp.). Microsoft Excel was also used.

Categorical data was described by n (%), mean and standard deviation [sd] for normally distributed data, median and interquartile range [IQR] for data which was nor normally distributed and where appropriate 95% confidence intervals [CI] were used for proportions.

Chapter 4 Comparison of Three Commonly Used Software for CTP

Introduction

Patient selection for reperfusion therapy is shifting from time-window -defined eligibility towards a more individual (or physiological) approach based on imaging profile.

Out of the landmark trials introduced in, SWIFT PRIME, EXTEND-IA, DAWN, DEFUSE-3, SELECT-2 and Angel-ASPECT used perfusion imaging as part of criteria to select patients for EVT -all of which used RAPID (Ischemaview) software to process the images (Saver et al., 2015, Campbell et al., 2015, Nogueira et al., 2017, Albers et al., 2018, Sarraj et al., 2023, Huo et al., 2023).

There are, however, several post-processing software available (research, commercial or available for free). Differences in post-processing algorithms may lead to varying results. These include defining the arterial input function and venous output function, motion correction, smoothing, selection of symmetry axis and selection of reference tissue -which is particularly relevant given core definition on CTP is most often based on a relative measure (CBF or CBV) as opposed to MRI which uses DWI and so is not dependent on reference tissue volumes (Soares et al., 2009).

Previous comparison of software packages has focused on the predictive value of RAPID perfusion maps in comparison to other software on follow-up MRI volume, or has focused on comparing ischaemic core from other software to RAPID (Austein et al., 2016, Koopman et al., 2019). A comprehensive analysis of ischaemic core and penumbra volumes using one software (MIStar) to compare six post-processing (six different deconvolution methods) methods showed marked variation (Bivard et al., 2013).

As CTP use becomes increasingly widespread, centres may opt to use different software for research, practicality or cost reasons. This may impact treatment decisions if different software produce different estimates of core and penumbra volumes.

We therefore aimed to examine the differences in parameters produced by three commonly used software platforms and how this may impact treatment decisions.

Methods

Patients

Imaging data from a local Stroke Research Imaging database of four prospective acute stroke studies – in which patients underwent multimodal CT less than 6h after symptom onset, were pooled. Data were used according to ethical approval and consent for secondary analysis. This was a convenience sample of available imaging and was not based upon a literature search because imaging needed to be manually run across three software.

These studies, MASIS, POSH, ATTEST and Australian TNK are detailed in General Methods (Chapter 3) (Wardlaw et al., 2013a, Macdougall et al., 2014, Huang et al., 2015, Parsons et al., 2012). Informed consent was obtained in all studies; consent forms included explicit permission for secondary analyses as part of collaborations.

In brief, MASIS and POSH were observational studies evaluating feasibility of complex imaging and the pathophysiology of hyperglycaemia, respectively (Wardlaw et al., 2013a, Macdougall et al., 2014). ATTEST and Australian TNK were phase 2 randomised-control trials which compared two different IV thrombolytic agents within 4.5h and 6h of symptom onset, respectively (Huang et al., 2015, Parsons et al., 2012). All patients were recruited within either 4.5 or 6 hours of AIS onset, with the Australian TNK population having additional imaging inclusion criteria of a CTP lesion greater than 20% of the ischaemic core with an associated vessel occlusion on CTA (Wardlaw et al., 2013a, Macdougall et al., 2014, Huang et al., 2015, Parsons et al., 2012).

Endovascular treatment was not undertaken.

Clinical details included demographic and risk factor data, admission blood glucose, known diagnosis of diabetes, National Institutes of Health Stroke Scale [NIHSS] (Brott et al., 1989) scores at onset and 24 h, estimated premorbid modified Rankin Scale (mRS) (van Swieten et al., 1988), day 90 mRS, time from symptom onset to computed tomography [CT] and to treatment (if applicable).

CT Acquisition

For all studies, acute CT imaging included whole brain NCCT, CTP and single-phase CTA using 64 or 320 slice scanners. Imaging is detailed in General Methods.

CT-Perfusion Analysis

CTP scans were processed using the following three software:

- MIStar version 3.2 (Apollo) – images were uploaded and analysed separately by two users (VB and AM) who manually highlighted regions of interest and supervised the AIF and VOF placement. Disagreements (i.e. with respect to hemisphere involvement or lesion presence) were resolved by both users analysing the images again. The software defined ischaemic core as DT>3s and rCBF<30% and penumbra as DT>3s (minus the ischaemic core).
- Brainomix (versions 9.001 to 11.001) – an automated software with no user input, ischaemic core was defined as Tmax>6s and rCBF<30% and penumbra as Tmax>6s.
- RAPID version 4.7 (Ischemaview) – an automated software with no user input, ischaemic core was defined as Tmax>6s and rCBF<30% and penumbra as Tmax>6s.

Perfusion lesions were classified according to hemisphere, size of total lesion volume, ischaemic core volume and size of potentially reversible ischaemia (mismatch, penumbra) as detailed in Table 4-1 below.

Software processing failure was defined as failure to produce an image or producing an image with bilateral lesions. None of studies reported bilateral lesions.

Target Mismatch

The imaging inclusion criteria used by the DEFUSE 3 and EXTEND trials were explored (Albers et al., 2018, Ma et al., 2019).

DEFUSE 3 Imaging Inclusion Criteria

The DEFUSE 3 trial included patients with ICA or MCA-M1 occlusions and a favourable target mismatch profile, defined as ischaemic core lesion<70ml, a ratio of total volume of ischaemic lesion to ischaemic core (Tmax>6s over CBF<30%) of $\geq$1.8 and a penumbra lesion $\geq$15ml (Albers et al., 2018).

EXTEND Imaging Inclusion Criteria

The EXTEND trial defined target mismatch as ischaemic core lesion<70ml, a ratio of volume of ischaemic lesion to ischaemic core (Tmax>6s over CBF<30%) of >1.2 and an absolute difference in volume >10ml (difference between perfusion lesion and core lesion) (Ma et al., 2019).

Table 4-1 Definition of Hypoperfusion According to Different Software

	Method	AIF + VOF	Ischaemic core	Hypoperfusion	Algorithm
MIStar	Two-observer consensus, regions of interest highlighted manually	Automatic (user-supervised)	DT>3s and rCBF<30%	DT>3s	Deconvolution
Brainomix	Automatic	Automatic	Tmax>6s and rCBF<30%	Tmax>6s	
RAPID	Automatic	Automatic	Tmax>6s and rCBF<30%	Tmax>6s	Delay-insensitive

AIF=arterial input function placement, VOF=venous output function placement, DT=delay time, rCBF=relative cerebral blood flow

Failure to process was defined as the software flagging up a failure to process, both sides of the brain being abnormally flagged as involved (e.g. whole brain flagged as ischaemic) or reports of a negative mismatch (i.e. Tmax>6s or DT>3s being labelled as less than rCBF<30%).

CT Angiogram Analysis

Site of Occlusion

The presence of baseline large vessel occlusion [LVO] was determined for hemisphere and site (Table 4-2) by consensus of at least two experienced stroke neurologists or neuroradiologists. The MASIS and POSH cohorts were assessed by KM (>10 years' experience), CP (>2 years' experience) and SYF (>2 years' experience). The ATTEST and Australian TNK scores had previously been analysed and only scans with flagged occlusions were analysed by KM and SYF; in cases of disagreement, the KM/SYF score was used. For this analysis, the licensed imaging software MIStar version 3.2 (Apollo) was used. Scans were assessed using maximum intensity projection [MIP] of 5mm, 10mm, 15mm and 20mm thickness.

Table 4-2 Classification of LVO Sites

Occlusion	Description
ICA	L or T shaped occlusion at the ICA-MCA bifurcation
Prox M1	Proximal M1 occlusion, within first 10mm of M1 segment of MCA
Dist M1	Distal M1 occlusion, remaining portion of M1 segment of MCA
M2	M2 segment of MCA occlusion
PCA	Any PCA occlusion
ACA	Any ACA occlusion

ICA=internal carotid artery, MCA=middle cerebral artery, M=portion of MCA, PCA=posterior cerebral artery, ACA=anterior cerebral artery.

Collateral Scoring

Collateral vessels determined by consensus of KM and SYF using the modified Tan score (see General Methods) (Tan et al., 2009b). Images were assessed at a MIP of 20mm on the MIStar software.

Statistical Analysis

Several comparisons between software were undertaken. The following analyses compared scans between individual software i.e. RAPID compared with MIStar, RAPID compared with Brainomix, Brainomix compared with MIStar. Scans which failed to process, scans showing a negative mismatch and scans with both sides affected were excluded. For each comparison, the following analyses took place.

Agreement between Hemispheres

Agreement between hemispheres was analysed using the Chi- squared method.

This is a non-parametric tool which assess differences between a nominally measured variable. The distribution of the data does not affect the outcome and the test provides detail about how each group performed within the study. It is a significance statistic but not a measure of strength. Limitations include large sample size requirements and its difficulty in handling large numbers of categories – neither of which are applicable to this analysis (McHugh, 2013).

Hemispheres were classified as being right sided, left sided or not applicable in the case of no lesion.

Comparison between Lesions

The following analyses were done for pairwise comparison between hypoperfusion defects.

Cohen's Kappa

The Cohen's κ coefficient was calculated to measure the strength of agreement.

Cohen originally suggested that values ≤ 0 indicated no agreement, 0.01-0.20 indicated none to slight agreement, 0.21-0.40 indicated fair agreement, 0.41-0.60 indicated moderate agreement, 0.61-0.80 indicated substantial agreement and 0.81-1.00 indicated almost perfect agreement (Cohen, 1960). An updated paper suggested that the original values were too low when applied to clinical data and instead proposed that 0-0.2 indicated no agreement, 0.21-0.39 indicated minimal agreement, 0.4 to 0.59 indicated weak agreement, 0.6 to 0.79 indicated moderate agreement, 0.8 to 0.9 indicated strong agreement and >0.9 indicated almost perfect agreement. The most commonly reported limitation is that the interpretation may be too lenient for health statistics (McHugh, 2012).

Bland-Altman

Absolute and percentage differences between core and penumbra volumes were calculated in separate analyses between individual software. The separate software analyses were as follows: MIStar minus RAPID, RAPID minus Brainomix, MIStar minus Brainomix. Bias and 95% limits of agreement were calculated by the Bland-Altman method.

Bland and Altman introduced a graphical method of comparing the agreement between quantitative measurements (Bland and Altman, 1986). These scatter plots are useful for evaluating agreement, visualising systemic bias and identifying outliers. The assumptions of a Bland-Altman plot are that the defined limitations of agreement are acceptable to the

population being measured, and that the data falls within a normal distribution pattern (Giavarina, 2015). Sample size is important too -without large numbers (i.e. 100 to 200 subjects) discrepancies between measurements may not be detected – although this is not relevant to our data given our sample size (Bunce, 2009).

Intraclass Correlation Coefficient

The intraclass correlation coefficient [ICC] was calculated to describe how closely lesion volumes resembled each other for each pairwise comparison.

First introduced in 1921, the concept of the ICC has evolved from examining the familial resemblance between siblings to a widely used measurement of the ability of two separate raters to measure variables similarly (RA, 1921, Bobak et al., 2018). Unlike the statistical methods previously mentioned, the ICC is subject to a sensitivity of assumption of both normality within the distribution and homogenous variance which must be taken into account (Bobak et al., 2018).

Target Mismatch Analysis

Agreement between software for target mismatch was analysed. Target mismatch was defined as the DEFUSE-3 definition: an ischaemic core volume <70ml, mismatch volume ≥15ml and a mismatch ratio of ≥1.8. The DEFUSE-3 investigators defined mismatch ratio as volume of ischaemic tissue over the ischaemic core volume i.e. Tmax>6s divided by the ischaemic core (Albers et al., 2018). For the TNK cohort, the Brainomix mismatch was calculated manually.

Results

The ATTEST, POSH, MASIS and Australian TNK trials are described in greater detail in General Methods (Chapter 3).

There were 376 patients recruited in total however the clinical database listed 374 patients -many of whom had missing data. This is described in the below flowchart –as is the

number of evaluable CTP which is further broken down into studies. There were 331 patients with CTP scans available for analysis. Of note, the oldest software (MIStar) had the fewest ‘non-evaluable’ scans.

The baseline characteristics of the patient are shown in Table 4-3. The mean age and standard deviation were 70±12 and median baseline NIHSS score was 12. Median time from onset to CTP was 2h56 (IQR 2h20 to 3h43)

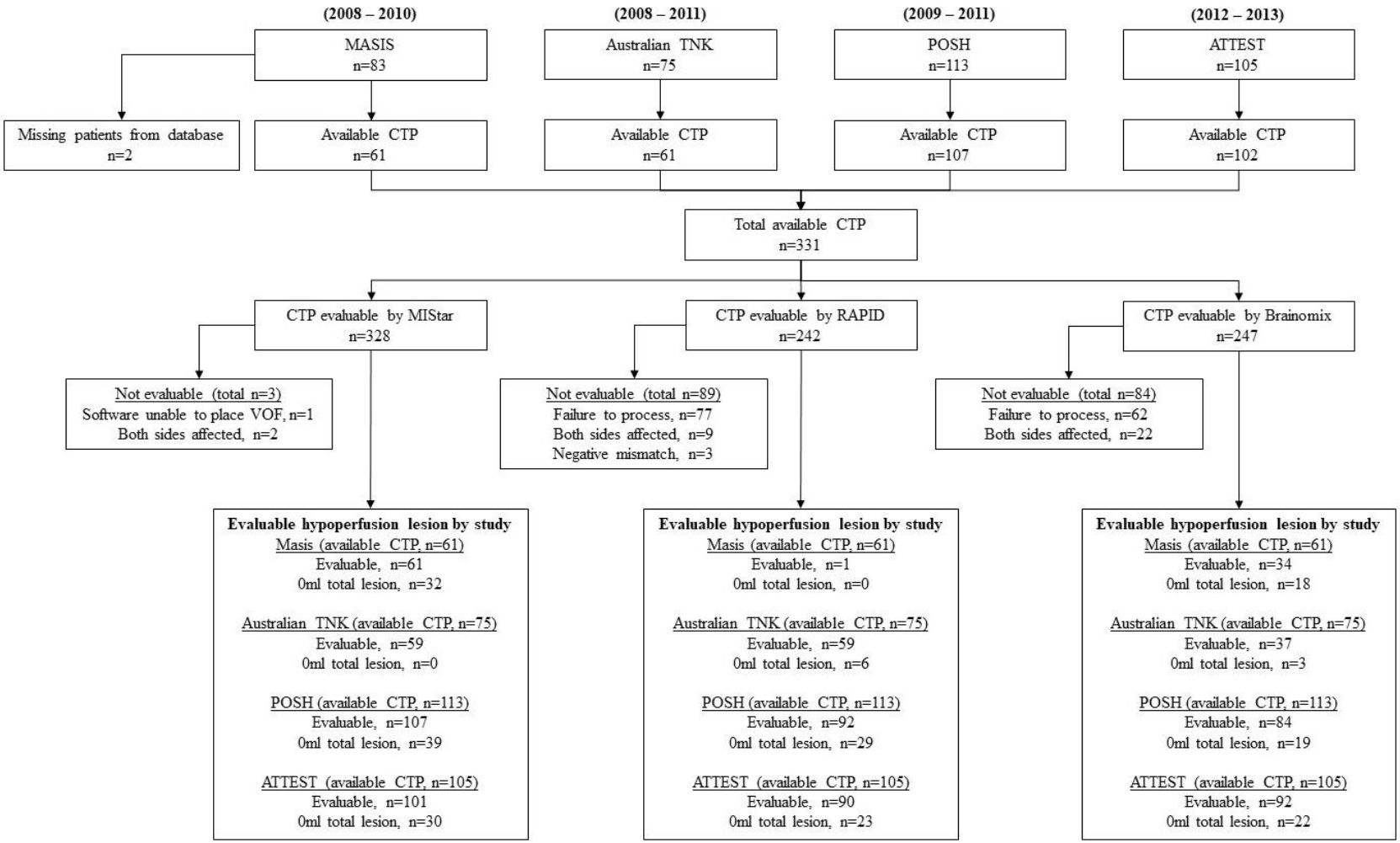

MASIS=Multi-Centre Acute Stroke Imaging Study, Australian TNK=Australian Tenecteplase Study, POSH=Post-Stroke Hyperglycaemia and Brain Arterial Patency Study, ATTEST= Alteplase-Tenecteplase Trial Evaluation for Stroke Thrombolysis, n=number, CTP=computed tomography perfusion, VOF=venous output function

Figure 4-1 Flowchart Detailing Inclusion Strategy of CTP Scans for Analysis

Table 4-3 Clinical Characteristics

Variable	Value, N=331
Age (n=315), range	32 – 95
Age (years), mean±SD	70±12
Age >70 years, n (%)	175 (53)
Risk Factors and Medical History	
Gender, n male (%)	182 (55)
Ischaemic heart disease, n (%)	76 (23)
Previous stroke or TIA, n (%)	61 (18)
Diabetes mellitus, n (%)	50 (15)
Hypertension, n (%)	181 (55)
Atrial fibrillation, n (%)	98 (30)
Current smoker, n (%)	93 (28)
Hyperlipidaemia, n (%)	160 (48)
Antiplatelet therapy, n (%)	170 (51)
Statin, n (%)	132 (426)
Antidiabetic agent, n (%)	28 (8)
Antihypertensive agent, n (%)	149 (45)
Stroke Characteristics	
Hemisphere	
Right, n (%)	135 (41)
Left, n (%)	163 (49)
Oxfordshire Classification	
TACS, n (%)	117 (35)
PACS, n (%)	102 (31)
LACS, n (%)	22 (7)
POCS, n (%)	9 (3)
Systolic blood pressure on admission (mmHg), mean±SD	149±23
Diastolic blood pressure on admission (mmHg), mean±SD	78±16
Number treated with IV rTPA, n (%)	251 (76)
Onset to treatment time (hours), median (IQR)	2h58 (2h30, 3h30)
Onset to CTP time (hours), median (IQR)	2h56 (2h20, 3h43)
Baseline NIHSS, median (IQR)	12 (7, 16)
24 hours NIHSS, median (IQR)	6 (2, 15)

Blood glucose on admission (mmol/L), mean±SD	7.1 (2.7)
Hyperglycaemia on admission (i.e. ≥7 mmol/l), n (%)	119 (36)
Pre-stroke excellent function (mRS 0-1), n (%)	58 (18)
Pre-stroke good function (mRS≤2), n (%)	77 (23)
Day 90 mRS outcome	
mRS 0, n (%)	39 (12)
mRS 1, n (%)	51 (15)
mRS 2, n (%)	57 (17)
mRS 3, n (%)	62 (19)
mRS 4, n (%)	40 (12)
mRS 5, n (%)	21 (6)
mRS 6, n (%)	43 (13)

N=number, SD=standard deviation, TIA=transient ischaemic attack, TACS=total anterior circulation stroke, PACS=partial anterior circulation stroke, LACS=lacunar stroke, POCS=posterior circulation stroke, IV=intravenous, rTPA=recombinant tissue plasminogen activator, IQR=interquartile range, CTP=computed tomography perfusion, NIHSS=National Institute of Health Stroke Scale, mRS=modified Rankin scale.

Pairwise Comparison

We compared software in pairs. Each comparison was separated into scans processed by both software, scans processed by one software and scans which were not processed by either software.

Software Processing

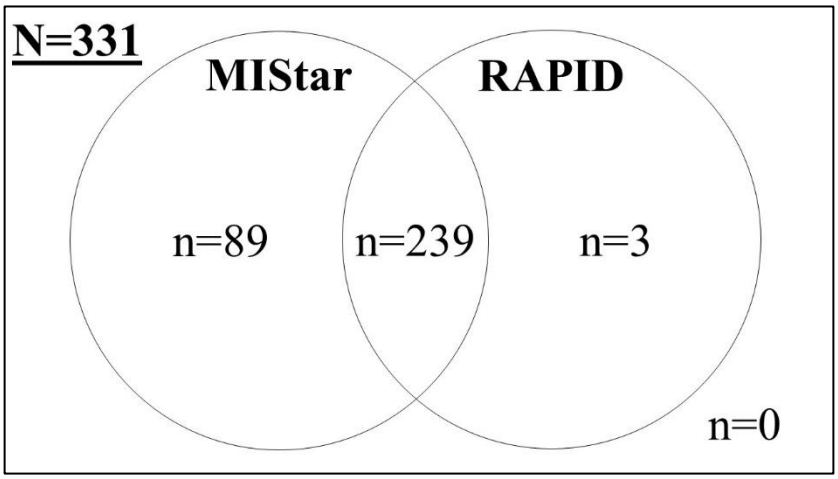

Figure 4-2 MIStar Compared with RAPID: Venn Diagram Detailing Scans which were Processed by the Software

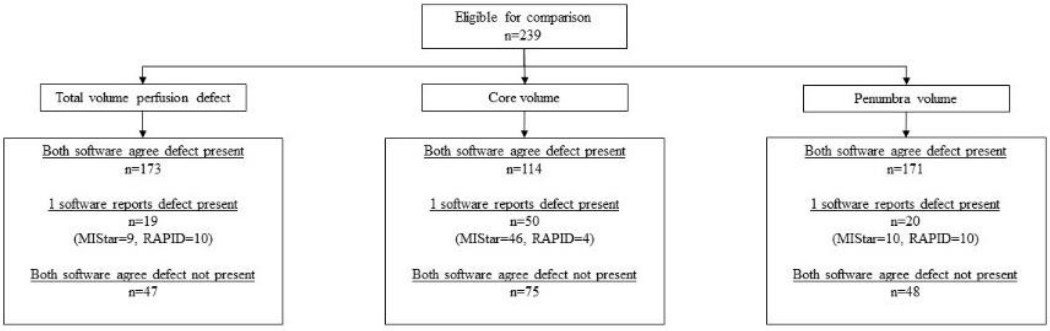

Figure 4-3 MIStar Compared with RAPID: Flowchart Detailing Breakdown of Scans Processed by Both Software

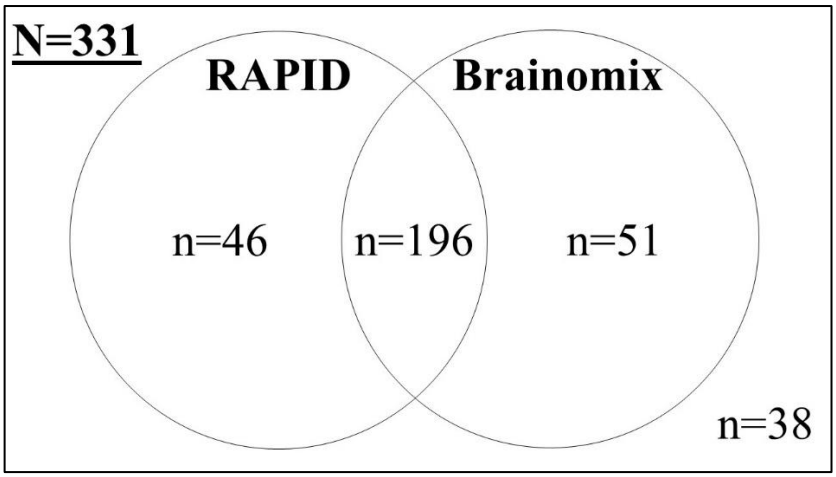

Figure 4-4 RAPID Compared with Brainomix: Venn Diagram Detailing Scans which were Processed by the Software

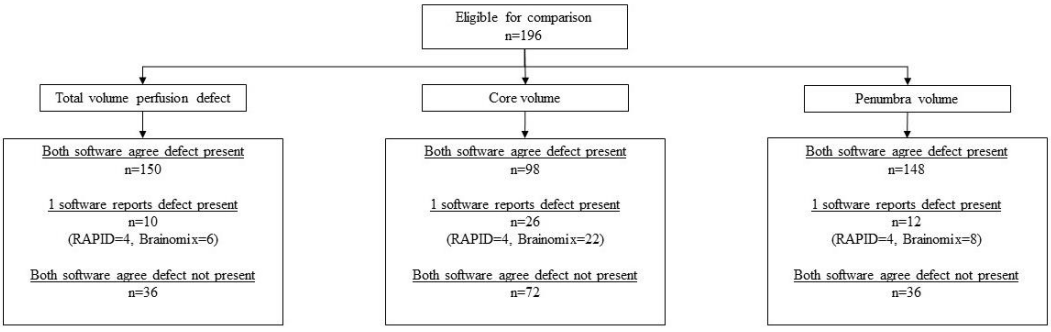

Figure 4-5 RAPID Compared with Brainomix: Flowchart Detailing Breakdown of Scans Processed by both Software

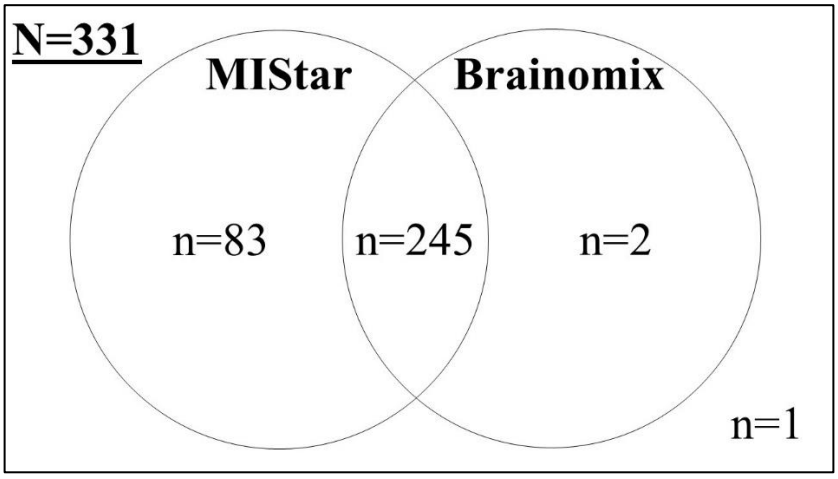

Figure 4-6 MIStar Compared with Brainomix: Venn Diagram Detailing Scans which were Processed by the Software

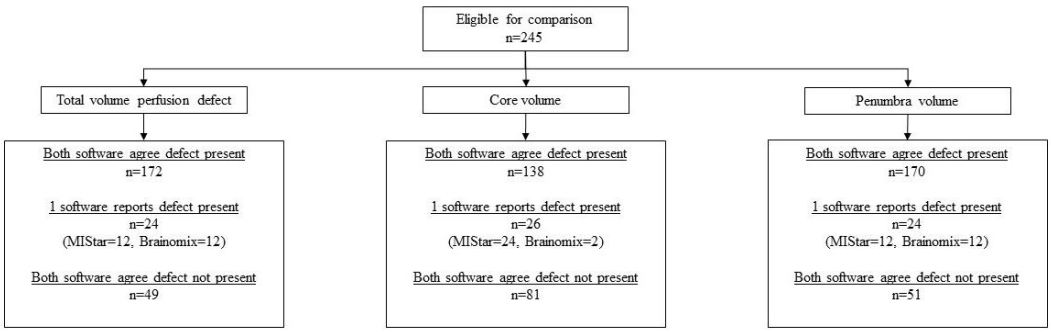

Figure 4-7 MIStar Compared with Brainomix: Flowchart Detailing Breakdown of Scans Processed by Both Software

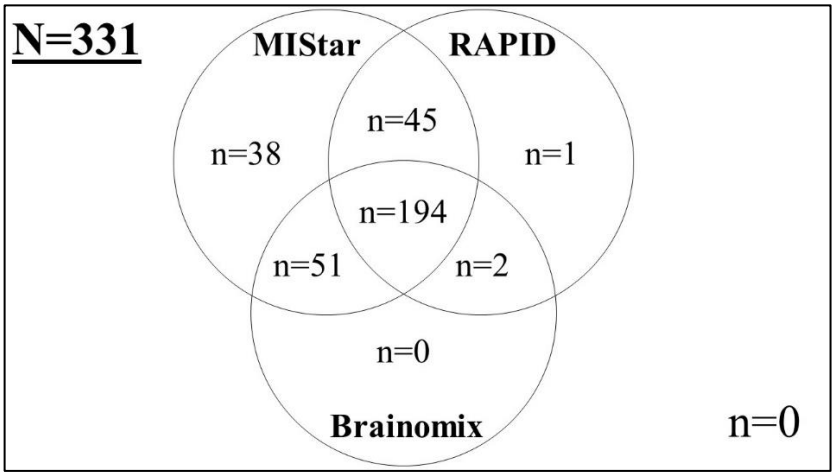

Figure 4-8 CTP Scans which were Processed by All Software

As mentioned above, the oldest software (MIStar) is able to process the most scans on a stand-alone basis -27% and 25% when compared pairwise with RAPID and Brainomix accordingly. When all three software were compared, MIStar was still able to process the most CTP scans on a stand-alone basis –11%.

Perfusion Defect Volumes

Pairwise comparison of perfusion defect volumes (as separated into total perfusion defect, core and penumbra) are listed below in Table 4-4 and Bland-Altmann plots for volumetric agreement are included in Table 4-5.

Affected Hemisphere

Absolute agreement for affected hemisphere was above 90% for all pairwise comparisons – of note, all disagreement was based on one software not recognising any perfusion defect -there were no instances where different hemispheres were suggested. Cohen's kappa coefficient suggested high strength of agreement (>0.8) across the software.

Total Perfusion Defect

Overall absolute agreement for presence of perfusion deficit was >90% for all pairwise comparisons with the highest strength of agreement being between RAPID and Brainomix (Cohen's kappa coefficient 0.85, 95% CI 0.75 to 0.94). Inter-rater reliability was within excellent range (>0.9) as analysed by intra-class coefficient for lesion volumes.

Core Volume

Compared with total deficit, agreements for presence of core were smaller with the lowest being between MIStar and RAPID (absolute agreement for presence of core being 92%, Cohen's kappa coefficient 0.58, 95% CI 0.49 to 0.68). Inter-rater reliability for volume was lowest between RAPID and Brainomix (intra-class coefficient 0.89 (0.78 to 0.93).

Penumbra Volume

Absolute agreement for presence of perfusion deficit was >90% for all pairwise comparisons. Strength of agreement was highest between RAPID and Brainomix - Cohen's kappa coefficient 0.82 (95% CI 0.72 to 0.92) and lowest between Brainomix and MIStar - Cohen's kappa coefficient 0.74 (95% CI 0.65 to 0.84). Inter-rater reliability for volume was highest between MIStar and RAPID, intra-class correlation coefficient 0.89 (95% CI 0.85 to 0.91) and lowest between MIStar and Brainomix, intra-class correlation coefficient 0.81 (95% CI 0.67 to 0.87).

Bland Altmann Plots

Table 4-5 demonstrates that total perfusion defects are spread equally around the mean difference (which is close to 0) in all three pairwise comparisons. In terms of core and penumbra volume differences, the steep lines of dots represent patients in whom one software detected a perfusion defect and the other did not (i.e. 0ml perfusion defect) making the mean difference 50% of the total difference resulting in a x=y/2 line. MIStar software, is more likely to display this in both core and penumbra. The general pattern is that Brainomix produces smaller core volumes than both MIStar and RAPID, smaller penumbra volumes than MIStar and larger penumbra volumes than RAPID. RAPID produces smaller core volumes than MIStar but larger penumbra volumes.

Target Mismatch Agreement

Agreement for meeting DEFUSE-3 criteria is strong across the pairwise comparisons – absolute agreement >90% and Cohen's kappa coefficient >0.8 throughout. Agreement for EXTEND is not as strong, with best agreement being between MIStar and RAPID (absolute agreement 88%, Cohen's kappa coefficient 0.74 (95% CI 0.66 to 0.83)) and worst between RAPID and Brainomix (absolute agreement 83%, Cohen's kappa coefficient 0.62 (95% CI 0.51 to 0.74)).

Table 4-4 Pairwise Comparison of Perfusion Defect Volumes

	MIStar and RAPID, N=239	RAPID and Brainomix, N=196	MIStar and Brainomix, N=245
Hemispheres			
Absolute agreement, %	92%	92%	91%
Cohen's κ coefficient (95% CI)	0.87 (0.82 to 0.92)	0.88 (0.82 to 0.94)	0.86 (0.81 to 0.91)
Total perfusion defect			
Absolute agreement %	92%	95%	90%
Cohen's κ coefficient (95% CI)	0.78 (0.69 to 0.87)	0.85 (0.75 to 0.94)	0.74 (0.64 to 0.84)
Inter-rater reliability			
Software 1, mean±SD (ml)	MIStar, 49±47	RAPID, 55±53	MIStar, 45±46
Software 2, mean±SD (ml)	RAPID, 53±54	Brainomix, 56±50	Brainomix, 51±51
Inter-item correlation matrix	0.87	0.87	0.84
Intra-class correlation coefficient, (95% CI)	0.92 (0.91 to 0.94)	0.93 (0.91 to 0.95)	0.91 (0.88 to 0.93)
p Value	<0.001	<0.001	<0.001
Core volume			
Absolute agreement %	79%	87%	89%
Cohen's κ coefficient (95% CI)	0.58 (0.49 to 0.68)	0.73 (0.64 to 0.83)	0.78 (0.70 to 0.86)
Inter-rater reliability			
Software 1, mean±SD (ml)	MIStar, 15±22	RAPID, 15±26	MIStar, 15±23
Software 2, mean±SD (ml)	RAPID, 14±24	Brainomix, 9±15	Brainomix, 9±15
Inter-item correlation matrix	0.89	0.95	0.94
Intra-class correlation coefficient, (95% CI)	0.93 (0.92 to 0.95)	0.89 (0.78 to 0.93)	0.90 (0.74 to 0.95)
p Value	<0.001	<0.001	<0.001
Penumbra volume			
Absolute agreement %	92%	94%	90%
Cohen's κ coefficient (95% CI)	0.77 (0.68 to 0.87)	0.82 (0.72 to 0.92)	0.74 (0.65 to 0.84)
Inter-rater reliability			
Software 1, mean±SD (ml)	MIStar, 33±33	RAPID, 39±40	MIStar, 29±30
Software 2, mean±SD (ml)	RAPID, 39±42	Brainomix, 47±42	Brainomix, 43±42
Inter-item correlation matrix	0.83	0.78	0.76
Intra-class correlation coefficient, (95% CI)	0.89 (0.85 to 0.91)	0.87 (0.82 to 0.90)	0.81 (0.67 to 0.87)
p Value	<0.001	<0.001	<0.001
DEFUSE 3 Target mismatch criteria			
Absolute agreement %	95%	92%	94%
Cohen's κ coefficient (95% CI)	0.87 (0.81 to 0.94)	0.81 (0.72 to 0.90)	0.86 (0.79 to 0.93)
EXTEND Target mismatch criteria			
Absolute agreement %	88%	83%	86%
Cohen's κ coefficient (95% CI)	0.74 (0.66 to 0.83)	0.62 (0.51 to 0.74)	0.71 (0.62 to 0.80)

This table shows comparison of volumes first separated into three columns detailing the three pairwise comparisons and then separated (by rows) into total perfusion, core and penumbra volumes. Finally, agreement for both DEFUSE-3 and EXTEND criteria were assessed. The previously described statistical tests were used appropriately, depending on measurement. N=number, CI=confidence intervals, SD=standard deviation, ml=millilitre, DEFUSE3=Diffusion and Perfusion Imaging Evaluation for Understanding Stroke Evolution 3, EXTEND=Extending the Time for Thrombolysis in Emergency Neurological Deficits.

Table 4-5 Bland-Altman Plots Demonstrating Software Agreement

	MIStar - RAPID, N=239	**RAPID - Brainomix, N=196**	**MIStar - Brainomix, N=245**
Total perfusion defect	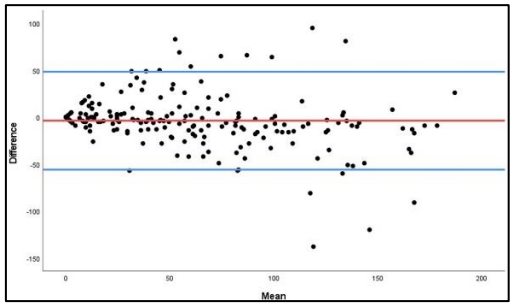	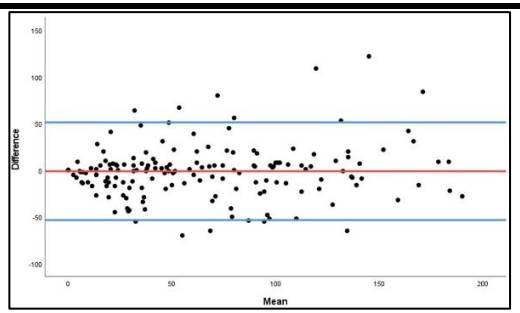	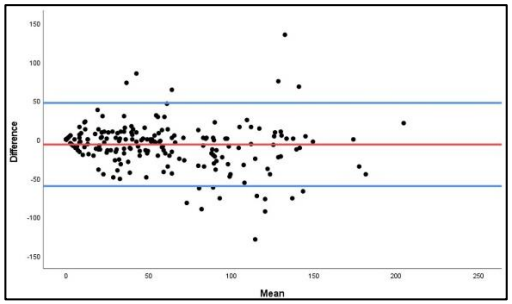
Core volume	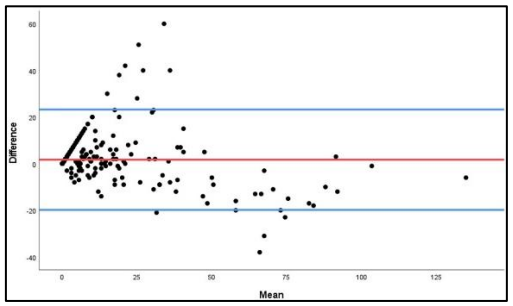	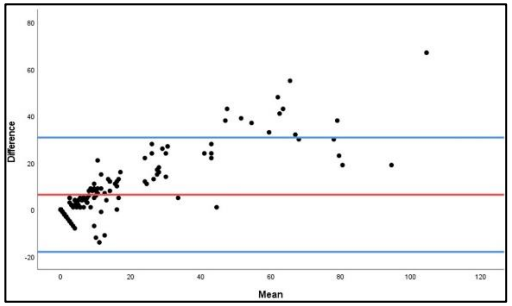	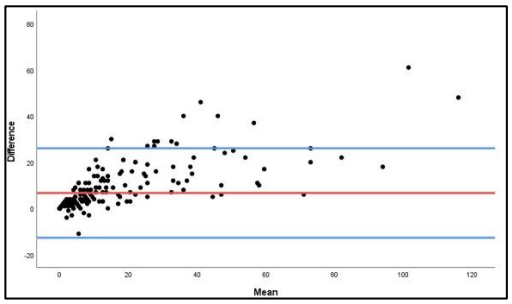
Penumbra	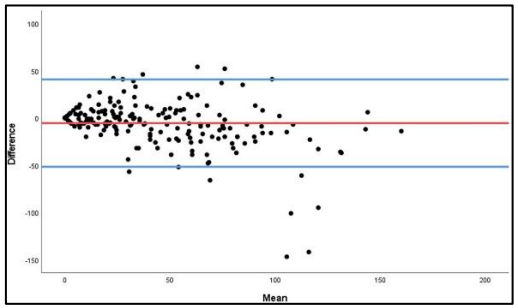	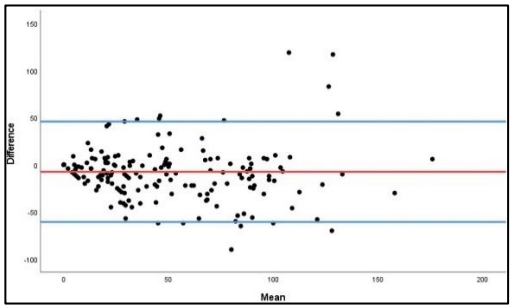	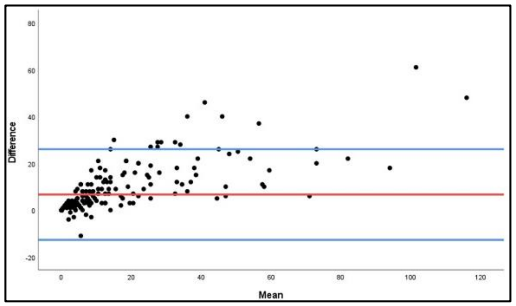

This table details the Bland-Altman plots, separated into columns of the three pairwise comparisons and rows detailing the three volume agreements measured: total perfusion lesion, core and penumbra volumes. N=number

Target Mismatch for all Software

There were 194 scans which were processed by all three software and were eligible for comparison for target mismatch. We assessed eligibility against both DEFUSE-3 and EXTEND criteria as demonstrated below in Figure 4-9 and Figure 4-10.

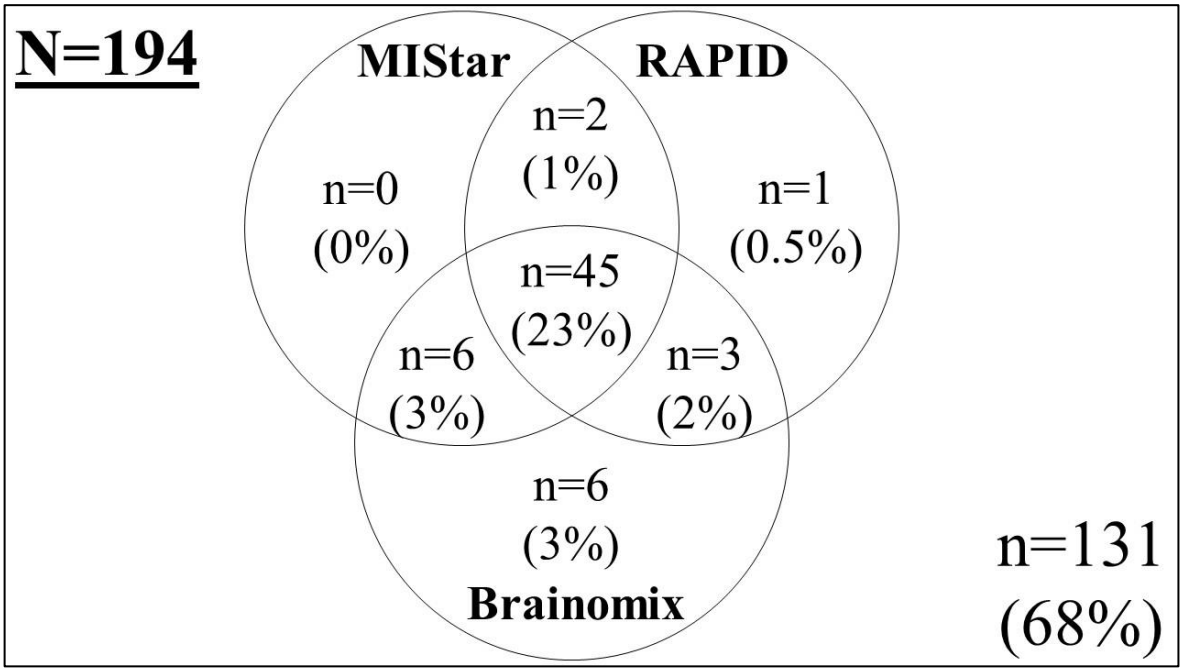

Figure 4-9 Venn Diagram Showing DEFUSE-3 Eligibility Across All Three Software

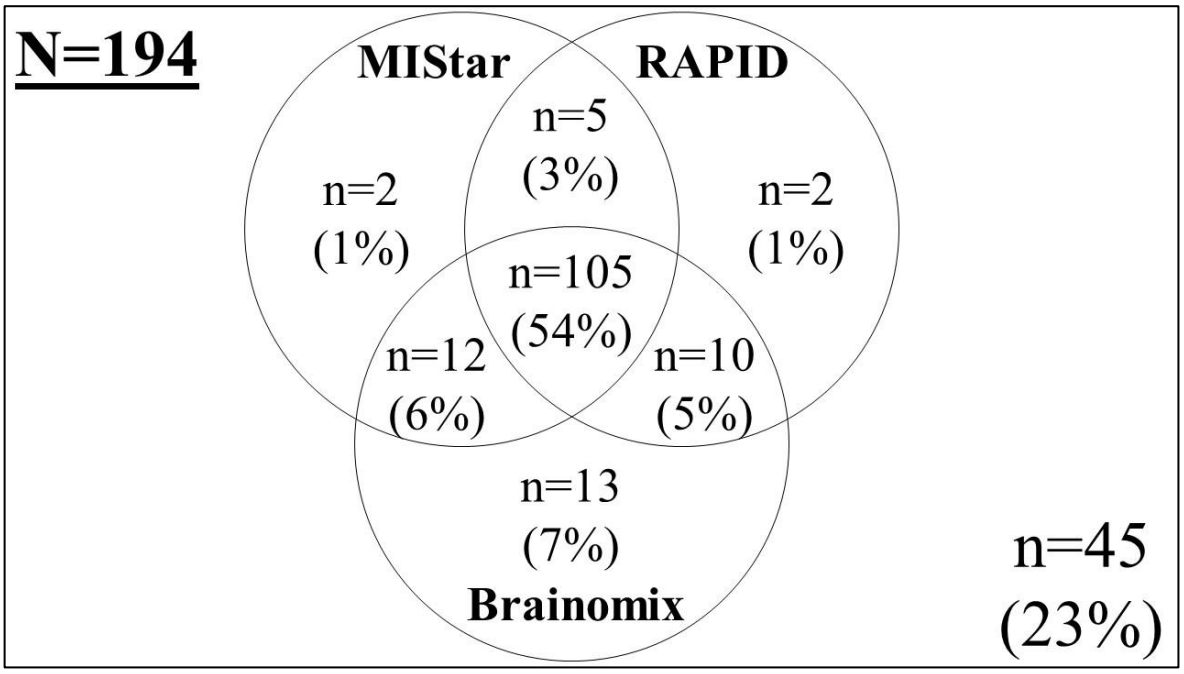

Figure 4-10 Venn Diagram Showing EXTEND Eligibility Across All Three Software

Absolute agreement for meeting target mismatch criteria was 91% and 77% for DEFUSE-3 and EXTEND respectively. Brainomix was the software with the highest amount of target mismatch eligibility on a stand-alone basis for both criteria (3% for DEFUSE-3 and 13% for EXTEND).

Discussion

We evaluated the agreement between CT perfusion studies processed with MIStar, RAPID and Brainomix and compared the differences between values for total perfusion lesion, core and penumbra volumes. We additionally compared the different software with respect to CTP studies meeting a definition of target mismatch.

Initially, comparison papers focused on accuracy of perfusion software, using follow up infarct volumes [FIV] as the standard (Koopman et al., 2019, Austein et al., 2016).

Koopman et al. analysed thirty-five datasets from EVT patients from the MR CLEAN trial and FIV were determined using NCCT five to seven days post-onset – and where this wasn't available, the twenty-four hour NCCT was used (exact number not reported). Austein et al used either NCCT or DWI to determine FIV in one hundred and forty-seven EVT patients between days one to eight following onset.

The Randomized Trial of Tirilazad Mesylate in Patients With Acute Stroke [RANTTAS] investigators showed the correlation between subacute (as defined by day six to day 11) NCCT infarct volume and clinical outcome to be moderate (Saver et al., 1999) and DWI has greater spatial resolution and sensitivity to ischaemic injury (van Everdingen et al., 1998). DWI lesion volumes change over several days and therefore consistent timing of follow-up is relevant. Brain swelling may also confound measurements. Finally, the problem with comparing different imaging modalities is that the total volume may not reflect anatomical distribution (i.e. infarct outside a perfusion lesion matched by perfusion lesion that does not infarct would cancel one another out and appear to agree perfectly). It is only possible to discriminate core from penumbra by knowledge of recanalization/reperfusion, which is based on an arbitrary time point. This is especially problematic in older studies and somewhat more uniformly available only for thrombectomy cases.

There is one retrospective analysis comparing RAPID and Brainomix software in patients admitted with stroke symptoms and had confirmed LVO on CTA who underwent CTP for extended window thrombectomy analysis (6 to 24 hours from symptom onset) which found high correlation for ischaemic core and penumbral volumes and 85% for meeting DEFUSE-3 thrombectomy criteria (Mallon et al., 2022). This was a retrospective analysis in a modest cohort of patients who were more likely to have perfusion defects and inter-rater reliability and volume comparison was not performed.

We sought to compare software output for inter-rater reliability and volume output in a large multi-centre imaging dataset of patients recruited prospectively to stroke trials within 6 hours' onset and assess eligibility against both DEFUSE-3 and EXTEND criteria. This is the scenario which clinicians will face at the time of patient presentation and we aimed to explore how this may influence treatment decision-making in a high-pressure, time-sensitive environment.

MIStar had the fewest (3 out of 328 - 1%) non-evaluable scans but the most (101 - 31%) 0ml total perfusion defects. Of note, there were no 0ml perfusion defects in the Australian TNK population who were selected using MIStar on the basis of significant mismatch (Parsons et al., 2012). By contrast, RAPID and Brainomix failed to process a higher proportion of the older scans. For example, of 61 available scans for MASIS, MIStar processed 61 (of which 32 were 0ml perfusion defects), RAPID processed 1 (2%) and Brainomix processed 34 (56%) (of which 18 were 0ml perfusion defects). Given that the MASIS paper reports 63 (76%) patients to have visible ischaemic lesions on structural imaging (Wardlaw et al., 2013a), this may reflect the limitations of analysing old data on new software. The variation between the software may represent differences in how software process images i.e. MIStar is more likely to produce an image regardless of data quality whereas RAPID or Brainomix do not produce necessarily produce images if data quality is poor. In these cases, not producing an output may be more informative than producing one.

The Bland Altmann plots demonstrate that overall Brainomix software is most conservative when it comes to assessing core volume. Both MIStar and Brainomix produce larger volumes of penumbra than RAPID. All three software use rCBF<30% to define ischaemic core. Commercial software purposefully under-estimates the ischaemic core volume by

around 15ml with best agreement between DWI lesion and CBF revealed to be rCBF<38% (Cereda et al., 2016). This is to ensure patients in whom CTP acquisition is sub-optimal and core is over-estimated do not miss out on reperfusion therapy.

We used a local Stroke Research Imaging Database of patients with AIS recruited to 4 studies within 6 hours of onset. There were 2 RCTs assessing thrombolysis of which one of the criteria for Australian TNK was a mismatch lesion on CTP. The concern being this population is likely to have a larger proportion of more disabled patients with LVO and would not accurately represent a typical stroke population. The Sentinel Stroke National Audit Programme [SSNAP] data records admissions to HASUs in England and Wales. Our population compares favourably to the 2023 data respectively in terms of age (mean 70±12 versus median 76 with IQR 65-86), female gender (45% versus 47%) and vascular risk factors such as hypertension (55% versus 56%), diabetes mellitus (15% versus 24%) and previous AIS/TIA (18% versus 24%). Our population has larger proportions of both AF (30% versus 19%) and patients receiving rTPA (76% versus 10%) which is to be expected in trials recruiting rTPA eligible patients where advanced neuroimaging is used. This is also reflected in our median NIHSS (12 with IQR 7-16 versus 4, IQR 2, 10) (SSNAP, 2023). Given that the aim of this chapter was to assess the imaging output of software programs this should not impact the findings other than the increased likelihood of there being a lesion to detect on CTP.

We performed a retrospective complete-case analysis due to availability. The main advantage of this approach was simplicity and availability of large data. The disadvantages included the loss of information when discarding incomplete cases (potentially missing out on large amounts of data contributing to bias and loss of precision). For example, our database held 374 cases despite the trials recruiting 376 patients in total. Further exclusions took place in that only 331 CTP scans were available for analysis. The clinical details table revealed more missing data.

Systematic bias towards Brainomix with both core and penumbral volumes was reflected in target mismatch agreement with greater proportions eligible against both DEFUSE-3 and EXTEND criteria. As mentioned previously, RAPID was used for processing in several key studies (Saver et al., 2015, Campbell et al., 2015, Nogueira et al., 2017, Albers et al., 2018)

but Brainomix in none at the time of writing. Additionally, unlike Brainomix, the accuracy of RAPID with regards to follow-up infarct volume has been widely corroborated (Austein et al., 2016, Cereda et al., 2016, Mokin et al., 2017, Hoving et al., 2018, Albers et al., 2016). Consequently, the reference standard with respect to treatment eligibility may be better represented by RAPID at present although it is not clear where the boundaries of treatment benefit truly lie. A meta-analysis from the Hermes collaboration demonstrated that although ischaemic core volume correlates with reduced likelihood of functional independence at 90 days, it does not modify the treatment effect of EVT (Campbell et al., 2019). Large ischaemic core volume is the topic of multiple ongoing trials with the SELECT-2 results demonstrating better functional outcomes with EVT versus medical care (Sarraj et al., 2023) and other trials yet to be completed -TENSION (Bendszus et al., 2019), LASTE (Costalat et al., 2023) and TESLA (Zaidat et al., 2023).

A limitation of this study is that the CTP imaging was obtained from multiple sites across Scotland and Australia which may have affected post-processing and contributed to the number of failed scans with possible processing failure as an artefact of data format conversion in the process of export, archiving and storage. Clinical data too was lost in this process and so bilateral lesions were not addressed. Whilst heterogeneity reflects daily clinical practice study datasets included much older scans, likely exaggerating processing failure rates. Another limitation is the lack of comparison with DWI given that MRI-DWI is the most accurate imaging method to diagnose ischaemia (González et al., 1999). Additionally, the patients included were selected based on study eligibility within 6 hours of AIS onset; perfusion defects are not necessarily reflective of real life. Finally, the Bland-Altmann approach may not fully represent the variation if only the mean differences are considered.

This was a retrospective analysis of an established database. In future chapters we hope to compare software perfusion defects in patients with wider timeframes, use follow-up DWI lesions as an infarct volume reference, compare perfusion defects to functional outcome and address the presentation of bilateral lesions across perfusion software.

Conclusion

There are variations in ischaemic core and penumbral volumes across different perfusion software which may affect EVT eligibility and functional outcome at 90 days. More patients are eligible for treatment according to the Brainomix software although this has not been validated though use in a trial.

Chapter 5 The WHISPER Study, Demographics and Main Outcomes

This chapter introduces the Whole Brain Ischaemic Stroke Perfusion and Extended Recanalisation [WHISPER] study.

Introduction

The rationale for favouring CT perfusion over other imaging modalities through the work is explored in Chapter 1.

The WHISPER-pilot study ran from 2018 to 2019 and recruited 20 patients -of whom 16 had a final diagnosis of AIS. CTP detected hypoperfusion in 7 patients (44%) with 1 patient (6%) meeting DEFUSE-3 criteria and none meeting DAWN criteria -both of which are described in Chapter 1 (El Tawil, 2020).

At the time of the pilot stroke guidelines recommended EVT for patients with AIS and an anterior circulation LVO within 6 hours' onset or last seen well (Turc et al., 2019). The confirmation of EVT being the gold-standard of care for this patient group was based on the publication of five pivotal trials in 2015 described in Chapter 1 (Berkhemer et al., 2014, Campbell et al., 2015, Goyal et al., 2015, Jovin et al., 2015, Saver et al., 2015). The PISTE trial provided further evidence for effectiveness of thrombectomy treatment in the UK; the trial was stopped early following the positive findings (Muir et al., 2017). Whilst the HERMES meta-analysis of these trials did not show significant benefit beyond 7.3 hours' onset, only two trials included late-window patients (i.e. >6 hours from symptom onset or last seen well) and this number was small (Goyal et al., 2015, Jovin et al., 2015, Saver et al., 2016).

In 2018, the DEFUSE-3 and DAWN trials used perfusion imaging to demonstrate benefit of EVT up to 16 hours (DAWN) and 24 hours (DEFUSE-3) based on a combination of clinical and perfusion imaging (estimating ischaemic core and penumbral volumes) criteria (Nogueira et al., 2017, Albers et al., 2018). The strict selection criteria and large treatment effects observed suggest more patients amongst the excluded may benefit from EVT.

There were no screening logs and both trials excluded a large proportion of patients following clinical review (Nogueira et al., 2017, Albers et al., 2018). The Multicentre Randomized Clinical trial of Endovascular treatment for late arrivals [MR CLEAN LATE] sought to address this and used collaterals assessed using CTA or MRA to confirm both safety and efficacy in patients with LVO (defined as distal ICA, M1 or proximal M2) within 6-24 hours (Olthuis et al., 2023b). MR CLEAN LATE promotes late-window EVT in patients for whom perfusion imaging may not be available, however the size of the subgroup with mismatch in unselected ischemic stroke patients within the first 24 hours' onset remains unclear.

More recently, trials have sought to assess the treatment effect of EVT in large core patients. RESCUE-Japan LIMIT and TENSION demonstrated better functional outcome with EVT in patients with LVO and ASPECTS 3-5 within 24 and 12 hours' onset respectively (Yoshimura et al., 2022, Bendszus et al., 2023). Both SELECT2 and ANGEL-ASPECT also demonstrated better functional outcome within 24 hours' onset and introduced additional optional inclusion criteria of core volumes of >50ml and between 70 to 100ml respectively (Sarraj et al., 2023, Huo et al., 2023). The trials recruiting up to 24 hours' onset demonstrated a significantly higher haemorrhagic transformation rate or vascular complications in the EVT arm (Yoshimura et al., 2022, Sarraj et al., 2023, Huo et al., 2023). The median core volumes for the EVT arms of SELECT2 and ANGEL-ASPECT were 74ml (IQR 50 to 111.5ml) and 60.5ml (IQR 29 to 86ml) respectively, which are relatively conservative for large core trials (Sarraj et al., 2023, Huo et al., 2023). The median total hypoperfusion lesion volume of 171ml (IQR 127 to 226ml) reported for SELECT2 suggests that this was more likely a large penumbra trial (Sarraj et al., 2023). The ANGEL-ASPECT hypoperfusion lesion volumes weren't reported.

Perfusion imaging was also used to extend the time window for rTPA therapy. The additional evidence from ECASS-4 and EXTEND (both 2019) added to the EPITHET data (2008) showed improved functional outcomes in patients treated with alteplase compared with placebo. ECASS-4 and EPITHET used perfusion-diffusion MRI exclusively and EXTEND used CTP (Campbell et al., 2019). Advanced brain imaging for treatment guidance is currently recommended in the European Stroke Organisation [ESO] guidelines

for thrombolysis between 4.5 and 9 h after symptom onset, or if presenting after waking up (Berge et al., 2021, Bhalla A, 2023).

The exact time after which collaterals fail and recanalisation therapy is futile differs between individuals (who are often referred to as either fast or slow progressors) and likely depends on genetic predisposition of the leptomeningeal collateral arteriole availability (Rocha and Jovin, 2017).

Current thresholds for prediction of tissue fate are informed by studies that recruited patients <6 hours after onset in which reperfusion was achieved through thrombolytic drugs (Campbell et al., 2011). It is not known whether the same thresholds apply in later presentations. If these differ, then current software will over or under-estimate volumes of tissue viability.

The accuracy of CTP has been challenged. The ghost-core concept suggests that CTP may over-estimate the ischaemic core volume in patients presenting within early time windows- the concern being that if CTP alone were used to select patients for reperfusion therapy, patients who may benefit may be excluded (Boned et al., 2017). Bivard et al. (2017) found that in the setting of early, complete reperfusion following EVT (median onset-to-reperfusion time 3h59 minutes, IQR 1h49 to 10h45), the optimal CTP threshold to estimate the baseline ischaemic core volume (compared with DWI at 24 hours) was rCBF<20% (using the MIStar software). Conversely, analysis of the SWIFT PRIME patients who achieved 100% reperfusion (median onset-to-reperfusion time 4h6, IQR 3h6 to 4h56) validated the rCBF value of <30% (compared with DWI at 27 hours) (Mokin et al., 2017). Thresholds may be dependent on onset-to-reperfusion-time with weaker association at late presentation with poorer initial collateral status contributing to over-estimation (Qiu et al., 2019, García-Tornel et al., 2021). A systematic review of patients who underwent CTP within six hours of symptom onset found the ghost core to be highly time and collateral-dependent with over-estimation more likely in patients with poor collaterals (Ballout et al., 2023).

We aimed to prospectively identify the numbers of patients with potentially reversible ischaemia (i.e. salvageable brain tissue) within different time windows with a view to informing the numbers of patients potentially eligible for delayed revascularisation. These data will assist service planning around endovascular treatment. We also aimed to explore factors associated with persistent salvageable tissue and with favourable clinical outcome. Identifying factors associated with slower ischaemic core growth would provide more information about neuroprotection -specifically how to enhance microvascular reperfusion and avoid reperfusion injury. This may be relevant to decisions regarding transfer between centres to receive mechanical thrombectomy.

The Whole Brain Ischaemic Stroke Perfusion and Extended Recanalisation [WHISPER] study was a single-centre prospective observational cohort study using whole-brain CT perfusion and subacute MRI to define follow-up tissue outcomes.

The prospective, single centre observational trial took place at the Queen Elizabeth University Hospital [QEUH], Glasgow, United Kingdom place between March 2018 and March 2022, with recruitment suspended between April 2020 and July 2020 due to the coronavirus disease 2019 [COVID-19] pandemic. This is a regional neurosciences centre providing a comprehensive stroke service to a population of approximately 450,000 with some additional secondary transfers for thrombolysis assessment from Glasgow Royal Infirmary, the Royal Alexander Hospital and Inverclyde Royal Infirmary. Total admissions with confirmed strokes were 1242 in 2022 with 173 (14%) treated with thrombolysis (SSCA, 2023).

The protocol was approved by the ethical committee responsible for research involving adults with incapacity (Scotland A REC, Reference:18/SS/0001). The study was funded by the Chief Scientist Office and the Neurosciences Foundation. This study was performed according to the Research Governance Framework for Health and Community Care (Second edition, 2006).

Clinical research staff recruited to the study and additionally supervised multimodal CT acquisitions. All investigators and key personnel had appropriate GCP training.

Methods

Patients

All patients presenting with stroke symptoms within 24 hours of onset or last-seen well were eligible. Prospective participants were identified from the Emergency Department or the Hyper-Acute Stroke Unit.

Baseline clinical data (including NIHSS) and study imaging (CTP+CTA) were obtained as soon as possible following recruitment.

We collected clinical data including relevant medical history (i.e. vascular risk factors which may contribute to aetiology). Prior antiplatelet regimes were not collected as this was not a trial of an interventional therapy and this would not have affected our outcome variables. As our outcome included disability, we collected admission mRS to assess the change.

Routine CT perfusion as part of multimodal CT (NCCT brain, CTP, CTA) was introduced at the QEUH in October 2020. Patients were excluded if they had known allergy to iodinated contrast, known renal dysfunction (eGFR<30mlmin) or in whom mechanical thrombectomy was planned.

Table 5-1 lists the full inclusion/exclusion criteria. Baseline clinical data included stroke severity by the NIHSS, risk factor data, medication, blood for HbA1c, admission blood glucose.

Functional outcome was determined by the modified Rankin Scale (mRS) using the Rankin Focused Assessment tool at day 90 using a central telephone or face-to-face follow-up.

Table 5-1 Inclusion and Exclusion Criteria for the WHISPER Study

Inclusion Criteria
1. Patients aged ≥18 years.
2. Male or non-pregnant females.
3. Clinical diagnosis of acute stroke.
4. Endovascular thrombectomy is not planned.
5. Scan can be obtained within 24 hours of last being seen well.
6. No contraindication to IV contrast.
7. Informed consent from patient or proxy (if patient lacks capacity).
Exclusion Criteria
1. Renal impairment with eGFR less than 30ml/min.
2. Known allergy to IV contrast.
3. Patient not expected to survive until or to be available for, final follow up due to stroke or other comorbidities.
4. Intracranial haemorrhage or non-stroke diagnosis on initial CT.
5. MRI incompatibility (follow-up CT is an option if MRI incompatible at the time of follow-up).
6. In patients treated with IV thrombolysis, substantial clinical improvement between treatment and imaging acquisition (NIHSS= 0 or 1 at time of imaging).

IV=intravenous, eGFR=estimated glomerular filtration rate, CT=computed tomography, MRI=magnetic resonance imaging, NIHSS=National Institute of Health Stroke Scale

Multi-modal CT Acquisition

Whole brain NCCT was acquired first, followed by CTP with 40 mm slab coverage (8 x 5 mm2 slices), using a 50 ml contrast bolus administered at 5 ml/second via a large-gauge peripheral venous cannula. Finally, a CTA was performed covering aortic arch to vertex using bolus tracking to enable correct timing of image acquisition. This was performed using a multi-detector Scanner (Toshiba Aquilion One Vision -research scanner) or the emergency department scanners -GE 660: 8cm detector in jog mode) which permitted post-processing of CTP to derive time-resolved angiographic data.

Follow-up Imaging

Follow-up imaging was performed at 24 to 72 hours, with repeat clinical examination and bloods (eGFR and glucose) performed at the same visit. MRI was the preferred follow up imaging modality, but this could be substituted by NCCT with CTA and CTP for patients in whom MRI was not tolerated, was contraindicated, or was unavailable. MRI involved a standard stroke protocol including T1, T2, DWI, SWI, FLAIR, time of flight MRA of the circle of Willis and ASL brain perfusion. Figure 1. summarises the recruitment process in a flowchart.

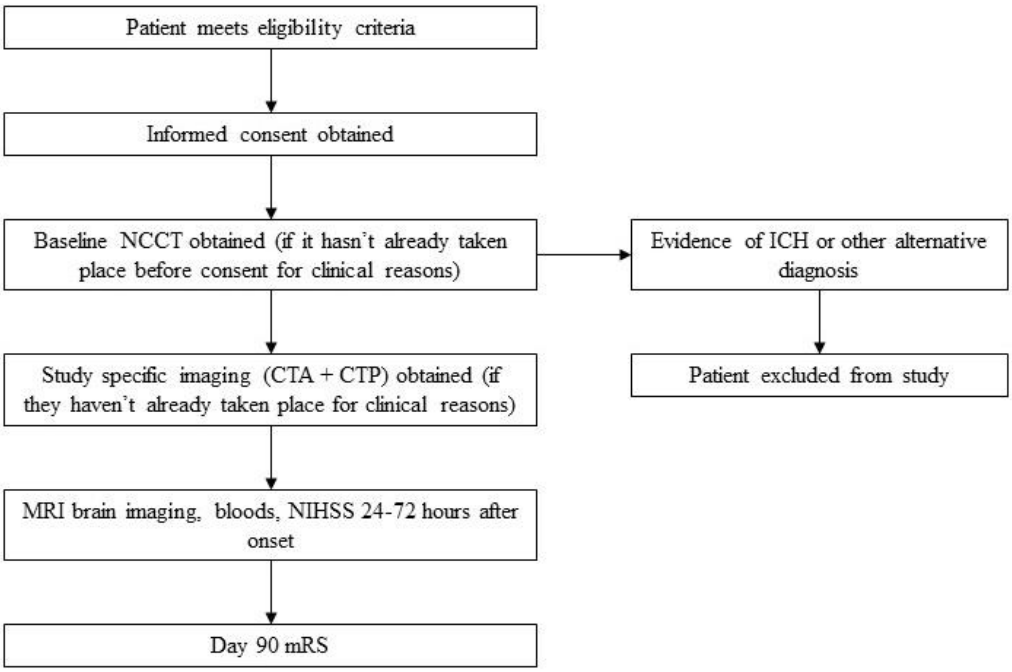

NCCT=non-contrast computed tomography, ICH=intracerebral haemorrhage, CTA=computed tomography angiogram, CTP=computed tomography perfusion, MRI=magnetic resonance imaging, NIHSS=National Institute of Health Stroke Scale, mRS=modified Rankin scale

Figure 5-1 WHISPER Study Flow Chart

Imaging Analysis

NCCT Analysis

The ASPECTS of all non-contrast CT scans were assessed by consensus by two experienced assessors: a stroke neurologist (AS) and a neuroradiologist (CP). The ASPECTS has been previously described in the General Methods section.

The scans were also processed through Brainomix (version 11.001) e-ASPECTS software which generated an e-ASPECT score, hyperdense artery sign with clot volume and hypodensity volume suggestive of early ischaemic change. The rate of hyperdense artery signs and early ischaemic change was calculated based on these reports.

CTP Analysis

CTP scans were processed using the following three software:

- MIStar version 3.2 (Apollo) – images were uploaded and analysed separately by two users (VB and AM) who manually highlighted regions of interest and supervised the AIF and VOF placement. Disagreements (i.e. with respect to hemisphere involvement or lesion presence) were resolved by both users analysing the images again. The software defined ischaemic core as DT>3s and rCBF<30% and penumbra as DT>3s (minus the ischaemic core).
- Brainomix (versions 9.001 to 11.001) – an automated software with no user input, ischaemic core was defined as Tmax>6s and rCBF<30% and penumbra as Tmax>6s.
- RAPID version 4.7 (Ischemaview) – an automated software with no user input, ischaemic core was defined as Tmax>6s and rCBF<30% and penumbra as Tmax>6s.

Target Mismatch

The imaging inclusion criteria used by the DEFUSE 3 and EXTEND trials were explored.(Albers et al., 2018, Ma et al., 2019)

DEFUSE 3 Imaging Inclusion Criteria

The DEFUSE 3 trial included patients with ICA or MCA-M1 occlusions and a favourable target mismatch profile, defined as ischaemic core lesion<70ml, a ratio of total volume of ischaemic lesion to ischaemic core (Tmax>6s over CBF<30%) of $\geq$1.8 and a penumbra lesion $\geq$15ml (Albers et al., 2018).

EXTEND Imaging Inclusion Criteria

The EXTEND trial defined target mismatch as ischaemic core lesion<70ml, a ratio of volume of ischaemic lesion to ischaemic core (Tmax>6s over CBF<30%) of >1.2 and an absolute difference in volume >10ml (difference between perfusion lesion and core lesion) (Ma et al., 2019).

The mismatch ratio 1.2 was first used in EPITHET (2008) and again in EXTEND (2019) (Davis et al., 2008, Ma et al., 2019).

The prevalence of target mismatch profile was explored in different time windows based on the most recent UK guidelines. These included comparisons of ≤4.5 hours, 4.5 to ≤9 hours and 9 hours to ≤24 hours based on the recommendation for IV treatment eligibility and ≤6 hours, 6 to ≤12 hours and 12 to ≤24 hours based on the recommendation for MT eligibility.

The Hypoperfusion Intensity Ratio

HIR was defined as the ratio of the volumes of tissue with Tmax >10s / tissue with Tmax>6s – these values were chosen based on the DEFUSE and DEFUSE2 studies (Olivot et al., 2009, Lansberg et al., 2012, Olivot et al., 2014). Higher HIR reflects poorer collateral flow and has been associated with faster infarct growth and poor clinical outcome (Olivot et al., 2014, Guenego et al., 2018). There is no uniform definition of low HIR but typically patients are dichotomised based on the median value -this has led to definitions such as <0.4, <0.5 and <0.54 (Olivot et al., 2014, Guenego et al., 2018, Baek et al., 2021).

CTA Analysis

CTA scans were scored by consensus by two experienced assessors (AS and CP) with a random sample of 10 patients confirmed by a third assessor (WI) chosen using a random numbers generator website. Scans were assessed for the presence and site of anterior circulation LVO, any vessel occlusion and collaterals were assessed using the rLMC score -see General Methods (Menon et al., 2011).

Large Vessel Occlusion

Definitions of anterior circulation LVO varied across the trials. Whilst all agree on ICA and M1 occlusion (SWIFT PRIME, REVASCAT, DAWN, DEFUSE-3, RESCUE-Japan LIMIT, SELECT2, ANGEL ASPECT and TENSION), some included M2 (MR CLEAN, MR CLEAN LATE, EXTEND-IA, PISTE, ESCAPE) (Saver et al., 2015, Jovin et al., 2015, Nogueira et al., 2017, Albers et al., 2018, Yoshimura et al., 2022, Sarraj et al., 2023, Huo et al., 2023, Bendszus et al., 2023, Berkhemer et al., 2014, Olthuis et al., 2023a, Campbell et al., 2015, Muir et al., 2017, Goyal et al., 2015).

Classifying M2 occlusions into either large or medium is difficult owing to the heterogeneity in angioarchitecture (Saver et al., 2020). We therefore defined anterior circulation LVO as occlusion of the internal carotid artery, M1 or >1 branch of M2 in keeping with the ESCAPE trial's definition -i.e. in keeping with the theory that multiple branches of M2 involvement are equal to M1 occlusion (Goyal et al., 2015).

MRI Analysis

MRI scans were reported by the radiologist on duty. Bleeds were noted and reviewed by a stroke neurologist (KM) against the Heidleberg Bleeding Classification (see General Methods).(von Kummer et al., 2015)

MRI scans were further scored by consensus by the above assessors (AS and CP) for ASPECTS. In the case of CTA-determined LVO, the MRA scans were scored for recanalisation at the primary occlusive site using the AOL score (described in General Methods) (Khatri et al., 2005).

DWI follow-up infarct volumes were calculated using Mango software by an assessor (SN).

Difficult-to-Read Images

Difficult-to-read images were interpreted if possible – with the view that all images are reviewed in clinical practice. We did not have criteria for image inclusion/exclusion but there were a few cases which were excluded with specific reasons detailed in the results section.

Inter-Observer Agreement Analysis

Inter-rater reliability was assessed using the Cohen's κ coefficient. In keeping with Cohen's suggestion, values ≤ 0 indicated no agreement, 0.01-0.20 indicated none to slight agreement, 0.21-0.40 indicated fair agreement, 0.41-0.60 indicated moderate agreement, 0.61-0.80 indicated substantial agreement and 0.81-1.00 indicated almost perfect agreement (Cohen, 1960).

Withdrawal of Subjects

Participants or their legal representative or consultee were able to withdraw at any stage of follow-up, but data acquired up to the point of withdrawal were retained for analysis.

Statistics and Data Analysis

The statistical approaches that were employed were predominantly descriptive. The study originally aimed to recruit a convenience sample of up to 149 patients. Patients with a final diagnosis of both AIS or TIA were included in the analysis; at the time of presentation these patients were assessed for AIS and were candidates for reperfusion therapy.

Study Objectives

The following objectives were predefined research objectives and included in the study protocol.

Null Hypothesis

The proportion of patients with target mismatch in late time windows is the same as in early time windows.

Sample Size Calculation

We used an online sample-size calculator (https://select-statistics.co.uk/calculators/sample-size-calculator-two-proportions/) to determine the appropriate sample size to detect a difference between the proportion with target mismatch in late time windows versus early.

McMeekin et al. (2017) published an estimation of the number of UK stroke patients eligible for EVT after using evidence from national registries (SSNAP and the SSCA) to estimate the number of patients hospitalised annually with AIS (n=9620). Evidence from RCTs was combined to create a decision-tree describing the EVT proportion who may be eligible. Out of 95,500 annual admissions, it was estimated that 9,620 (10%) of patients would be eligible for EVT within 4 hours with a further 1,310 (1%) eligible who presented later (McMeekin et al., 2017).

Using these proportions, with a power of 80% and requirement of 95% CI, the recommended sample size was 97.

Primary Objective

The primary objective was to establish the proportion of patients with prolonged penumbral survival (and therefore eligibility for endovascular treatment) in unselected ischaemic stroke patients within the first 24 hours after onset of symptoms. Time windows were analysed as follows:

- <4.5 hours, 4.5 to ≤9 hours, 9 to ≤24 hours
- <6 hours, 6 to ≤12 hours and 12 to ≤24 hours

Secondary Objectives and Post Hoc Analysis

The secondary objectives were as follows:

- To investigate the mechanisms underlying failure to recruit leptomeningeal collaterals in a clinical population through comparison of leptomeningeal collateral flow (graded on time-resolved baseline CTA derived from the CTP examination), between normoglycaemic and hyperglycaemic groups

Following the initial analysis, we decided to perform the following post hoc analysis:

- To explore whether thresholds for prediction of tissue fate vary by time from symptom onset by assessing modified Rankin Scale distribution at day 90 and follow-up infarct volume as calculated on MRI among those with and without vessel recanalization or brain reperfusion at 48-72h follow-up

Results

This chapter details the clinical characteristics of the patients recruited to WHISPER and addresses the primary objective.

The study was approved by Scotland A REC (Reference:18/SS/0001).

Between March 2018 and March 2022, 2,312 patients admitted to the Queen Elizabeth University Hospital had a final discharge diagnosis of AIS. Research study recruitment was suspended between April 2020 and July 2020 due to the COVID-19 pandemic, and access to research staff and facilities remained restricted for several months after the period of suspension. Recruitment was therefore dependent on availability of research staff and access to research scanners during working hours and was feasible for a maximum of 30% of the working week making the denominator 693 cases during working hours – reduced to 635 following the 4 month suspension during the COVID-19 pandemic.

We recruited 185 patients to WHISPER (29% recruitment rate), of whom 174 had a final diagnosis of AIS or TIA. Clinical characteristics and final diagnoses of all subjects are

described in Table 5-2 and final diagnoses in Table 5-3. All recruited patients had baseline NCCT.

Table 5-2 Clinical Characteristics

Variable		**Value, N=174**
Age	range	19-102
Age (years)	mean±SD	67±13
Age >70 years	n (%)	77 (44%)
Risk Factors and Medical History		
Gender	n male (%)	106 (61%)
Myocardial infarction	n (%)	16 (9%)
Other ischaemic heart disease	n (%)	23 (13%)
Previous stroke	n (%)	26 (15%)
Ischaemic	n (%)	22 (13%)
Haemorrhagic	n (%)	2 (1%)
Unknown	n (%)	2 (1%)
Diabetes mellitus	n (%)	33 (19%)
Hypertension	n (%)	87 (50%)
Atrial fibrillation	n (%)	27 (16%)
Current smoker	n (%)	36 (21%)
Excessive alcohol consumption	n (%)	12 (7%)
Aspirin	n (%)	32 (18%)
Clopidogrel	n (%)	22 (13%)
Warfarin	n (%)	3 (2%)
Direct oral anticoagulant	n (%)	9 (5%)
Statin	n (%)	77 (44%)
Antihypertensive agent	n (%)	88 (51%)
Stroke Characteristics		
Hemisphere		
Right	n (%)	73 (42%)
Left	n (%)	100 (57%)
Both	n (%)	1 (1%)
Oxfordshire Classification		
TACS	n (%)	29 (17%)
PACS	n (%)	92 (53%)
POCS	n (%)	23 (13%)
LACS	n (%)	30 (17)

Systolic blood pressure on admission (mmHg)	mean±SD	152±22
Diastolic blood pressure on admission (mmHg)	mean±SD	85±18
Number treated with IV rTPA	n (%)	85 (49)
Alteplase	n (%)	68 (39)
Tenecteplase	n (%)	17 (10)
Onset to treatment time (minutes)	median (IQR)	196 (140, 251)
Number treated with known onset time	n (%)	73 (42)
Proportion of total rTPA	%	86
Number treated ≤4.5h	n (%)	70 (40)
Number treated >4.5h	n (%)	15 (8)
Baseline NIHSS	median (IQR)	6 (3, 11)
24-72 hours NIHSS	median (IQR)	3 (1, 6)
Blood glucose on admission (mmol/L)*	mean±SD	7.3±3.6
Hyperglycaemia on admission (i.e. ≥7 mmol/l)	n (%)	57 (33)
Blood glucose at 24-72 hours (mmol/L)**	mean±SD	6.9±2.6
Hyperglycaemia at 24-72 hours (i.e. ≥7 mmol/l)	n (%)	31 (18)
HbA1c +/- 3 months of event (mmol/mol)***	mean±SD	46±16
eGFR on admission (ml/min/1.73 m^2)	mean±SD	49±9
eGFR decline at 24-72 hours****	n (%)	19 (11)
Pre-stroke excellent function (mRS 0-1)	n (%)	160 (92)
Pre-stroke good function (mRS≤2)	n (%)	166 (95)
Day 90 mRS outcome*****		
mRS 0	n, %	22 (13)
mRS 1	n, %	43 (26)
mRS 2	n, %	45 (27)
mRS 3	n, %	27 (16)
mRS 4	n, %	18 (11)
mRS 5	n, %	3 (2)
mRS 6	n, %	8 (5)

*n=172, **n=96, ***n=89, ****n=136,*****n=166. AIS=acute ischaemic stroke, TIA=transient ischaemic attack, SD=standard deviation, TACS=total anterior circulation stroke, PACS=partial anterior circulation stroke, POCS=posterior circulation stroke, LACS=lacunar stroke, rTPA=recombinant tissue plasminogen activator, IQR=interquartile range, NIHSS=national institutes of health stroke scale, HbA1c=haemoglobin A1C, eGFR=estimated glomerular filtration rate, mRS=modified Rankin scale

Table 5-3 Final Diagnoses for WHISPER Patients

Diagnosis	**n (%), N=185**
AIS	168 (91)
TIA	6 (3)
Migraine	1 (0.5)
Seizure	1 (0.5)
Syncope	1 (0.5)
Vestibular neuritis	1 (0.5)
Alcohol withdrawal	1 (0.5)
Infection	1 (0.5)
Lung cancer	1 (0.5)
Pain	2 (1)
Unclear	2 (1)

WHISPER=whole brain ischaemic stroke perfusion and extended recanalisation, n=number, AIS=acute ischaemic stroke, TIA=transient ischaemic attack

Figure 5-2 is a flowchart showing the number of patients who underwent study specific imaging.

All the recruited patients had baseline NCCT. There were 167 (90%) patients who received all of the study-specific imaging -of which 157 (85%) had a final diagnosis of AIS or TIA.

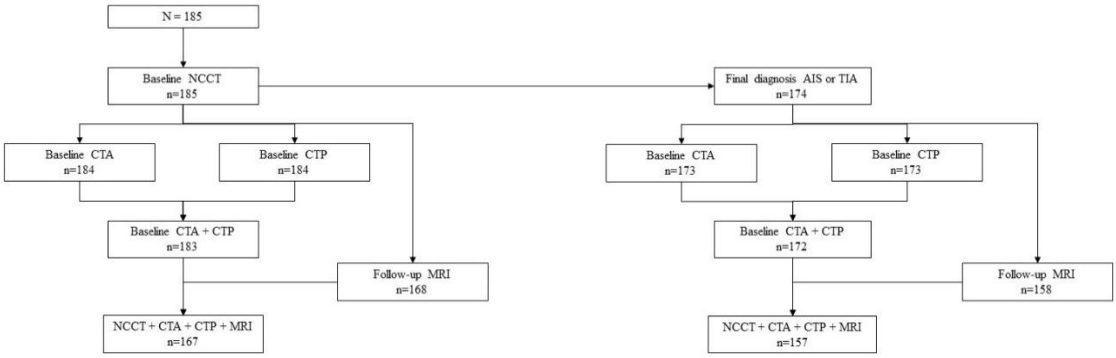

n=number, NCCT=non-contrast computed tomography scan, AIS=acute ischaemic stroke, TIA=transient ischaemic attack, CTA=computed tomography angiography, CTP=computed tomography perfusion, MRI=magnetic resonance imaging

Figure 5-2 Patients with Study-Specific Imaging

Table 5-4 Imaging Details for WHISPER Patients

Variable	Value (N=185)
NCCT	
NCCT conducted (n, %)	185 (100)
Onset to NCCT (median, IQR) (hours)	4.0 (2.5, 9.5)
ASPECTS (median, IQR)	9.0 (8, 10)
ASPECTS 0-4 (n, %)	6 (3)
ASPECTS 5-7 (n, %)	39 (21)
ASPECTS 8-10 (n, %)	140 (76)
ASPECTS 10 (n, %)	85 (46)
CTP	
CTP conducted (n, %)	184 (99%)
Onset to CTP (median, IQR) (hours)	4.8 (3.0, 14.8)
NCCT to CTP (median, IQR) (hours)	0.1 (0.1, 1.9)
Lesion deficit (n, %)	122 (66%)
Core Volume (median, IQR) (ml) - Tmax>6 seconds and relative CBF<30%	0 (0, 5)
Penumbra Volume (median, IQR) (ml) - Tmax>6 seconds	13 (0, 68)
HIR (median, IQR)	0.0 (0.0, 0.5)
CTP conducted (n, %)	184 (99%)
CTA	
CTA conducted (n, %)	184 (99)
Onset to CTA (median, IQR) (hours)	5.0 (3.1, 15.0)
CTP to CTA (median, IQR) (hours)	0.1 (0.1, 0.1)
Number with LVO (n, %)*	45 (24)
rLMC (median, IQR)	20 (14, 20)
rLMC 0-10 (n, %)	22 (12)
rLMC 11-16 (n, %)	40 (22)
rLMC 17-20 (n, %)	120 (65)
MRB	
MRB conducted (n, %)	168 (91%)
Onset to MRB (median, IQR) (hours)	52.8 (39.7, 69.7)
ASPECTS (median, IQR)	8 (5, 10)
ASPECTS 0-4 (n, %)	34 (20%)
ASPECTS 5-7 (n, %)	40 (24%)
ASPECTS 8-10 (n, %)	92 (55%)
DWI Follow-up infarct volume (median, IQR) (ml)***	4 (1, 16)
MRA conducted (n, %)	158 (85%)
MRA AOL score (median, IQR)	2 (0, 3)

*N=182, Additionally two further CTA scans were poor quality and not interpretable by AS and CP, **N=45, ***N=164 (quality) n=number, NCCT=non-contrast computed tomography, IQR=interquartile range, ASPECTS=Alberta stroke programme early computed tomography score, CTP=computed tomography perfusion, Tmax=time to maximum, CBF=cerebral blood-flow, HIR=hypoperfusion intensity ratio, CTA=computed tomography angiography, LVO=large vessel occlusion, rLMC=relative leptomeningeal collateral score, MRB=magnetic resonance brain imaging, MRA=magnetic resonance angiography

Inter-Observer Agreement

The third assessor's independent analysis was compared with the consensus of the first and second assessor's analysis in ten randomly selected cases using the Cohen's κ coefficient as detailed in Table 5-5.

Table 5-5 Inter-Observer Agreement for Imaging Analysis

Imaging Assessment	Cohen's κ coefficient (95% CI) (N=10)
NCCT ASPECTS	0.79 (0.62 to 0.96)
CTA LVO presence	1
CTA LVO hemisphere	1
CTA LVO site	0.72 (0.57 to 0.87)
CTA rLMC score	0.71 (0.52 to 0.91)
MR ASPECTS*	0.67 (0.51 to 0.83)
MRA AOL score**	0.58 (0.26 to 0.91)

*N=9, one of the patients randomly selected did not have follow-up imaging, **N=5, five patients did not have MRA. NCCT=non-contrast computed tomography, ASPECTS=Alberta stroke programme early computed tomography score, CTA=computed tomography angiography, LVO=large vessel occlusion, rLMC=regional leptomeningeal collateral, MR=magnetic resonance, MRA=magnetic resonance angiography, CI=confidence intervals.

Agreement among raters was substantial except for MRA AOL scoring (of which there were five scans) which was moderate (Cohen, 1960).

Target Mismatch Separated into Time Thresholds

Of 174 patients who had a final diagnosis of AIS or TIA, 4 patients who did not have a CTP and CTP scans which were not evaluable by RAPID were excluded as shown in Figure X. There were 7 scans which showed bilateral lesions and these were included. The number of patients whose CTP scans were evaluated was 170. Further analysis used those with anterior circulation LVO (48 patients). Table X and X summarise the clinical characteristics and radiological features.

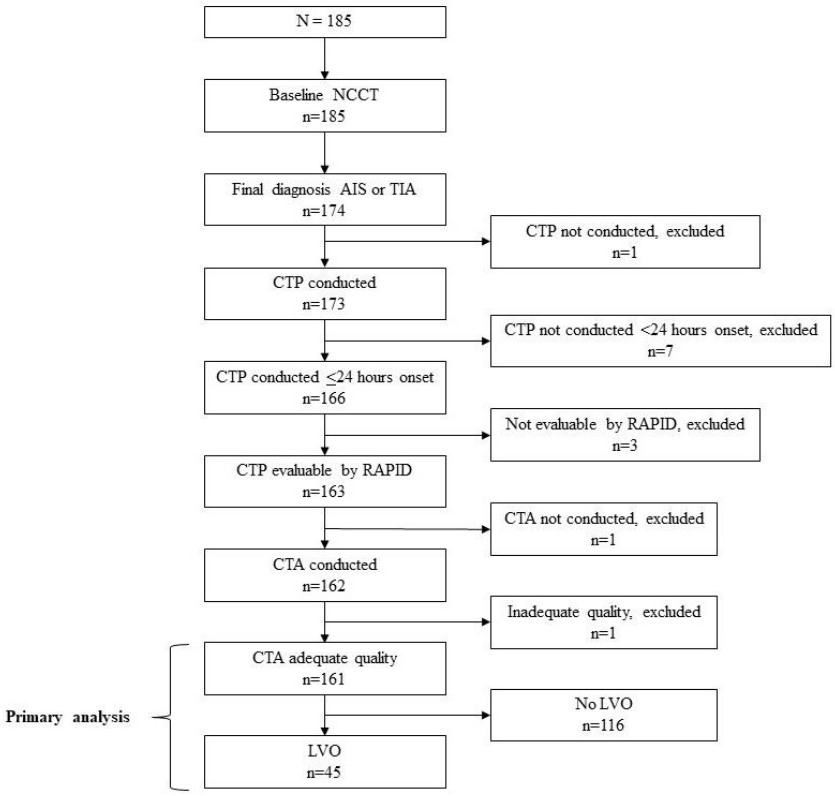

n=number, NCCT=non-contrast computed tomography scan, AIS=acute ischaemic stroke, TIA=transient ischaemic attack, CTP=computed tomography perfusion, CTA=computed tomography angiography, LVO=large vessel occlusion

Figure 5-3 The Number of Patients with CTP Scans Eligible for Analysis

Table 5-6 Clinical Characteristics within the LVO Subgroup

Variable		All Eligible Patients, N=161	LVO subgroup, N=45
Age (years)	mean±SD	67±14	67±14
Male Gender	n (%)	100 (62)	25 (56)
Myocardial infarction	n (%)	15 (9)	2 (4)
Other ischaemic heart disease	n (%)	20 (12)	7 (16)
Previous stroke	n (%)	24 (15)	6 (13)
Ischaemic	n (%)	20 (12)	5 (11)
Haemorrhagic	n (%)	2 (1)	0 (0)
Unknown	n (%)	2 (1)	1 (2)
Diabetes mellitus	n (%)	31 (19)	9 (20)
Hypertension	n (%)	81 (50)	22 (49)
Atrial fibrillation	n (%)	25 (15)	8 (18)
Current smoker	n (%)	35 (22)	8 (18)
Excessive alcohol consumption	n (%)	11 (7)	3 (7)
Baseline NIHSS	median (IQR)	6 (4, 11)	14 (8, 18)
Pre-stroke mRS 0-1	n (%)	148 (92)	39 (87)
Pre-stroke mRS$\leq$2	n (%)	153 (95)	41 (91)
Onset to CTP (hours)	median (IQR)	6h9 (2h39, 13h5)	3h28 (2h, 8h34)
Wake-up	n (%)	55 (34)	13 (29)

n-number, SD=standard deviation, NIHSS=National Institute of Health Stroke Scale, IQR=interquartile range mRS=modified Rankin Score, CTP=computed tomography perfusion

Table 5-7 Radiological Features of Patients with Eligible CTP Scans

Variable		All patients, N=161	LVO, N=45
NCCT			
ASPECTS	median (IQR)	9 (8, 10)	7 (5, 9)
CTP			
Total lesion volume (ml)	median (IQR)	21 (0, 81)	145 (84, 185)
Core volume (ml)	median (IQR)	0 (0, 7)	11 (0, 21)
Penumbra volume (ml)	median (IQR)	16 (0, 71)	110 (76, 166)
HIR	median (IQR)	0.1 (0.0, 0.5)	0.4 (0.2, 0.6)
Meets DEFUSE-3 criteria	n (%)	31 (19)	31 (69)
Meets EXTEND criteria	n (%)	88 (55)	39 (87)
CTA			
LVO (n, %)	n (%)	45 (28)	
Collateral score	median (IQR)	19 (14, 20)	11 (9, 15)
Follow-up MRI			
ASPECTS	median (IQR)		4 (1, 6)
Follow-up MRA			
AOL 0	n (%)		10 (22)
AOL 1	n (%)		1 (2)
AOL 2	n (%)		12 (27)
AOL 3	n (%)		12 (27)

*N=161, **N=146, ***N=71, ****N=37, *****N=35. NCCT=non-contrast computed tomography, ASPECTS=Alberta Stroke Program Early Computed Tomography Score, IQR=interquartile range, CTP=computed tomography perfusion, HIR=hypoperfusion intensity ratio, CTA=computed tomography angiography, MRI=magnetic resonance imaging, MRA=magnetic resonance angiography, AOL=Arterial Occlusive Lesion recanalisation score

Table 5-8 Radiological and Clinical Features of Patients Meeting or not Meeting Target Mismatch Criteria in the CTP Eligible Population

	N=161	DEFUSE 3	EXTEND
Meets criteria	n (%)	31 (19)	88 (55)
Total lesion volume (ml)	median (IQR)	148 (105, 185)	64 (29, 125)
Core volume (ml)	median (IQR)	11 (0, 16)	0 (0, 12)
Penumbra volume (ml)	median (IQR)	132 (92, 180)	54 (22, 113)
NIHSS	median (IQR)	15 (10, 18)	8 (4, 13)
LVO	n (%)	31 (19)	39 (44)
Does not meet criteria	n (%)	130 (81)	73
Total lesion volume (ml)	median (IQR)	11 (0, 38)	0 (0, 5)
Core volume (ml)	median (IQR)	0 (0, 0)	0 (0, 0)
Penumbra volume (ml)	median (IQR)	9 (0, 34)	0 (0, 3)
NIHSS	median (IQR)	5 (3, 9)	5 (3, 9)
LVO	n (%)	14 (9)	6 (4)

IQR=interquartile range, NIHSS=National Institute of Health Stroke Scale, LVO=Large Vessel Occlusion

Table 5-9 Radiological Features of Patients with Eligible CTP Scans with Separation into Relevant Time Windows

Variable	Time Threshold (hours), N=161		
	≤4.5	**4.5 to ≤9**	**9 to ≤24**
n (%)	86	19	56
NCCT			
ASPECTS (median, IQR)	9 (7, 10)	9 (6, 10)	10 (8, 10)
CTP			
Total lesion volume (median, IQR) (ml)	34 (3, 106)	53 (5, 127)	4 (0, 19)
Core volume (median, IQR) (ml)	0 (0, 11)	0 (0, 10)	0 (0, 0)
Penumbra volume (median, IQR) (ml)	32 (3, 88)	53 (5, 121)	0 (0, 17)
HIR (median, IQR)	0.3 (0.0, 0.5)	0.2 (0.0, 0.4)	0.0 (0.0, 0.3)
Meets DEFUSE-3 criteria (n, %)	18	8	5
Meets EXTEND criteria (n, %)	57	13	18
CTA			
LVO (n, %)	27	8	10
Collateral score (median, IQR)	18 (13, 20)	15 (11, 20)	20 (16, 20)
MR*			
ASPECTS (median, IQR)			
MRA**			
AOL 0 (n, %)			
AOL 1 (n, %)			
AOL 2 (n, %)			
AOL 3 (n, %)			

**N=146, ***N=71. NCCT=non-contrast computed tomography, ASPECTS=Alberta Stroke Program Early Computed Tomography Score, IQR=interquartile range, CTP=computed tomography perfusion, HIR=hypoperfusion intensity ratio, CTA=computed tomography angiography, MRI=magnetic resonance imaging, MRA=magnetic resonance angiography, AOL=Arterial Occlusive Lesion recanalisation score

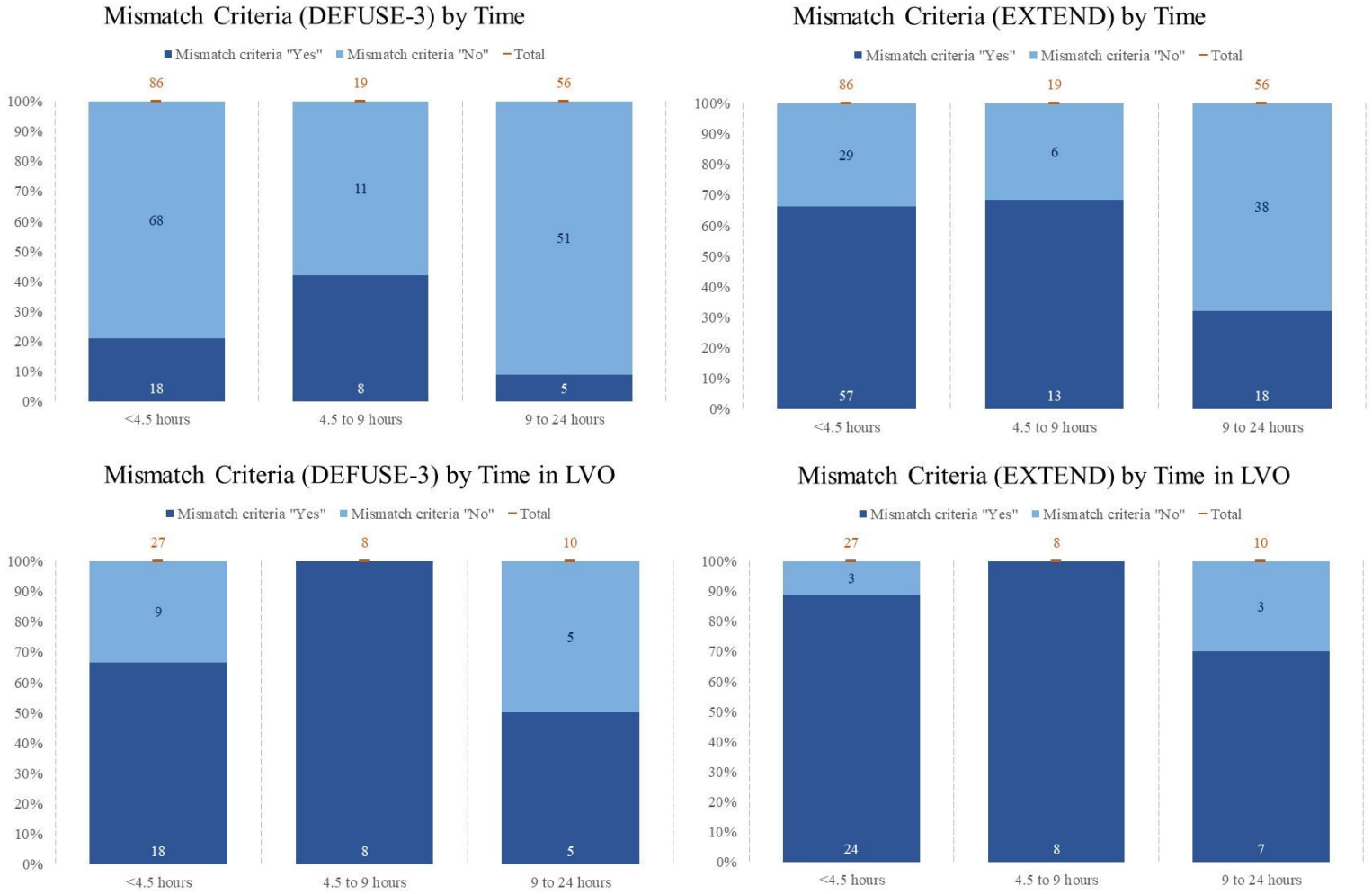

Figure 5-4 Charts Demonstrating the Proportions of Patients meeting DEFUSE-3 and EXTEND Criteria within Relevant Time Windows

Using time categories as initially defined, among 161 patients with evaluable CTP scans, and including 10 in whom CTP lesions were bilateral, 31 (19%) met DEFUSE-3 criteria for target mismatch and 89 (55%) met EXTEND criteria. Compared with the EXTEND criteria. those meeting more restrictive DEFUSE-3 criteria had greater severity (median NIHSS 15 versus 8 for EXTEND), larger core (median 11ml versus 0ml) and penumbra volumes (median 132ml versus 54ml).

There was a significant difference in the proportion meeting both DEFUSE-3 and EXTEND criteria by time window (Fisher's exact test, p=0.005, 95% CI 0.003 to 0.007 and p<0.0001, 95% CI <0.0001 to <0.001 respectively) with a lower proportion in the later time windows.

Among 45 patients with LVO, there was no significant difference in the proportion meeting DEFUSE-3 or EXTEND criteria by time window (Fisher's exact test, p=0.190, OR 0.158, 95% CI 0.151 to 0.165 and p=0.162, OR=0.236, 95% CI 0.228 to 0.244 respectively).

Table 5-10 Radiological Features of Patients with Eligible CTP Scans with Separation into Relevant Time Windows

Variable	Time Threshold (hours), N=161		
	≤6	**6 to ≤12**	**12 to ≤24**
n (%)	98 (61)	17 (11)	46 (29)
NCCT			
ASPECTS (median, IQR)	9 (7, 10)	10 (9, 10)	10 (8, 10)
CTP			
Total lesion volume (median, IQR) (ml)	36 (6, 107)	5 (0, 98)	4 (0, 17)
Core volume (median, IQR) (ml)	0 (0, 11)	0 (0, 0)	0 (0, 0)
Penumbra volume (median, IQR) (ml)	34 (6, 92)	5 (0, 80)	0 (0, 15)
HIR (median, IQR)	0.2 (0.0, 0.5)	0.0 (0.0, 0.3)	0.0 (0.0, 0.2)
Meets DEFUSE-3 criteria (n, %)	24	2	5
Meets EXTEND criteria (n, %)	66	7	15
CTA			
LVO (n, %)	33	4	8
Collateral score (median, IQR)*	17 (12, 20)	20 (15, 20)	20 (17, 20)
MR*			
ASPECTS (median, IQR)			
MRA**			
AOL 0 (n, %)			
AOL 1 (n, %)			
AOL 2 (n, %)			
AOL 3 (n, %)			

*N=160, **N=146, ***N=71. NCCT=non-contrast computed tomography, ASPECTS=Alberta Stroke Program Early Computed Tomography Score, IQR=interquartile range, CTP=computed tomography perfusion, HIR=hypoperfusion intensity ratio, CTA=computed tomography angiography, MRI=magnetic resonance imaging, MRA=magnetic resonance angiography, AOL=Arterial Occlusive Lesion recanalisation score

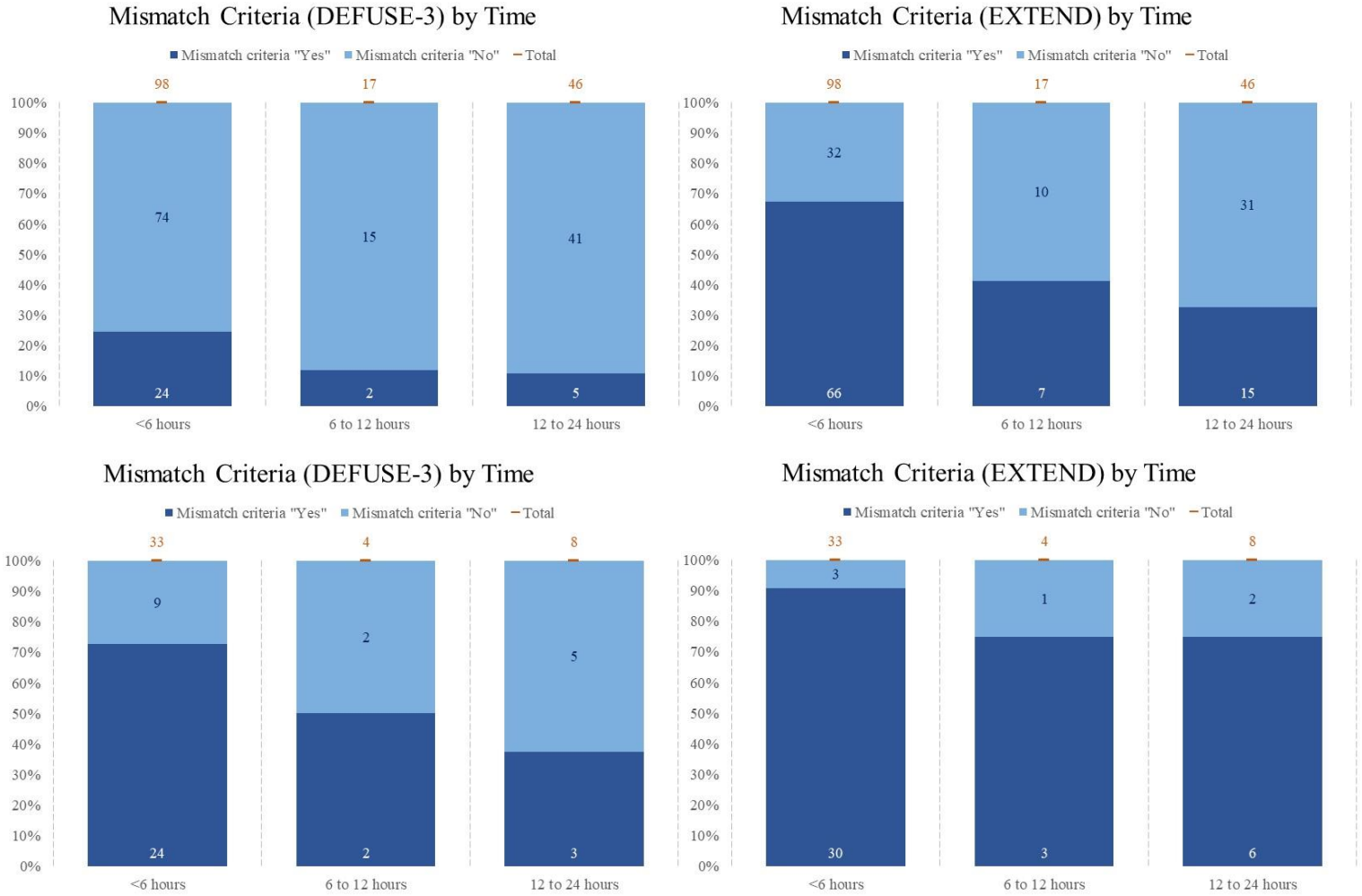

Figure 5-5 Charts Demonstrating the Proportions of Patients meeting DEFUSE-3 and EXTEND Criteria within Relevant Time Windows

Among 161 patients with evaluable CTP scans, there was no significant difference in the proportion meeting DEFUSE-3 criteria by time window (Fisher's exact test, p=0.126, 95% CI 0.118 to 0.135). There was a significant difference in the proportion meeting EXTEND criteria (Fisher's exact test, p<0.001, 95% CI 0.000 to <0.001) with a lower proportion in later windows.

Among 45 patients with LVO, there was no significant difference in the proportion meeting DEFUSE-3 criteria by time window (Fisher's Exact test, p=0.659, OR 0.659, 95% CI 0.649 to 0.668 and p=0.206, OR 0.608, 95% CI 0.599 to 0.618 respectively).

The LVO Subset

We sought to characterise core and penumbra volumes associated with the 45 patients with LVO occlusion sites.

Table 5-11 Perfusion Volumes by LVO Site

Occlusion Site	n (%)	Core Volume, ml median (IQR)	Penumbra Volume, ml median (IQR)	Proportion meeting DEFUSE-3 %
ICA	12	16 (3, 37)	142 (106, 192)	9
Proximal M1*	12	9 (0, 40)	127 (76, 175)	10
Distal M1	13	6 (0, 13)	107 (57, 161)	12
M2>1 branch	8	2 (0, 16)	84 (57, 117)	0

*including 1 patient who had an ICA + prox M1 occlusion. N=Number, IQR=Interquartile Range, ICA=Internal Carotid Artery

Neither core nor penumbra volumes differed significantly by occlusion site (Kruskal-Wallis test, p=0.261 core, p=0.233 penumbra).

Onset-to-CTP time

We explored the possibility that the more severely affected stroke patients had presented earlier. Onset-to-CTP time (minutes) was divided by 60 before analysis to represent hourly intervals.

NIHSS Across Time

NIHSS=National Institute of Health Stroke Scale

Figure 5-6 Association between Onset-to-CTP and NIHSS is a scatter plot depicting admission NIHSS against onset-to-CTP per 60 minute interval. The overall trend is of the more severely disabled patients presenting earlier.

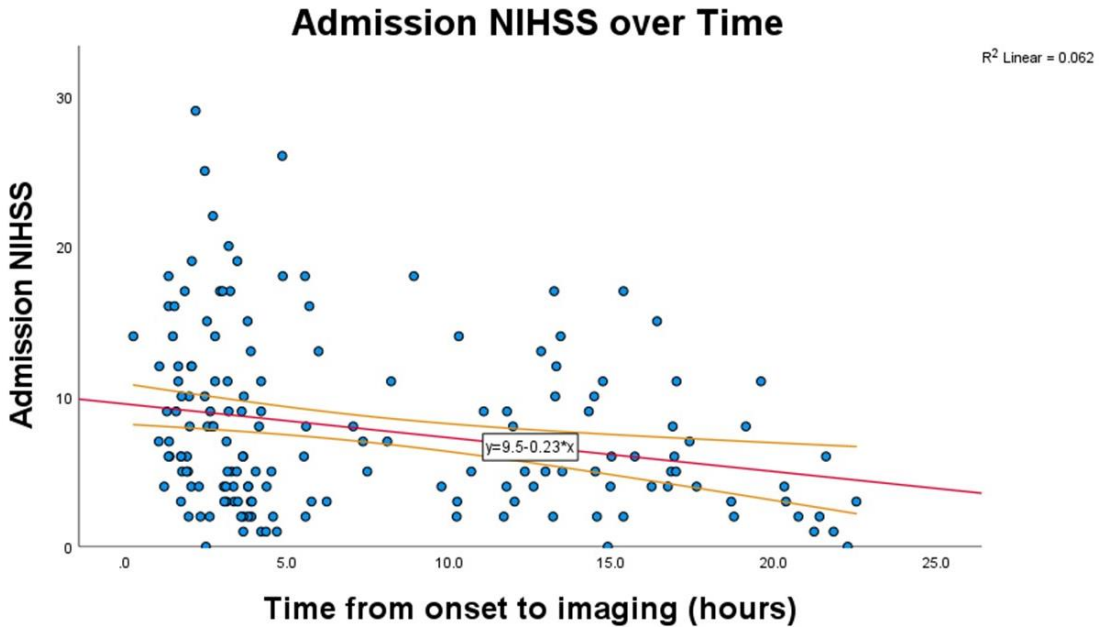

NIHSS=National Institute of Health Stroke Scale

Figure 5-6 Association between Onset-to-CTP and NIHSS

We further assessed how NIHSS differed by time window. Higher scoring patients presented earlier when time windows were divided into 4.5, 4.5 to 9 and 9 to 24 hours (Kruskal-Wallis test, p=0.049) but not when divided into 6, 6 to 12 and 12 to 24 hours (Kruskal-Wallis test, p=0.086).

Table 5-12 NIHSS by Time Window

Variable, N=161	**Time Window (hours)**		
	≤4.5	4.5 to ≤9	9 to ≤24
n (%)	86	19	56
Baseline NIHSS (median, IQR)	7 (2, 12)	7 (3, 16)	5 (3, 9)
	Alternate Time Window (hours)		
	≤6	6 to ≤12	12 to ≤24
n (%)	98	17	46
Baseline NIHSS (median, IQR)	7 (4, 12)	7 (4, 9)	5 (3, 9)

N=number, NIHSS=National Institute of Health Stroke Scale, IQR=interquartile range

The majority of patients presented within the first time-window with higher median NIHSS, again suggesting most stroke patients present early which may be related to severity.

Association between Onset-to-CTP Scan and Target Mismatch Profile

In binary logistic regression, after adjusting for age, both the presence of DEFUSE-3 and EXTEND target mismatch profiles were significantly associated with onset-to-CTP interval (per 60-minute interval).

Table 5-13 Binary Logistic Regression Analysis to Assess Association with DEFUSE-3 Eligibility

Variable	**Odds Ratio**	**95 % CI**		**p**
Onset-to-CTP/60	0.922	0.854	0.996	0.038
Age	1.007	0.977	1.038	0.657

CI=confidence intervals, CTP=computed tomography perfusion

Table 5-14 Binary Logistic Regression Analysis to Assess Association with EXTEND Eligibility

Variable	**Odds Ratio**	**95 % CI**		**p**
Onset-to-CTP/60	0.88	0.831	0.932	<0.001
Age	1.019	0.994	1.046	0.137

CI=confidence intervals, CTP=computed tomography perfusion

Association between Hypoperfusion Lesion and Onset-to-CTP Imaging Time

We assessed the relationship between core, penumbra and HIR with onset-to-CTP imaging time per 60 minute interval. We explored the definitions of "good HIR" as <0.2, <0.3, <0.4 and <0.5. Each model was run individually and was adjusted for age and admission NIHSS.

Table 5-15 Linear Regression Analyses to Assess Association with Onset-to-CTP Time per 60 Minute Interval

Variable	Unstandardised Coefficients		Standardised Coefficients			95% Confidence Intervals	
	B	Standard Error	Beta	t	Significance	Lower	Upper
Core	0.024	0.031	0.068	0.773	0.441	-0.037	0.085
Penumbra	-0.021	0.01	-0.197	-2.191	0.03	-0.04	-0.002
HIR	-6.201	1.991	-0.25	-3.114	0.002	-10.134	-2.267
Good HIR<0.2	3.231	1.011	0.257	3.196	0.002	1.234	5.227
Good HIR<0.3	2.479	1.026	0.193	2.416	0.017	0.452	4.507
Good HIR<0.4	3.289	1.051	0.244	3.129	0.002	1.213	5.365
Good HIR<0.5	3.728	1.103	0.261	3.381	<0.001	1.55	5.905
Good HIR<0.6	2.248	1.374	0.127	1.636	0.104	-0.466	4.962

NIHSS=National Institute of Health Stroke Scale, HIR=Hypoperfusion Intensity Ratio

We assessed the association between onset-to-CTP imaging time (per 60-minute interval) and total lesion, core lesion, penumbral lesion volumes and HIR as seen below in Figure X in both the CTP-eligible population and the subset of patients with LVO.

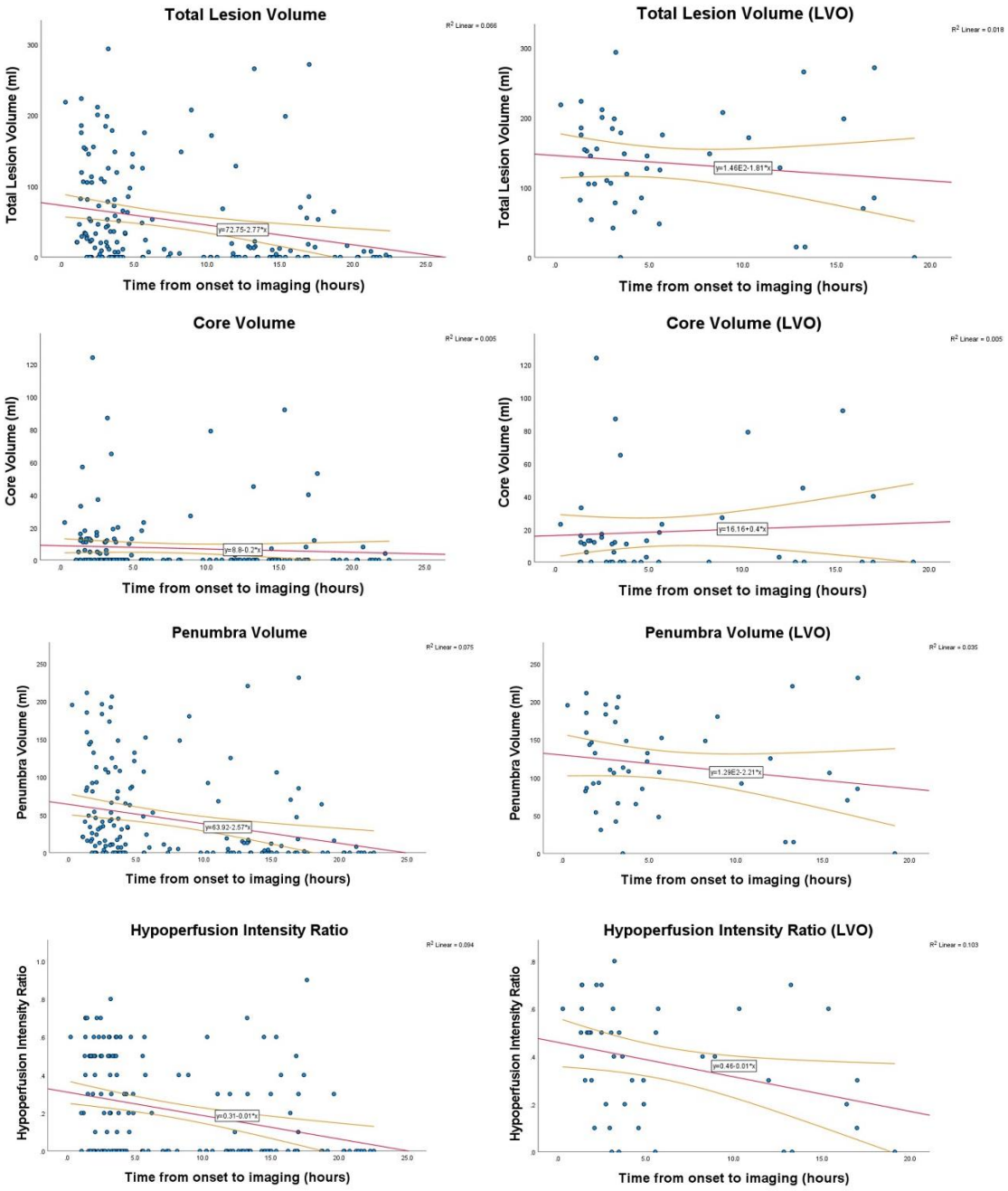

Figure 5-7 Association between Onset-to-CTP imaging time and Total Lesion Volume, Core Volume, Penumbral Volume and HIR (including LVO subset)

Discussion

In this single centre, prospective observational cohort study of acute stroke patients imaged up to 24h from onset of symptoms we found that the proportion of patients with significant volumes of salvageable tissue remained high at any time point and that the volumes of salvageable tissue declined slowly over time.

Patients who present later with severe strokes, still meet criteria for reperfusion therapy. Of the overall population (eligible for analysis), the proportion of patients meeting DEFUSE-3 and EXTEND criteria were 20% and 55% respectively. Across the time windows (including within the LVO subgroup), there was no significant difference in the proportion meeting DEFUSE-3 criteria but there was a significant difference in those meeting EXTEND - with a lower proportion in the later time windows. The proportion of patients meeting criteria was larger within the LVO subgroup but numbers were too small to assess whether this varied across the time windows. Nevertheless, this suggests that when a patient with a more severe-LVO driven AIS presents within a later time window, they are more likely to be eligible for EVT.

Within our cohort, most stroke patients presented earlier. We sought collect an unselected dataset of stroke patients up to 24 hours from onset however, our dataset is skewed towards the earlier time windows with most of our patients presenting earlier: 58% of patients with a final diagnosis of AIS or TIA presented within 6 hours of onset. This is in keeping with previous data that 61% AIS patients present within the first 6 hours (Lacy et al., 2001). More severe stroke patients present earlier. Admission NIHSS decreased with time: the median NIHSS in the <4.5 hour group being 7 (IQR 4-12) and in the >18 hour group 3 (IQR 2–6). The decrease was significant across the groups with the main difference being between the first and last time windows. It is known that admission delay is related to severity of initial symptoms (Jørgensen et al., 1996).

Within the LVO subset, the most common occlusion site was M1. Whilst most trials defined LVO as ICA or M1 occlusion, our definition extended to multiple branches of the M2 in keeping with the ESCAPE trial's definition (Goyal et al., 2015). This was based on the logic that multiple occluded M2 branches have a similar clinical presentation to an M1 occlusion and most would be removed by EVT. The majority of patients within each occlusion site met DEFUSE-3 criteria; the proportions increased the more distal the presenting occlusion site with 100% of the >1 branch M2 occlusions meeting criteria. Neither core nor penumbra volumes differed significantly by occlusion site when limiting the population to our chosen definition of LVO. Again the numbers were not sufficiently large to allow for comparison across time window but this also supports our previous finding that within 24 hours, patients presenting with LVO are more likely to meet DEFUSE-3 criteria. Additionally, patients with more distal occlusions may have better

collateral circulation which could be explained by the ICA and MCA supplying microvascular anastomoses between the ACA and the MCA, and the MCA and the PCA allowing retrograde flow if the MCA supply has not been completely occluded (Liebeskind, 2003).

We found penumbra but not core volume to be significantly negatively associated with onset-to-imaging time (both through measurement of mismatch lesion and HIR). The concept of the penumbra translates clinically as disabling ischaemia within the brain may be reversible if the occluded vessel is reperfused. This was demonstrated by Thomas et al. (1981) whose temporary occlusion of the MCA in Macaca irus monkeys demonstrated reversible hemiparalysis. There have been few human studies surrounding the natural history of stroke. Beaulieu et al. (1999) demonstrated larger infarct growth up to 30 days in patients with a PWI - DWI mismatch. The lack of mismatch in some patients may be explained by their being ‘fast progressors’ whilst those with may have been slow (Rocha and Jovin, 2017). Lesion volumes were dynamic: remaining stable up to 12 hours, increasing markedly between 24-36 hours with 25% demonstrating maximum DWI volumes at 24-36 hours and the rest at 5-7 day. The findings were not statistically significant (the number recruited was 21) however, 53% of patients were thrombolysed which does not explain the variability amongst lesion volumes which further supports the fast/slow progressor theory (Beaulieu et al., 1999, Rocha and Jovin, 2017). Previous datasets have shown the ischaemic penumbra to be persistent and constant within the first 6 hours of symptom onset in patients with acute MCA occlusion (Jovin et al., 2003). The physiology of retrograde collateral flow is unclear. The idea of such flow temporarily maintaining penumbra but ultimately failing to replace antegrade perfusion has led to the concept of collateral failure: the persistence of penumbra depends on the collateral endurance (Liebeskind et al., 2010). Collateral flow failure is associated with infarct growth (Jones et al., 1981). The DEFUSE2 study introduced the target mismatch profile - patients with which have more favourable clinical outcome following early reperfusion by EVT as compared with those without (Lansberg et al., 2012). Whilst our data would support the concept of collateral failure beyond 6 hours onset especially as median penumbra volumes for both definitions of late window were 0ml, having not taken sequential measurements, we can only conclude that the chance of a larger penumbra at presentation significantly decreases with time and not penumbra itself.

Our data show HIR to also be significantly associated with time. The HIR provides an index of collateral flow (Olivot et al., 2014). Higher HIR reflects poorer collateral flow and has been associated with faster infarct growth and poor clinical outcome (Olivot et al., 2014, Guenego et al., 2018). The DEFUSE investigators (and originators of the HIR) defined high HIR (i.e. poorer collaterals) as above the median value (0.39, interquartile range 0.23-0.51) (Olivot et al., 2014). As a result, the definition of high HIR is traditionally $\geq$0.4 but there is no concrete value. We therefore explored several "good HIR" definitions of <0.2, <0.3, <0.4, <0.5 and <0.6 based on our median value (0.4) and interquartile range (0.2 to 0.6). The definitions of <0.2 to <0.5 were significant against time (and not that of <0.6) further supporting the idea that collateral availability is time dependent. The value of a volumetric index of collateral status (rather than the conventional CTA scoring) would be especially useful in the context of selecting patients for interhospital transfer. We will explore this further in Chapter 6.

Previously, only estimates of the proportion of patients who might be eligible for treatment have been available to inform clinical services since there had been few observational data on those presenting >6h from onset in a typical hospital population. This is particularly relevant at a time when not only has the window for intervention been extended but the more restrictive DEFUSE-3 criteria is being questioned (Nogueira et al., 2017, Albers et al., 2018). MR CLEAN LATE and the large core trials have opened up EVT to patients who present later with larger core volumes (although as mentioned previously, these patients most likely had larger penumbra volumes) (Olthuis et al., 2023a, Yoshimura et al., 2022, Bendszus et al., 2023, Sarraj et al., 2023, Huo et al., 2023). Within our data, more patients met EXTEND criteria than DEFUSE-3 (55% versus 19%) which adds further support to there being a cohort of patients who would benefit from reperfusion therapy outside of the DEFUSE-3 criteria. The WHISPER study provides an estimate on the proportion of patients with viable brain tissue at later times after onset of stroke symptoms and supports the idea of collateral failure at later time windows.

Inter-observer agreement for image analysis using Cohen's κ coefficient was substantial with perfect agreement in LVO presence and affected hemisphere (Cohen, 1960). The other imaging assessments relevant to this chapter were NCCT ASPECTS and CTA LVO site. There was only one discrepancy with the LVO site analysis -a P1 lesion versus a P2 which

represents a degree of human subjectivity and overall is not concerning. Admittedly, this sample size is small but represents 5% of our overall recruitment.

This study has several limitations. Whilst our sample size is small (although not for an observational study), we aimed to recruit 149 patients but were able to recruit 185. Most patients presented earlier which made comparisons between the time windows difficult however we expect acute, severely disabling stroke patients to come to hospital earlier. Nevertheless, having more LVO patients within our cohort with a more even distribution of severity would strengthen our conclusions.

Our criteria were deliberately wide in order to recruit as many patients with AIS symptoms as possible. Owing to a lack of availability of research imaging, recruitment was only possible when advanced imaging was available. In February 2020, CTP and CTA became standard front-door investigations at the Queen Elizabeth University Hospital which will have influenced admissions to the HASU and study recruitment i.e. patients with identifiable lesions were more likely to be recruited. The imaging was available 24/7 but was used selectively; clinicians requested it based on admission NIHSS and on the grounds that the results would inform treatment decisions. It may have biased the sample recruited.

This was a single-centre study which makes generalisability difficult. We had a good recruitment rate of 29% and our population compared favourably to national audit data although the high rTPA rate (49%) within our population may reflect recruitment bias once advanced imaging became part of routine assessment (SSNAP, 2023).

Our data were collected at a time when EVT was not routinely available in Scotland but overall 19% of our population met DEFUSE-3 criteria. We will explore the radiological outcome for these patients in Chapter 7. Furthermore, we present cross-sectional evidence of patients presenting within different time windows rather than sequential imaging of the same patients, further sequential imaging, in larger populations of late-presenting AIS patients would provide valuable information on the relationship between penumbra and time.

Chapter 6 The WHISPER Study: Collateral Status

Introduction

Leptomeningeal collaterals [LMCs] are a prognostic marker in AIS. Better collaterals are associated with smaller ischaemic core and larger mismatch volumes with CTP (Vagal et al., 2016). Poorer collaterals are associated with increased risk of symptomatic haemorrhagic transformation following EVT (Bang et al., 2011). Collateral blood supply (as measured using multiphase CTA) predicts treatment effect and final clinical outcome in patients with LVO treated with EVT (Berkhemer et al., 2016a, Menon et al., 2015). LMCs were not formally used to recruit patients to EVT trials except for ESCAPE although are likely to have informed selection in trials which did not use perfusion (Goyal et al., 2015). Like many other imaging prognostic markers, a treatment-modifying interaction effect has not been demonstrable (Gensicke et al., 2022).

More recently in the large core trials, none included collateral status in the inclusion criteria (Yoshimura et al., 2022, Bendszus et al., 2023, Sarraj et al., 2023, Huo et al., 2023). Secondary analysis is needed to determine the association with outcome. A recent retrospective analysis of collateral status in patients with anterior LVO and an ASPECTS of $\leq$5 who underwent EVT demonstrated significantly better clinical outcome associated with reperfusion in patients with good collaterals (Broocks et al., 2020).

Single-phase CTA [sCTA] is widely available and is the most used CTA modality. Assessment of LMCs however may over- or under-estimate collaterals according to acquisition phase of the CTA (Beyer et al., 2015, Boers et al., 2018). Timing of image acquisition and contrast arrival varies widely among patients. The predictive proportion of sCTA scans with poor collaterals is better in the early arterial phase but better in the late venous phase for good collaterals (Gensicke et al., 2022). Many scoring systems are limited to anterior circulation large vessel occlusion (LVO) and use broad categories which are often collapsed further in analysis into a dichotomous moderate-good versus poor-none. The most commonly used is the modified Tan collateral grading system which was proposed in 2009 and was derived from patients with MCA occlusion (Tan et al., 2009a).

CTA collateral scoring that provides greater levels of detail relevant to more distal vessel occlusions or non-MCA vascular territories is labour intensive and likely prone to greater observer variation. A retrospective analysis using three scores (the modified Tan, the Miteff and the Rosenthal scales) found that whilst the best measure of consistency was found for the simplest method of scoring - modified Tan scale (weighted kappa value 0.72 versus 0.49 and 0.59 for the more complex Miteff and Rosenthal scales respectively), the difference did not reach statistical significance (Dolotova et al., 2023).

The regional Leptomeningeal Collateral [rLMC] score (20 points) is a semi-quantitative system of scoring the leptomeningeal pathways as divided into anatomic regions in accordance with the ASPECTS method, based on the extent of contrast opacification in multi-phase CTA. Better collateral status is indicated by higher total scores which correlate with clinical outcome at 90 days (Menon et al., 2011). Interrater reliability is good. The rLMC score has been previously analysed as a continuous variable or trichotomized into 0-10, 11-16 and 17-20 (Menon et al., 2011, Chatterjee et al., 2020). Although it was derived from patients who underwent multiphase CTA, we applied it to our single CTA scans based on its more detailed assessment of collateral circulation.

CTP imaging estimates cerebral haemodynamics based on a dynamic acquisition and also represents collateral status (Liebeskind, 2003). The hypoperfusion intensity ratio (HIR) was proposed to provide an index of collateral flow on the basis that the greater the Tmax delay, the poorer the collateral status. It is defined as the proportion of Tmax >6 second delay lesion with Tmax >10 second delay i.e. Tmax>6s/Tmax10s (Olivot et al., 2014).

The chosen values of Tmax >6s and Tmax >10s are based on the findings of the Diffusion and Perfusion Imaging Evaluation for Understanding Stroke Evolution Study (DEFUSE) and DEFUSE 2 studies (Olivot et al., 2009, Lansberg et al., 2012). Tmax >6s provides the most accurate assessment of penumbra volume compared with Tmax >2s, Tmax >4s, Tmax 8s and Tmax >10s. Penumbra salvage volume only defined by a Tmax >6 second delay was significantly increased in patients with favourable outcomes, patients who experienced reperfusion and among mismatch patients (Olivot et al., 2009). Tmax >6s lesions encompass regions of variable delay – including severe hypoperfusion associated with irreversible necrosis regardless of reperfusion and tissue with delays of >8s and >10s

(Calamante et al., 2010, Olivot et al., 2014, Guadagno et al., 2008). Tmax >10s was associated with poor outcome following reperfusion in the DEFUSE and the Echoplanar Imaging Thrombolytic Evaluation Trial (EPITHET) meta-analysis (Mlynash et al., 2011).

Higher HIR reflects poorer collateral flow and has been associated with faster infarct growth and poor clinical outcome (Olivot et al., 2014, Guenego et al., 2018). There is no uniform definition of low HIR but typically patients are dichotomised based on the median value -this has led to definitions such as <0.4, <0.5 and <0.54 (Olivot et al., 2014, Guenego et al., 2018, Baek et al., 2021).

Collateral scores as determined by CTA or CTP have been developed using anterior-circulation LVO populations.

This chapter examines the correlation between collateral scores as determined by CTA and CTP, the definitions of low HIR and explores biological determinants of collateral status, within the WHISPER population who had a final diagnosis of AIS or TIA.

Methods

Patients

The inclusion criteria, study design and primary results of WHISPER have been described in the preceding chapter.

Definitions

Perfusion lesion volumes (Tmax >4, 6, 8, 10s) were estimated by RAPID version 4.7 (Ischemaview) -an automated software program.

HIR was defined by the proportion of Tmax>6s with Tmax>10s (Olivot et al., 2014). Patients were dichotomised into high (poor) and low (good) HIR groups based on the

median value for LVO patients (0.4) – we also explored the quartiles (0.2 and 0.6) as HIR thresholds.

Angiographic collateral scores were assessed by two experienced assessors with a random sample confirmed by a third assessor. Good collaterals as defined by rLMC≥17 and moderate-to-good as defined by rLMC≥11 were explored.

Intracranial VO [IVO] was defined as occlusion of the internal carotid artery [ICA], middle cerebral artery [MCA] M1 or >1 branch of M2. Other IVO were defined as occlusion of anterior cerebral artery [ACA] M2 (1 branch), M3, posterior cerebral artery [PCA], basilar artery, vertebral artery or superior cerebellar artery [SCA].

AOL revascularisation scores were dichotomised first into revascularisation (AOL 2-3) versus no revascularisation (AOL 0-1) and then into good revascularisation (AOL 3) versus poor revascularisation (AOL 0-2).

Hyperglycaemia was defined as admission glucose >7.0mmol/l.

Scans separated by thrombolysis were defined by patients who had either CTP or CTA after thrombolysis.

Outcome was measured by follow-up NIHSS at 24-72 hours, day 90 mRS, follow-up infarct volume on MRI and AOL score on MRA.

Analyses

We analysed the following aspects of collateral status as determined by CTA and CTP:

Collateral Score Analysis

The radiological characteristics of patients separated into high (unfavourable) and low (favourable) HIR with thresholds of low HIR as <0.2, <0.4 and <0.6 in all patients, IVO and LVO.

We used the Kruskal-Wallis test to compare groups to assess if one dominated the other. This test assumes that the intervention (in this case the definition of low/good HIR) affects the response level (the other radiological characteristics measured) with a rank order among the responses (Lehmann E.L., 1975).

We also assessed the ability of the rLMC to predict low/good HIR (as defined by separate thresholds) using receiver operating characteristic [ROC] curve analysis. This test evaluates ability of tests to diagnose or predict the state of objects and finds the optimal cut-off values (Hajian-Tilaki, 2013).

The area under the curve [AUC] was calculated. This is a widely used measure of accuracy. The closer the ROC curve is to the upper left corner of the graph, the more closely the two variables measured align – the upper left corner has a sensitivity and specificity of 1 i.e. no false positives. Therefore an AUC of 1 represents perfect alignment. An AUC of 0.5 would correspond with a curve in the shape of a straight 45 degree line i.e. x=y. Any value below this number indicates random guessing. We used the following definitions for interpretation of AUC: $\geq$0.9 represented excellent, $\geq$0.8 to <0.9 represented good, $\geq$0.7 to <0.8 represented fair, $\geq$0.6 to <0.7 represented poor and <0.6 represented a fail (Hajian-Tilaki, 2013).

The limitation of the ROC-AUC analysis is that there is an assumption that both distributions are normal with comparable standard deviations. Additionally, it summarises the comparison into a single number (the AUC) which means valuable information about the pattern of alignment may be lost (Hajian-Tilaki, 2013).

Biological Determinants of Collateral Status

We explored the possibility that HIR and rLMC would be affected by risk factors such as age, hypertension status, presence of atrial fibrillation, smoking status, admission blood glucose, admission hyperglycaemia and HbA1c through regression analysis.

We used binary logistic regression modelling to identify relationship to low HIR (as defined by HIR<0.2, HIR<0.4 and HIR<0.6) and high rLMC (as defined by rLMC≥17 and rLMC≥11).

The advantage of linear regression is that it both tests for relationships and then quantifies direction and strength. The regression coefficient describes the expected change in the dependent variable for each unit of change in the independent variable. Assumptions by the model include normal distribution, no repeated measurements and including appropriate interactions to adjust the model to avoid biased estimates (Schober and Vetter, 2021). Similar to linear regression, binary logistic regression provides an odds ratio in the context of more than one explanatory variable. However, the dependent variable is binomial and a further advantage is that analysing the association of variables together avoids confounding effects (Sperandei, 2014).

Collateral Status and Outcome

The association of collateral status with clinical and radiological outcomes was assessed.

We assessed the following outcomes:

1. Decrease in follow-up NIHSS
2. day 90 mRS
3. MRI volume
4. MRA recanalisation in patients with IVO

Statistics

Statistical analysis was performed using IBM SPSS Statistics for Windows (version 28.0, Armonk, New York: IBM Corp.).

Results

The flowchart of inclusion for the analyses in this chapter is shown below in Figure 6-1.

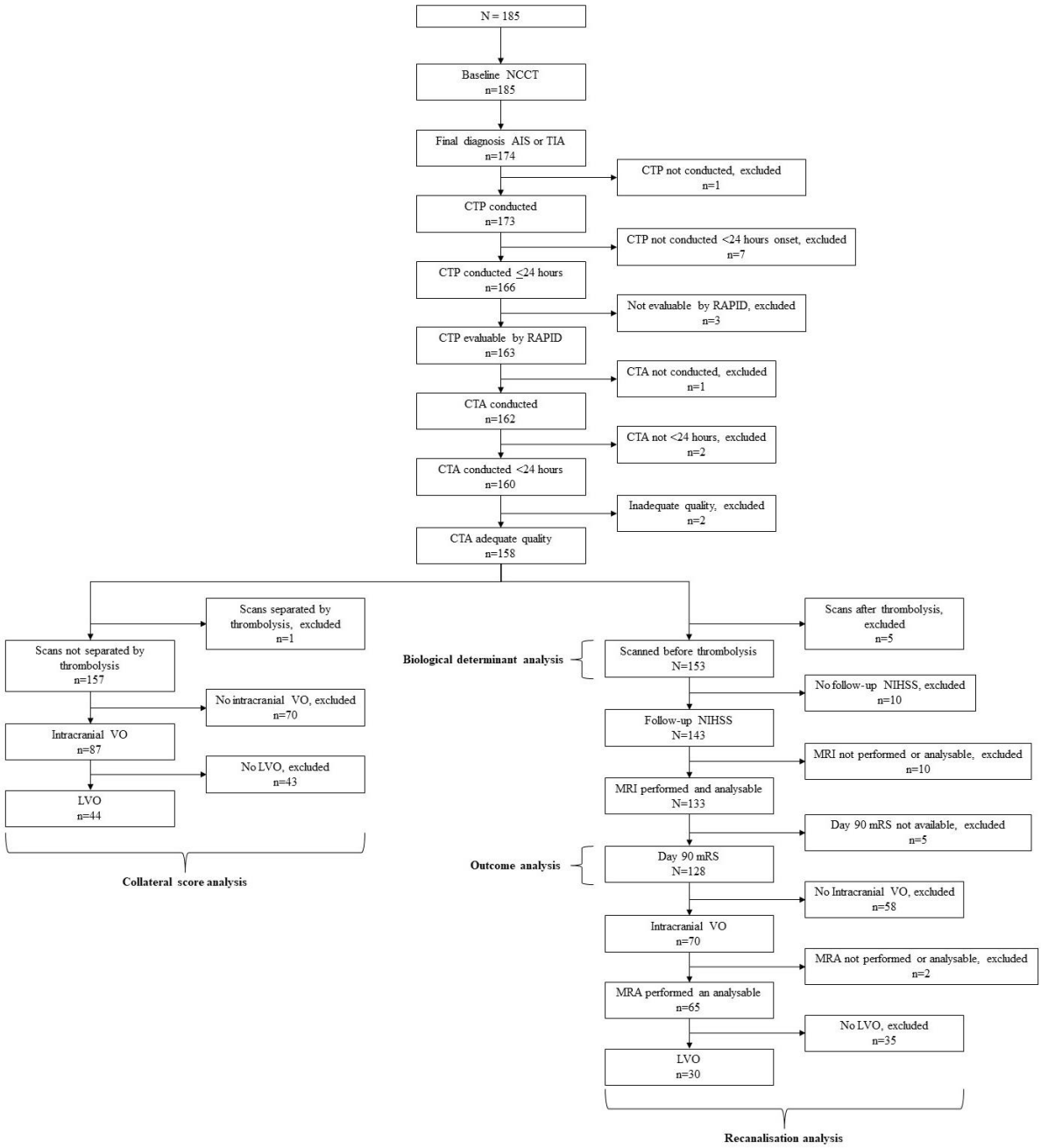

N=number, NCCT=non-contrast computed tomography, AIS=acute ischaemic stroke, TIA=transient ischaemic attack, CTP=computed tomography perfusion, CTA=computed tomography angiography,

VO=vessel occlusion, LVO=large vessel occlusion, NIHSS=National Institute of Health Stroke Scale, MRI=magnetic resonance imaging, mRS=modified Rankin, MRA=magnetic resonance angiography

Figure 6-1 Flowchart of Inclusion for Analyses

Collateral Score Analysis

Baseline characteristics are described below in Table 6-1.

Table 6-1 Clinical Characteristics

Variable	**All patients N =157**	**IVO N=87**	**LVO N=44**
Age (mean±SD) (years)	67±14	66±14	67±15
Gender (% male)	97 (62)	53 (61)	24 (55)
Myocardial infarction (n, %)	14 (9)	9 (10)	2 (5)
Other ischaemic heart disease (n, %)	20 (13)	13 (15)	7 (16)
Previous stroke (n, %)	23 (15)	13 (15)	6 (14)
Ischaemic (n, %)	19 (12)	11 (13)	5 (11)
Haemorrhagic (n, %)	2 (1)	1 (1)	0 (0)
Unknown (n, %)	2 (1)	1 (1)	1 (2)
Diabetes mellitus (n, %)	20 (19)	15 (17)	8 (18)
Hypertension (n, %)	79 (50)	39 (45)	21 (48)
Atrial fibrillation (n, %)	24 (15)	17 (20)	8 (18)
Current smoker (n, %)	35 (22)	17 (20)	8 (18)
Excessive alcohol consumption (n, %)	10 (6)	5 (6)	3 (7)
Admission blood glucose (mean±SD (mmol/L)	7.4±3.7*	7.6±3.8[a]	8.2±4.9[∞]
Hyperglycaemia on admission (i.e. ≥7 mmol/l) (n, %)	53 (34)*	33 (38) [a]	20 (46) [∞]
HbA1c +/- 3 months of event (mean±SD (mmol/mol)	46.4±14.7**	45.8±13.2[≠]	45.8±15.0
Baseline NIHSS (median, IQR)	6 (4, 11)	8 (5, 14)	14 (8, 18)
Pre-stroke excellent function (mRS 0-1) (n, %)	144 (92)	79 (91)	38 (87)
Pre-stroke good function (mRS≤2) (n, %)	149 (95)	82 (94)	40 (91)
Onset to CTP (median, IQR) (hours)	249 (161, 785)	217 (125, 449)	209 (118, 525)
Onset to CTA (median, IQR) (hours)\	247 (164, 775)	215 (129, 397)	215 (121, 471)
Wake-up (n, %)	52 (33)	21 (24)	12 (27)

*N=156, **N=81, [a]N=86, [≠]N=45, [∞]N=43. IVO=intracranial vessel occlusion, LVO=large vessel occlusion, n=number, SD=standard deviation, NIHSS=National Institute of Health Stroke Scale, IQR=interquartile range, mRS=modified Rankin Scale, CTP=computed tomography perfusion, CTA=computed tomography angiography

Table 6-2 Proportion of Vessel Occlusion Sites

Vessel Occlusion Site	n	IVO %, N=87	LVO %, N=44
ICA	12	14%	27%
Proximal M1	12	14%	27%
Distal M1	13	15%	30%
M2 > 1 branch	7	8%	16%
M2 1 branch	22	25%	
M3	7	8%	
PCA	9	10%	
Basilar	2	2%	
Vertebral	2	2%	
SCA	1	1%	

N=number, IVO=intracranial vessel occlusion, LVO=large vessel occlusion, ICA=internal carotid artery, PCA=posterior cerebral artery, SCA=superior cerebellar artery

Table 6-2 is a breakdown of the vessel occlusion sites -the largest proportion being M2 1 branch (25% of IVO) which were not included in the LVO analysis. The largest LVO proportions were tied between ICA and proximal MI (27% of LVO each).

Table 6-3 details the radiological characteristics of patients included in the collateral score analysis. Patients were separated in columns into “All patients”, “IVO” and “LVO” and into rows using the low/good HIR thresholds. Difference between HIR thresholds was assessed using Kruskal-Wallis.

ASPECTS were significantly different at all HIR threshold definitions except in the LVO subgroup; scores were only significant at the HIR<0.6 threshold with no significant difference at lower thresholds. Perfusion deficit volumes were significantly different across all thresholds except for mismatch at the HIR<0.6 threshold subgroup in the IVO patients. The rLMC score was not significantly different in LVO patients when separated into HIR thresholds<0.4 and <0.6.

Table 6-3 Radiological Characteristics Separated into Low HIR Threshold Definitions

Characteristics		All (N=157) All	All (N=157) Low HIR	All (N=157) High HIR	All (N=157) p value	Intracranial VO (N=87) All	Intracranial VO (N=87) Low HIR	Intracranial VO (N=87) High HIR	Intracranial VO (N=87) p value	LVO (N=44) All	LVO (N=44) Low HIR	LVO (N=44) High HIR	LVO (N=44) p value
Low HIR<0.2													
n (%)			85 (54)	72 (46)			25 (29)	62 (71)			10 (23)	34 (77)	
ASPECTS	median (IQR)	9 (8, 10)	10 (9, 10)	8 (6, 9)	<**0.001**	8 (6, 10)	9 (8, 10)	8 (6, 9)	**0.001**	7 (5, 9)	9 (7, 9)	7 (5, 8)	0.09
CBF<30% (ml)	median (IQR)	0 (0, 6)	0 (0, 0)	6 (0, 18)	<**0.001**	0 (0, 13)	0 (0, 0)	7 (0, 18)	<**0.001**	11 (0, 22)	0 (0, 0)	13 (2, 29)	<**0.001**
Tmax>6s (ml)	median (IQR)	21 (0, 80)	0 (0, 12)	75 (35, 151)	**0.000**	68 (24, 145)	13 (5, 45)	105 (51, 159)	<**0.001**	137 (83, 183)	45 (12, 90)	153 (119, 198)	<**0.001**
Tmax>10s (ml)	median (IQR)	0 (0, 25)	0 (0, 0)	31 (13, 73)	**0.000**	20 (5, 63)	0 (0, 3)	37 (17, 80)	<**0.001**	56 (15, 96)	0 (0, 6)	75 (37, 109)	<**0.001**
Mismatch (ml)	median (IQR)	16 (0, 69)	0 (0, 12)	67 (26, 130)	**0.000**	54 (18, 113)	13 (3, 44)	82 (40, 144)	<**0.001**	109 (73, 157)	45 (11, 87)	132 (92, 181)	<**0.001**
rLMC score	median (IQR)	19 (14, 20)	20 (19, 20)	14 (10, 18)	<**0.001**	15 (11, 18)	18 (16, 20)	13 (10, 17)	<**0.001**	11 (9, 15)	16 (11, 17)	10 (9, 13)	**0.005**
Low HIR<0.4													
n (%)			109 (69)	48 (31)			46 (53)	41 (47)			20 (46)	24 (55)	
ASPECTS	median (IQR)		10 (8, 10)	8 (6, 9)	<**0.001**		9 (7, 10)	7 (6, 9)	**0.002**		8 (6, 9)	6 (5, 9)	0.228
CBF<30% (ml)	median (IQR)		0 (0, 0)	12 (0, 23)	<**0.001**		0 (0, 0)	13 (0, 25)	<**0.001**		0 (0, 9)	16 (7, 42)	<**0.001**
Tmax>6s (ml)	median (IQR)		5 (0, 34)	94 (34, 175)	<**0.001**		43 (11, 85)	119 (53, 181)	<**0.001**		85 (44, 125)	175 (146, 205)	<**0.001**
Tmax>10s (ml)	median (IQR)		0 (0, 5)	49 (19, 94)	**0.000**		5 (0, 15)	63 (31, 97)	<**0.001**		13 (0, 26)	93 (69, 116)	<**0.001**
Mismatch (ml)	median (IQR)		5 (0, 34)	81 (24, 148)	<**0.001**		42 (11, 85)	92 (36, 156)	<**0.001**		85 (44, 118)	148 (96, 190)	**0.001**
rLMC score	median (IQR)		20 (17, 20)	14 (10, 19)	<**0.001**		16 (13, 20)	11 (10, 17)	**0.004**		13 (10, 16)	10 (8, 13)	0.032
Low HIR<0.6													
n (%)			135 (86)	22 (14)			67 (77)	20 (23)			32 (73)	12 (27)	
ASPECTS	median (IQR)		9 (8, 10)	7 (5, 8)	<**0.001**		9 (7, 10)	6 (5, 8)	**0.001**		8 (6, 9)	6 (4, 8)	**0.04**
CBF<30% (ml)	median (IQR)		0 (0, 0)	20 (12, 54)	<**0.001**		0 (0, 8)	20 (12, 54)	<**0.001**		0 (0, 12)	28 (15, 85)	<**0.001**
Tmax>6s (ml)	median (IQR)		13 (0, 58)	137 (35, 201)	<**0.001**		55 (16, 113)	163 (40, 208)	**0.002**		108 (66, 148)	198 (172, 222)	<**0.001**
Tmax>10s (ml)	median (IQR)		0 (0, 13)	87 (22, 117)	<**0.001**		12 (0, 38)	97 (25, 119)	<**0.001**		30 (6, 67)	115 (101, 140)	<**0.001**
Mismatch (ml)	median (IQR)		11 (0, 53)	84 (17, 193)	<**0.001**		53 (16, 108)	89 (31, 194)	0.063		107 (65, 140)	176 (96, 204)	**0.01**
rLMC score	median (IQR)		20 (15, 20)	12 (9, 17)	<**0.001**		15 (11, 19)	11 (9, 17)	**0.023**		11 (9, 15)	10 (8, 11)	0.106

N=number, VO=vessel occlusion, LVO=large vessel occlusion, HIR=hypoperfusion intensity ratio, ASPECTS=Alberta stroke programme early computed tomography score, CBF=cerebral blood flow, Tmax=time to maximum, rLMC=regional leptomeningeal collateral score

Table 6-4 ROC Curve Analysis of the rLMC to Predict Low HIR separated into HIR Threshold Definitions

	All (N=157)	Intracranial VO (N=87)	LVO (N=44)
Low HIR<0.2	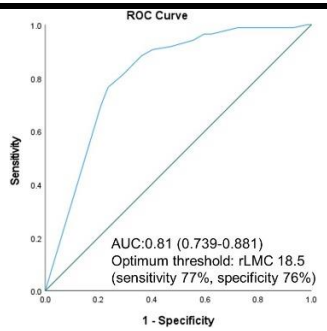	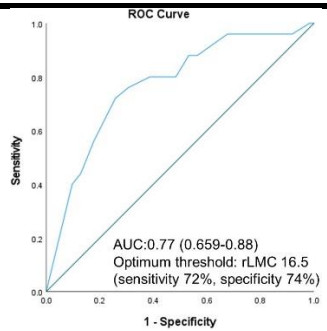	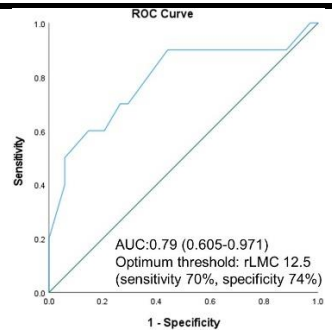
Low HIR<0.4	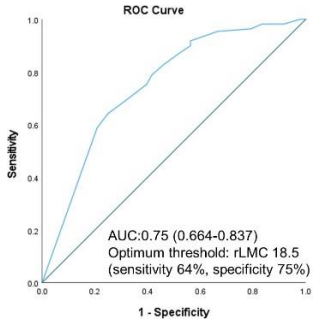	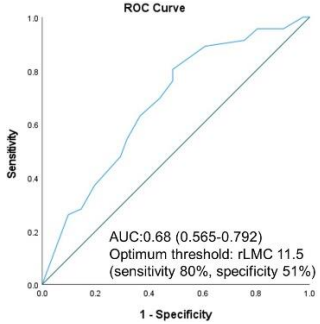	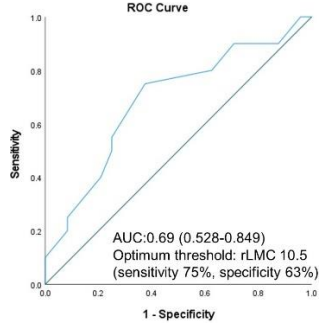
Low HIR<0.6	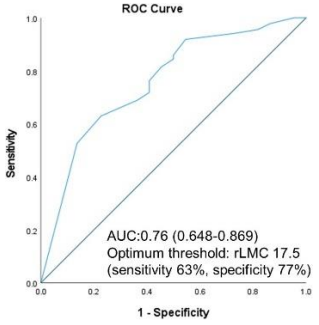	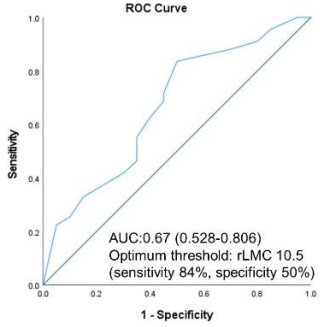	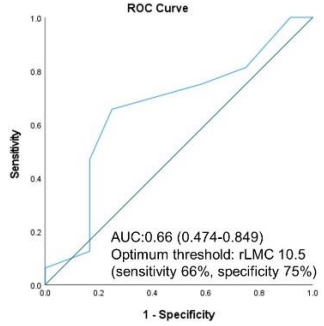

ROC= receiver operating characteristic, N=number, VO=vessel occlusion, LVO=large vessel occlusion, HIR=hypoperfusion intensity ratio, AUC=area under the curve, rLMC=regional leptomeningeal collateral score

Table 6-4 is a series of ROC curve analyses to determine the relationship between HIR (at separate thresholds) and rLMC score.

In terms of AUC assessment, only the “All patients” group achieved an “excellent” status within the 0.2 threshold i.e. the rLMC score was able to predict low/good HIR as defined by HIR<0.2. There were no “good” statuses and at higher thresholds for low/good HIR (i.e. <0.4 and <0.6) the subgroups of IVO and LVO demonstrated “poor” prediction.

On visual inspection of the ROCs, in all patients and the LVO subgroup, the HIR thresholds do not discriminate between rLMC scores -they remain between 17.5 and 18.5 and 10.5 and 12.5 respectively. Within the IVO subgroup, lower HIR (i.e. better collaterals) corresponds to higher rLMC score.

Biological Determinants of Collateral Status

We assessed biological determinants of collateral status. Baseline characteristics are described below in Table 6-5.

.

Table 6-5 Clinical Characteristics within the Biological Determinants Subgroup

Variable	**All patients N =153**
Age (mean±SD) (years)	67±14
Gender (% male)	94 (61)
Myocardial infarction (n, %)	14 (9)
Other ischaemic heart disease (n, %)	20 (13)
Previous stroke (n, %)	22 (14)
Ischaemic (n, %)	18 (12)
Haemorrhagic (n, %)	2 (1)
Unknown (n, %)	2 (1)
Diabetes mellitus (n, %)	28 (18)
Hypertension (n, %)	77 (50)
Atrial fibrillation (n, %)	24 (16)
Current smoker (n, %)	32 (21)
Excessive alcohol consumption (n, %)	10 (7)
Admission blood glucose (mean±SD (mmol/L)	7.3±3.7*
Hyperglycaemia on admission (i.e. ≥7 mmol/l) (n, %)	51 (33)*
HbA1c +/- 3 months of event (mean±SD (mmol/mol)	46.3±14.7**
Baseline NIHSS (median, IQR)	6 (3, 11)
Pre-stroke excellent function (mRS 0-1) (n, %)	140 (92)
Pre-stroke good function (mRS≤2) (n, %)	145 (95)
Onset to CTP (median, IQR) (hours)	253 (163, 785)
Onset to CTA (median, IQR) (hours)	253 (165, 775)
Wake-up (n, %)	51 (33)

*N=152, **N=77. n=number, SD=standard deviation, NIHSS=National Institute of Health Stroke Scale, IQR=interquartile range, mRS=modified Rankin Scale, CTP=computed tomography perfusion, CTA=computed tomography angiography

Table 6-6 Series of Univariable Linear Regression Analyses for HIR versus Biological Determinants

N=153	Unstandardised Coefficients		Standardised Coefficients			95% Confidence Intervals	
Variable	**B**	**Standard Error**	**Beta**	**t**	**Significance**	**Lower**	**Upper**
Age	-5.75E-5	0.001	-0.003	-0.038	0.97	-0.003	0.003
Hypertension	-0.017	0.041	-0.034	-0.416	0.678	-0.099	0.064
Atrial fibrillation	0.1	0.056	0.144	1.792	0.075	-0.01	0.211
Smoking	-0.05	0.051	-0.08	-0.982	0.328	-0.149	0.05
Blood glucose	0.007	0.005	0.103	1.272	0.205	-0.004	.018
Hyperglycaemia	0.077	0.043	0.144	1.785	0.076	-0.008	0.161
HbA1c	0.0	0.002	0.021	0.18	0.858	-0.004	0.004

N=number

Table 6-6 is a series univariable linear regression analysis with biological determinants run separately as independent variables to demonstrate relationship with HIR. There are no significant determinants.

Table 6-7 Series of Univariable Linear Regression Analyses for rLMC versus Biological Determinants

N=153	Unstandardised Coefficients		Standardised Coefficients			95% Confidence Intervals	
Variable	**B**	**Standard Error**	**Beta**	**t**	**Significance**	**Lower**	**Upper**
Age	-0.028	0.025	-0.09	-1.11	0.269	-0.077	0.022
Hypertension	0.005	0.695	0.001	0.007	0.995	-1.369	1.379
Atrial fibrillation	-1.36	0.95	-0.116	-1.4433	0.154	-3.237	0.516
Smoking	0.96	0.851	0.091	1.128	0.261	-0.722	2.642
Blood glucose	-0.198	0.092	-0.174	-2.159	0.032	-0.378	-0.017
Hyperglycaemia	-1.63	0.723	-0.181	-2.254	0.026	-3.059	-0.201
HbA1c	-0.015	0.033	-0.053	-0.462	0.645	-0.081	0.051

N=number

Table 6-6 Series of Univariable Linear Regression Analyses for HIR versus Biological Determinants

Table 6-7 is a series univariable linear regression analysis with biological determinants run separately as independent variables to demonstrate relationship with rLMC score. Both

blood glucose and admission hyperglycaemia are significantly associated with a reduction in rLMC score (p=0.032, 95% CI -0.378 to -0.017, B coefficient -0.198 and p=0.026, 95%CI -3.059 to -0.201, B coefficient -1.63).

Table 6-8 Univariate Binary Logistic Regression Modelling to Identify Predictors of Low HIR

N=153	HIR	Odds Ratio	95 % CI		p
Age	<0.2	1.001	0.979	1.025	0.9
	<0.4	1.001	0.977	1.026	0.931
	<0.6	0.999	0.967	1.032	0.945
Hypertension	<0.2	1.334	0.705	2.526	0.376
	<0.4	1.225	0.616	2.439	0.562
	<0.6	0.821	0.332	2.032	0.669
Atrial fibrillation	<0.2	0.349	0.139	0.873	0.025
	<0.4	0.696	0.28	1.727	0.434
	<0.6	0.425	0.147	1.228	0.114
Smoking	<0.2	1.071	0.489	2.348	0.863
	<0.4	1.764	0.703	4.424	0.227
	<0.6	1.801	0.498	6.513	0.37
Blood glucose	<0.2	0.942	0.859	1.034	0.212
	<0.4	0.966	0.885	1.054	0.431
	<0.6	0.938	0.852	1.034	0.197
Hyperglycaemia	<0.2	0.539	0.273	1.064	0.075
	<0.4	0.537	0.262	1.101	0.09
	<0.6	0.501	0.197	1.273	0.146
HbA1c	<0.2	0.996	0.966	1.027	0.789
	<0.4	0.995	0.964	1.028	0.781
	<0.6	0.987	0.949	1.026	0.514

N=number

Table 6-8 demonstrates a series of binary logistic regression analysis with biological determinants run separately as independent variables to demonstrate relationships with low/good HIR. We explored low/good HIR as <0.2, <0.4 and <0.6 as previously explained. Atrial fibrillation was significantly associated with HIR<0.2 (p=0.025, OR 0.349, 95% CI 0.139 to 0.873).

Table 6-9 Univariate Binary Logistic Regression Modelling to Identify Predictors of High rLMC

N=153	rLMC	Odds Ratio	95 % CI		p
Age	≥17	0.979	0.954	1.004	0.105
	≥11	0.991	0.956	1.027	0.612
Hypertension	≥17	1.02	0.526	1.981	0.952
	≥11	0.499	0.187	1.33	0.165
Atrial fibrillation	≥17	0.394	0.163	0.955	0.039
	≥11	0.5	0.163	1.536	0.226
Smoking	≥17	1.513	0.644	3.555	0.342
	≥11	1.58	0.433	5.766	0.489
Blood glucose	≥17	0.954	0.874	1.041	0.294
	≥11	0.874	0.787	0.97	0.011
Hyperglycaemia	≥17	0.663	0.33	1.331	0.247
	≥11	0.313	0.117	0.836	0.021
HbA1c	≥17	1.001	0.97	1.033	0.952
	≥11	0.972	0.937	1.008	0.127

N=number

Table 6-9 demonstrates a series of binary logistic regression analysis with biological determinants run separately as independent variables to demonstrate relationships with high/good rLMC. We explored high/good rLMC as ≥17 and ≥11. Atrial fibrillation was significantly associated with rLMC>17 (p=0.039, OR 0.394, 95% CI 0.163 to 0.955).

Collateral Status and Outcome

We analysed the relationship between collateral status and outcome (clinical and radiological) as detailed in the flowchart of analysis at the beginning of the chapter. There were 128 patients included in this analysis – clinical details are listed in Table 6-10.

Table 6-10 Clinical Characteristics within the Collateral Status and Outcome Subgroup

Variable	All patients N =128
Age (mean±SD) (years)	68±14
Gender (% male)	80 (63)
Myocardial infarction (n, %)	13 (10)
Other ischaemic heart disease (n, %)	16 (13)
Previous stroke (n, %)	17 (13)
Ischaemic (n, %)	14 (11)
Haemorrhagic (n, %)	1 (1)
Unknown (n, %)	2 (2)
Diabetes mellitus (n, %)	25 (20)
Hypertension (n, %)	66 (52)
Atrial fibrillation (n, %)	17 (13)
Current smoker (n, %)	27 (21)
Excessive alcohol consumption (n, %)	8 (6)
Baseline NIHSS (median, IQR)	6 (3, 11)
Follow-up NIHSS at 24-72 hours (median, IQR)	2 (0, 6)
Pre-stroke excellent function (mRS 0-1) (n, %)	119 (93)
Pre-stroke good function (mRS≤2) (n, %)	123 (96)
90-day excellent function (mRS 0-1) (n, %)	52 (41)
90-day good function (mRS≤2) (n, %)	86 (67)
90-day mortality (mRS=6) (n, %)	4 (3)
Onset to CTP (median, IQR) (hours)	2h16 (2h38, 12h18)
Onset to CTA (median, IQR) (hours)	6h1 (2h42, 12h13)
Onset to MRI (median, IQR) (hours)	52h25 (39h22, 67h54))
Wake-up (n, %)	44 (34)

n=number, SD=standard deviation, NIHSS=National Institute of Health Stroke Scale, IQR=interquartile range, mRS=modified Rankin Scale, CTP=computed tomography perfusion, CTA=computed tomography angiography, MRI=magnetic resonance imaging.

Follow-up NIHSS at 24-72 hours

We undertook multivariable regression models and binary logistic regression seeking the association of collateral scores with change in NIHSS at 24-72 hours. We assessed HIR and rLMC separately. All models were adjusted for age, admission NIHSS, onset-to-scan time

and thrombolysis. These variables are likely to be strongly associated with collateral scores or outcome prediction.

Table 6-11 demonstrates how multivariable linear regression showed rLMC but not HIR to be significantly associated with a reduction in NIHSS (p=0.029, 95% CI -0.412 to -0.022, B coefficient -0.217). Admission NIHSS and thrombolysis are also significantly associated.

Table 6-11 Multivariable Linear Regression Analyses to Assess Prediction of ΔNIHSS at 24-72 Hours

N=128	**Unstandardised Coefficients**		**Standardised Coefficients**			**95% Confidence Intervals**	
Variable	**B**	**Standard Error**	**Beta**	**t**	**Significance**	**Lower**	**Upper**
HIR	1.534	1.591	0.087	0.97	0.334	-1.605	4.692
Age	0.014	0.025	.043	0.542	0.589	-0.036	0.064
Admission NIHSS	-0.357	0.068	-0.45	-5.248	**<0.001**	-4.92	-0.223
Onset-to-CTP	0.000	0.001	0.022	0.214	0.831	-0.002	0.003
Thrombolysis	-1.785	0.885	-0.207	-2.016	**0.046**	-3.537	-0.033
rLMC	-0.217	0.098	-0.202	-2.207	**0.029**	-0.412	-0.022
Age	0.01	0.025	0.031	0.394	0.694	-0.039	0.059
Admission NIHSS	-0.418	0.073	-0.526	-5.705	**<0.001**	-0.563	-0.273
Onset-to-CTA	0.000	0.001	0.01	0.105	0.917	-0.002	0.002
Thrombolysis	-1.803	0.846	-0.209	-2.13	**0.035**	-3.478	-0.127

HIR=hypoperfusion intensity ratio, NIHSS=National Institute of Health Stroke Scale, CTP=computed tomography perfusion, rLMC=regional Leptomeningeal Collateral score, CTA=computed tomography angiography

Table 6-12 and Table 6-13 demonstrate that HIR as a continuous variable and run separately as binary variables <0.2, <0.4 and <0.6 did not demonstrate a significant association with decrease in NIHSS at 24-72 hours. However, rLMC both as a continuous variable and as ≥17 demonstrated a significant association with a decrease in NIHSS

(p=0.014, OR 1.247, 95% CI 1.046 to 1.487 and p=0.007, OR 6.071, 95% CI 1.625 to 22.677 respectively).

Additionally, we explored the interaction HIR*thrombolysis and rLMC*thrombolysis to assess for evidence these variables demonstrate a synergistic effect on the outcome – which they did not.

Table 6-12 Multivariate Binary Logistic Regression Analyses to Assess Prediction of Decrease in NIHSS at 24-72 Hours

Variable	Odds Ratio	95 % CI		p
HIR	0.604	0.029	12.401	0.743
Age	0.985	0.952	1.019	0.375
Admission NIHSS	1.05	0.947	1.165	0.353
Onset-to-CTP	0.999	0.998	1.001	0.192
Thrombolysis	0.785	0.189	3.259	0.739
Thrombolysis by HIR score	31.683	0.291	3346.207	0.149
HIR<0.2	2.019	0.551	7.401	0.289
Age	0.984	0.951	1.018	0.353
Admission NIHSS	1.063	0.958	1.179	0.25
Onset-to-CTP	0.999	0.997	1.0	0.137
Thrombolysis	0.668	0.163	2.748	0.576
Thrombolysis by HIR score	80.622	0.735	8838.234	0.067
HIR<0.4	0.574	0.106	3.098	0.518
Age	0.985	0.953	1.019	0.379
Admission NIHSS	1.04	0.941	1.148	0.443
Onset-to-CTP	0.999	0.998	1.001	0.261
Thrombolysis	0.972	0.246	3.846	0.968
Thrombolysis by HIR score	7.66	0.072	815.518	0.393
HIR<0.6	1.84	0.287	11.805	0.52
Age	0.985	0.953	1.019	0.385
Admission NIHSS	1.049	0.95	1.159	0.341
Onset-to-CTP	0.999	0.997	1.0	0.176
Thrombolysis	0.765	0.193	3.033	0.703
Thrombolysis by HIR score	28.002	0.619	1265.905	0.087

CI=confidence interval, HIR=hypoperfusion intensity ratio, NIHSS=National Institute of Health Stroke Scale, CTP=computed tomography perfusion

Table 6-13 Multivariate Binary Logistic Regression Analyses to Assess Prediction of Decrease in NIHSS at 24-72 Hours

Variable	Odds Ratio	95 % CI		p
rLMC	1.247	1.046	1.487	0.014
Age	0.991	0.957	1.026	0.603
Admission NIHSS	1.118	0.992	1.0	0.093
Onset-to-CTA	0.999	0.997	1.0	0.093
Thrombolysis	119.335	1.07	13304.811	0.047
Thrombolysis by rLMC score	0.772	0.59	1.01	0.059
rLMC≥17	6.071	1.625	22.677	0.007
Age	0.992	0.958	1.027	0.662
Admission NIHSS	1.107	0.988	1.241	0.081
Onset-to-CTA	0.999	0.997	1.0	0.107
Thrombolysis	131.666	0.935	18531.438	0.053
Thrombolysis by rLMC score	0.77	0.582	1.018	0.066
rLMC≥11	2.433	0.419	14.122	0.322
Age	0.987	0.954	1.02	0.427
Admission NIHSS	1.069	0.955	1.198	0.245
Onset-to-CTA	0.999	0.998	1.0	0.161
Thrombolysis	8.047	0.148	438.326	0.307
Thrombolysis by rLMC score	0.904	0.723	1.131	0.377

CI=confidence interval, rLMC=regional Leptomeningeal Collateral score, NIHSS=National Institute of Health Stroke Scale, CTA=computed tomography angiography

mRS at Day 90

We undertook multivariate binary logistic regression to assess the associations of collateral score with mRS 0-2 (good) or mRS 0-1 (excellent) at day 90. We assessed HIR and rLMC separately. As previously described, models were adjusted for age, admission NIHSS, onset-to-scan and thrombolysis. Once again, we explored the interaction HIR*thrombolysis and rLMC*thrombolysis

Neither HIR a continuous variable or run separately as low/good HIR <0.2, <0.4 and <0.6 were significantly associated with mRS 0-2 or mRS 0-1 at day 90 in a model adjusted for age, admission NIHSS, onset-to-CTP, thrombolysis and thrombolysis*HIR.

There was no significant association between rLMC and mRS 0-1. Table 6-14 demonstrates that the relationship between rLMC (as a continuous variable) with mRS0-2 almost reached significance (p=0.052, OR 1.117, 95% CI 0.998 to 1.387) and did reach significance when separated into rLMC≥11 (p=0.028, OR 6.569, 95% CI 1.22 to 35.375).

Table 6-14 Series of Multivariate Binary Logistic Regression Analyses to Assess Prediction of Good (mRS<2) Function at day 90

Variable	Odds Ratio	95 % CI		p
rLMC	1.117	0.998	1.387	0.052
Age	0.97	0.936	1.005	0.092
Admission NIHSS	0.852	0.775	0.937	<0.001
Onset-to-CTA	1.0	0.998	1.002	0.894
Thrombolysis	22.992	0.609	867.411	0.091
Thrombolysis by rLMC score	0.823	0.667	1.017	0.072
rLMC≥17	1.32	0.404	4.314	0.646
Age	0.968	0.935	1.003	0.074
Admission NIHSS	0.831	0.756	0.914	<0.001
Onset-to-CTA	1.0	0.998	1.002	0.957
Thrombolysis	3.272	0.136	78.754	0.465
Thrombolysis by rLMC score	0.927	0.77	1.116	0.424
rLMC≥11	6.569	1.22	35.375	0.028
Age	0.965	0.931	1.001	0.053
Admission NIHSS	0.848	0.771	0.932	<0.001
Onset-to-CTA	1.0	0.998	1.002	0.931
Thrombolysis	7.935	0.357	176.278	0.19
Thrombolysis by rLMC score	0.874	0.733	1.042	0.133

CI=confidence interval, rLMC=regional Leptomeningeal Collateral score, NIHSS=National Institute of Health Stroke Scale, CTA=computed tomography angiography

Volumetric Outcome

We undertook multivariable linear regression models seeking the association of collateral scores with follow-up infarct volume [FIV] on DWI at 24-72 hours. We assessed HIR and rLMC separately. All models were adjusted for age, onset-to-CTP/CTA, thrombolysis and Tmax>6s.

Table 6-15 demonstrates that rLMC but not HIR was significantly associated with FIV (p=0.027, 95% CI -3.464 to -0.211, B coefficient -1.837 – a reduction in rLMC i.e. worse collaterals, was associated with increased FIV).

Table 6-15 Multivariable Linear Regression Analyses to Assess Prediction of Total Follow-Up Infarct Volume at 24-72 Hours

Variable	Unstandardised Coefficients		Standardised Coefficients			95% Confidence Intervals	
	B	Standard Error	Beta	t	Significance	Lower	Upper
HIR	10.1	13.281	0.072	0.76	0.448	-16.192	36.392
Age	-0.125	0.165	-0.05	-0.758	0.45	-0.452	0.202
Tmax>6s	0.336	0.045	0.677	7.433	<0.001	0.247	0.426
Onset-to-CTP	-0.002	0.008	-0.026	-0.302	0.763	-0.018	0.013
Thrombolysis	-14.451	5.794	-0.212	-2.494	0.014	-23.92	-2.982
rLMC	-1.837	0.822	-0.216	-2.236	0.027	-3.464	-0.211
Age	-0.169	0.163	-0.067	-1.033	0.303	-0.492	0.154
Tmax>6s	0.279	0.049	0.561	5.702	<0.001	0.182	0.375
Onset-to-CTA	-0.002	0.008	-0.024	-0.3	0.764	-0.017	0.013
Thrombolysis	-13.359	5.566	-0.196	-2.4	0.018	-24.377	-2.341

HIR=Hypoperfusion intensity ratio, CTP=computed tomography perfusion, rLMC=regional Leptomeningeal Collateral score, CTA=computed tomography angiography

Recanalisation Outcome

As seen in Figure 6-1, there were 65 patients with intracranial VO and 30 patients with LVO who had MRA scans in which analysis was possible. Table 6-16 details the clinical characteristics.

Table 6-16 Clinical Characteristics within the Imaging Outcomes Subgroup

Variable	IVO N=65	LVO N=30
Age (mean±SD) (years)	69±14	70±13
Gender (% male)	40 (62)	17 (57)
Myocardial infarction (n, %)	8 (12)	2 (7)
Other ischaemic heart disease (n, %)	8 (12)	4 (13)
Previous stroke (n, %)	10 (15)	4 (13)
Ischaemic (n, %)	8 (12)	3 (10)
Haemorrhagic (n, %)	1 (2)	0 (0)
Unknown (n, %)	1 (2)	1 (3)
Diabetes mellitus (n, %)	11 (17)	6 (20)
Hypertension (n, %)	29 (45)	14 (47)
Atrial fibrillation (n, %)	13 (20)	6 (20)
Current smoker (n, %)	12 (19)	5 (17)
Excessive alcohol consumption (n, %)	3 (5)	2 (7)
Baseline NIHSS (median, IQR)	9 (5, 14)	14 (9, 17)
Follow-up NIHSS at 24-72 hours (median, IQR)	3 (1, 9)	9 (2, 15)
Pre-stroke excellent function (mRS 0-1) (n, %)	60 (92)	28 (93)
Pre-stroke good function (mRS≤2) (n, %)	62 (95)	29 (97)
90-day excellent function (mRS 0-1) (n, %)	21 (32)	8 (27)
90-day good function (mRS≤2) (n, %)	37 (57)	12 (40)
90-day mortality (mRS=6) (n, %)	3 (5)	1 (3)
Onset to CTP (median, IQR) (hours)	3h29 (2h5, 7h38)	3h12 (2h2, 8h44))
Onset to CTA (median, IQR) (hours)	3h29 (2h9, 6h52)	3h14 (2h5, 7h2)
Onset to MRI (median, IQR) (hours)	59h22 (43h45 to 71h53)	55h29 (44h9, 68h53)
Wake-up (n, %)	18 (28)	10 (33)

n=number, SD=standard deviation, NIHSS=National Institute of Health Stroke Scale, IQR=interquartile range, mRS=modified Rankin Scale, CTP=computed tomography perfusion, CTA=computed tomography angiography, MRI=magnetic resonance imaging.

Infarct Growth Related to Time

We sought to determine the relationship between HIR and infarct growth over time. We performed a repeated measures ANOVA test to assess the effect of good HIR change in infarct volume at the time of CTP (core volume) and follow-up MRI (DWI volume) in patients with intracranial VO (Figure 6-2) and anterior circulation LVO (Figure 6-3). As with previous analysis, we explored the thresholds of good HIR as <0.2, <0.4 and <0.6.

Regardless of HIR threshold and recanalisation status, ‘good’ HIR patients are more likely to present with smaller core volumes and have smaller FIV. In patients who did not recanalise, this difference is greater.

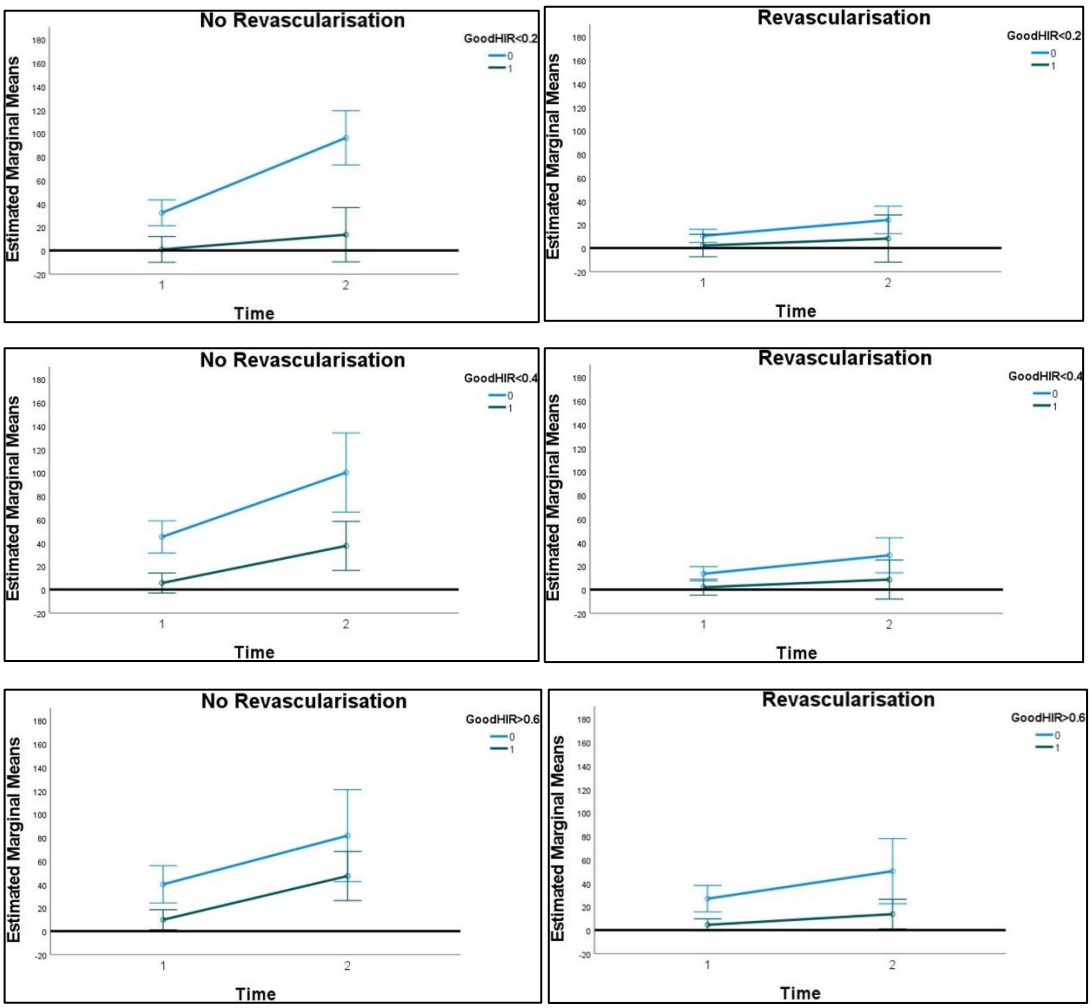

Figure 6-2 Estimated Marginal Means of Infarct Volume at Baseline and Follow-Up Time Points in Intracranial Vessel Occlusion

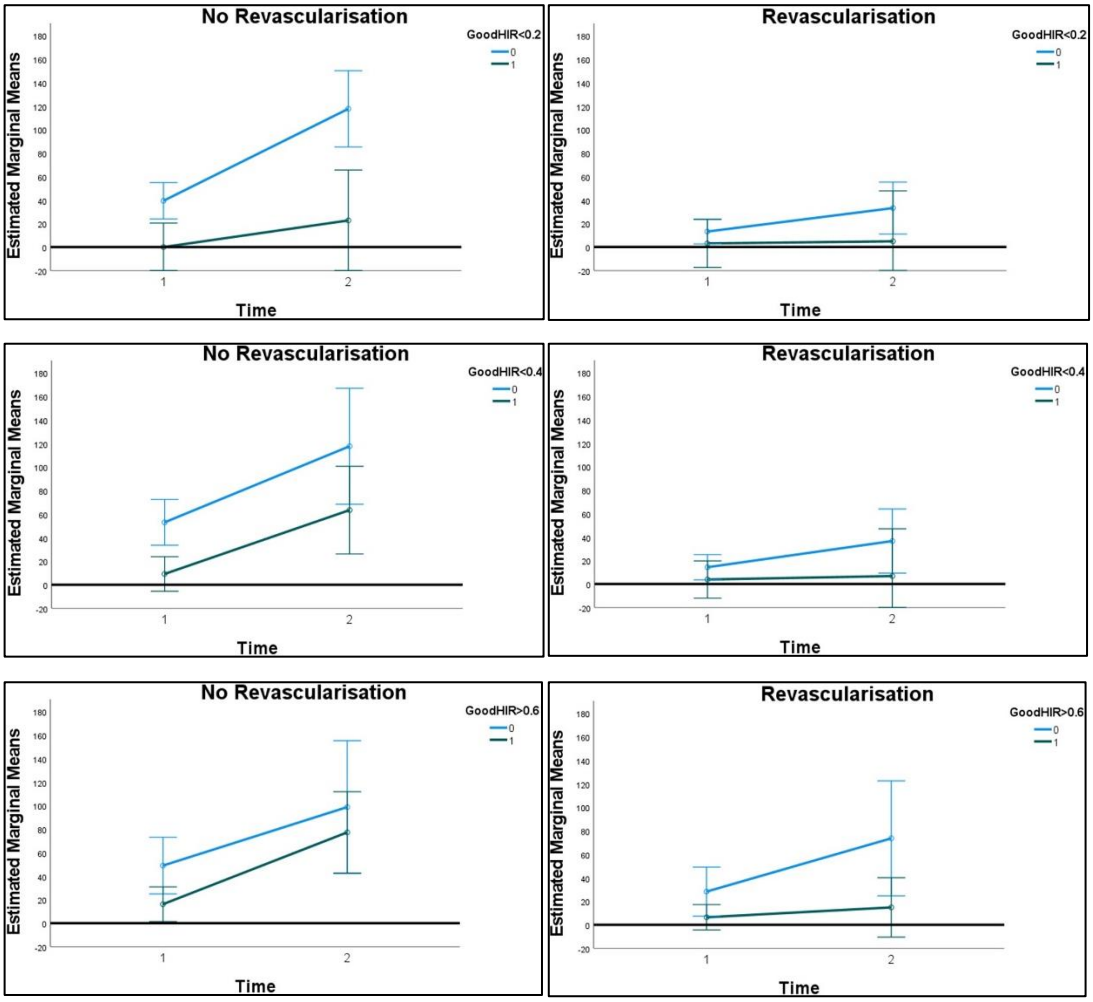

Figure 6-3 Estimated Marginal Means of Infarct Volume in Anterior Circulation Large Vessel Occlusion

Discussion

Radiological characteristics separated into ASPECTS, perfusion deficit and collateral scoring on CTA were significantly different across all thresholds of HIR as expected. We separated patients into all patients, IVO and LVO for all analyses.

In our dataset, although the AUCs from the ROC curves were consistently > 0.66 suggesting at the very least, acceptable performance of the rLMC to predict HIR, there is no discrimination between the HIR thresholds for the 'all patients' and 'LVO' subgroups - rLMC remained good at >17 or moderate at 10.5-12.5 accordingly. The IVO group HIR thresholds corresponded to a change in rLMC ranging from good to poor and previous analysis has demonstrated how high HIR is significantly correlated with poorer collateral score (Wang et al., 2021). This may reflect that HIR was developed using an LVO

population but our LVO dataset is too small for this analysis. HIR is derived from CTP and although has been correlated with collateral flow (Olivot et al., 2014), provides a more detailed measure of collateral flow at tissue level. Furthermore, HIR is derived from automated software whereas the collateral scores in our dataset were assessed by humans.

Out of the biological risk factors assessed, only AF was significantly associated with both increased HIR and reduced rLMC. This may be explained by AF being associated with increased volumes of severe hypoperfusion at baseline CTP (Tu et al., 2013). It has also been postulated that patients with AF do not recruit collaterals as well as patients with chronic hypoperfusion from athero-stenotic lesions (Rebello et al., 2017). Glucose and in particular hypergylcaemia at admission were significantly related to poor rLMC score. This link, which we could not confirm in our meta-analysis in Chapter 2, has not always reached significant status in smaller datasets. HIR was not significantly associated with glycaemic status and whilst some previous studies have reported significant association between glucose and collateral status, none has demonstrated a link between glucose as a continuous variable and HIR.

Finally, in our dataset, HIR but not rLMC was significantly correlated to good outcome as defined by improvement in NIHSS and good to excellent day 90 mRS. Neither HIR nor rLMC were significantly associated with FIV, but HIR was related to smaller admission core volumes and smaller FIV regardless of recanalisation status. Previous studies have shown HIR to be significantly associated with infarct growth and FIV but this was in an LVO population (Olivot et al., 2014).

Limitations are that there may be other relationships between the variables confounding outcome which we have not discovered. Regression modelling assumes relationships to be linear and data to be normally distributed. Our population seems to be one of "good collaterals" which should also be taken into account as it skews our data towards better collateral scores.

Our choice of collateral scoring system is pertinent. In Chapter 3, we described two commonly used methods of CTA collateral flow grading. We selected the modified Tan

score to assess collateral flow in a retrospective analysis of a research database in Chapter 4. However, for a more detailed assessment of leptomeningeal collateral vessels the Tan score may be considered basic and has moderate inter-observer agreement (Berkhemer et al., 2016b). For this analysis, we opted for the rLMC score. Originally developed using multi-phase CTA, we nevertheless used it on our single-phase CTA with the view that it would provide a more detailed anatomical analysis of collateral flow and it may be a more reliable assessment tool given the high inter-observer agreement (Menon et al., 2011). The limitation of scoring collaterals using single-phase CTA is that the quality is dependent on acquisition phase; too early and collaterals may not have a chance to fill and will therefore be under-estimated (Demchuk et al., 2016). However, single-phase CTA remains the most widely used assessment method for reperfusion therapy eligibility on a global scale (Wintermark et al., 2015). One of the objectives of this study, as detailed in Chapter 5, is to assess implications for the National Health Service [NHS]. This paired with availability is why single-phase CTA was used as part of our assessment.

Conclusion

Although HIR and collateral score are correlated, thresholds of good HIR are not predicted by thresholds of collateral score when assessed by rLMC. HIR is a significant predictor of outcome as determined by NIHSS improvement and day 90 mRS. HIR is related to smaller FIV regardless of recanalisation status.

Chapter 7 Thresholds of Ischaemia

Introduction

Several studies have validated CTP parameters as substitutes for DWI imaging. CBF corresponds with the DWI lesion better than CBV (Campbell et al., 2011). However, there is substantial variability in penumbra and infarct prediction depending on deconvolution techniques and variation in thresholds across post-processing platforms (Bivard et al., 2013, Kamalian et al., 2011). In Chapter 4 we performed a software comparison which confirmed variations in ischaemic core and penumbral volumes with implications towards EVT eligibility. Perfusion processing therefore requires standardisation although the more recent trials use RAPID software.

Since perfusion imaging was introduced, there has been a wide range of optimal thresholds of CBF proposed to identify the ischaemic core ranging from <15% to <60% (Schaefer et al., 2015, Wintermark et al., 2006). Cereda et al. (2016) used an in-house developed CTP-software algorithm to demonstrate volumetric accuracy of DWI lesions at rCBF<38%. The threshold rCBF<30% is commonly deployed for detecting ischaemic core regardless of onset-time (Yoshie et al., 2020). Post-processing software therefore may under-estimate the ischaemic core volume by around 15ml with best agreement (Cereda et al., 2016).

The proposed thresholds assume DWI to be the definitive benchmark for core. There is evidence that some DWI lesions are reversible. A systematic review found 1 in 4 patients to have a reversible component with complete reversal being rare. Reversibility was associated with early reperfusion and rates were higher with complete reperfusion as opposed to partial (Nagaraja et al., 2020). We used follow up DWI to define the ischaemic core as the follow up scans took place 24-72 hours after onset of AIS.

We discussed in Chapter 5 how thresholds developed to predict tissue status / tissue outcome are estimates derived from specific populations, using specific software and older studies included those with thrombolysis or natural reperfusion as the only modalities of modifying tissue outcome (Campbell et al., 2011). The time after which collaterals fail and reperfusion therapy is futile is unclear (Rocha and Jovin, 2017). The ghost core is highly time and collateral-dependent with over-estimation more likely in earlier-presenting

patients with poor collaterals (Ballout et al., 2023). The SELECT-2 trial attempted to combat this by using both NCCT and CTP to calculate core -using the larger of the two volumes (Sarraj et al., 2023).

This chapter focuses on imaging outcome. We examined correlation between ischaemic core and FIV in the IVO and LVO subsets. We explore the roles of CBF thresholds, reperfusion and time in a population who did not undergo EVT and were imaged up to 24 hours after onset.

Methods

We analysed admission CTP and follow-up MRI at 24-72 hours limiting the analysis to patients with IVO at baseline since knowledge of recanalisation status is a prerequisite for defining thresholds.

Patients

Please refer to Chapter 5 for a full description of the WHISPER study. Owing to an update in software, the CBF values required for this analysis (specifically CBF<20%) were not available until November 2018 which has been factored into the flowchart of inclusion (Figure 7-1).

Definitions

CTP defect volumes (Tmax >4, 6, 8, 10s and CBF<20%, 30%, 34%, 38%) were estimated by RAPID version 4.7 (Ischemaview).

Anterior circulation IVO and LVO as detected by CTA were defined in Chapter 6, as was revascularisation according to AOL score on follow-up MRI.

Outcome was measured by follow-up NIHSS at 24-72 hours, day 90 mRS, follow-up infarct volume on MRI and AOL score on MRA.

Analyses

We compared the Spearman's rank correlation coefficients for FIV with 1) initial hypoperfused volumes among those who did not recanalize (AOL=0-1 at follow-up vascular imaging), and 2) initial core volumes among those who recanalised (AOL≥2) dividing patients into early (<6h) and late (6-24h) time windows.

Spearman's rank correlation coefficient provides a measure of strength of the association between FIV and initial hypoperfused volumes on CTP. This particular correlation coefficient calculates the ranks of values as opposed to the actual values themselves. As any (including ordinal) data can be ranked, the Spearman's rank correlation is not limited to continuous data. By measuring ranks, the coefficient is able to quantify a monotonic relationship between FIV and CTP volumes and can convert a nonlinear relationship to a linear relationship. This property ensures the coefficient is protected against outliers. Limitations of this coefficient are that an observed correlation does not always ensure that the relationship exists: the two variables may be increasing together (or decreasing) for many reasons. Correlations also do not measure strength of agreement. Finally, a correlation close to 0 does not necessarily mean the variables are not related (Schober et al., 2018). We aim to plot the data for visual inspection of the relationship to address the latter point.

We undertook multivariate linear regression to determine the predictors of FIV, including in the model core and total ischaemia volumes and onset-to-CTP scan interval.

Statistics

Statistical analysis was performed using IBM SPSS Statistics for Windows (version 28.0, Armonk, New York: IBM Corp.).

Results

The flowchart of inclusion is depicted below in Figure 7-1.

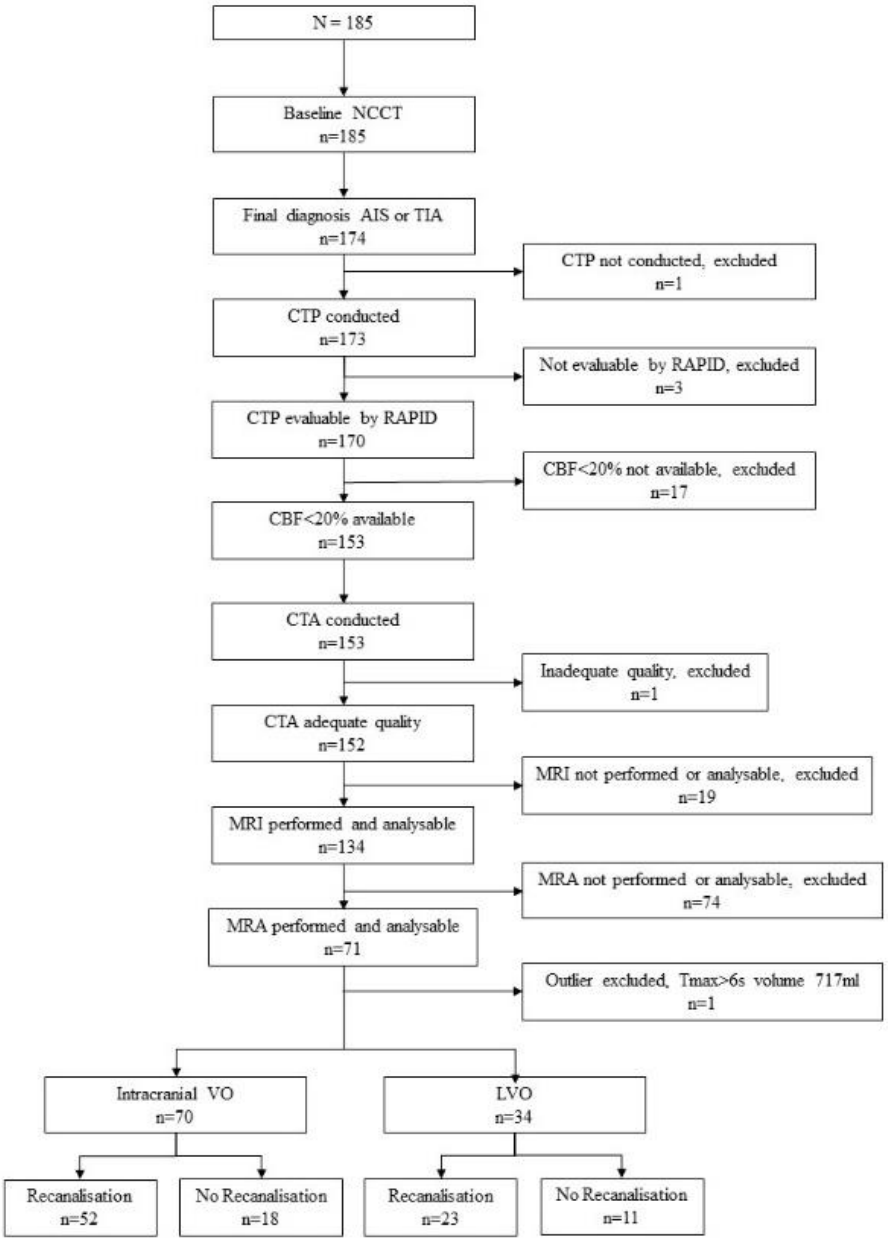

mRS=modified Rankin scale, n=number, VO=vessel occlusion, MRA=magnetic resonance angiography, CBF=cerebral blood flow, LVO=large vessel occlusion

Figure 7-1 Flowchart of Inclusion

There were 70 patients with intracranial VO of whom 52(74%) recanalised and 34 patients with LVO of whom 23(68%) recanalised. Following initial analysis, one patient with a Tmax>6s volume of 717ml was excluded as an outlier.

Clinical details are listed below in Table 7-1.

Table 7-1 Clinical Characteristics

Variable	IVO, N=70	LVO, N=34
Age (mean±SD) (years)	68±15	68±15
Gender (% male)	41 (59)	18 (53)
Myocardial infarction (n, %)	9 (13)	3 (9)
Other ischaemic heart disease (n, %)	10 (14)	5 (15)
Previous stroke (n, %)	11 (16)	4 (12)
Ischaemic (n, %)	9 (13)	3 (9)
Haemorrhagic (n, %)	1 (1)	0 (0)
Unknown (n, %)	1 (1)	1 (3)
Diabetes mellitus (n, %)	10 (14)	5 (15)
Hypertension (n, %)	29 (41)	14 (40)
Atrial fibrillation (n, %)	14 (20)	7 (21)
Current smoker (n, %)	13 (19)	6 (18)
Excessive alcohol consumption (n, %)	3 (4)	2 (6)
Admission blood glucose (mean±SD (mmol/L)*	6.9±2.4	7.7±2.6
Hyperglycaemia on admission (i.e. ≥7 mmol/l) (n, %)*	22	12 (35)
HbA1c +/- 3 months of event (mean±SD (mmol/mol)**	44±10	41±8.0
Baseline NIHSS (median, IQR)	9 (5, 13)	13 (8, 17)
Pre-stroke excellent function (mRS 0-1) (n, %)	64 (91)	30 (88)
Pre-stroke good function (mRS≤2) (n, %)	66 (94)	32 (91)
Onset to CTP (median, IQR) (hours)	205 (123, 386)	192 (111, 374)
Onset to CTA (median, IQR) (hours)	207 (128, 383)	194 (110, 355)
Wake-up (n, %)	15 (21)	9 (27)

*1 patient missing data, **33 patients missing data. N=number, SD=standard deviation, IQR=interquartile range, NIHSS=national institutes of health stroke scale, HbA1c=haemoglobin A1C, mRS=modified Rankin scale, CTP=computed tomography perfusion, CTA=computed tomography angiography

Thresholds of Ischaemia

Table 7-2 compares the Spearman's rank correlation coefficients divided into time windows.

In patients presenting <6 hours who recanalised, core defined as both CBF<20% and CBF<30% was significantly correlated with FIV (Spearman's rank coefficient 0.458, p=0.002, 95% CI 0.177 to 0.669 and Spearman's rank coefficient 0.584, p<0.001, 95% CI 0.339 to 0.755 respectively). Patients who did not recanalise did not have significantly

correlated total lesion volumes with FIV regardless of time window -numbers were small for these subgroups.

Table 7-2 Spearman's Rank Coefficients for Recanalised and Non-Recanalised Follow-Up Infarct Volumes

	≤6 hours		>6 hours		Total
Recanalised (CBF<20% compared with FIV)	n=44	Spearman's rho=0.458 p=0.002 95% CI 0.177 to 0.669	n=8	Spearman's rho=0.577 p=0.134 95% CI -0.239 to 0.916	52
Recanalised (CBF<30% compared with FIV)		Spearman's rho=0.584 p<0.001 95% CI 0.339 to 0.755		Spearman's rho=0.546 p=0.162 95% CI -0.283 to 0.908	
Did not recanalise (Tmax>6s compared with FIV)	n=8	Spearman's rho=0.619 p=0.102 95% CI -0.177 to 0.925	n=10	Spearman's rho=0.573 p=0.083 95% CI -0.110 to 0.889	18
Total	52		18		70

CBF=cerebral blood flow, FIV=follow up infarct volume, Tmax=time to maximum, rho=rank correlation coefficient, CI=confidence intervals

Figure 7-2 is a series of scatter plots demonstrating correlation divided into time windows. In patients with IVO who recanalised, the relationship between FIV and CBF<20% is similar for both time windows and patients presenting >6 hours tend to have larger FIV when comparison with CBF<30%. In IVO patients who did not recanalise, Tmax>6 volumes in patients presenting <6 hours are more closely associated with FIV than those presenting >6 hours, suggesting that patients presenting later with larger admission ischaemic core volumes are more likely to have viable tissue. Similar patterns are seen in patients with LVO although the total number is much smaller.

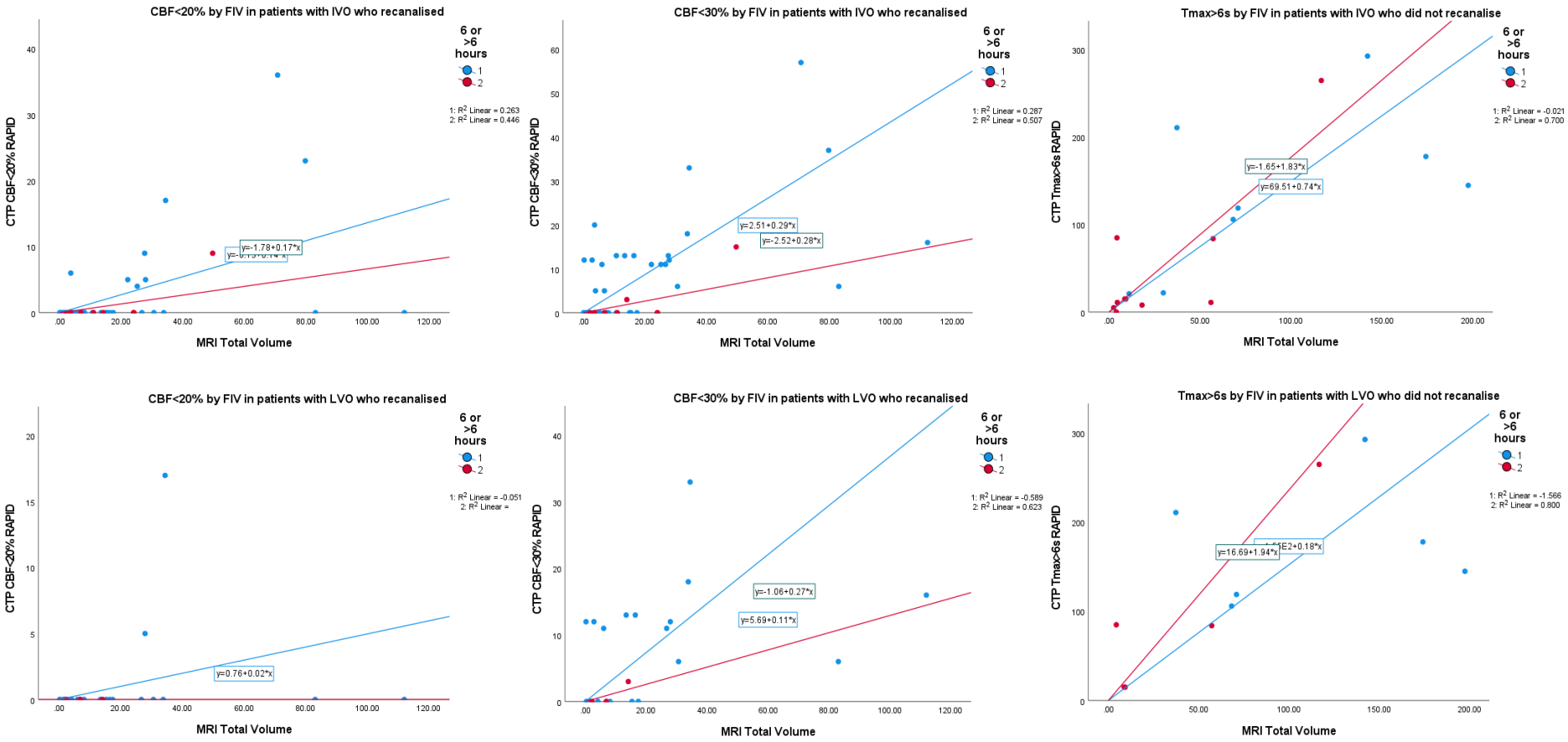

CTP=computed tomography perfusion, CBF=cerebral blood flow, FIV=follow-up infarct volume, IVO=intracranial vessel occlusion, LVO= large vessel occlusion, MRI=magnetic resonance imaging

Figure 7-2 Scatter plots Demonstrating Correlation between Core or Total Lesion Volume in IVO and LVO Separated into Time Windows

Predictors of FIV

We undertook multivariable linear regression models seeking the association of core volume (both CBF<20% and CBF<30%) and total hypoperfusion lesion (Tmax>6s) with FIV at 24-72 hours. We assessed patients who recanalised and patients who did not separately. Our models included CBF<20%, CBF<30%, Tmax>6s and onset-to-CTP time -variables which are likely to interact with one another and be associated with outcome.

Table 7-3 demonstrates that CBF<30% (but not CBF<20%) and Tmax>6s significantly predicted FIV (B coefficient 1.124, p=0.042, 95% CI 0.042 to 2.205, and B coefficient 0.115, p=0.021, 95% CI 0.018 to 0.213 respectively) and onset-to-CTP was not significant (p=0.094) in patients with IVO.

Among those who did not recanalise, no variables were significantly associated.

Table 7-3 Multivariable Linear Regression Analyses to Assess Association of Lesion Volumes with Follow-Up Infarct Volume at 24-72 Hours in Patients with IVO who Recanalised

N=52	**Unstandardised Coefficients**		**Standardised Coefficients**			**95% Confidence Intervals**	
Variable	**B**	**Standard Error**	**Beta**	**t**	**Significance**	**Lower**	**Upper**
CBF<20%	0.186	0.892	0.051	0.208	0.836	-1.608	1.979
CBF<30%	1.124	0.538	0.532	2.090	**0.042**	0.042	2.205
Tmax>6s	0.115	0.048	0.290	2.389	**0.021**	0.018	0.213
Onset-to-CTP	0.015	0.009	0.195	1.710	0.094	-0.003	0.033

N=number, CBF=cerebral blood flow, Tmax=time to maximum, CTP=computed tomography perfusion

There were no significant associations with FIV in patients with LVO in both recanalised and non-recanalised subgroups.

Discussion

This analysis has demonstrated that patients with IVO who present within 6 hours of onset and recanalise have admission core volumes (as defined by both CBF<20% and 30%) significantly correlated with FIV. Out dataset consists of patients who have been treated with medical management or IV thrombolysis where the time of recanalisation is uncertain. Previous datasets in such patients found CBF<30% to be a reliable predictor of ischaemic core volume as defined by DWI (Campbell et al., 2011, Lin et al., 2016). Inevitably, these studies had a time delay between CTP and DWI acquisition leading to the suggestion of the ischaemic core expanding between the imaging acquisitions causing overestimation of the core (Bivard et al., 2010, Bivard et al., 2017).

Successful EVT leads to rapid and definitive recanalisation at a known time point and in these patients CTP may overestimate the FIV leading to the concept of the 'ghost' core (Boned et al., 2017). In these cohorts, the optimal CTP threshold to estimate ischaemic core may be CBF<20% (Bivard et al., 2017). Both CBF<20% and <30% were significantly correlated to FIV in our cohort, suggesting that ischaemic core estimates with either threshold are valid even in the absence of EVT. There was no significant correlation with Tmax>6s in those who did not recanalise, nor was there any correlation in the later time window, however the number of patients in these subgroups were small and we are therefore unable to draw a reliable conclusion.

Whilst the scatter plots comparing core volume against FIV demonstrated a trend between admission perfusion deficit (CBF<20% and <30% in those who recanalised, and Tmax>6s in those who did not) and FIV, numbers were small and it is difficult to draw robust conclusions from small datasets.

Linear regression demonstrated that both CBF<30% (and not <20%) and Tmax>6s were significant predictors of FIV in patients who recanalised, which is consistent with non-EVT datasets mentioned previously (Campbell et al., 2011, Lin et al., 2016). Time from onset to imaging did not significantly modify the relationship between perfusion lesions and follow-up infarct volume. Previous evidence suggests that optimal CTP thresholds associated with FIV vary depending on CTP-to-recanalisation time but not onset-to-CTP or

onset-to-recanalisation times (d'Esterre et al., 2015, Qiu et al., 2019). Infarct growth may be slower in many late presenters including in wake-up strokes. This is consistent with thresholds of tissue viability being similar across the time window.

This analysis is limited by our not being able to assess onset-to-recanalisation time. We included wake-up strokes in our analysis who may present late and have imprecise onset times. Our sub-groups were also too small to analyse effectively; we must be careful to not over interpret the “p” value in this case.

Conclusion

In patients presenting earlier who do not receive EVT but achieve recanalisation, both CBF<20% and <30% are significantly associated with FIV. Thresholds of tissue viability remain similar across time windows.

Chapter 8 Conclusion and Future Directions

Attitudes towards AIS

Patients and (equally importantly) their relatives often describe stroke as sudden, unexpected and terrifying. This perception has endured (and continues to do so) over thousands of years. Stroke, or apoplexy was seen as a catastrophic, irreversible event usually resulting in death. Oscar Wilde's protagonist Jack Worthing considered using it as an excuse when in need of a quick, clean end to his alter ego (although after reflecting on the enormity of the event he would inflict upon his imagined character, he opted to kill him with a severe chill instead)(Wilde, 1895).

The pathophysiology is simple and was determined in the 17th century. A blood clot prevents cerebral bloodflow causing cell death and subsequent neurological deficit. The treatment approach is also straightforward: bloodflow must be restored quickly, completely and safely (Muir and White, 2016). Despite this, the idea (and truth) of stroke being an irreversibly catastrophic event persisted until the 1960s.

Patients and their relatives' attitudes are still clouded by fear and a sense of inevitable deterioration. This is unsurprising given the portrayal of stroke in the media (relatively unchanged since Wilde's play in 1895). Doctors' attitudes are similar; many non-stroke specialists fear AIS and are unsure of symptoms, no doubt they too would prefer to be treating "a severe chill". As well as the classic face, arm and leg disability, there seems to be a fear that almost any acute neurological symptom can be a stroke. The trouble is that it often can. The overlap between AIS and stroke mimics is broad and many stroke specialists appreciate that the more experienced they become, the less confident they are in describing an event as not an AIS.

Developments in Neuro-Imaging

How might clinicians differentiate between patients urgently requiring AIS reperfusion therapy and patients presenting with a stroke-mimic? The answer is in the imaging.

The humble non-contrast CT head remains the bastion of the junior doctor's initial stroke investigation. Some have even argued that it can be used single-handedly to select patients for EVT (Nguyen et al., 2022). We believe this to be an over-reach. Quicker and cheaper than an MRI, NCCT continues to reliably exclude patients from reperfusion treatment or even admittance to the HASU.

The emergence of advanced neuro-imaging has elevated imaging from exclusion tools to selection tools. The modalities of CTA, CTA and MR perfusion may be considered as physiological imaging; a way of visualising and quantifying tissue at risk by providing an estimation of hypoperfused tissue either through collateral vessel assessment or mismatch volume. In this thesis, we considered both as representative of the penumbra.

The Timing of the WHISPER Study

The timing of the WHISPER which ran from 2018 to 2023 study coincided with a change in landscape of stroke treatment.

At the beginning of the study, the efficacy of EVT had been established following a meta-analysis of data from five trials suggesting a NNT of 26, leading to the HERMES collaboration (Goyal et al., 2016, Muir and White, 2016) . DAWN and DEFUSE-3 had confirmed that late window EVT could be successful but questions were raised about the very selective criteria which excluded a large proportion of patients (Nogueira et al., 2017, Albers et al., 2018). There appeared to be room to expand the inclusion.

The expected expansion in EVT centres was slow. Lack of ability (training of interventional radiologists to perform EVT takes at least 3 years) and a strong concentration of ability in London rendered a post code lottery which persists today.

Mid-way through our study, following evidence that perfusion imaging could select patients for rtPA up to 9 hours after onset of symptoms, the European Stroke Guidelines were updated accordingly (Turc et al., 2019).

Whilst not all of the EVT trials had used perfusion imaging to select patients, it seemed as though perfusion imaging was going to play a key role in reperfusion therapy.

Towards the end of our study, the arrival of large core trials shifted the emphasis to late-window, large core patients – with some studies defining a low core as low ASPECTS on NCCT (Yoshimura et al., 2022, Bendszus et al., 2023). Whilst better functional outcome following EVT was demonstrated, two "large core" studies (SELECT2 and ANGEL-ASPECT) used perfusion imaging to demonstrate median core volumes of 74ml (IQR 50 to 111.5ml) and 60.5ml (IQR 29 to 86ml) respectively (Sarraj et al., 2023, Huo et al., 2023). This does not appear to be so revolutionary when judged against the 70ml standard set by DEFUSE-3 and EXTEND and so an upper limit resulting in futile recanalisation has yet to be determined (Albers et al., 2018, Ma et al., 2019). The median total hypoperfusion lesion volume of 171ml (IQR 127 to 226ml) reported for SELECT2 suggests that this was also a dataset with "large penumbrae" (Sarraj et al., 2023). The significantly higher haemorrhagic transformation rate and vascular complications reported within the EVT arms suggest that the treatment of "large core" has not been fully resolved (Yoshimura et al., 2022, Sarraj et al., 2023, Huo et al., 2023).

This piece of work is an assessment of penumbra with confirmation that the concept of the penumbra is still valid.

Describing the population with viable tissue separated into time windows

The size of the subgroup of patients who could benefit from delayed treatment based on imaging selection was not clear. There were no studies that looked at prevalence of mismatch in unselected ischemic stroke patients within the first 24 hours after onset of symptoms. In the DEFUSE 2 study, "target mismatch" (a patient with a perfusion defect significantly exceeding the volume of core tissue defined by the diffusion weighted MRI lesion) was detected in 46% of patients treated after 6 hours (Lansberg et al., 2012).

Retrospective reviews reported a positive mismatch in hundreds of patients who received endovascular therapy more than 6 hours after symptom onset. However, the imaging criteria used for patient selection were not uniform across different centres, and there are no details on numbers excluded due to unfavourable imaging profile (Jovin et al., 2011, Nogueira et al., 2017). Additionally, since these data generally reflect single-centre experience at neurovascular centres, the proportion of patients in whom transfer from primary stroke centres was declined is not reported. A favourable imaging profile as described in these studies is not directly equivalent to penumbra survival, with other factors such as absolute core size, total deficit size and presence of a large artery occlusion included in the treatment selection criteria.

Our primary aim was to identify the proportion of patients with viable penumbra within separate time windows for reperfusion.

We conducted a single centre, prospective, observational study of acute stroke patients imaged up to 24h from onset of symptoms (the WHISPER study). We demonstrated that the proportion of patients with significant volumes of salvageable tissue remained high at any time point and that the volumes of salvageable tissue declined slowly over time. Overall, the proportion of patients meeting DEFUSE-3 and EXTEND criteria were 20% and 55% respectively with patients who presented later, with severe disability still meeting criteria. There was no significant difference in the proportion of those meeting DEFUSE-3 criteria across time windows but there was for those meeting EXTEND criteria, with a lower proportion in the later time windows. Numbers were too small to assess this within the LVO subgroup but the proportion of patients meeting both criteria was larger. The proportion of patients meeting criteria was larger within the LVO subgroup but numbers were too small to assess whether this varied across the time windows.

We found that a substantial proportion of patients presenting in later time windows have viable brain tissue throughout the 24-hour time period. Whilst numbers in the later time windows were smaller, this is in keeping with evidence that the majority of patients with AIS present before 6 hours (Lacy et al., 2001).

In recent years, there appears to have been a shift in emphasis from penumbra to core with several trials demonstrating good functional outcome following EVT in “large core” patients (Yoshimura et al., 2022, Bendszus et al., 2023, Sarraj et al., 2023, Huo et al., 2023). However, as mentioned, within these ‘large core’ populations, viable, rescuable brain tissue was a pre-requisite for good outcome. In the SELECT2 trial, whilst there was no upper limit for ischaemic core volume all patients underwent CT perfusion imaging or perfusion-diffusion MRI prior to recruitment and patients who did not demonstrate a mismatch were not randomised (Sarraj et al., 2023). Knowing in whom perfusion imaging can be omitted remains a challenge especially as have yet to identify an upper threshold for core volume.

The proportion of patients eligible for EVT is also dependent on the frequency of LVO, our study identified an LVO rate of 24%. This is smaller than the 39% rate reported by El Tawil et al. (2016), a figure based analysis of the MASIS, POSH and ATTEST studies which have been described earlier and included patients presenting within 6 hours (Wardlaw et al., 2013a, Macdougall et al., 2014, Huang et al., 2015).

As well as demonstrating eligibility for EVT across time windows we also used the EXTEND criteria to demonstrated eligibility for extended thrombolysis (Ma et al., 2019). This is particularly useful in stroke centres where EVT is not available. A recent publication of an RCT of patients with LVO (most of whom did not receive EVT) who were selected using perfusion imaging for treatment with Tenecteplase versus routine medical therapy demonstrated significantly better mRS outcome, no difference in mortality rate and a slightly increased rate of sICH (Xiong et al., 2024).

All of this information will guide service planning at a time when EVT remains unavailable to many parts of the UK. It will also serve to inform future studies aimed at delayed reperfusion and more specifically investigation of the fate of the penumbra.

Investigating biological mechanisms underlying failure to recruit leptomeningeal collaterals

Within this population, we aimed to investigate biological mechanisms underlying failure to recruit leptomeningeal collaterals (as representatives of penumbra) with a focus on hyperglycaemia.

As with the perfusion-defined penumbra, the short time window for beneficial reperfusion has been conceptualised as progressive “collateral failure”. Previous studies in patients <6 hours after stroke onset indicate stable volumes of penumbra over time in those with moderate or good collaterals (Cheripelli et al., 2016). Patients with poor collaterals are therefore the time-critical group for treatment, and will either derive less benefit from delayed perfusion, or be excluded from treatment altogether. Better understanding of collateral pathophysiology would identify therapeutic targets that offer potential gains in this group.

We focused on hyperglycaemia as there is a clear a link between admission hyperglycaemia and poor collateral status, reduction in penumbral salvage and accelerated infarct expansion causing poor outcome but so far correction therapy has proven to be unsafe (Wiegers et al., 2020, MacDougall, 2013). This may be related to the use of insulin, itself a potentially dangerous and lethal drug with wide variations in response.

We first performed a systematic-review and meta-analysis of published data. Our relatively small number of papers (n=24) spanned over a large time period -not least in terms of developments in imaging and treatment (1994 to 2023).

Whilst the mean blood glucose was higher in patients with poorer collaterals, our meta-analysis of 7 papers (1994 to 2022) did not find a significant link between hyperglycaemia and poor collateral status. This analysis was hindered by the varying definitions of hyperglycaemia and the many methods of collateral status grading. For the purpose of the review, we assumed that baseline glucose and admission glucose to be identical but it was difficult to know if definitions varied between centres and when exactly measurements

took place in relation to onset time. The largest study population within our dataset was the most recently published: a sub-analysis of the MR CLEAN dataset. This arguably included the most robustly assessed collateral vessels and admission glycaemic monitoring (Genceviciute et al., 2022b).

Within our observational study, we assessed how collateral status, as defined by both perfusion (HIR) and angiographic (rLMC score) imaging was affected by biological determinants such as AF, smoking status, admission blood glucose, admission hyperglycaemia and HbA1c within 3 months of AIS.

We demonstrated through regression analysis that AF was significantly associated with both increased HIR and reduced rLMC. This supports previous reports that AF is associated with severe hypoperfusion on baseline CTP and that patients with AF do not recruit collaterals as well as those without (Tu et al., 2013, Rebello et al., 2017).

Both admission glucose and hyperglycaemia were significantly associated with poor rLMC. We already discussed the varying reports of the impact of glycaemic status on collateral vessels. Given the current environment of advanced imaging, more studies will be published reporting collateral vessels and glycaemic monitoring data and our systematic review can be repeated with high-quality and robust data.

Comparison of Two Methods of Collateral Assessment

We assessed patients using both CTP and CTA imaging and we used both HIR and rLMC to assess collateral circulation.

The HIR was developed and validated using an LVO population (Olivot et al., 2014). However, the RAPID software output provides HIR data regardless of vessel occlusion status and we assessed the clinical significance. The original investigators (the DEFUSE-2 team) dichotomised “good/low HIR” from “poor/high HIR” using the median value of their population (0.4) (Olivot et al., 2014). Our median value (within our LVO group) was similarly 0.4 with IQR 0.2-0.6. We used all three values to dichotomise our data separately

and found significantly different radiological characteristics as defined by NCCT ASPECTS, size of perfusion defect and rLMC scoring on CTA. We also found this to be true within subgroups of IVO and LVO. However, only the 0.0 to 0.2 HIR quartile (the lower numbers representing better collaterals) was significantly associated with improvement in NIHSS. Given that HIR as a continuous variable was significantly associated with admission NIHSS, this may reflect less severe AIS and a "good collateral" population – overall median HIR was 0.1, IQR 0.0 – 0.5.

Previous analysis has demonstrated how high HIR is significantly correlated with poor collateral status (Wang et al., 2021). We used ROC analysis to assess the ability of rLMC scoring to predict HIR as dichotomised once again into "low HIR" and "high HIR". The rLMC scores were best able to predict low HIR when defined as <0.2. This again points to our population having "good collaterals" as confirmed by a median rLMC score of 20, IQR 16 – 20. The numbers of patients with both IVO and LVO were possibly too low to assess being 87 (55%) and 44 (28%) respectively.

Collateral assessment tools (as demonstrated in our systematic review and meta-analysis Chapter 2) have evolved over time and become more detailed. In Chapter 4, we used the modified Tan score as a basic assessment of collateral vessels (Tan et al., 2007). When assessing the WHISPER population in Chapters 5 and 6 we chose to use the rLMC score for its more anatomically detailed scoring system and better interrater agreement (Menon et al., 2011).

CTA scans were scored by consensus by two experienced assessors with a random sample of 10 patients confirmed by a third assessor. We demonstrated perfect inter-observer agreement for detection of LVO and affected hemisphere. There was moderate inter-observer agreement for LVO site and rLMC score with a Cohen's κ coefficient of 0.72 (95% CI 0.57 to 0.87) and 0.71 (95% CI 0.52 to 0.91) respectively.

Whilst this score was originally developed for use in multi-phase CTA, the rLMC scores pointing to a population with good collaterals was confirmed by HIR suggesting that there is scope to use this score to assess single-phase CTA scans. Limitations of single-phase

CTA need to be taken into account; the main issue being that the quality of the scan (and subsequent collateral assessment) is dependent on acquisition timing (Demchuk et al., 2016). We did not collect acquisition timings for our patients but this would be a useful measure to further assess rLMC against acquisition phase. The clinical relevance is that the majority of stroke centres in the UK use single-phase CTA to assess patients. It is both quicker and cheaper to obtain whilst being easier to interpret It should be noted however, that the more detailed the collateral assessment, the more experience needed to grade this score.

The LVO subset (and our introduction of the term IVO)

Whilst definitions of anterior circulation LVO varied across the trials, all agreed on ICA and M1 occlusion with some including M2 (MR CLEAN, MR CLEAN LATE, EXTEND-IA, PISTE, ESCAPE) (Saver et al., 2015, Jovin et al., 2015, Nogueira et al., 2017, Albers et al., 2018, Yoshimura et al., 2022, Sarraj et al., 2023, Huo et al., 2023, Bendszus et al., 2023, Berkhemer et al., 2014, Olthuis et al., 2023a, Campbell et al., 2015, Muir et al., 2017, Goyal et al., 2015).

We defined anterior circulation LVO as occlusion of the internal carotid artery, M1 or >1 branch of M2 in keeping with the ESCAPE trial's definition -i.e. in keeping with the theory that multiple branches of M2 involvement are equal to M1 occlusion (Goyal et al., 2015).

Additionally, we introduced the term Intracranial Vessel Occlusion [IVO] to capture other vessel occlusions which may not fit without definition of LVO. This information is important and may inform future reperfusion trials targeting medium or posterior circulation vessels. Similarly, whilst these patients may not be eligible for EVT they may be eligible for thrombolysis.

In terms of IVO, 43% had either ICA, proximal or distal M1 occlusions (separated into 14%, 14% and 15% respectively). The majority (25%) had M2-1 branch occlusions i.e. not

amenable to thrombectomy. Incidence of other vessel occlusions was low with 2 patients (2%) presenting with a basilar occlusion.

Assessment of Ghost Core

We aimed to validate current thresholds for prediction of tissue fate in later presentations. Since perfusion imaging was introduced, there has been a wide range of optimal thresholds of CBF proposed to identify the ischaemic core ranging from <15% to <60% (Schaefer et al., 2015, Wintermark et al., 2006). The thresholds developed to predict tissue status / tissue outcome are estimates derived from specific populations, using specific software and older studies included those with thrombolysis or natural reperfusion as the only modalities of modifying tissue outcome (Campbell et al., 2011).

Successful EVT leads to rapid and definitive recanalisation at a known time point and in these patients CTP may overestimate the FIV leading to the concept of the 'ghost' core (Boned et al., 2017). In these cohorts, the optimal CTP threshold to estimate ischaemic core may be CBF<20% (Bivard et al., 2017). Both CBF<20% and <30% were significantly correlated to FIV in our cohort, suggesting that ischaemic core estimates using either threshold are valid even in the absence of EVT

The time after which collaterals fail and reperfusion therapy is futile is unclear (Rocha and Jovin, 2017). The ghost core is highly time and collateral-dependent with over-estimation more likely in earlier-presenting patients with poor collaterals (Ballout et al., 2023). The SELECT-2 trial attempted to combat this by using both NCCT and CTP to calculate core - using the larger of the two volumes (Sarraj et al., 2023).

Linear regression demonstrated that CBF<30% (but not <20%) and Tmax>6s were significant predictors of FIV in patients who recanalised, which is consistent with non-EVT datasets mentioned previously (Campbell et al., 2011, Lin et al., 2016). Time from onset to imaging did not significantly modify the relationship between perfusion lesions and follow-up infarct volume. Infarct growth may be slower in many late presenters

including in wake-up strokes. This is consistent with thresholds of tissue viability being similar across the time window.

Amongst patients with IVO who recanalised, both Tmax>6s and CBF<30% but not CBF<20% significantly predicted FIV using multivariate linear regression. This was not true in the patient group that did not recanalise.

Our analysis is limited by our not being able to assess onset-to-recanalisation time. We included wake-up strokes in our analysis who may present late and have imprecise onset times. Our sub-groups were also too small to analyse effectively. Within the group presenting <6 hours, 44 patients recanalised compared with 8 patients who did not and the numbers for the >6 hour group were 8 and 10 patients respectively. Finally, the only reperfusion therapy available was thrombolysis – complete recanalisation rates for thrombolysis lie between 30-56% with point of recanalisation between 2-6 hours after administration which will have confounded out data(Zangerle et al., 2007).

Perfusion Software Imaging

Finally, we evaluated differences between current post-processing software for CTP in Chapter 4.

Most stroke trials used RAPID AI software. There are, however, several post-processing software available with the concern being that differences in post-processing algorithms may lead to varying results. As CTP use becomes increasingly widespread, centres may opt to use different software for research, practicality or cost reasons.

We used a pooled database to evaluate the agreement between CT perfusion studies processed with MIStar, RAPID and Brainomix. Bland Altmann plots demonstrated that overall Brainomix software was the most conservative in assessing core volume. Both MIStar and Brainomix produce larger volumes of penumbra than RAPID. Greater proportions of Brainomix processed scans met both DEFUSE-3 and EXTEND target mismatch criteria.

In terms of clinical impact, the Brainomix software has not been validated in a stroke trial. Most stroke trials used RAPID and there is widespread corroboration with follow-up infarct volume (Austein et al., 2016, Cereda et al., 2016, Mokin et al., 2017, Hoving et al., 2018, Albers et al., 2016).

This may impact treatment decisions if different software produce different estimates of core and penumbra volumes.

Limitations of our data

We encountered several difficulties in recruiting to the WHISPER study.

Availability of research scanners was an issue before COVID-19 but became worse during and after the pandemic when COVID-19 trials took priority.

Our population had a mean age of 69, a 49% thrombolysis rate and a median NIHSS 6 (3-11). During this study, CTP and CTA became routine practice on admission and this may have influenced recruitment to trials. This suggests more severely disabled AIS patients were recruited especially when compared with SSNAP data – median age 76, thrombolysis rate 10%, median NIHSS 4 (2-10) (SSNAP, 2023). This suggests that more disabling AIS may be overrepresented within our data although notably our LVO rate is much lower than previously suggested (El Tawil et al., 2016). The disabling AIS was more prevalent within the population within our pooled analysis (representative of two of the pooled trials being thrombolysis trials) – there was a mean age of 70, a 76% thrombolysis rate and admission NIHSS was 12 (7-16). SSNAP data represents all AIS admissions within England and Wales (including patients who may have dementia, patients with minor AIS who may not be admitted and many other AIS patients who are unlikely to be recruited into acute stroke trials). Our population represents people able to give consent and who are potentially within a treatment window which may explain the younger, more disabled populations.

Our population was 61% male, a bias seen in other stroke trials and also seen in our pooled analysis (55% male) in Chapter 4. This is not, however, in keeping with the evidence that the lifetime risk of stroke for women is higher than men (25.1% versus 24.7% respectively) (Feigin et al., 2018). Women are reportedly more likely to die from AIS although timeframes are unclear (Heron, 2021). In 2023, Office for National Statistics reported that there were 1.68 million women over the age of 75 living alone as opposed to 786,000 men (Statistics, 2023). It may be that women are less likely to have a relative to consent on their behalf but we do not have screening logs to back this up.

Impact on Stroke Treatment and Future Directions

We found that a substantial proportion of patients presenting in later time windows have viable brain tissue throughout the 24-hour time period. Whilst numbers in the later time windows were smaller, this is in keeping with evidence that the majority of patients with AIS present before 6 hours (Lacy et al., 2001). Patients presenting later with LVO in our dataset are still likely to be eligible for both EVT and thrombolysis up to 24 hours and potentially even later. Further evaluation is necessary, firstly in populations with more evenly distributed numbers (including of LVO) across the time windows and secondly in populations presenting later than 24 hours. Next, as more ‘large core’ trial data is published, analysis of the perfusion thresholds for good outcome is necessary, in order to quantify the mismatch ratio necessary for patients with larger core volumes to improve following EVT. The upper threshold of core volume for futile recanalisation is not clear: we have yet to define the group of severely hypoperfused patients who may be harmed by EVT. No trials have assessed reperfusion therapy in patients with all core and no penumbra.

From an organisational perspective, emphasis has always been placed on restoring perfusion as quickly as possible. Optimally, 24/7 service availability is desirable. Not all stroke centres have access to EVT and some only have partial access within certain hours. Given that we demonstrated that a substantial proportion would still be eligible at later time windows, our data would support a system to ensure repeat imaging or possibly transfer when EVT becomes available within 24 hours.

Mechanisms around collaterals remain incompletely investigated. Is it possible to modify collateral status within relevant timeframes? We still do not have clarity around hypergylcaemia and collateral vessels. Our data suggests that hyperglycaemia is associated with worse collateral status. This suggests an opportunity to intervene: modifying blood glucose may modify collateral status and change outcome. In practice, this has been historically difficult to do but therapies without the life-threatening risks of insulin are worth exploring. The ability to modulate and improve collateral flow would radically enhance AIS treatment – especially in places where EVT is not available 24/7.

We confirmed that collaterals as represented by the HIR are still important as an index of tissue viability for outcome. We found AF to be significantly associated with poor collaterals (as determined by HIR and rLMC) which is in keeping with current evidence (Tu et al., 2013).

We sought to validate thresholds of ischaemia for prediction of tissue fate against time windows in the intracranial vessel occlusion population. Current data are based on patients who have had EVT, this is a select population in terms of baseline fitness, occlusion site and the exact time point of recanalisation is known. It is difficult to know how generalisable these findings especially in patients who may not meet eligibility criteria for EVT. Our dataset demonstrated significant correlation between patients who presented within 6 hours and recanalised between FIV and admission CBF<20% and 30% confirming current findings in the absence of EVT (Campbell et al., 2011, Lin et al., 2016, Bivard et al., 2017). The numbers in the group that did not recanalise and in the >6 hour subgroups were too small to draw any reliable conclusion. Further evaluation in these populations is necessary.

Finally, we compared CTP analysis produced by three commonly used software and found variations in ischaemic core and penumbral volumes which may affect EVT eligibility. This is relevant at a time when resources are limited and patients may need to travel (potentially far distances) for EVT based on an AI generated analysis. The other (and equally relevant) implication is how AI software affects clinical decision making. It would be useful to explore if scan analysis software were able to take into account clinical details (i.e. affected hemisphere, similar to the information provided on scan requests to

radiologists) and even process NCCT, CTA and CTP as one linked analysis – with each scan informing the analysis of the others.

One aspect of stroke which we did not address was the minor stroke population. The recent publication of the TEMPO2 trial has confirmed that thrombolysis is potentially dangerous in the treatment of minor stroke. This study recruited on the basis of a perfusion imaging mismatch or occlusion seen on CTA to randomise minor AIS patients to either thrombolysis (with Tenecteplase) or best medical treatment (Coutts et al., 2024). This does not necessarily mean that perfusion imaging would not be useful in this cohort and this would be worth exploring.

We present a complete dataset of patients who presented with AIS within 24 hours' onset who did not have access to EVT but did have access to advanced neuro-imaging and with both radiological and clinical follow up. We focused on analysis of the penumbra but this dataset could be further explored to answer other imaging questions.

References

Acheampong, P., et al. 2014. Bolus-infusion delays of alteplase during thrombolysis in acute ischaemic stroke and functional outcome at 3 months. *Stroke Res Treat,* 2014**,** 358640-358640.

Adams, H. P., Jr., et al. 1993. Classification of subtype of acute ischemic stroke. Definitions for use in a multicenter clinical trial. TOAST. Trial of Org 10172 in Acute Stroke Treatment. *Stroke,* 24**,** 35-41.

Aho, K., et al. 1980. Cerebrovascular disease in the community: results of a WHO collaborative study. *Bull World Health Organ,* 58**,** 113-30.

Albers, G. W., et al. 2016. Ischemic core and hypoperfusion volumes predict infarct size in SWIFT PRIME. *Ann Neurol,* 79**,** 76-89.

Albers, G. W., et al. 2018. Thrombectomy for stroke at 6 to 16 hours with selection by perfusion imaging. *N Engl J Med,* 378**,** 708-718.

Alkjaersig, N., Fletcher, A. P. & Sherry, S. 1959. The mechanism of clot dissolution by plasmin. *J Clin Invest,* 38**,** 1086-1095.

An, H., et al. 2011. Signal evolution and infarction risk for apparent diffusion coefficient lesions in acute ischemic stroke are both time- and perfusion-dependent. *Stroke,* 42**,** 1276-81.

Anderson, T. J., et al. 1995. The effect of cholesterol-lowering and antioxidant therapy on endothelium-dependent coronary vasomotion. *N Engl J Med,* 332**,** 488-493.

Arboix, A., et al. 2001. Ischemic stroke of unusual cause: clinical features, etiology and outcome. *Eur J Neurol,* 8**,** 133-9.

Arteaga, D. F., et al. 2022. Collateral status, hyperglycemia, and functional outcome after acute ischemic stroke. *BMC Neurol,* 22**,** 408.

Asinger, R. W., et al. 1981. Incidence of left-ventricular thrombosis after acute transmural myocardial infarction. Serial evaluation by two-dimensional echocardiography. *N Engl J Med,* 305**,** 297-302.

Astrup, J., Siesjö, B. K. & Symon, L. 1981. Thresholds in cerebral ischemia - the ischemic penumbra. *Stroke,* 12**,** 723-725.

Atalay, Y. B., et al. 2021. Prevalence of cervical artery dissection among hospitalized patients with stroke by age in a nationally representative sample from the united states. *Neurology,* 96**,** e1005-e1011.

Austein, F., et al. 2016. Comparison of perfusion ct software to predict the final infarct volume after thrombectomy. *Stroke,* 47**,** 2311-2317.

Baek, J.-H., et al. 2021. Low hypoperfusion intensity ratio is associated with a favorable outcome even in large ischemic core and delayed recanalization time. *J Clin Med* [Online], 10.

Ballout, A. A., et al. 2023. Ghost infarct core: A systematic review of the frequency, magnitude, and variables of CT perfusion overestimation. *J Neuroimaging,* 33**,** 716-724.

Bamford, J., et al. 1991. Classification and natural history of clinically identifiable subtypes of cerebral infarction. *Lancet,* 337**,** 1521-6.

Bang, O. Y., et al. 2011. Collateral flow averts hemorrhagic transformation after endovascular therapy for acute ischemic stroke. *Stroke,* 42**,** 2235-9.

Barber, P. A., et al. 2000. Validity and reliability of a quantitative computed tomography score in predicting outcome of hyperacute stroke before thrombolytic therapy. ASPECTS Study Group. Alberta Stroke Programme Early CT Score. *Lancet,* 355**,** 1670-4.

Beaulieu, C., et al. 1999. Longitudinal magnetic resonance imaging study of perfusion and diffusion in stroke: evolution of lesion volume and correlation with clinical outcome. *Ann Neurol,* 46**,** 568-78.

Bendszus, M., et al. 2019. A randomized controlled trial to test efficacy and safety of thrombectomy in stroke with extended lesion and extended time window. *Int J Stroke,* 14**,** 87-93.

Bendszus, M., et al. 2023. Endovascular thrombectomy for acute ischaemic stroke with established large infarct: multicentre, open-label, randomised trial. *Lancet,* 402**,** 1753-1763.

Berge, E., et al. 2021. European Stroke Organisation (ESO) guidelines on intravenous thrombolysis for acute ischaemic stroke. *Eur Stroke J,* 6**,** I-LXII.

Berkhemer, O. A., et al. 2014. A randomized trial of intraarterial treatment for acute ischemic stroke. *N Engl J Med,* 372**,** 11-20.

Berkhemer, O. A., et al. 2016a. Collateral status on baseline computed tomographic angiography and intra-arterial treatment effect in patients with proximal anterior circulation stroke. *Stroke,* 47**,** 768-76.

Berkhemer, O. A., et al. 2016b. Collateral status on baseline computed tomographic angiography and intra-arterial treatment effect in patients with proximal anterior circulation stroke. *Stroke,* 47**,** 768-776.

Bernhardt, J., et al. 2017. Agreed definitions and a shared vision for new standards in stroke recovery research: The Stroke Recovery and Rehabilitation Roundtable taskforce. *Int J Stroke,* 12**,** 444-450.

Beyer, S. E., et al. 2015. Strategies of collateral blood flow assessment in ischemic stroke: prediction of the follow-up infarct volume in conventional and dynamic CTA. *AJNR Am J Neuroradiol,* 36**,** 488-94.

Bhalla A, C. L., Fisher R, James M. 2023. *National clinical guideline for stroke for the united kingdom and ireland* [Online]. strokeguideline.org. Available: https://www.strokeguideline.org/ [Accessed 08.09.2023 2023].

Bhatia, R., et al. 2010. Low rates of acute recanalization with intravenous recombinant tissue plasminogen activator in ischemic stroke: real-world experience and a call for action. *Stroke,* 41**,** 2254-8.

Birenbaum, D., Bancroft, L. W. & Felsberg, G. J. 2011. Imaging in acute stroke. *West J Emerg Med,* 12**,** 67-76.

Bivard, A., et al. 2017. Ischemic core thresholds change with time to reperfusion: A case control study. *Ann Neurol,* 82**,** 995-1003.

Bivard, A., et al. 2013. Perfusion CT in acute stroke: a comprehensive analysis of infarct and penumbra. *Radiology,* 267**,** 543-50.

Bivard, A., et al. 2010. Defining the extent of irreversible brain ischemia using perfusion computed tomography. *Cerebrovasc Dis,* 31**,** 238-245.

Bland, J. M. & Altman, D. G. 1986. Statistical methods for assessing agreement between two methods of clinical measurement. *Lancet,* 1**,** 307-10.

Bobak, C. A., Barr, P. J. & O'malley, A. J. 2018. Estimation of an inter-rater intra-class correlation coefficient that overcomes common assumption violations in the assessment of health measurement scales. *BMC Med Res Methodol,* 18**,** 93.

Boden-Albala, B., et al. 2012. Daytime sleepiness and risk of stroke and vascular disease: findings from the Northern Manhattan Study (NOMAS). *Circ Cardiovasc Qual Outcomes,* 5**,** 500-7.

Boers, A. M. M., et al. 2018. Value of quantitative collateral scoring on ct angiography in patients with acute ischemic stroke. *AJNR Am J Neuroradiol,* 39**,** 1074-1082.

Boned, S., et al. 2017. Admission CT perfusion may overestimate initial infarct core: the ghost infarct core concept. *J Neurointerv Surg,* 9**,** 66-69.

Borggrefe, J. G., B.; Maus, V.; Onur, O.; Abdullayev, N.; Barnikol, U.; Kabbasch, C.; Fink, G. R.; Mpotsaris, A. 2018. Clinical outcome after mechanical thrombectomy in patients with diabetes with major ischemic stroke of the anterior circulation. *World Neurosurgery.*

Bozzao, L., et al. 1989. Early collateral blood supply and late parenchymal brain damage in patients with middle cerebral artery occlusion. *Stroke,* 20**,** 735-740.

Bracard, S., et al. 2016. Mechanical thrombectomy after intravenous alteplase versus alteplase alone after stroke (THRACE): a randomised controlled trial. *Lancet Neurol,* 15**,** 1138-47.

Broocks, G., et al. 2020. Elevated blood glucose is associated with aggravated brain edema in acute stroke. *J Neurol,* 267**,** 440-448.

Brott, T., et al. 1989. Measurements of acute cerebral infarction: a clinical examination scale. *Stroke,* 20**,** 864-70.

Brott, T. G., et al. 1992. Urgent therapy for stroke. Part I. Pilot study of tissue plasminogen activator administered within 90 minutes. *Stroke,* 23**,** 632-40.

Bruno, A., et al. 2008. Treatment of hyperglycemia in ischemic stroke (THIS). *Stroke,* 39**,** 384-389.

Bulwa, Z. B., Mendelson, S. J. & Brorson, J. R. 2021. Acute secondary prevention of ischemic stroke: Overlooked no longer. *Front Neurol,* 12**,** 701168.

Bunce, C. 2009. Biochem J. *Am J Ophthalmol,* 148**,** 4-6.

Calamante, F., et al. 2010. The physiological significance of the time-to-maximum (Tmax) parameter in perfusion MRI. *Stroke,* 41**,** 1169-1174.

Calamante, F., et al. 1999. Measuring cerebral blood flow using magnetic resonance imaging techniques. *J Cereb Blood Flow Metab,* 19**,** 701-35.

Call, G. K., et al. 1988. Reversible cerebral segmental vasoconstriction. *Stroke,* 19**,** 1159-1170.

Campbell, B. C., et al. 2011. Cerebral blood flow is the optimal CT perfusion parameter for assessing infarct core. *Stroke,* 42**,** 3435-40.

Campbell, B. C., et al. 2015. Endovascular therapy for ischemic stroke with perfusion-imaging selection. *N Engl J Med,* 372**,** 1009-18.

Campbell, B. C. V., et al. 2019. Penumbral imaging and functional outcome in patients with anterior circulation ischaemic stroke treated with endovascular thrombectomy versus medical therapy: a meta-analysis of individual patient-level data. *Lancet Neurol,* 18**,** 46-55.

Capes, S. E., et al. 2001. Stress hyperglycemia and prognosis of stroke in nondiabetic and diabetic patients. *Stroke,* 32**,** 2426-2432.

Casp 2018. CASP qualitative checklist. *CASP*.

Cereda, C. W., et al. 2016. A benchmarking tool to evaluate computer tomography perfusion infarct core predictions against a DWI standard. *J Cereb Blood Flow Metab,* 36**,** 1780-1789.

Chatterjee, D., et al. 2020. Regional leptomeningeal collateral score by computed tomographic angiography correlates with 3-month clinical outcome in acute ischemic stroke. *Brain Circ,* 6**,** 107-115.

Chen, Z. 1997. CAST: randomised placebo-controlled trial of early aspirin use in 20,000 patients with acute ischaemic stroke. CAST (Chinese Acute Stroke Trial) Collaborative Group. *Lancet,* 349**,** 1641-9.

Chen, Z. M., et al. 2000. Indications for early aspirin use in acute ischemic stroke : A combined analysis of 40 000 randomized patients from the chinese acute stroke trial and the international stroke trial. On behalf of the CAST and IST collaborative groups. *Stroke,* 31**,** 1240-9.

Cheripelli, B. K., et al. 2016. What is the relationship among penumbra volume, collaterals, and time since onset in the first 6 h after acute ischemic stroke? *Int J Stroke,* 11**,** 338-46.

Chopp, M., et al. 1987. Intracellular acidosis during and after cerebral ischemia: in vivo nuclear magnetic resonance study of hyperglycemia in cats. *Stroke,* 18**,** 919-23.

Christensen, S. & Lansberg, M. G. 2019. CT perfusion in acute stroke: Practical guidance for implementation in clinical practice. *J Cereb Blood Flow Metab,* 39**,** 1664-1668.

Chung, J. W., et al. 2016. Determinants of Basal Collaterals in Moyamoya Disease: Clinical and Genetic Factors. *Eur J Neurol,* 75**,** 178-85.

Clarke, E. 1963. Apoplexy in the hippocratic writings. *Bull Hist Med,* 37**,** 301-314.

Cohen, J. 1960. A coefficient of agreement for nominal scales. *Educ Psychol Meas,* 20**,** 37-46.

Cole, W. & Kimberley, S. 1689. *A physico-medical essay concerning the late frequency of apoplexies together with a general method of their prevention and cure : in a letter to a physician,* Oxford : Printed at the Theater.

Cooke, J. 1820. *A treatise on nervous diseases: Vol. I on apoplexy. [vol. Ii on palsy and on epilepsy.],* Longman.

Cooper, A. 1836a. Account of the first successful operation performed on the common carotid artery for aneurysm in the year 1808 with postmortem examination in 1821. *Guy's Hospital Reports,* 1**,** 53-59.

Cooper, A. 1836b. Some experiments and observations on tying the carotid and vertebral arteries and the pneumogastric, phrenic and sympathetic nerves. *Guy's Hospital Reports,* 1**,** 457-475.

Cordonnier, C., Al-Shahi Salman, R. & Wardlaw, J. 2007. Spontaneous brain microbleeds: systematic review, subgroup analyses and standards for study design and reporting. *Brain,* 130**,** 1988-2003.

Costalat, V., et al. 2023. Evaluation of acute mechanical revascularization in large stroke (ASPECTS ⩽5) and large vessel occlusion within 7 h of last-seen-well: The LASTE multicenter, randomized, clinical trial protocol. *Int J Stroke***,** 17474930231191033.

Courten-Myers, G. D., Myers, R. E. & Schoolfield, L. 1988. Hyperglycemia enlarges infarct size in cerebrovascular occlusion in cats. *Stroke,* 19**,** 623-630.

Coutts, S. B., et al. 2024. Tenecteplase versus standard of care for minor ischaemic stroke with proven occlusion (TEMPO-2): a randomised, open label, phase 3 superiority trial. *Lancet,* 403**,** 2597-2605.

Coutts, S. B., et al. 2004. Interobserver variation of ASPECTS in real time. *Stroke,* 35**,** e103-5.

D'esterre, C. D., et al. 2015. Time-dependent computed tomographic perfusion thresholds for patients with acute ischemic stroke. *Stroke,* 46**,** 3390-7.

Davis, S. M., et al. 2008. Effects of alteplase beyond 3 h after stroke in the Echoplanar Imaging Thrombolytic Evaluation Trial (EPITHET): a placebo-controlled randomised trial. *Lancet Neurol,* 7**,** 299-309.

Day, A. L. 1984. Indications for surgical intervention in middle cerebral artery obstruction. *J Neurosurg,* 60**,** 296.

Debette, S., et al. 2011. Differential features of carotid and vertebral artery dissections. *The CADISP Study,* 77**,** 1174-1181.

Demchuk, A. M., Menon, B. K. & Goyal, M. 2016. Comparing vessel imaging. *Stroke,* 47**,** 273-281.

Dersimonian, R. & Laird, N. 1986. Meta-analysis in clinical trials. *Control Clin Trials,* 7**,** 177-88.

Dolotova, D. D., et al. 2023. Inter-rater reliability of collateral status assessment based on ct angiography: A retrospective study of middle cerebral artery ischaemic stroke. *J Clin Med* [Online], 12.

Dorn, F., et al. 2012. Order of CT stroke protocol (CTA before or after CTP): impact on image quality. *Neuroradiology,* 54**,** 105-112.

Doubal, F. N., et al. 2010. Enlarged perivascular spaces on MRI are a feature of cerebral small vessel disease. *Stroke,* 41**,** 450-4.

Drake, C. G. & Peerless, S. J. 1997. Giant fusiform intracranial aneurysms: review of 120 patients treated surgically from 1965 to 1992. *J Neurosurg,* 87**,** 141-62.

Drake, C. G., Peerless, S. J. & Ferguson, G. G. 1994. Hunterian proximal arterial occlusion for giant aneurysms of the carotid circulation. *J Neurosurg,* 81**,** 656-65.

Dregan, A., et al. 2014. Chronic inflammatory disorders and risk of type 2 diabetes mellitus, coronary heart disease, and stroke. *Circulation,* 130**,** 837-844.

Dresser, H. 1899. Pharmakologisches uber aspirin (acetylsalicylsaure). *Pflugers Arch,* 76**,** 306–18.

Ducros, A., et al. 2007. The clinical and radiological spectrum of reversible cerebral vasoconstriction syndrome. A prospective series of 67 patients. *Brain,* 130**,** 3091-3101.

Duering, M., et al. 2023. Neuroimaging standards for research into small vessel disease-advances since 2013. *Lancet Neurol,* 22**,** 602-618.

Duval, X., et al. 2010. Effect of early cerebral magnetic resonance imaging on clinical decisions in infective endocarditis. *Ann Intern Med,* 152**,** 497-504.

Dziewas, R., et al. 2003. Cervical artery dissection--clinical features, risk factors, therapy and outcome in 126 patients. *J Neurol,* 250**,** 1179-84.

Earley, C. J., et al. 1998. Stroke in children and sickle-cell disease: Baltimore-Washington Cooperative Young Stroke Study. *Neurology,* 51**,** 169-76.

Egger, M., et al. 1997. Bias in meta-analysis detected by a simple, graphical test. *BMJ Med,* 315**,** 629-34.

El Tawil, S. 2020. *Computed Tomography Perfusion imaging in acute ischemic stroke.* PhD, University of Glasgow.

El Tawil, S., et al. 2016. How many stroke patients might be eligible for mechanical thrombectomy? *Eur Stroke J,* 1**,** 264-271.

Ema 2002. Actilyse. *In:* AGENCY, E. M. (ed.). London, UK.

Endo, A., Kuroda, M. & Tsujita, Y. 1976. ML-236A, ML-236B, and ML-236C, new inhibitors of cholesterogenesis produced by Penicillium citrinium. *J Antibiot (Tokyo),* 29**,** 1346-8.

Engelhardt, E. 2017. Apoplexy, cerebrovascular disease, and stroke: Historical evolution of terms and definitions. *Dement Neuropsychol,* 11**,** 449-453.

Farrell, B., et al. 1991. The United Kingdom transient ischaemic attack (UK-TIA) aspirin trial: final results. *J Neurol Neurosurg Psychiatry,* 54**,** 1044-54.

Fda 1996. Drug approval package: Alteplase. *In:* ADMINISTRATION, F. A. D. (ed.). Rockville, Maryland, USA.

Fda. 2024. *Center for drug evaluation and research. Automated radiological image processing software k233512 approval letter.* [Online]. 10903 New Hampshire Avenue, Silver Spring, MD 20993: U.S. Food & Drug Administration. Available: https://www.accessdata.fda.gov/cdrh_docs/pdf23/K233512.pdf [Accessed 06.08.2024 2024].

Feigin, V. L., et al. 2018. Global, regional, and country-specific lifetime risks of stroke, 1990 and 2016. *N Engl J Med,* 379**,** 2429-2437.

Feigin, V. L., et al. 2021. Global, regional, and national burden of stroke and its risk factors, 1990-2019: a systematic analysis for the Global Burden of Disease Study 2019. *Lancet Neurol,* 20**,** 795-820.

Fog, M. 1938. The relationship between the blood pressure and the tonic regulation of the pial arteries. *J Neurol Psychiatry,* 1**,** 187-197.

Fulop, N., et al. 2013. Innovations in major system reconfiguration in England: a study of the effectiveness, acceptability and processes of implementation of two models of stroke care. *Implementation Science,* 8**,** 5.

Furlan, A., et al. 1999. Intra-arterial prourokinase for acute ischemic stroke. The PROACT II study: a randomized controlled trial. Prolyse in Acute Cerebral Thromboembolism. *JAMA,* 282**,** 2003-11.

Furuta, A., et al. 1991. Medullary arteries in aging and dementia. *Stroke,* 22**,** 442-6.

Gács, G., et al. 1983. CT visualization of intracranial arterial thromboembolism. *Stroke,* 14**,** 756-762.

Gao, Y., et al. 2024. Immediate or delayed intensive statin in acute cerebral ischemia: The inspires randomized clinical trial. *JAMA Neurol,* 81**,** 741-751.

García-Tornel, Á., et al. 2021. Ischemic core overestimation on computed tomography perfusion. *Stroke,* 52**,** 1751-1760.

Garner, R. L. & Tillett, W. S. 1934. Biochemical studies on the fibrinolytic activity of hemolytic streptococci : I. Isolation and characterization of fibrinolysin. *J Exp Med,* 60**,** 239-254.

Genceviciute, K., et al. 2022a. Association of diabetes mellitus and admission glucose levels with outcome after endovascular therapy in acute ischaemic stroke in anterior circulation. *Eur J Neurol,* 29**,** 2996-3008.

Genceviciute, K., et al. 2022b. Association of diabetes mellitus and admission glucose levels with outcome after endovascular therapy in acute ischaemic stroke in anterior circulation. *Eur J Neurol,* 29**,** 2996-3008.

Gensicke, H., et al. 2022. Comparison of three scores of collateral status for their association with clinical outcome: The HERMES collaboration. *Stroke,* 53**,** 3548-3556.

Giavarina, D. 2015. Understanding Bland Altman analysis. *Biochemia Medica (Zagreb),* 25**,** 141-51.

Ginsberg, M. D., Welsh, F. A. & Budd, W. W. 1980. Deleterious effect of glucose pretreatment on recovery from diffuse cerebral ischemiain the cat: I. Local cerebral blood flow and glucose utilization. *Stroke,* 11**,** 347-354.

Gissi 1986. Effectiveness of intravenous thrombolytic treatment in acute myocardial infarction. Gruppo Italiano per lo Studio della Streptochinasi nell'Infarto Miocardico (GISSI). *Lancet,* 1**,** 397-402.

Go, A. S., et al. 2004. Chronic kidney disease and the risks of death, cardiovascular events, and hospitalization. *N Engl J Med,* 351**,** 1296-305.

Gobbel, G. T., Cann, C. E. & Fike, J. R. 1991. Measurement of regional cerebral blood flow using ultrafast computed tomography. Theoretical aspects. *Stroke,* 22**,** 768-771.

Gong, Q., et al. 2021. Predictive value of CT perfusion imaging on the basis of automatic segmentation algorithm to evaluate the collateral blood flow status on the outcome of reperfusion therapy for ischemic stroke. *J Healthc Eng,* 2021**,** 4463975.

González, R. G., et al. 1999. Diffusion-weighted MR imaging: diagnostic accuracy in patients imaged within 6 hours of stroke symptom onset. *Radiology,* 210**,** 155-62.

Goyal, M., et al. 2015. Randomized assessment of rapid endovascular treatment of ischemic stroke. *N Engl J Med,* 372**,** 1019-30.

Goyal, M., et al. 2016. Endovascular thrombectomy after large-vessel ischaemic stroke: a meta-analysis of individual patient data from five randomised trials. *Lancet,* 387**,** 1723-1731.

Grau, A. J., et al. 2004. Periodontal disease as a risk factor for ischemic stroke. *Stroke,* 35**,** 496-501.

Gray, C. S., et al. 2007. Glucose-potassium-insulin infusions in the management of post-stroke hyperglycaemia: the UK Glucose Insulin in Stroke Trial (GIST-UK). *Lancet Neurol,* 6**,** 397-406.

Gray, C. S., et al. 1987. The prognostic value of stress hyperglycaemia and previously unrecognized diabetes in acute stroke. *Diabet Med,* 4**,** 237-40.

Guadagno, J. V., et al. 2008. Selective neuronal loss in rescued penumbra relates to initial hypoperfusion. *Brain,* 131**,** 2666-78.

Guenego, A., et al. 2018. Hypoperfusion ratio predicts infarct growth during transfer for thrombectomy. *Ann Neurol,* 84**,** 616-620.

Gür-Özmen, S., Güngör-Tunçer, Ö. & Krespi, Y. 2019. The effects of diffusion and perfusion MRI mismatch on the admission blood glucose and blood pressure values measured in the first 12 hours of acute stroke. *Medicine (Baltimore),* 98**,** e16212.

Hacke, W., et al. 2008. Thrombolysis with alteplase 3 to 4.5 hours after acute ischemic stroke. *N Engl J Med,* 359**,** 1317-29.

Hajian-Tilaki, K. 2013. Receiver operating characteristic (ROC) curve analysis for medical diagnostic test evaluation. *Caspian J Intern Med,* 4**,** 627-35.

Haley, E. C., Jr., et al. 1992. Urgent therapy for stroke. Part II. Pilot study of tissue plasminogen activator administered 91-180 minutes from onset. *Stroke,* 23**,** 641-5.

Hall Je, G. A. 2011. *Guyton and Hall Textbook of Medical Physiology,* Philadelphia, USA, Saunders Elsevier.

Hart, R. G., et al. 2014. Embolic strokes of undetermined source: the case for a new clinical construct. *Lancet Neurol,* 13**,** 429-438.

Heiss, W. D. & Rosner, G. 1983. Functional recovery of cortical neurons as related to degree and duration of ischemia. *Ann Neurol,* 14**,** 294-301.

Heron, M. 2021. Deaths: leading causes for 2019.

Heubner, O. 1875. Die luetischen Erkrankungen der Hirnarterien. *Jenaer Literatur-Zeitung,* 22**,** 381.

Higashida, R. T. & Furlan, A. J. 2003. Trial design and reporting standards for intra-arterial cerebral thrombolysis for acute ischemic stroke. *Stroke,* 34**,** e109-e137.

Higgins Jpt, T. J., Chandler J, Cumpston M, Li T, Page Mj, Welch Va (Editors) 2023. Cochrane handbook for systematic reviews of interventions version 6.4 (updated august 2023). *In:* COCHRANE (ed.).

Hoksbergen, A. W. J., et al. 1999. Influence of the collateral function of the circle of willis on hemispherical perfusion during carotid occlusion as assessed by transcranial colour-coded duplex ultrasonography. *Eur J Vasc Endovasc Surg,* 17**,** 486-492.

Hommel, M., et al. 1996. Thrombolytic therapy with streptokinase in acute ischemic stroke. *N Engl J Med,* 335**,** 145-50.

Hossmann, K. A. & Schuier, F. J. 1980. Experimental brain infarcts in cats. I. Pathophysiological observations. *Stroke,* 11**,** 583-92.

Hounsfield, G. N. 1973. Computerized transverse axial scanning (tomography). 1. Description of system. *Br J Radiol,* 46**,** 1016-22.

Hoving, J. W., et al. 2018. Volumetric and spatial accuracy of computed tomography perfusion estimated ischemic core volume in patients with acute ischemic stroke. *Stroke,* 49**,** 2368-2375.

Hoylaerts, M., et al. 1982. Kinetics of the activation of plasminogen by human tissue plasminogen activator. Role of fibrin. *J Biol Chem,* 257**,** 2912-9.

Huang, X., et al. 2015. Alteplase versus tenecteplase for thrombolysis after ischaemic stroke (ATTEST): a phase 2, randomised, open-label, blinded endpoint study. *Lancet Neurol,* 14**,** 368-76.

Huang, X. M., Kw. 2012. Does alteplase bolus infusion delay affect outcome? *UK Stroke Forum.* Harrogate, North Yorkshire, UK.

Huang, Y. N., et al. 1997. Vascular lesions in Chinese patients with transient ischemic attacks. *Neurology,* 48**,** 524-5.

Huo, X., et al. 2023. Trial of endovascular therapy for acute ischemic stroke with large infarct. *N Engl J Med,* 388**,** 1272-1283.

Isis-2 1988. Randomised trial of intravenous streptokinase, oral aspirin, both, or neither among 17 187 cases of suspected acute myocardial infarction: Isis-2. *Lancet,* 332**,** 349-360.

Ist 1997. The International Stroke Trial (IST): a randomised trial of aspirin, subcutaneous heparin, both, or neither among 19435 patients with acute ischaemic stroke. International Stroke Trial Collaborative Group. *Lancet,* 349**,** 1569-81.

Jennett, W. B., Harper, A. M. & Gillespie, F. C. 1966. Measurement of regional cerebral blood-flow during carotid ligation. *Lancet,* 2**,** 1162-3.

Jensen, M. & Thomalla, G. 2020. Causes and secondary prevention of acute ischemic stroke in adults. *Hamostaseologie,* 40**,** 22-30.

Johnson, A. J. & Tillett, W. S. 1952. The lysis in rabbits of intravascular blood clots by the streptococcal fibrinolytic system (streptokinase). *J Exp Med,* 95**,** 449-464.

Johnston, K. C., et al. 2019. Intensive vs standard treatment of hyperglycemia and functional outcome in patients with acute ischemic stroke: The shine randomized clinical trial. *JAMA,* 322**,** 326-335.

Johnston, K. C., et al. 2009. Glucose regulation in acute stroke patients (GRASP) trial. *Stroke,* 40**,** 3804-3809.

Johnston, S. C., et al. 2018. Clopidogrel and aspirin in acute ischemic stroke and high-risk TIA. *N Engl J Med,* 379**,** 215-225.

Jones, T. H., et al. 1981. Thresholds of focal cerebral ischemia in awake monkeys. 54**,** 773.

Jørgensen, H. S., et al. 1996. Factors delaying hospital admission in acute stroke: the Copenhagen Stroke Study. *Neurology,* 47**,** 383-7.

Jovin, T. G., et al. 2015. Thrombectomy within 8 hours after symptom onset in ischemic stroke. *N Engl J Med,* 372**,** 2296-306.

Jovin, T. G., et al. 2011. Imaging-based endovascular therapy for acute ischemic stroke due to proximal intracranial anterior circulation occlusion treated beyond 8 hours from time last seen well: retrospective multicenter analysis of 237 consecutive patients. *Stroke,* 42**,** 2206-11.

Jovin, T. G., et al. 2003. The cortical ischemic core and not the consistently present penumbra is a determinant of clinical outcome in acute middle cerebral artery occlusion. *Stroke,* 34**,** 2426-33.

Kamalian, S., et al. 2011. CT cerebral blood flow maps optimally correlate with admission diffusion-weighted imaging in acute stroke but thresholds vary by postprocessing platform. *Stroke,* 42**,** 1923-8.

Kamalian, S. & Lev, M. H. 2019. Stroke Imaging. *Radiol Clin North Am,* 57**,** 717-732.

Keating, C. 2015. The social history of ISIS-2: the early history. *Lancet,* 386**,** 646-647.

Kersten, C., et al. 2022. Association of hyperglycemia and computed tomographic perfusion deficits in patients who underwent endovascular treatment for acute ischemic stroke caused by a proximal intracranial occlusion: A subgroup analysis of a randomized phase 3 trial (MR CLEAN). *J Neurol Sci,* 440**,** 120333.

Keyt, B. A., et al. 1994. A faster-acting and more potent form of tissue plasminogen activator. *Proc Natl Acad Sci U S A,* 91**,** 3670-3674.

Khatri, P., et al. 2005. Revascularization end points in stroke interventional trials. *Stroke,* 36**,** 2400-2403.

Kim, J. J., et al. 2004. Regional angiographic grading system for collateral flow: correlation with cerebral infarction in patients with middle cerebral artery occlusion. *Stroke,* 35**,** 1340-4.

Kim, J. T., et al. 2018. Impact of hyperglycemia according to the collateral status on outcomes in mechanical thrombectomy. *Stroke,* 49**,** 2706-2714.

Knauth, M., et al. 1997. Potential of CT angiography in acute ischemic stroke. *AJNR Am J Neuroradiol,* 18**,** 1001-1010.

Kono, S., Oka, K. & Sueishi, K. 1990. Histopathologic and morphometric studies of leptomeningeal vessels in moyamoya disease. *Stroke,* 21**,** 1044-1050.

Konstas, A. A., et al. 2009. Theoretic basis and technical implementations of CT perfusion in acute ischemic stroke, part 1: Theoretic basis. *AJNR Am J Neuroradiol,* 30**,** 662-8.

Koopman, M. S., et al. 2019. Comparison of three commonly used CT perfusion software packages in patients with acute ischemic stroke. *J Neurointerv Surg,* 11**,** 1249.

Lacy, C. R., et al. 2001. Delay in presentation and evaluation for acute stroke. *Stroke,* 32**,** 63-69.

Lansberg, M. G., et al. 2012. MRI profile and response to endovascular reperfusion after stroke (DEFUSE 2): a prospective cohort study. *Lancet Neurol,* 11**,** 860-7.

Lassen, N. A. 1959. Cerebral blood flow and oxygen consumption in man. *Physiol Rev,* 39**,** 183-238.

Lassen, N. A. 1985. Normal average value of cerebral blood flow in younger adults is 50 ml/100 g/min. *J Cereb Blood Flow Metab,* 5**,** 347-9.

Laughlin, B. C., Alex. Tai, Waimei Amy. Moftakhar, Parham 2019. *RAPID automated CT perfusion in clinical practice* [Online]. Available: https://practicalneurology.com/articles/2019-nov-dec/rapid-automated-ct-perfusion-in-clinical-practice#:~:text=Automated%20CT%20perfusion%20(CTP)%20has,tissue%20and%20should%20have%20thrombectomy. [Accessed 04/11/2023 2023].

Le Bihan, D., et al. 1988. Separation of diffusion and perfusion in intravoxel incoherent motion MR imaging. *Radiology,* 168**,** 497-505.

Lees, K. R., et al. 2010. Time to treatment with intravenous alteplase and outcome in stroke: an updated pooled analysis of ECASS, ATLANTIS, NINDS, and EPITHET trials. *Lancet,* 375**,** 1695-703.

Lehmann E.L., D. a. H. J. 1975. *Nonparametrics: Statistical methods based on ranks,* Oxford, England, Holden-Day.

Leys, D., Falcou, A. & Mas, J. L. 2022. Acute stroke care in France: Survey in the 138 stroke units. *Rev Neurol (Paris),* 178**,** 1072-1078.

Li, S. ORIGINAL: a phase III, multicentre, prospective, randomized, open-label, blinded endpoint (PROBE), active-controlled, parallel-group trial to assess the efficacy and safety of tenecteplase versus alteplase in Chinese patients with acute ischaemic stroke within 4.5 hours after stroke onset. 10th European Stroke Organisation Conference, 16.05.24 2024 Basel, Switzerland.

Liebeskind, D. S. 2003. Collateral circulation. *Stroke,* 34**,** 2279-84.

Liebeskind, D. S., et al. 2014a. Impact of collaterals on successful revascularization in Solitaire FR with the intention for thrombectomy. *Stroke,* 45**,** 2036-40.

Liebeskind, D. S., et al. 2010. Collateral failure? Late mechanical thrombectomy after failed intravenous thrombolysis. *J Neuroimaging,* 20**,** 78-82.

Liebeskind, D. S., et al. 2022. Collateral circulation in thrombectomy for stroke after 6 to 24 hours in the DAWN trial. *Stroke,* 53**,** 742-748.

Liebeskind, D. S., et al. 2014b. Collaterals at angiography and outcomes in the interventional management of stroke (IMS) III trial. *Stroke,* 45**,** 759-764.

Lin, L., et al. 2016. Whole-brain ct perfusion to quantify acute ischemic penumbra and core. *Radiology,* 279**,** 876-87.

Lin, M. P. & Liebeskind, D. S. 2016. Imaging of ischemic stroke. *Continuum (Minneapolis, Minn.),* 22**,** 1399-1423.

Linfante, I., et al. 2001. Diffusion-weighted imaging and National Institutes of Health Stroke Scale in the acute phase of posterior-circulation stroke. *Arch Neurol,* 58**,** 621-8.

Lownie, S. P., et al. 2000. Clinical presentation and management of giant anterior communicating artery region aneurysms. *J Neurosurg,* 92**,** 267.

Luitse, M. J., et al. 2013. Admission hyperglycaemia and cerebral perfusion deficits in acute ischaemic stroke. *Cerebrovasc Dis,* 35**,** 163-7.

Lyden, P., et al. 1994. Improved reliability of the NIH Stroke Scale using video training. NINDS TPA Stroke Study Group. *Stroke,* 25**,** 2220-2226.

Ma, H., et al. 2019. Thrombolysis guided by perfusion imaging up to 9 hours after onset of stroke. *N Engl J Med,* 380**,** 1795-1803.

Macdougall, N. 2013. *Pathophysiology of post-stroke hyperglycaemia and brain arterial patency.* Doctor of Medicine, University of Glasgow.

Macdougall, N., et al. 2014. *Post-stroke hyperglycaemia is associated with adverse evolution of acute ischaemic injury*.

Mackey, J., et al. 2011. Population-based study of wake-up strokes. *Neurology,* 76**,** 1662-7.

Macmanus, J. P. & Buchan, A. M. 2000. Apoptosis after experimental stroke: fact or fashion? *J Neurotrauma,* 17**,** 899-914.

Mallon, D. H., et al. 2022. Comparison of automated ASPECTS, large vessel occlusion detection and CTP analysis provided by Brainomix and RapidAI in patients with suspected ischaemic stroke. *J Stroke Cerebrovasc Dis,* 31**,** 106702.

Mannismäki, L., et al. 2023. Association of admission plasma glucose level and cerebral computed tomographic perfusion deficit volumes. *J Neurol Sci,* 451**,** 120722.

Marcoux, F. W., et al. 1982. Differential regional vulnerability in transient focal cerebral ischemia. *Stroke,* 13**,** 339-46.

Marini, C., et al. 2005. Contribution of atrial fibrillation to incidence and outcome of ischemic stroke: results from a population-based study. *Stroke,* 36**,** 1115-9.

Markus, H. S. 2004. Cerebral perfusion and stroke. *J Neurol Neurosurg Psychiatry,* 75**,** 353-61.

Mast-I 1995. Randomised controlled trial of streptokinase, aspirin, and combination of both in treatment of acute ischaemic stroke. Multicentre Acute Stroke Trial--Italy (MAST-I) Group. *Lancet,* 346**,** 1509-14.

Matsubara, S., et al. 2020. Statin treatment can reduce incidence of early seizure in acute ischemic stroke: A propensity score analysis. *Sci Rep,* 10**,** 1968.

Mchugh, M. L. 2012. Interrater reliability: the kappa statistic. *Biochemia Medica (Zagreb),* 22**,** 276-82.

Mchugh, M. L. 2013. The chi-square test of independence. *Biochemia Medica (Zagreb),* 23**,** 143-9.

Mcmeekin, P., et al. 2017. Estimating the number of UK stroke patients eligible for endovascular thrombectomy. *Eur Stroke J,* 2**,** 319-326.

Mcverry, F., Liebeskind, D. S. & Muir, K. W. 2012. Systematic review of methods for assessing leptomeningeal collateral flow. *AJNR Am J Neuroradiol,* 33**,** 576-82.

Menon, B. K., et al. 2015. Differential Effect of Baseline Computed Tomographic Angiography Collaterals on Clinical Outcome in Patients Enrolled in the Interventional Management of Stroke III Trial. *Stroke,* 46**,** 1239-44.

Menon, B. K., et al. 2013. Leptomeningeal collaterals are associated with modifiable metabolic risk factors. *Ann Neurol,* 74**,** 241-8.

Menon, B. K., et al. 2011. Regional leptomeningeal score on CT angiography predicts clinical and imaging outcomes in patients with acute anterior circulation occlusions. *AJNR Am J Neuroradiol,* 32**,** 1640.

Meyer, J. S. 1958. Circulatory changes following occlusion of the middle cerebral artery and their relation to function. *J Neurosurg,* 15**,** 653.

Meyer, J. S. & Denny-Brown, D. 1957. The cerebral collateral circulation. *Neurology,* 7**,** 447.

Mhra 2024. Impact of AI on the regulation of medical products. *In:* AGENCY, M. H. P. R. (ed.). United Kingdom.

Mi, D. H., et al. 2017. Hyperglycemia indicates poor cerebral collaterals in patients underwent acute ischemic stroke. *Int J Clin Exp Med,* 10**,** 14792-14797.

Mies, G., et al. 1991. Ischemic thresholds of cerebral protein synthesis and energy state following middle cerebral artery occlusion in rat. *J Cereb Blood Flow Metab,* 11**,** 753-761.

Miller-Fisher, C. 1965. Lacunes. *Neurology,* 15**,** 774.

Mlynash, M., et al. 2011. Refining the definition of the malignant profile: insights from the DEFUSE-EPITHET pooled data set. *Stroke,* 42**,** 1270-5.

Mocco, J., et al. 2016. Aspiration thrombectomy after intravenous alteplase versus intravenous alteplase alone. *Stroke,* 47**,** 2331-8.

Modi, N. B., et al. 2000. Pharmacokinetics and pharmacodynamics of tenecteplase: results from a phase II study in patients with acute myocardial infarction. *J Clin Pharmacol,* 40**,** 508-515.

Moher, D., et al. 2009. Preferred reporting items for systematic reviews and meta-analyses: the PRISMA Statement. *PLoS Med,* 3**,** e123-30.

Mohr, J. P., et al. 1978. Broca aphasia: Pathologic and clinical. *Neurology,* 28**,** 311-311.

Mokin, M., et al. 2017. Predictive value of RAPID assessed perfusion thresholds on final infarct volume in SWIFT PRIME (Solitaire With the Intention for Thrombectomy as Primary Endovascular Treatment). *Stroke,* 48**,** 932-938.

Molinari, G. F. & Laurent, J. P. 1976. A classification of experimental models of brain ischemia. *Stroke,* 7**,** 14-17.

Moore, P. M. 1989. Diagnosis and management of isolated angiitis of the central nervous system. *Neurology,* 39**,** 167-73.

Moreton, F. C., Mccormick, M. & Muir, K. W. 2007. Insular cortex hypoperfusion and acute phase blood glucose after stroke: a CT perfusion study. *Stroke,* 38**,** 407-410.

Morris, S., et al. 2014. Impact of centralising acute stroke services in English metropolitan areas on mortality and length of hospital stay: difference-in-differences analysis. *BMJ Med,* 349**,** g4757.

Muir, K. W. Alteplase-Tenecteplase Trial Evaluation for Stroke Thombolysis: A multi-centre randoimised, controlled phase III trial. 15th World Stroke Congress, 10-12/10/2023 2023 Toronto, Canada.

Muir, K. W., et al. 2017. Endovascular therapy for acute ischaemic stroke: the Pragmatic Ischaemic Stroke Thrombectomy Evaluation (PISTE) randomised, controlled trial. *J Neurol Neurosurg Psychiatry,* 88**,** 38.

Muir, K. W., et al. 2011. Prevalence, predictors and prognosis of post-stroke hyperglycaemia in acute stroke trials: Individual patient data pooled analysis from the Virtual International Stroke Trials Archive (VISTA). *Cerebrovasc Dis Extra,* 1**,** 17-27.

Muir, K. W. & White, P. 2016. HERMES: messenger for stroke interventional treatment. *Lancet,* 387**,** 1695-1697.

Müller, M. & Schimrigk, K. 1996. Vasomotor reactivity and pattern of collateral blood flow in severe occlusive carotid artery disease. *Stroke,* 27**,** 296-299.

Murros, K., et al. 1993. Serum cortisol and outcome of ischemic brain infarction. *J Neurol Sci,* 116**,** 12-17.

Nagaraja, N., et al. 2020. Reversible diffusion-weighted imaging lesions in acute ischemic stroke. *Neurology,* 94**,** 571-587.

Nedergaard, M. 1987. Transient focal ischemia in hyperglycemic rats is associated with increased cerebral infarction. *Brain Res,* 408**,** 79-85.

Nederkoorn, P. J., Van Der Graaf, Y. & Hunink, M. G. M. 2003. Duplex ultrasound and magnetic resonance angiography compared with digital subtraction angiography in carotid artery stenosis. *Stroke,* 34**,** 1324-1331.

Nguyen, T. N., et al. 2022. Noncontrast Computed Tomography vs Computed Tomography Perfusion or Magnetic Resonance Imaging Selection in Late Presentation of Stroke With Large-Vessel Occlusion. *JAMA Neurol,* 79**,** 22-31.

Nice 2022. Evidence overview: Software with artificial intelligence-derived algorithms for analysing CT brain scans in people with a suspected acute stroke.

Nice 2024. Artificial intelligence (AI)-derived software to help clinical decision making in stroke. Diagnostics guidance [DG57].

Nicholson, P., et al. 2020. Per-region interobserver agreement of Alberta Stroke Program Early CT Scores (ASPECTS). *J Neurointerv Surg,* 12**,** 1069.

Nih 1980. Thrombolytic therapy in treatment: summary of an NIH Consensus Conference. *BMJ Med,* 280**,** 1585-1587.

Ninds 1995. Tissue plasminogen activator for acute ischemic stroke. *N Engl J Med,* 333**,** 1581-7.

Nogueira, R. G., et al. 2017. Thrombectomy 6 to 24 hours after stroke with a mismatch between deficit and infarct. *N Engl J Med,* 378**,** 11-21.

Ntaios, G., et al. 2011. Persistent hyperglycemia at 24-48 h in acute hyperglycemic stroke patients is not associated with a worse functional outcome. *Cerebrovasc Dis,* 32**,** 561-6.

O'donnell, M. J., et al. 2016. Global and regional effects of potentially modifiable risk factors associated with acute stroke in 32 countries (INTERSTROKE): a case-control study. *Lancet,* 388**,** 761-775.

O'donnell, M. J., et al. 2010. Risk factors for ischaemic and intracerebral haemorrhagic stroke in 22 countries (the INTERSTROKE study): a case-control study. *Lancet,* 376**,** 112-23.

Obi, C., et al. 2009. Inhibition of platelet-rich arterial thrombus in vivo: acute antithrombotic effect of intravenous HMG-CoA reductase therapy. *Arterioscler Thromb Vasc Biol,* 29**,** 1271-6.

Olivot, J.-M., et al. 2009. Optimal tmax threshold for predicting penumbral tissue in acute stroke. *Stroke,* 40**,** 469-475.

Olivot, J. M., et al. 2014. Hypoperfusion intensity ratio predicts infarct progression and functional outcome in the DEFUSE 2 Cohort. *Stroke,* 45**,** 1018-23.

Olthuis, S. G. H., et al. 2023a. Endovascular treatment versus no endovascular treatment after 6-24 h in patients with ischaemic stroke and collateral flow on CT angiography (MR CLEAN-LATE) in the Netherlands: a multicentre, open-label, blinded-endpoint, randomised, controlled, phase 3 trial. *Lancet,* 401**,** 1371-1380.

Olthuis, S. G. H., et al. 2023b. Endovascular treatment versus no endovascular treatment after 6–24 h in patients with ischaemic stroke and collateral flow on CT angiography (MR CLEAN-LATE) in the Netherlands: a multicentre, open-label, blinded-endpoint, randomised, controlled, phase 3 trial. *Lancet,* 401**,** 1371-1380.

Oppenheimer, S. M., et al. 1985. Diabetes mellitus and early mortality from stroke. *BMJ Med,* 291**,** 1014-1015.

Ostergaard, L., et al. 1996. High resolution measurement of cerebral blood flow using intravascular tracer bolus passages. Part I: Mathematical approach and statistical analysis. *Magn Reson Med,* 36**,** 715-25.

Overell, J. R., Bone, I. & Lees, K. R. 2000. Interatrial septal abnormalities and stroke: a meta-analysis of case-control studies. *Neurology,* 55**,** 1172-9.

Palaiodimou, L. Tenecteplase versus alteplase in the treatment of acute ischemic stroke within 4.5 hours: A systematic review and meta-analysis. 10th European Stroke Organisation Conference, 16.05.24 2024 Basel, Switzerland.

Paljärvi, L., et al. 1983. Brain lactic acidosis and ischemic cell damage: Quantitative ultrastructural changes in capillaries of rat cerebral cortex. *Acta Neuropathol,* 60**,** 232-240.

Pansera, F. 1990. The integration of the cerebral and coronary circulations with the dynamic system structure of brain and myocardium and the form of the cerebral and coronary artery trees. *Med Hypotheses,* 32**,** 297-305.

Pantoni, L. 2010. Cerebral small vessel disease: from pathogenesis and clinical characteristics to therapeutic challenges. *Lancet Neurol,* 9**,** 689-701.

Parsons, M. Tenecteplase versus alteplase for stroke thrombolysis evaluation with perfusion imaging selection within 4.5 hours of onset (TASTE): a multicentre, randomized, controlled phase III non-inferiority trial. 10th European Stroke Organisation Conference, 15.05.2024 2024 Basel, Switzerland.

Parsons, M., et al. 2012. A randomized trial of tenecteplase versus alteplase for acute ischemic stroke. *N Engl J Med,* 366**,** 1099-107.

Parsons, M. W., et al. 2002. Acute hyperglycemia adversely affects stroke outcome: A magnetic resonance imaging and spectroscopy study. *Ann Neurol,* 52**,** 20-28.

Paschen, W., Mies, G. & Hossmann, K. A. 1992. Threshold relationship between cerebral blood flow, glucose utilization, and energy metabolites during development of stroke in gerbils. *Exp Neurol,* 117**,** 325-333.

Petersen, J. E., Jp. 1937. The anatomical end results of cerebral arterial occlusion. *Transactions of the American Neurological Association,* 63**,** 88-93.

Poirier, J. & Derouesné, C. 1985. The concept of cerebral lacunae from 1838 to the present. *Rev Neurol (Paris),* 141**,** 3-17.

Powers, W. J., et al. 2019. Guidelines for the early management of patients with acute ischemic stroke: 2019 update to the 2018 guidelines for the early management of acute ischemic stroke: A guideline for healthcare professionals from the American Heart Association/American Stroke Association. *Stroke,* 50**,** e344-e418.

Powers, W. J. & Raichle, M. E. 1985. Positron emission tomography and its application to the study of cerebrovascular disease in man. *Stroke,* 16**,** 361-76.

Prado, R., et al. 1988. Hyperglycemia increases infarct size in collaterally perfused but not end-arterial vascular territories. *J Cereb Blood Flow Metab,* 8**,** 186-192.

Prasad, K., et al. 2018. Dual antiplatelet therapy with aspirin and clopidogrel for acute high risk transient ischaemic attack and minor ischaemic stroke: a clinical practice guideline. *BMJ Med,* 363**,** k5130.

Pulsinelli, W. 1992. Pathophysiology of acute ischaemic stroke. *Lancet,* 339**,** 533-6.

Qiu, W., et al. 2019. Confirmatory study of time-dependent computed tomographic perfusion thresholds for use in acute ischemic stroke. *Stroke,* 50**,** 3269-3273.

Quinn, T. J., et al. 2009. Reliability of the modified Rankin Scale: a systematic review. *Stroke,* 40**,** 3393-5.

Ra, F. 1921. On the "probable error" of a coefficient of correlation deduced from a small sample. *Metron,* 1**,** 1-32.

Rankin, J. 1957. Cerebral vascular accidents in patients over the age of 60. II. Prognosis. *Scott Med J,* 2**,** 200-15.

Rasmussen, L. M., et al. 2001. Diverse effects of inhibition of 3-hydroxy-3-methylglutaryl-CoA reductase on the expression of VCAM-1 and E-selectin in endothelial cells. *Biochem Journal,* 360**,** 363-70.

Rebello, L. C., et al. 2017. Stroke etiology and collaterals: atheroembolic strokes have greater collateral recruitment than cardioembolic strokes. *Eur J Neurol,* 24**,** 762-767.

Reddy, K. N. & Markus, G. 1972. Mechanism of activation of human plasminogen by streptokinase. Presence of active center in streptokinase-plasminogen complex. *J Biol Chem,* 247**,** 1683-91.

Rehncrona, S., Rosén, I. & Siesjö, B. K. 1981. Brain lactic acidosis and ischemic cell damage: 1. Biochemistry and neurophysiology. *J Cereb Blood Flow Metab,* 1**,** 297-311.

Reshi, R., et al. 2017. Hyperglycemia in acute ischemic stroke: Is it time to re-evaluate our understanding? *Med Hypotheses,* 107**,** 78-80.

Rha, J.-H. & Saver, J. L. 2007. The impact of recanalization on ischemic stroke outcome. *Stroke,* 38**,** 967-973.

Ribo, M., et al. 2007. Hyperglycemia during ischemia rapidly accelerates brain damage in stroke patients treated with tPA. *J Cereb Blood Flow Metab,* 27**,** 1616-1622.

Riedel, C. H., et al. 2011. The importance of size: successful recanalization by intravenous thrombolysis in acute anterior stroke depends on thrombus length. *Stroke,* 42**,** 1775-7.

Riggs He, R. C. 1963. Variation in form of circle of Willis: The relation of the variations to collateral circulation: Anatomic analysis. *Arch Neurol,* 8**,** 8-14.

Rocha, M. & Jovin, T. G. 2017. Fast versus slow progressors of infarct growth in large vessel occlusion stroke: Clinical and research implications. *Stroke,* 48**,** 2621-2627.

Rosso, C., et al. 2011. Hyperglycemia and the fate of apparent diffusion coefficient-defined ischemic penumbra. *AJNR Am J Neuroradiol,* 32**,** 852-856.

Rost, N. S., et al. 2010. White matter hyperintensity volume is increased in small vessel stroke subtypes. *Neurology,* 75**,** 1670-7.

Sacco, R. L., et al. 2013. An updated definition of stroke for the 21st century: a statement for healthcare professionals from the American Heart Association/American Stroke Association. *Stroke,* 44**,** 2064-89.

Salehi Omran, S., et al. 2020. Association between pregnancy and cervical artery dissection. *Ann Neurol,* 88**,** 596-602.

Sarraj, A., et al. 2023. Trial of endovascular thrombectomy for large ischemic strokes. *N Engl J Med,* 388**,** 1259-1271.

Saver, J. L., et al. 2017. Long-term outcomes of patent foramen ovale closure or medical therapy after stroke. *N Engl J Med,* 377**,** 1022-1032.

Saver, J. L., et al. 2020. Thrombectomy for distal, medium vessel occlusions: A consensus statement on present knowledge and promising directions. *Stroke,* 51**,** 2872-2884.

Saver, J. L., et al. 2015. Stent-retriever thrombectomy after intravenous t-PA vs. t-PA alone in stroke. *N Engl J Med,* 372**,** 2285-95.

Saver, J. L., et al. 2016. Time to treatment with endovascular thrombectomy and outcomes from ischemic stroke: A meta-analysis. *JAMA,* 316**,** 1279-88.

Saver, J. L., et al. 1999. Infarct volume as a surrogate or auxiliary outcome measure in ischemic stroke clinical trials. The RANTTAS Investigators. *Stroke,* 30**,** 293-8.

Schaefer, P. W., et al. 2015. Limited reliability of computed tomographic perfusion acute infarct volume measurements compared with diffusion-weighted imaging in anterior circulation stroke. *Stroke,* 46**,** 419-424.

Scheidecker, E., et al. 2022. Role of diabetes in collateral status assessed in CT perfusion-derived dynamic CTA in anterior circulation stroke. *Neuroradiology,* 64**,** 1195-1199.

Schiller, F. 1970. Concepts of stroke before and after Virchow. *Med Hist,* 14**,** 115-131.

Schober, P., Boer, C. & Schwarte, L. A. 2018. Correlation coefficients: Appropriate use and interpretation. *Anesth Analg,* 126**,** 1763-1768.

Schober, P. & Vetter, T. R. 2021. Linear regression in medical research. *Anesth Analg,* 132**,** 108-109.

Schuier, F. J. & Hossmann, K. A. 1980. Experimental brain infarcts in cats. II. Ischemic brain edema. *Stroke,* 11**,** 593-601.

Sharbrough, F. W., Messick, J. M., Jr. & Sundt, T. M., Jr. 1973. Correlation of continuous electroencephalograms with cerebral blood flow measurements during carotid endarterectomy. *Stroke,* 4**,** 674-83.

Shetty, S. K. & Lev, M. H. 2005. CT perfusion in acute stroke. *Neuroimaging Clin N Am,* 15**,** 481-501, ix.

Shimoyama, T., et al. 2013. Admission hyperglycemia causes infarct volume expansion in patients with ICA or MCA occlusion: association of collateral grade on conventional angiography. *Eur J Neurol,* 20**,** 109-116.

Singhal, A. B., et al. 2011. Reversible cerebral vasoconstriction syndromes: analysis of 139 cases. *Arch Neurol,* 68**,** 1005-12.

Smith, W. S., et al. 2005. Safety and efficacy of mechanical embolectomy in acute ischemic stroke. *Stroke,* 36**,** 1432-1438.

Soares, B. P., et al. 2009. Automated versus manual post-processing of perfusion-CT data in patients with acute cerebral ischemia: influence on interobserver variability. *Neuroradiology,* 51**,** 445-51.

Sorteberg, W., et al. 1989. Blood velocity and regional blood flow in defined cerebral artery systems. *Acta Neurochir,* 97**,** 47-52.

Sperandei, S. 2014. Understanding logistic regression analysis. *Biochemia Medica (Zagreb),* 24**,** 12-8.

Ssca 2023. Scottish stroke improvement programme Annual report 2023. Public Health Scotland.

Ssnap 2023. SSNAP acute organisational audit report 2023. London: King's College London.

Staniforth, D. H., Smith, R. a. G. & Hibbs, M. 1983. Streptokinase and anisoylated streptokinase plasminogen complex. *Eur J Clin Pharmacol,* 24**,** 751-756.

Statistics, O. F. N. 2023. Families and households in the UK: 2023. UK.

Stone, E. 1763. An account of the success of the bark of the willow in the cure of agues. In a letter to the Right Honourable George Earl of Macclesfield, President of R. S. from the Rev. Mr. Edward Stone, of Chipping-Norton in Oxfordshire. *Philosophical Transactions of the Royal Society of London,* 53**,** 195-200.

Strandgaard, S., et al. 1973. Autoregulation of brain circulation in severe arterial hypertension. *BMJ Med,* 1**,** 507-10.

Sutc 2013. Organised inpatient (stroke unit) care for stroke. *Cochrane Database Syst Rev*.

Symon, L. 1960. Observations on the leptomeningeal collateral circulation in dogs. *J Physiol,* 154**,** 1-14.2.

Symon, L., Branston, N. M. & Chikovani, O. 1979. Ischemic brain edema following middle cerebral artery occlusion in baboons: relationship between regional cerebral water content and blood flow at 1 to 2 hours. *Stroke,* 10**,** 184-191.

Tan, I. Y., et al. 2009a. CT angiography clot burden score and collateral score: correlation with clinical and radiologic outcomes in acute middle cerebral artery infarct. *AJNR Am J Neuroradiol,* 30**,** 525-31.

Tan, I. Y. L., et al. 2009b. CT angiography clot burden score and collateral score: correlation with clinical and radiologic outcomes in acute middle cerebral artery infarct. *AJNR Am J Neuroradiol,* 30**,** 525-531.

Tan, J. C., et al. 2007. Systematic comparison of perfusion-CT and CT-angiography in acute stroke patients. *Ann Neurol,* 61**,** 533-43.

Tanswell, P., et al. 1989. Pharmacokinetics and systemic effects of tissue-type plasminogen activator in normal subjects. *Clin Pharmacol Ther,* 46**,** 155-62.

Tanswell, P., et al. 1992. Pharmacokinetics and fibrin specificity of alteplase during accelerated infusions in acute myocardial infarction. *J Am Coll Cardiol,* 19**,** 1071-1075.

Tarr, D., et al. 2013. Hyperglycemia accelerates apparent diffusion coefficient-defined lesion growth after focal cerebral ischemia in rats with and without features of metabolic syndrome. *J Cereb Blood Flow Metab,* 33**,** 1556-63.

Thomalla, G., et al. 2018. MRI-guided thrombolysis for stroke with unknown time of onset. *N Engl J Med,* 379**,** 611-622.

Thomas, H. J., et al. 1981. Thresholds of focal cerebral ischemia in awake monkeys. *J Neurosurg,* 54**,** 773-782.

Tillett, W. S. & Garner, R. L. 1933. The fibrinolytic activity of hemolytic streptococci. *J Exp Med,* 58**,** 485-502.

Tillett, W. S. & Sherry, S. 1949. The effect in patients of streptococcal fibrinolysin (streptokinase) and streptococcal desoxyribonuclease on fibrinous, purulent, and sanguinous pleural exudations. *J Clin Invest,* 28**,** 173-190.

Timi 1985. The Thrombolysis in Myocardial Infarction (TIMI) trial. Phase I findings. *N Engl J Med,* 312**,** 932-6.

Toni, D., et al. 1994. Influence of hyperglycaemia on infarct size and clinical outcome of acute ischemic stroke patients with intracranial arterial occlusion. *J Neurol Sci,* 123**,** 129-33.

Trojaborg, W. & Boysen, G. 1973. Relation between EEG, regional cerebral blood flow and internal carotid artery pressure during carotid endarterectomy. *Electroencephalogr Clin Neurophysiol,* 34**,** 61-9.

Tu, H. T. H., et al. 2013. Worse stroke outcome in atrial fibrillation is explained by more severe hypoperfusion, infarct growth, and hemorrhagic transformation. *Int J Stroke,* 10**,** 534-540.

Turc, G., et al. 2019. European Stroke Organisation (ESO) - European society for minimally invasive neurological therapy (ESMINT) guidelines on mechanical thrombectomy in acute ischaemic stroke endorsed by stroke alliance for europe (SAFE). *Eur Stroke J,* 4**,** 6-12.

Vagal, A., et al. 2016. Association between CT angiogram collaterals and CT perfusion in the interventional management of stroke III trial. *Stroke,* 47**,** 535-8.

Van Everdingen, K. J., et al. 1998. Diffusion-weighted magnetic resonance imaging in acute stroke. *Stroke,* 29**,** 1783-90.

Van Ommen, F., et al. 2019. Effect of prolonged acquisition intervals for CT-perfusion analysis methods in patients with ischemic stroke. *Med Phys,* 46**,** 3156-3164.

Van Seeters, T., et al. 2016. Determinants of leptomeningeal collateral flow in stroke patients with a middle cerebral artery occlusion. *Neuroradiology,* 58**,** 969-977.

Van Swieten, J. C., et al. 1988. Interobserver agreement for the assessment of handicap in stroke patients. *Stroke,* 19**,** 604-7.

Vander Ecken Hm, A. R. 1953. The anatomy and functional significance of the meningeal arterial anastamoses of the human brain. *J Neuropathol Exp Neurol,* 12**,** 132-57.

Vane, J. R. 1971. Inhibition of prostaglandin synthesis as a mechanism of action for aspirin-like drugs. *Nat New Biol,* 231**,** 232-5.

Vavilala Ms, L. L. 2002. Cerebral blood flow and vascular physiology. *Anesthesiol Clin North Am,* 20**,** 247-264.

Venables, G. S., et al. 1985. The effects of hyperglycaemia on changes during reperfusion following focal cerebral ischaemia in the cat. *J Neurol Neurosurg Psychiatry,* 48**,** 663-9.

Vermeer, S. E., Longstreth, W. T., Jr. & Koudstaal, P. J. 2007. Silent brain infarcts: a systematic review. *Lancet Neurol,* 6**,** 611-9.

Verro, P., et al. 2002. CT angiography in acute ischemic stroke. *Stroke,* 33**,** 276-278.

Viechtbauer, W. & Cheung, M. W. 2010. Outlier and influence diagnostics for meta-analysis. *Res Synth Methods,* 1**,** 112-25.

Villringer, A., et al. 1988. Dynamic imaging with lanthanide chelates in normal brain: contrast due to magnetic susceptibility effects. *Magn Reson Med,* 6**,** 164-74.

Von Kummer, R., et al. 2015. The Heidelberg bleeding classification: Classification of bleeding events after ischemic stroke and reperfusion therapy. *Stroke,* 46**,** 2981-6.

Von Kummer, R. & Hacke, W. 1992. Safety and efficacy of intravenous tissue plasminogen activator and heparin in acute middle cerebral artery stroke. *Stroke,* 23**,** 646-52.

Von Kummer, R., et al. 1994. Sensitivity and prognostic value of early CT in occlusion of the middle cerebral artery trunk. *AJNR Am J Neuroradiol,* 15**,** 9-15.

Wagner, A. H., et al. 2000. Improvement of nitric oxide-dependent vasodilatation by HMG-CoA reductase inhibitors through attenuation of endothelial superoxide anion formation. *Arterioscler Thromb Vasc Biol,* 20**,** 61-9.

Wang, C. M., et al. 2021. Hypoperfusion index ratio as a surrogate of collateral scoring on ct angiogram in large vessel stroke. *J Clin Med,* 10.

Wang, F., et al. 2018. Higher admission fasting plasma glucose levels are associated with a poorer short-term neurologic outcome in acute ischemic stroke patients with good collateral circulation. *Acta Diabetol,* 55**,** 703-714.

Wang, Y., et al. 2013. Clopidogrel with aspirin in acute minor stroke or transient ischemic attack. *N Engl J Med,* 369**,** 11-19.

Warach, S., et al. 1992. Fast magnetic resonance diffusion-weighted imaging of acute human stroke. *Neurology,* 42**,** 1717-23.

Wardlaw, J. M., et al. 2013a. Clinical relevance and practical implications of trials of perfusion and angiographic imaging in patients with acute ischaemic stroke: a multicentre cohort imaging study. *J Neurol Neurosurg Psychiatry,* 84**,** 1001-7.

Wardlaw, J. M., et al. 2012. Recombinant tissue plasminogen activator for acute ischaemic stroke: an updated systematic review and meta-analysis. *Lancet,* 379**,** 2364-72.

Wardlaw, J. M., et al. 2013b. Neuroimaging standards for research into small vessel disease and its contribution to ageing and neurodegeneration. *Lancet Neurol,* 12**,** 822-38.

Weimar, W., et al. 1981. Specific lysis of an iliofemoral thrombus by administration of extrinsic (tissue-type) plasminogen activator. *Lancet,* 318**,** 1018-1020.

Weir, C. J., et al. 1997. Is hyperglycaemia an independent predictor of poor outcome after acute stroke? Results of a long-term follow up study. *BMJ Med,* 314**,** 1303-6.

Wesbey, G. E., Moseley, M. E. & Ehman, R. L. 1984. Translational molecular self-diffusion in magnetic resonance imaging. II. Measurement of the self-diffusion coefficient. *Invest Radiol,* 19**,** 491-8.

Who 1975. International classification of diseases 9th revision. United States.

Who 2015. World Health Organisation best practices for the naming of new human infectious diseases. Geneva: World Health Organization.

Wiegers, E. J. A., et al. 2020. Clinical and Imaging Determinants of Collateral Status in Patients With Acute Ischemic Stroke in MR CLEAN Trial and Registry. *Stroke,* 51**,** 1493-1502.

Wilde, O. 1895. *The Importance of Being Earnest,* Forgotten Books.

Williams, D. S., et al. 1992. Magnetic resonance imaging of perfusion using spin inversion of arterial water. *Proc Natl Acad Sci U S A,* 89**,** 212-6.

Wing, S. C. & Markus, H. S. 2019. Interpreting CT perfusion in stroke. *Pract Neurol,* 19**,** 136-142.

Wintermark, M., et al. 2006. Perfusion-CT assessment of infarct core and penumbra: receiver operating characteristic curve analysis in 130 patients suspected of acute hemispheric stroke. *Stroke,* 37**,** 979-85.

Wintermark, M., et al. 2015. International survey of acute stroke imaging used to make revascularization treatment decisions. *Int J Stroke,* 10**,** 759-62.

Wolverson, M. K., et al. 1983. Hyperdensity of recent hemorrhage at body computed tomography: incidence and morphologic variation. *Radiology,* 148**,** 779-84.

Woo, D., et al. 1999. Does the National Institutes of Health Stroke Scale favor left hemisphere strokes? NINDS t-PA Stroke Study Group. *Stroke,* 30**,** 2355-9.

Wso. 2022. *WSO global stroke fact sheet* [Online]. Available: https://www.world-stroke.org/news-and-blog/news/wso-global-stroke-fact-sheet-2022 [Accessed 09/07 2023].

Xiong, Y. Tenecteplase for ischemic stroke due to large vessel occlusion at 4.5 to 24 hours with perfusion imaging selection. 10th European Stroke Organisation Conference, 16.05.24 2024 Basel, Switzerland.

Xiong, Y., et al. 2024. Tenecteplase for ischemic stroke at 4.5 to 24 hours without thrombectomy. *N Engl J Med,* 391**,** 203-212.

Yang, Q. 2005. Method and system of obtaining improved data in perfusion measurements. PCT International Application PCT/AU2004/000821. *International Publication on,* 10.

Yoshie, T., et al. 2020. Perfusion parameter thresholds that discriminate ischemic core vary with time from onset in acute ischemic stroke. *AJNR Am J Neuroradiol,* 41**,** 1809-1815.

Yoshimura, S., et al. 2022. Endovascular therapy for acute stroke with a large ischemic region. *N Engl J Med,* 386**,** 1303-1313.

Zaidat, O. O., et al. 2023. TESLA trial: rationale, protocol, and design. *Stroke vasc interv neurol,* 3**,** e000787.

Zamarron, C., Lijnen, H. R. & Collen, D. 1984. Kinetics of the activation of plasminogen by natural and recombinant tissue-type plasminogen activator. *J Biol Chem,* 259**,** 2080-3.

Zangerle, A., et al. 2007. Recanalization after thrombolysis in stroke patients. *Neurology,* 68**,** 39-44.

Appendix A

Prospero Protocol

Systematic review

Please select one of the options below to edit your record. Either option will create a new version of the record - the existing version will remain unchanged.

A list of fields that can be edited in an update can be found here

1. * Review title.

Give the title of the review in English

The relevance of hyperglycaemia in collateral flow in acute ischaemic stroke

2. Original language title.

For reviews in languages other than English, give the title in the original language. This will be displayed with the English language title.

3. * Anticipated or actual start date.

Give the date the systematic review started or is expected to start.

26/10/2018

4. * Anticipated completion date.

Give the date by which the review is expected to be completed.

26/04/2019

5. * Stage of review at time of this submission.

This field uses answers to initial screening questions. It cannot be edited until after registration.

Tick the boxes to show which review tasks have been started and which have been completed.

Update this field each time any amendments are made to a published record.

The review has not yet started: No

Review stage	Started	Completed
Preliminary searches	Yes	No
Piloting of the study selection process	No	No
Formal screening of search results against eligibility criteria	No	No
Data extraction	No	No
Risk of bias (quality) assessment	No	No
Data analysis	No	No

Appendix B

Ovid Medline Search Strategy

1. exp Stroke
2. exp Stroke, Lacunar/
3. exp Ischemia/
4. exp Cerebrovascular Disorders/
5. exp Infarction
6. exp Brain Ischemia/
7. (stroke or cerebrovascular accident or cerebro-vascular accident or cerebro vascular accident or brain vascular accident or CVA or cerebrovascular attack cerebro-vascular attack cerebro vascular attack or brain vascular attack brain attack or cerebrovascular insult* or cerebro-vascular insult* or cerebro vascular insult* or brain vascular insult* or cerebrovascular injury or cerebro-vascular injury or cerebro vascular injury or infarct* or isch?em* or occlusive cerebrovascular disease or occlusive cerebro-vascular disease or occlusive cerebro vascular disease or cerebral artery occlusion or cerebrovascular disease or cerebro-vascular disease or cerebro vascular disease or cerebrovascular disorders or cerebro-vascular disorders or cerebro vascular disorders or acute cerebrovascular lesion or acute cerebro-vascular lesion or acute cerebro vascular lesion or intracranial embolism or intra-cranial embolism or intra cranial embolism or intracranial thrombosis or intra-cranial thrombosis or intra cranial thrombosis).tw.
8. 1 or 2 or 3 or 4 or 5 or 6 or 7
9. exp Cerebrovascular Circulation/
10. Collateral Circulation/
11. Regional Blood Flow/
12. (collateral* or cerebrovascular circulation or cerebro-vascular circulation or cerebro vascular circulation or cerebral circulation or cerebrovascular bloodflow or cerebro-vascular bloodflow or cerebro vascular bloodflow or cerebrovascular blood-flow or cerebro-vascular blood-flow or cerebro vascular blood-flow or cerebrovascular blood flow or cerebro-vascular blood flow or cerebro vascular blood flow or cerebral bloodflow or cerebral blood-flow or cerebral blood flow or regional bloodflow or regional blood-flow or regional blood flow or perfusion).tw.
13. 9 or 10 or 11 or 12
14. exp Blood Glucose/

15. exp Hyperglycemia/
16. exp Hypoglycemia/
17. (blood glucose or blood sugar or glucose blood level or sugar blood level or serum glucose or serum sugar or plasma glucose or plasma sugar or glucos?emi* or glyc?emi* or hypergl?c?emi* or hyper-gl?c?emi* or hypogl?c?emi* or hypo-gl?c?emi* or eugl?c?emi* or eu-gl?c?emi* or normogl?c?emi* or normo-gl?c?emi*).tw.
18. 14 or 15 or 16 or 17
19. 8 and 13 and 18
20. limit 19 to english language

Embase Search Strategy

1. exp cerebrovascular accident/
2. exp brain infarction/
3. brain ischemia/
4. (stroke or cerebrovascular accident or cerebro-vascular accident or cerebro vascular accident or brain vascular accident or CVA or cerebrovascular attack cerebro-vascular attack cerebro vascular attack or brain vascular attack brain attack or cerebrovascular insult* or cerebro-vascular insult* or cerebro vascular insult* or brain vascular insult* or cerebrovascular injury or cerebro-vascular injury or cerebro vascular injury or infarct* or isch?em* or occlusive cerebrovascular disease or occlusive cerebro-vascular disease or occlusive cerebro vascular disease or cerebral artery occlusion or cerebrovascular disease or cerebro-vascular disease or cerebro vascular disease or cerebrovascular disorders or cerebro-vascular disorders or cerebro vascular disorders or acute cerebrovascular lesion or acute cerebro-vascular lesion or acute cerebro vascular lesion or intracranial embolism or intra-cranial embolism or intra cranial embolism or intracranial thrombosis or intra-cranial thrombosis or intra cranial thrombosis).tw.
5. 1 or 2 or 3 or 4
6. exp collateral circulation/
7. exp collateral artery/
8. exp blood flow/
9. exp brain perfusion/

10. (collateral* or cerebrovascular circulation or cerebro-vascular circulation or cerebro vascular circulation or cerebral circulation or cerebrovascular bloodflow or cerebro-vascular bloodflow or cerebro vascular bloodflow or cerebrovascular blood-flow or cerebro-vascular blood-flow or cerebro vascular blood-flow or cerebrovascular blood flow or cerebro-vascular blood flow or cerebro vascular blood flow or cerebral bloodflow or cerebral blood-flow or cerebral blood flow or regional bloodflow or regional blood-flow or regional blood flow or perfusion).tw.
11. 6 or 7 or 8 or 9 or 10
12. exp glucose blood level/
13. exp hyperglycemia
14. exp hypoglycemia
15. (blood glucose or blood sugar or glucose blood level or sugar blood level or serum glucose or serum sugar or plasma glucose or plasma sugar or glucos?emi* or glyc?emi* or hypergl?c?emi* or hyper-gl?c?emi* or hypogl?c?emi* or hypo-gl?c?emi* or eugl?c?emi* or eu-gl?c?emi* or normogl?c?emi* or normo-gl?c?emi*).tw.
16. 12 or 13 or 14 or 15
17. 5 and 11 and 16
18. limit 17 to english language

Cochrane Library Search Strategy

1. MeSH descriptor: [Stroke] explode all trees
2. MeSH descriptor: [Stroke, Lacunar] explode all trees
3. MeSH descriptor: [Ischemia] explode all trees
4. MeSH descriptor: [Cerebrovascular Disorders] explode all trees
5. MeSH descriptor: [Infarction] explode all trees
6. MeSH descriptor: [Brain Ischemia] explode all trees
7. (stroke or cerebrovascular accident or cerebro-vascular accident or cerebro vascular accident or brain vascular accident or CVA or cerebrovascular attack cerebro-vascular attack cerebro vascular attack or brain vascular attack brain attack or cerebrovascular insult* or cerebro-vascular insult* or cerebro vascular insult* or brain vascular insult* or brain insult* or cerebrovascular injury or cerebro-vascular injury or cerebro vascular injury or brain vascular injury or brain injury or infarct* or isch?em* or occlusive cerebrovascular disease or occlusive cerebro-vascular

disease or occlusive cerebro vascular disease or cerebral artery occlusion or cerebrovascular disease or cerebro-vascular disease or cerebro vascular disease or cerebrovascular disorders or cerebro-vascular disorders or cerebro vascular disorders or acute cerebrovascular lesion or acute cerebro-vascular lesion or acute cerebro vascular lesion or intracranial embolism or intra-cranial embolism or intra cranial embolism or intracranial thrombosis or intra-cranial thrombosis or intra cranial thrombosis):ti,ab

8. #1 or #2 or #3 or #4 or #5 or #6 or #7
9. MeSH descriptor: [Cerebrovascular Circulation] explode all trees
10. MeSH descriptor: [Collateral Circulation] explode all trees
11. MeSH descriptor: [Microcirculation] explode all trees
12. MeSH descriptor: [Regional Blood Flow] explode all trees
13. (collateral* or cerebrovascular circulation or cerebro-vascular circulation or cerebro vascular circulation or cerebral circulation or neurovascular coupling or cerebrovascular bloodflow or cerebro-vascular bloodflow or cerebro vascular bloodflow or cerebrovascular blood-flow or cerebro-vascular blood-flow or cerebro vascular blood-flow or cerebrovascular blood flow or cerebro-vascular blood flow or cerebro vascular blood flow or cerebral bloodflow or cerebral blood-flow or cerebral blood flow or regional bloodflow or regional blood-flow or regional blood flow or perfusion or h?emodynamic brain response or h?emo-dynamic brain response or h?emo dynamic brain response or microcirculation):ti,ab
14. #9 or #10 or #11 or #12 or #13
15. MeSH descriptor: [Blood Glucose] explode all trees
16. MeSH descriptor: [Hyperglycemia] explode all trees
17. MeSH descriptor: [Hypoglycemia] explode all trees
18. (blood glucose or blood sugar or glucose blood level or sugar blood level or serum glucose or serum sugar or plasma glucose or plasma sugar or glucos?emi* or glyc?emi* or hypergl?c?emi* or hyper-gl?c?emi* or hypogl?c?emi* or hypo-gl?c?emi* or eugl?c?emi* or eu-gl?c?emi* or normogl?c?emi* or normo-gl?c?emi*):ti,ab
19. #15 or #16 or #17 or #18
20. #8 and #14 and #19

Appendix C

A series of images to illustrate the imaging modalities and interpretations of collateral flow.

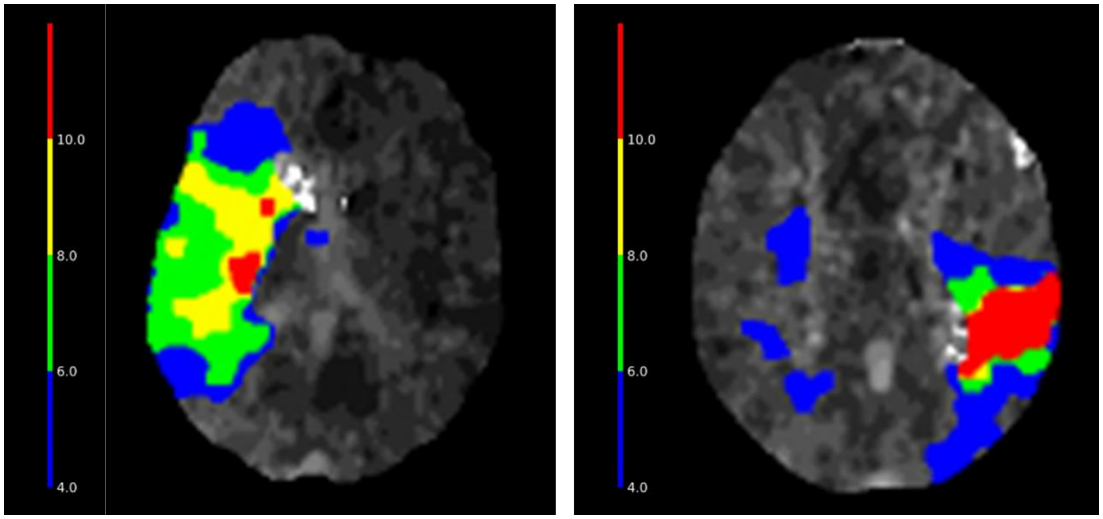

Left image: 59 year-old female, NIHSS 15, onset-to-CTP 27h2, HIR=0.2
Right image: 64 year-old male, NIHSS 6, onset-to-CTP 1h22, HIR 0.6

Figure 0-1 Examples of HIR

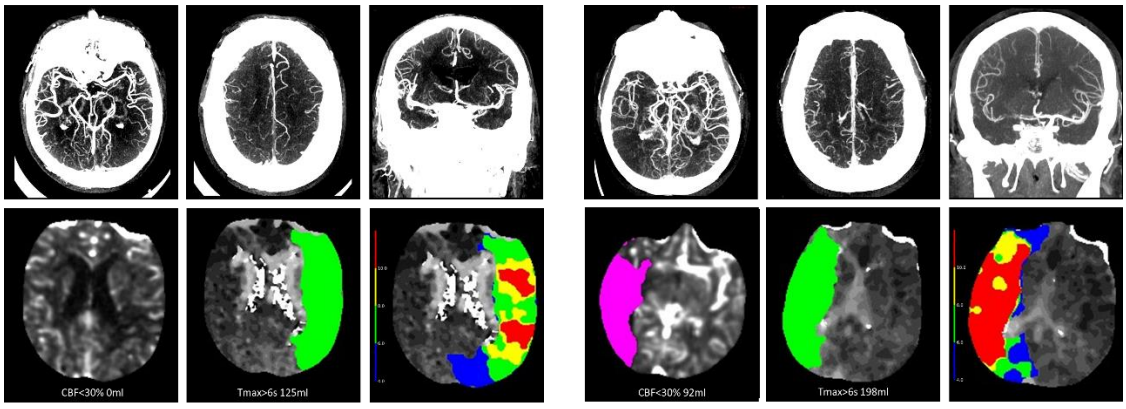

Left images: 83 year-old male, NIHSS 9, onset-to-CTP 3h13, left M2 occlusion (1 branch) rLMC 18, HIR 0.2
Right images: 64 year-old female, NIHSS 17, onset-to-CTP 15h25, right ICA occlusion, rLMC 7, HIR 0.6

Figure 0-2 Collateral Status as assessed using CTA (rLMC) and CTP (HIR)